Low-density lipoprotein (LDL) influences the immunomodulatory response of endothelial cells through promyelocytic leukemia protein (PML) activation

Inaugural-Dissertation
to obtain the academic degree
Doctor rerum naturalium (Dr. rer. nat.)

submitted to the Department of Biology, Chemistry, Pharmacy

of Freie Universität Berlin

by

Kerrin Roos

2022

This thesis as well as all involved experiments were planned, prepared and carried out within the years 2018 to 2022 at Charité Universitätsmedizin Berlin. The experiments and thesis were performed under the supervision of Prof. Dr. Günter Siegel (2018 to 2019) and Prof. Dr. Helmut Habazettl (2019 to 2022), both from the Institute for Physiology, Charité Universitätsmedizin Berlin.

1st reviewer: Prof. Dr. Helmut Habazettl
Charité Universitätsmedizin Berlin
Institute for Physiology
Charitéplatz 1
10117 Berlin

2nd reviewer: Prof. Dr. Katja Nowick
Freie Universität Berlin
Institute of Biology – Zoology
Königin-Luise-Str. 1-3
14195 Berlin

Date of defence: 16.01.2023

Acknowledgements

Für Prof. Dr. Günter Siegel (1942 - 2019).

First of all, I want to thank Prof. Dr. Helmut Habazettl for taking over supervision of this thesis, for his trust and patience in me and in my work. Furthermore, I want to thank Prof. Dr. Katja Nowick for being my second reviewer and for always being reachable and open to any questions or problems. Dr. Andreas Zakrzewicz deserves special acknowledgements for opening so many possibilities for me, without which I could not have brought this thesis to an end.

I want to thank Charité Universitätsmedizin Berlin, Freie Universität Berlin and Studienstiftung des Deutschen Volkes for giving me the opportunity to engage in my research and this thesis.

I want to acknowledge the collaborations with Prof. Dr. Christoph Knosalla, Prof. Dr. Michael Walter, Prof. Dr. Britta Eickholt, Prof. Dr. Karl Winkler, PD Dr. Thorsten Braun and PD Dr. Peter Hemmerich. A kind thanks to all patients and probands involved in this study. Without their kind support in the procuration of materials, none of my experiments could have been conducted.

I further want to thank the best working group ever, especially Dr. Janine Berkholz, for guiding me through this whole project with great kindness, helpfulness, knowledge and insights, as well as Angela Becker and PD Dr. Oliver Baum. Thank you for your expertise, for teaching me so much, for letting me be part of this team and for your support when things didn't always go the way they were supposed to.

A heartfelt thank-you to my family, in particular my parents - especially to my mum for being so supportive and proud of me at any time and to my siblings for their endless support, particularly to Aycke, not only for his great expertise, but for his couch in endless nights and to Yngve, for trying to help at any time.

Additionally, I want to thank my friends whose support has been, and always is, of huge value for me, especially in the hard times of my research. I particularly want to thank Judith, Robert, Martha and Eddi for a roof over my head and feeling at home at any time and Diana, Louise, Nicola, Jasmin, Anastasia and Tomma, for their helpful critics, and also for their open ears at any time.

Last but not least, I want to thank Benjamin. For always having my back, for his unconditional trust in me, for always being there and understanding me so well, and for always believing in me, even when I don't do so myself. I wouldn't be where am right now, if it wasn't for him.

Selbstständigkeitserklärung

Hierdurch versichere ich, dass ich meine Dissertation selbstständig verfasst und keine anderen als die von mir angegebenen Quellen und Hilfsmittel verwendet habe. Die Dissertation ist in keinem früheren Promotionsverfahren angenommen oder abgelehnt worden.

Datum

Unterschrift

0. Zusammenfassung/ Abstract

Zusammenfassung:

Arteriosklerose und Morbus Alzheimer stellen Volkskrankheiten dar, deren Prävalenz in der Gesellschaft stetig ansteigt. Aus diesem Grund ist es von großer Bedeutung, bestehende Zusammenhänge zu finden, mehr über die Erkrankungen in Erfahrung zu bringen und daraus entstehende Risiken besser einschätzen und eindämmen zu können. Da bei Arteriosklerose und Morbus Alzheimer neben einer z.T. durch Lipoproteine verursachten charakteristischen Nanoplaquebildung Inflammationsvorgänge bekannt sind, an denen PML und dessen Interaktionspartner beteiligt sind, stellt die genauere Untersuchung von Lipoproteinen und deren Wechselwirkung mit PML den Hauptgegenstand dieser Dissertation dar. Da Lipoproteine, wenn sie Apolipoprotein E4-homozygot sind, ein besonderes Risiko für den Ausbruch einer Alzheimererkrankung darstellen, wurden nicht nur Lipoproteine mit gepooltem apoE, sondern auch apoE4-homozygote Lipoproteine für die Experimente verwendet.

Um die Rolle von PML bei Entzündungsvorgängen der Arteriosklerose näher zu beschreiben, wurden verschiedene Endothelzellen (EA.hy926, HUVEC) mit verschiedenen Zusammensetzungen (an LDL, HDL oder in Mischungen aus VLDL, IDL und HDL mit variierenden LDL-Konzentrationen) von Lipoproteinen inkubiert. RT-qPCR, Immunblotting und Immunfluoreszenzanalysen zeigten, dass die PML-Expression und die Anzahl der PML-Kernkörperchen bereits nach 3 Stunden Inkubation mit den Lipoproteinmischungen oder den einzelnen Lipoproteinen höher war. Besonders ausgeprägt war dieser Anstieg nach Inkubation mit hohen LDL-Konzentrationen (in Mischungen oder als einzelnes Lipoprotein).

Darüber hinaus wurden auch die Aktivität der Proteinkinase C (PKC) sowie die Sekretion der Zytokine IL-6 und IL-8 positiv durch Inkubation mit Lipoproteinmischungen, apoE-gepooltem oder apoE4-homozygotem LDL dosisabhängig von LDL beeinflusst. Um herauszufinden, ob PML an dieser Signalkaskade in Endothelzellen beteiligt ist, wurden EA.hy926-Zellen mit einem für PML codierenden Vektor transfiziert und mit einem bekannten PKC-Inhibitor (sc-3088) oder PKC-Aktivator (PMA) behandelt. Die IL-6 und IL-8-Expression in solchen PML-überexprimierenden Zellen war erhöht. Außerdem bewirkte die Inkubation von EA.hy926-Zellen mit sc-3088 eine verringerte PML-Expression und weniger PML-Kernkörperchen, während sich die Inkubation mit PMA gegenteilig auf die PML-Expression auswirkte. Eine Kombination der Zellstimulation mit der physiologisch konzentrierten Lipoproteinmischung und der Behandlung mit einem Inhibitor oder mit der Transfektion mit dem PML-Vektor zeigte, dass der LDL-induzierte Effekt auf IL-6 und IL-8 von der PKC-Aktivität und der PML-

Konzentration der Zellen abhängig war. Inkubation mit LDL über 24 Stunden sowie die Aktivierung der PKC erhöhten außerdem die Expression und Aktivierung von STAT3, während die Inhibierung der STAT3-Aktivierung mit dem Inhibitor STATTIC eine leichte Absenkung der PML-Expression bewirkte. STAT3 könnte damit ein weiteres Zwischenglied der Signalkette darstellen, wobei gezeigt werden konnte, dass STAT3 die PKC-Aktivität negativ rückkoppelnd beeinflusst. Eine Inhibierung von STAT3 verringerte die IL-6 und IL-8-Expression, weshalb davon ausgegangen werden kann, dass STAT3 die Sekretion dieser Zytokine unabhängig von PML beeinflusst. Der über LDL vermittelte PKC-aktivierende Signalweg in Endothelzellen beeinflusst zudem die Proteinexpression von p53 positiv, jedoch zeigten Überexpressionsversuche mit PML, dass dies unabhängig von PML geschieht. Im Gegensatz dazu konnte für die Expression von eNOS keine LDL-abhängige Beeinflussung gezeigt werden. Die eNOS-Expression in Endothelzellen wird jedoch über HDL vermittelt, während eine erniedrigte eNOS-Expression in Überexpressionsversuchen mit PML beobachtet wurde.

Insgesamt zeigen die Ergebnisse dieser Facharbeit einen neuen Signalweg in Endothelzellen auf, der die Aktivierung von PKC durch LDL beinhaltet, was zu einer erhöhten PML-Expression führt, die wiederum zu einer Erhöhung der Expression von IL-6 und IL-8 führt. Als weitere (zum Teil) involvierte Faktoren konnten STAT3 und p53 identifiziert werden.

Abstract:

Atherosclerosis and Alzheimer's disease are wide-spread diseases with rising prevalence. Therefore it is important to uncover more about the diseases themselves and thus understanding and contain the risks they bring along. As blood lipoproteins are involved in nanoplaque formation as well as in inflammatory processes in both diseases, which are linked to PML and its interaction partners, this study concentrates on the question if PML expression is modulated by lipoproteins. As apoE4-homozygous lipoproteins cause a genetic predisposition and thus a high risk for developing Alzheimer's disease, not only lipoproteins with pooled apoE, but also apoE4-homozygous lipoproteins were used.

To determine the role of PML in inflammatory processes in atherosclerosis, endothelial cells (EA.hy926 and HUVECs) were incubated with variations of lipoproteins (of LDL, HDL or in compositions containing VLDL, IDL, HDL and different concentrations of LDL). RT-qPCR, immunoblotting and immunofluorescence analysis showed that PML expression and the number of PML nuclear bodies (PML-NBs) increased after only 3 hours of incubation with the compositions or the single lipoproteins. This increase was especially high when treated with high concentrations of LDL in a composition or as a single apoE-pooled or apoE4-homozygous lipoprotein. Moreover, the activity of protein kinase C (PKC) and the secretion of the cytokines IL-6 and IL-8 were also positively regulated by lipoprotein compositions, pooled and apoE4-homozygous LDL in a dose-dependent manner.

To investigate whether PML is a component of this signalling cascade in endothelial cells, EA.hy926 cells were transfected with an expression vector encoding PML, in the presence or absence of a known PKC inhibitor (sc-3088) or PKC activator (PMA). The expression of IL-6 and IL-8 was higher in PML-overexpressing cells, suggesting that IL-6 and IL-8 act downstream of PML. Furthermore, treatment of the cells with sc-3088 demonstrated lower PML expression and PML-NB assembly, while treatment with PMA resulted in opposing effects. Combining the stimulation of the cells with blood lipoprotein compositions and inhibitor treatment or transfection with a PML vector showed that the LDL-induced effect on IL-6 and IL-8 was dependent on PKC activity and PML concentrations. Incubation with LDL for 24 hours as well as activation of PKC further led to an increase in STAT3 expression and activation, while inhibition of STAT3 activity with the inhibitor STATTIC caused PML expression to slightly decrease. Therefore,

STAT3 might be another link in this signalling cascade, whereas it was shown to negatively influence the activity of PKC as a feedback.

The inhibition of STAT3 activation in endothelial cells resulted in lower expression of IL-6 and IL-8, thus it is assumed that the influence of STAT3 on these cytokines is independent of PML. The LDL-induced PKC activating pathway in endothelial cells also positively affected p53 protein expression. However, experiments with PML-overexpressing cells indicate that this increase is independent of PML. In contrast, eNOS-expression was not influenced by LDL, yet eNOS expression in endothelial cells was induced by HDL. PML-overexpressing cells showed a decrease in eNOS expression.

Taken together, the results of this thesis indicate that a so far non-described signalling pathway is present in endothelial cells that includes activation of PKC by LDL in an early response, leading to an increased PML expression, followed by an increase in the expression of the PML targets IL-6 and IL-8. Other factors that are (partly) involved in this signalling cascade are STAT3 and p53.

I . Abbreviations

ABCA1: ATP-binding cassette transporter 1
Aβ40/42: Beta-amyloid 40 or 42
AD: AD
AKT: Protein kinase B
aPKC: Atypical PKC
apo: Apolipoprotein
APP: Amyloid precursor protein
APRF: Acute phase response factor
ATP: Adenosine triphosphate
BH_4: Tetrahydrobiopterin
BMI: Body Mass Index
BSA: Bovine serum albumin
CAD: Coronary artery disease
CaM: Calmodulin
cAMP: Cyclic adenosine monophosphate
CCE: Capacitive calcium entry
CEPT: Cholesteryl ester transfer protein
CK2: Casein kinase 2
CSF: Colony-stimulating factor
cGMP: Cyclic guanosine monophosphate
cPKC: Conventional PKC
CRP: C-reactive protein
DAG: Diacylglycerol
DMEM: Dulbecco's modified Eagle's medium
EA.hy926: Homo sapiens hybrid cell line
EDTA: Ethylenediaminetetraacetic acid
ELISA: Enzyme-linked immunosorbent assay
eNOS: Endothelial nitric oxide synthase
ERK: Extracellular signal-regulated kinases
FAD: Flavin adenine dinucleotide
FCS: Foetal calf serum
FMN: Flavin mononucleotide
GAPDH: Glyceraldehyde-3-Phosphate Dehydrogenase
gp130: Glycoprotein 130
HCAEC: Human coronary artery endothelial cells
HDL: High-density Lipoprotein
HUVEC: Human umbilical vein endothelial cells
HS-PG: Heparan sulfate proteoglycan
HTGL: Hepatic triglyceride lipase
ICAM-1: Intercellular adhesion molecule 1
IDL: Intermediate-density Lipoprotein
IFN: Interferon

IGFBP-5:	Insulin-like growth factor-binding protein 5
IL:	Interleukin
IMT:	Intima-media-thickness
iNOS:	Nitric oxide synthase
JAK:	Janus kinase
KLHL20:	Kelch-like protein 20
LCAT:	lecithin-cholesterol acyltransferase
LDL:	Low-density Lipoprotein
LPS:	Lipopolysaccharide
MAP4:	Microtubule-associated protein 4
MAPK:	Mitogen-activated protein kinase
M-CSF:	Macrophage colony-stimulating factor
MCP-1:	Monocyte chemoattractant protein 1
MDM2:	mouse double minute 2 homolog
mmHG:	Unit millimetre of mercury
mTOR:	Mechanistic target of rapamycin
NADPH:	Nicotinamide adenine dinucleotide phosphate
NFkB:	Nuclear factor “kappa-light-chain-enhancer” of activated B-cells
NLRP3:	NLR family pyrin domain containing 3
NMDA:	N-Methyl-D-aspartic acid
NO:	Nitric oxide
nPKC:	Novel PKC
oxLDL:	Oxidized low-density lipoprotein
p53:	Tumour protein p53
PAD:	Peripheral arterial occlusive disease
PAI-1:	Plasminogen activator inhibitor-1
PBS:	Phosphate-buffered saline
PHF:	Paired helical filaments
PI3K:	Phosphoinositide 3-kinase
PIN1:	Peptidyl-prolyl cis-trans isomerase NIMA-interacting 1
PKC:	Protein kinase C
PLTP:	Phospholipid transport protein
PMA:	Phorbol 12-myristate 13-acetate
PML:	Promyelocytic Leukemia Protein
PML-NB:	PML nuclear body
PS:	Presenilin
pSTAT3:	Phosphorylated STAT3
PTK:	Protein tyrosine kinase
RBCC:	Ring-B-boxes-coiled-coil
ROS:	Reactive oxygen species
RNF4:	Ring finger protein 4
SDS-PAGE:	Sodium dodecyl sulfate polyacrylamide gel electrophoresis
SENP1:	SUMO specific peptidase 1
SIM:	SUMO interaction motif
Sirt1:	Sirtuin 1
SH2:	Src Homology 2 domain

SHP-2:	Src Homology region 2 domain-containing phosphatase 2
STAT:	Signal transducer and activator of transcription
STATTIC:	STAT3 inhibitory compound
SUMO:	Small ubiquitin-related modifier
rpm:	Rounds per minute
TGF-ß:	Transforming growth factor beta
TNF:	Tumor necrosis factor
TPA:	Total plaque area
Tyk2:	Tyrosine kinase 2
UBC9:	SUMO-E2-conjugating enzyme
UV-VIS:	Ultraviolet-visible
VCAM-1:	Vascular cell adhesion protein 1
VEGF:	Vascular endothelial growth factor
VLDL:	Very Low-density Lipoprotein
VSMC:	Vascular smooth muscle cells
WHO:	World Health Organization

1. Introduction

Atherosclerosis and AD are non-communicable diseases that affect patients worldwide. The World Health Organization (WHO) reported that AD became more prevalent in 2019 than in the years before. The WHO also named ischaemic heart disease the main cause of death in 2019 [1]. Therefore, it is of prime relevance to find out more about existing correlations between the two diseases and their etiopathology in order to assess emerging risks.

1.1. Atherosclerosis

Atherosclerosis is characterized by chronic inflammation of coronary and peripheral arteries [2], leading to the narrowing of their lumen of the blood vessels and the loss of functionality [3]. It also includes nanoplaque formation (for more details on nanoplaques s. chapter 1.1.1), which cause obstruction, thrombosis and embolism, leading to the clinical manifestation of disturbed blood circulation with permanent structural changes. As a consequence, atherosclerosis bears an increased cardiovascular risk to develop effects of stenosis such as myocardial infarcts, apoplexy and peripheral arterial occlusive disease (PAD) [4].

1.1.1. Aetiology and pathophysiology of atherosclerosis

Hypercholesterolemia and high triglyceride levels [5] contribute to the vascular changes and thereby are crucial risk factors for developing atherosclerotic vessel alterations [6]. The first manifestations, so-called “fatty streaks”, caused by a local increase of lipoprotein levels, are found in the intima [7]. From a pathological perspective, it comes to a lesion of the endothelium upstream of the site of platelet aggregation due to the structural damage of the tissue.
Subsequently, microthrombi accumulate at the endothelium surface, followed by the release of various cytokines and growth factors, such as monocyte chemoattractant protein-1 (MCP-1), interleukin-6 (IL-6) and tumor necrosis factor-α (TNF-α) from the endothelial cells [8, 9]. Consequentially, both monocytes and lymphocytes invade the damaged tissue, where the monocytes differentiate into macrophages. LDL-proteoglycan and oxidized LDL (oxLDL) complexes accumulate in the injured tissue to be then phagocytosed by these macrophages. However, as macrophages are unable to demount the incorporated LDL-complexes, the intracellular lipoproteins cause foam cell formation, which leads to an additional invasion of monocytes and lymphocytes, provoking the whole process being subject to a circulus vitiosus

[6]. On the molecular level, a nanoplaque formation under the involvement of blood lipids and heparan sulfate proteoglycan (HS-PG) takes place, which is accelerated by increasing concentrations of Ca^{2+} [10].

1.1.2. Clinical manifestation of atherosclerosis

The American Heart Association distinguishes between six lesson stages of atherosclerosis [7]: the types *I* to *III* are preliminary stages without clinical symptoms, while the types *IV* to *VI* describe advanced vascular lesions.

Although all six atherosclerotic stages are found in adults, type *I* lesions mostly occur in children. They often remain undetected which is the reason for limited knowledge about the arterial vessel changes caused by these lesions [7]. As reported by Stary and colleagues [11, 12], type *I* lesions consist of unconnected groups of macrophages, already containing small concentrations of lipids. Foam cells express pathological concentrations of lipoproteins which start to accumulate in the intima, in regions corresponding to those where type *II* and *III* lesions take place as well [7].

The demeanour of fatty streaks, yellowish portions that can be seen with the bare eye, indicate the presence of type *II* lesions. Type *II* lesions are composed of adjoining layers of foam cells, no longer consisting of isolated small groups only. However, they must be identified by their microscopic composition, since the appearance of fatty streaks alone is not defining the lesions. Furthermore, lipid droplets are incorporated which are mainly composed of cholesterol esters, cholesterol and phospholipids [7, 13-15]. Type *II* lesions have greater concentrations of macrophages and mast cells but fewer T-lymphocytes compared to corresponding vascular sections of healthy controls [16].

Type III lesions feature extracellular lipid droplets, which are corresponding to the ones that are found in small concentrations in some type *II* lesions. A “lipid core”, which is distinctive for progressive lesions, is not established yet [7].

Type *IV* lesions, also called atheroma, are the first of the advanced lesions characterized by a strong accumulation of the extracellular lipids that appear as a “lipid core” [17]. Remarkably, Ca^{2+} is found in lipid core formations. In consequence, macrophages along with smooth muscle cells with or without lipid droplets show up between the lipid core and the endothelial surface [17]. Even though the lesions do not cause significant narrowing of the vessel lumen, these structural alterations are of clinical relevance, if they lead to fissures. If the lipid core converts into fibrous tissue, it can reduce the intima luminally of the lipid core [17]. As soon as this

transition of the intima into fibrous tissue progresses, the lesion transforms from a type *IV* to a type *V* lesion.

The formation of extrusive new fibrous connective tissue is the main feature of type *V* lesions [17]. There is a subdivision in type *Va, Vb* and *Vc* lesions, whereas, in type *Va* lesions, possibly multi-layered, the new tissue is part of a type *IV* lesion, while in type *Vb* the lipid core is calcified along with other components. Low lipid levels and the absence of a lipid core characterize *Vc* lesions. At this point, the arteries constrict more than in type *IV* lesions. Same Fissures and thrombi may occur, which underlines the clinical relevance of type *V* lesions [17]. "Complicated" or type *VI* lesions are type *IV* or *V* lesions in which thrombosis, hematoma or haemorrhage as well as disruptions of the lesion surface are observed [17]. These lesions may cause death of the patients. Type *VI* lesions are subdivided into further groups. Type *VIa* lesions consist of disruption of the endothelial surface, type *VIb* lesions include hematoma or haemorrhage, while type *VIc* lesions contain thrombosis. If all these features come together, the lesion is classified as a type *VIabc* lesion [17].

1.1.3. Risk factors for atherosclerosis

In a longitudinal 13-year follow-up study, the so-called Tromsø Study, Herder et al. collected ultrasound data on the progression of intima-media thickness (IMT) as well as increase of total plaque area (TPA) in the right coronary artery of 1307 male and 1436 female patients [18]. Risk factors that were also attained included levels of total cholesterol, HDL cholesterol, blood pressure, body mass index (BMI), as well as information about smoking habits, prevalent diabetes and cardiovascular disease [18]. The outcome of the study showed that total cholesterol levels, systolic blood pressure and smoking were significant predictors of both TPA and IMT: the impact on TPA was stronger than on IMT, while on the other hand sex and age had a stronger impact on IMT. Systolic blood pressure and smoking had a significant impact on the progression of TPA, while total cholesterol levels affected the progression of TPA and IMT [18]. Consequently, it was concluded that the factors do not generally indicate a high risk for atherosclerosis but that there are two different phenotypes of atherosclerosis in plaque TPA and IMT [18].

Risk factors of atherosclerosis were also determined in the Prospective Cardiovascular Münster Study (PROCAM-Study) [19]. In this longitudinal study, Schulte and Assmann tested 20060 male and female employees in the age of 17 to 65 from 52 industrial companies for cardiovascular risk factors with respect to signs of atherosclerosis such as myocardial

infarction, stroke and coronary death [19]. The study showed that in men aged 40 to 65, who had not had a myocardial infarction prior to the study, 73 myocardial infarctions or coronary deaths were recorded after four years of follow-up, whereas 2681 subjects suffered from neither infarctions nor apoplexy. The authors defined a collective of high-risk patients by regarding hyper-/dyslipoproteinemia, age, HDL cholesterol, systolic blood pressure, smoking habits, diabetes mellitus, angina pectoris and a family history of myocardial infarction [19]. Besides the Tromsø- and the PROCAM-study, van der Meer et al. observed risk factors for the progression of atherosclerosis in the so-called "Rotterdam Study" [20]. The authors examined a group of 7983 participants (male and female) aged 55 or older in a population-based cohort study. In the end, data from 6.5 years were obtained for 3409 participants. The study showed that age, smoking, total cholesterol levels, systolic blood pressure and/or hypertension were independent parameters for both a moderate and a severe progression of atherosclerosis. In contrast, diabetes mellitus only predicted severe progression, while the sex did not predict any atherosclerotic progression [20].

1.1.4. Atherosclerosis and inflammation

Even marginal inflammatory processes induce immunological responses of the organism. Endothelial lesions additionally trigger these inflammatory reactions. Especially when it comes to the progression of atherosclerosis, such inflammatory processes are of vital relevance [21]. Especially monocytes, macrophages and T lymphocytes are the first cells linked up to the immune system when it comes to the progression of atherosclerosis, with a special focus on the nanoplaque formation. While TH1 cells start to secrete several cytokines, for example interferon-gamma (IFN-γ), interleukin (IL)-2 and TNF as well as IL-12 and IL-18, all of which are proinflammatory [21], TH2 cells have an impact on the expression of cytokines involved in inflammation, namely IL-4, IL-5 and IL-10 [21]. As previously described in chapter 1.1.1, monocytes start binding to the endothelium of the developing atheroma via vascular cell adhesion protein 1 (VCAM-1), intercellular adhesion molecule 1 (ICAM-1) and several selectins, which empower the IL-8 and MCP-1-facilitated migration of the monocytes to the intima where they then differentiate into macrophages [6, 21, 22], whereas their differentiation is triggered by macrophage colony-stimulating factor (M-CSF). Several known inflammatory biomarkers, such as high-sensitivity C-reactive protein (CRP), IL-1 and IL-6 [21], but also many different components of the NLRP3 (NLR family pyrin domain containing 3) inflammasome are of biological relevance to the processes of inflammation in atherosclerosis.

1.2. Alzheimer's disease (AD)

AD is a neurodegenerative disease causing 70 % of dementia cases [23]. Nanoplaques named "senile plaques" consisting of β-amyloid, HS-PG, blood lipids and Ca^{2+} [10, 24, 25] and neurofibrillary tangles primarily composed of tau protein [23] are found in the vascular samples of AD patients. It comes to the loss of nerve cells and synapses. This causes macroscopic brain atrophy, most severely emerging in the neocortex, the hippocampus, the basal forebrain, the dorsal raphe nucleus and the locus coeruleus [6]. Clinical symptoms usually occur when about 70 % of the affected neurons are degenerated [26].

1.2.1. Pathophysiology

Three hypotheses have been developed to explain the pathophysiology behind the aetiology of AD, namely the amyloid hypothesis, the acetylcholine hypothesis and the glutamate hypothesis [6]. The amyloid hypothesis implies that soluble or insoluble β-amyloid is in charge of the psychopathology of AD [6]. β-amyloid proteins are generated by the amyloid precursor protein (APP), a transmembrane protein [23, 26]. Especially α-, β- and γ-secretases catalyse the cleavage of APP. α-secretase generates soluble APP, while β- and γ-secretases generate β-amyloids [26]. The secretases release the resulting β-amyloid outside of the cell, where it is dismantled. When found in senile plaques, β-amyloid mostly appears as a peptide consisting of 40 or 42 amino acid residues [27]. Increased concentrations of Aβ 40 and Aβ 42 are present in pathological processes, therefore β-amyloid is not easily dismantled due to its hydrophobic properties and accumulates [23]. Mutations in APP and presenilin-genes (PS) cause hereditary forms of AD and facilitate the formation of β-amyloids [27]. As treatment of Aβ in AD mostly fails, an issue of APP metabolism along with tau-pathology is described as a more fitting explanation for the cause of the disease [23].

Spillantini et al [28] describe the tau protein as a microtubule-associated phosphoprotein. This protein plays a role in microtubule assembly and stabilization. Especially tau protein phosphorylation is relevant to its physio- and pathophysiological influence [28]. Aggregated tau proteins are found in neurodegenerative disorders, where they build up neurofibrillary tangles. In AD, paired helical filaments (PHF) [29] are derived from native tau proteins and pathological tau protein seems to be relevant in the development of other neurodegenerative diseases [29] besides AD.

As about 90% of the cholinergic neuronal pathways to the neocortex originate in the nucleus basalis Meynert, it is heavily affected when it comes to the degeneration of neurons. This is noticeable as the deteriorating of the cholinergic neurons causes clinical symptoms such as the derangement of memory [26], caused directly or indirectly through the interference with attentional processing [30] induced by an acetylcholine deficiency. This statement builds the foundation of the acetylcholine-hypothesis [6]. This hypothesis is represented by the glutamate-hypothesis – a hypothesis based on the fact that N-methyl-D-aspartate (NMDA)-receptors in patients are unusually high active in AD patients [31]. Freissmuth et al. showed that this increased NMDA-receptor signalling leads to the breakdown of long-term potentiation and the increase in glutamate-dependent neurotoxicity [6].

1.2.2. Genetic predisposition for AD

Advanced age, female sex [32], mutations in presenilin-genes 1 (PS-1) and 2 (PS-2) along with mutations in APP and more [33] have an impact on the development of AD in individuals. A very high genetic risk factor for developing AD is Apolipoprotein E4 (apoE4) [34]. It belongs to the group of apolipoproteins, which play a role in cholesterol transport (see chapters 1.3.2 and 1.3.3). apoE is produced mainly in the liver but also in astrocytes, skin, adrenal glands, the spleen, and the lung [35-37]. There are three apoE isoforms, E2, E3 and E4, with three different alleles causing six possible phenotypes, three of them homozygous and three of them heterozygous. However, most of the humans carry apoE3/E3 as a phenotype [36, 38, 39]. ApoE4 acts as a ligand for LDL-receptors [40]. Similarly to apoE2, apoE4 increases LDL levels and plays a role in the aetiology of neurodegenerative diseases, where it is involved in tau phosphorylation but also causes mitochondrial dysfunction [40]. 65 to 80 % of patients with AD are carrying at least one allele of apoE4, underlining the importance of apoE4 as a genetic marker in developing AD. Mahley et al. described that when being apoE4-homozygous, the point of the outbreak of AD was reduced by 8 years for each allele the patient carries [40], the stakes of developing the disease when carrying one allele enhance 4-fold compared to a patient who is apoE4-negative. In comparison with an apoE3/3-positive patient, a patient carrying two alleles of apoE4 (apoE4-homozygous) develops AD by a 14-fold higher probability, even in patients without any family history of dementia, where the age for the outbreak of AD was lowered significantly [41].

1.3. Lipoproteins

Lipoproteins are made of apolipoproteins and lipids, which are packed together in several complexes mainly for the transport of hydrophobic lipids in the aqueous blood compartment (*Table 1*) [42]. Lipoprotein particles are classified through their physiochemical properties. Every class exhibits a specific density (*Figure 1*), allowing their biochemical isolation in addition to their naming [42]. Most important classes are chylomicrons, very low-density lipoprotein (VLDL), intermediate-density lipoprotein (IDL), LDL and HDL. As the experiments conducted for this thesis did not involve chylomicrons, this chapter mainly focusses on VLDL, IDL, LDL and HDL.

Lipoprotein	*Density in g/mL*	*Size (diameter) in nm*	*Apolipoprotein involved*	*Location of origin*	*Lipids proportion in %*	*Proteins proportion in %*
Chylomicrons	0,93	100-500	A, B48, C-II, E	Small intestine	99	1
VLDL	0.95-1.006	30-80	A, B100, CII, E	Liver	85- 90	10-15
IDL	1.006-1.019	25-50	B100, C, E	VLDL	85	15
LDL	1.019-1.063	18-28	B100	IDL	80	20
HDL	1.063-1.210	5-15	AI, AII, C-II, E	Liver, intestine	50	50

Table 1. Lipoprotein summary. *Different lipoproteins and their compound and locations of origin. Based on [42-47] . Created by the author.*

Even though the lipoproteins have different concentrations of triglycerides, cholesterol and cholesterol esters as well as several apolipoproteins, their structure is similar. The core mainly consists of non-polar triglycerides and cholesterol esters, while the coat consists of amphiphile cholesterol, phospholipids and apolipoproteins (*Figure 1*) [45].

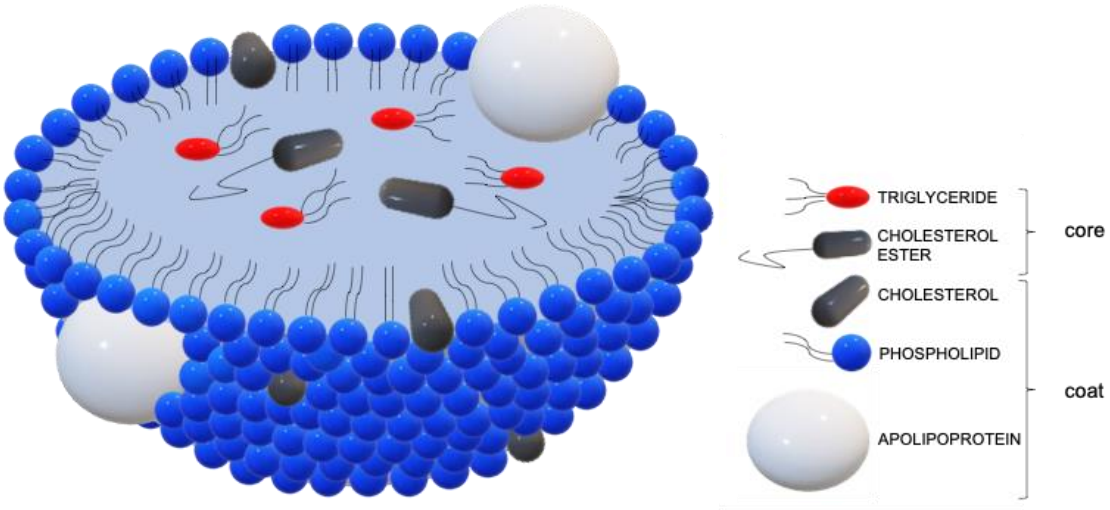

Figure 1. Schematic representation of a lipoprotein particle, cross section. *A lipoprotein particle is made of various components. The core consists of different triglycerides and cholesterol esters, while the coat consists of cholesterol, phospholipids and apolipoproteins. Based on [45]. Created by the author.*

As shown in Figure 2, chylomicrons contain the highest concentration of triglycerides, while LDL has the highest concentration of cholesterol. HDL embodies the highest levels of apolipoproteins and phospholipids but the lowest triglyceride levels. IDL is composed of about 35 % triglycerides and 34 % cholesterol [6, 48]

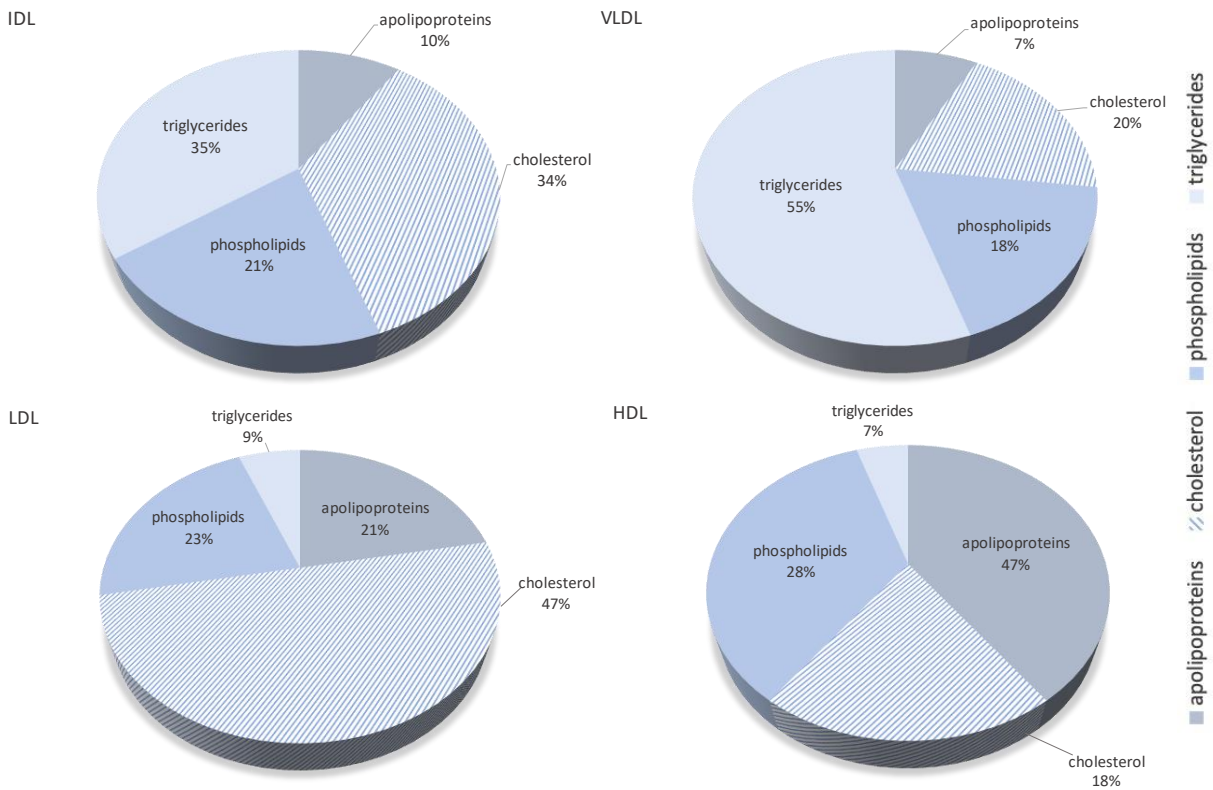

Figure 2. Composition of the different lipoprotein classes. *Shown are relative levels of cholesterol, phospholipids, triglycerides as well as apolipoproteins. As chylomicrons were not tested in this thesis, their data is not shown in this graph. Based on [44, 48].*

1.3.1. Lipoproteins in the human organism

The plasma concentrations of lipoproteins are crucial for a stable function of cholesterol transport, whereas unbalanced levels of lipoproteins lead to the development of diseases. VLDL is usually found in a concentration of 30 mg/dL, while IDL occurs in 10 mg/dL [10, 49-51]. HDL levels should be at least 50 mg/dL [6, 52]. For people with low risk of developing atherosclerosis, LDL levels should be between 100 and a maximum of 115 mg/dL, whereas they should not be higher than 70 mg/dL for high-risk patients. Hypercholesterolaemia mostly develops due to increased LDL concentrations, possibly in combination with increased triglyceride levels, which are risk factors for cardiovascular diseases such as atherosclerosis or diabetes mellitus. Treatment of hypercholesterolaemia includes changes of lifestyle and medical therapy. Further risk factors for the development of lipoprotein-related diseases are smoking, low HDL levels (below 40 mg/dL) or hypertension [6]. The LDL/HDL ratio is of relevance for the development of cardiovascular disease. The higher the ratio, the higher the cardiovascular risk. As concluded in the PROCAM study (chapter 1.1.3), the optimal ratio is lower than 2.5, whereas coronary death occurred with higher probability when the ratio was between 3.7 and 4.3 [6, 19, 53, 54].

1.3.2. Apolipoproteins and their functions

Apolipoproteins are held accountable for most of the lipoprotein functions [55]. By now, 10 different classes of apolipoproteins have been identified. The various apolipoproteins exhibit different functions. Apolipoproteins are soluble in water, which qualifies them for the transport of cholesterol and triglycerides through the circulatory system [42, 56]. They interact with specific cell receptors and stabilize the lipid fraction of the lipoproteins [56, 57]. ApoAI, apoAII, apoB100 and apoE are important due to their involvement in physiological and pathophysiological processes [34, 58, 59]. ApoAI and apoAII are found in HDL particles (*Table 2*). apoAI plays a role in the activation of the lecithin-cholesterol acyltransferase (LCAT), while apoAII contributes to the activation of the hepatic triglyceride lipase (HTGL) [56, 59, 60].
LDL contains only apoB100, which is also a main component of VLDL and acts as a ligand for the LDL receptor, highlighting its role in the development of atherosclerosis and cardiovascular diseases [61].
apoE plays a role in the reversed cholesterol transport and thereby gains protective attributes in atherosclerosis and AD [58, 62]. As previously described in chapter 1.2.2, particularly apoE4

is relevant in the genetic predisposition for AD [34]. In comparison to apoB, apoE4 has an increased binding affinity to the LDL receptor [63].

class	*Representative/ further subdivision*	*Approx. Molecular weight (Da)*	*Corresponding lipoprotein*
apolipoprotein A	apoAI, apoAII, apo AIV, apoAV	17.414-46.465	HDL, chylomicrons, VLDL (AV)
apolipoprotein B	apoB48, apoB100	264.000-549.000	IDL, Lp(a) B48: chylomicrons B100: LDL, IDL, VLDL
apolipoprotein C	apoCI, apoCII, apoCIII, apoCIV	6.630-8.800	VLDL, IDL, HDL, chylomicrons
apolipoprotein D	apoD	29.000	HDL
apolipoprotein E	apoE2, apoE3, apoE4	34.000	VLDL, IDL, HDL
apolipoprotein F	apoF	26.000-32.000	HDL
apolipoprotein H	-	43.000	Unknown
apolipoprotein L	apoL1-6, apoLD1	42.000	HDL
apolipoprotein M	apoM	21.253	HDL, LDL, VLDL
apolipoprotein(a)	-	250.000-800.000	Lp(a) (Lipoprotein (a))

Table 2. Biochemical properties of apolipoproteins *in subdivision of classes, molecular weight, corresponding receptors as well as corresponding lipoproteins. Based on [55, 56, 64-72]. Created by the author.*

1.3.3. Metabolism of lipoproteins

The exogenous lipoprotein pathway (*Figure 3*) begins after the intake of lipids with food, where both cholesterol and triglycerides are being absorbed by the intestinal endothelium. Triglycerides are cleaved into diacylglycerides, monoacylglycerides and fatty acids. In the endoplasmic reticulum of the enterocytes, large chylomicrons are synthesized, composed of

triglycerides, apoA, apoB48 and low levels of cholesterol, and released at the basal pole. The chylomicrons then reach the lymphatic system and enter the circulatory blood system via the *ductus thoracicus* and left *angulus venosus*. Due to a change in their apolipoprotein composition through interaction with HDL, microvascular lipoprotein lipase in the capillaries of the peripheral fat is activated. As this enzyme hydrolyses the cleavage of fatty acids out of triglycerides to have them absorbed by adipocytes, the number of triglycerides inside the chylomicrons continuously decreases, while the relative concentration of cholesterol esters increases. Finally, the so-called 'chylomicron remnants' are taken up into hepatocytes by inducing endocytosis via apoE binding to the LDL receptor [73, 74].

VLDL particles are formed in hepatocytes and function as a transporter for endogenous triglycerides (from metabolized carbohydrates), phospholipids, cholesterol and cholesterol esters [75]. The lipoprotein lipases in the endothelium of capillaries in the peripheral fat also deplete triglycerides from circulating VLDL particles, thereby forming IDL particles. These IDL particles are equipped with apoB100 and apoE to facilitate the uptake into hepatocytes. The remaining IDL particles in the circulation lose apoE molecules and thus convert into LDL. LDL particles are taken up into all peripheral cells by the LDL receptor, as cholesterol is necessary for the integrity of their cell membranes [26, 43, 76].

HDL incorporates precipitated cholesterol but also phospholipids and triglycerides. The uptake takes place via the ATP-binding cassette transporter 1 (ABCA1) and LCAT. Subsequentially, saturated HDL is transported to the liver (to form bile acids) and steroid hormone-synthesizing cells, such as the ovaries, testicles and adrenal glands. HDL also executes the reversed cholesterol transport, where cholesterol from macrophages and atheroma is taken back to the liver [77].

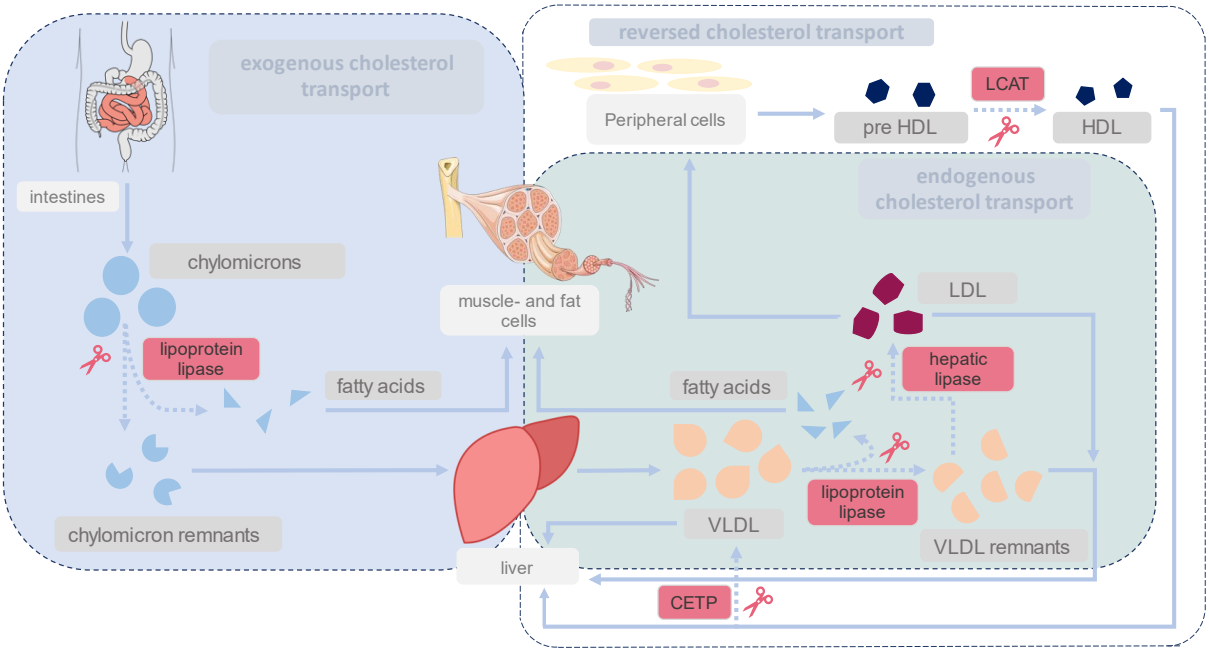

Figure 3. Schematic representation of the lipoprotein metabolism. *The blue shaded box depicts the exogenous cholesterol transport, in which fatty acids are esterified in the enterocytes and packed together with apoB48 and triglycerides to form chylomicrons which then end up in the circulatory system via the lymphatic system. Here, the chylomicrons get rid of fatty acids, a process catalysed by lipoprotein lipase, expressed by capillary endothelial cells. While the fatty acids find their way to muscle- and fat cells, the chylomicron remnants make their way to the liver, where they are taken up. The endogenous cholesterol transport is depicted by the turquoise shaded box. The liver forms VLDL which is also decomposed by the lipoprotein lipase as soon as it reaches the circulatory system. Fatty acids which, besides VLDL remnants, are the product of VLDL decomposition, pass over to LDL. VLDL remnants are either taken back up into the liver or develop into LDL particles, a process catalysed by the lipoprotein lipase. These LDL particles either get back to the liver to be taken up via scavenger receptors [6, 78], or reach peripheral cells, where the cholesterol the LDL is carrying is metabolized. If peripheral cells require no more cholesterol, yet still possess concentrations of it, it comes to reversed cholesterol transport. This reversed cholesterol transport is pictured by the white shaded box. Cholesterol from peripheral cells is taken up by pre-HDL and is esterified with help from LCAT. HDL transports cholesterol through the circulation to the liver, where it either is disposed through direct HDL uptake or through the CETP-catalysed transformation of HDL to VLDL, which gets taken up by the liver [79]. Created by the author.*

1.3.4. VLDL

With a concentration of 85 to 90 % of lipids, VLDL consists of only 10 to 15 % protein [43-45] (*Table 1)*. VLDL is sub-divided into three distinct classes due to their densities: $VLDL_1$, $VLDL_2$ and $VLDL_3$. The subclass $VLDL_1$ includes particles with the lowest density and a size of 60 to 100 nm, while $VLDL_2$ covers particles with intermediate density and the size of 40 to 60 nm.

The $VLDL_3$ subclass contains the particles with the highest density, yet the smallest size of 30 to 40 nm [47].

All VLDL particles contain the apolipoproteins apoE and apoB100, which are relevant in LDL formation. In the circulatory system, HDL particles pass apoE and apoC-II to VLDL particles. ApoC-II is responsible for the depletion of triglycerides by activating lipoprotein lipase located in the capillary endothelium of peripheral tissues [74, 80, 81].

1.3.5. IDL

Not only the loss of triglycerides through the lipoprotein lipase causes VLDL to turn into IDL, but also the esterification of cholesterol by the cholesteryl ester transfer protein (CEPT). The freshly generated lipoproteins contain apoE and apoB100. Some particles are taken up in hepatocytes, whereas the remaining particles lose their apoE molecules to transform into LDL. IDL is divided into two subclasses from which the low-density class particles are about 28 to 30 nm, while the intermediate density particles are 27 to 28 nm [47].

1.3.6. LDL

After its CETP-mediated generation out of IDL, LDL has only one remaining apolipoprotein, apoB100. The LDL particles contain more cholesterol than triglycerides (*Table 1*) [26]. The LDL subclasses divide LDL into low, intermediate and high-density particles, of which the low-density particles have a size of 23 to 30 nm, intermediate particles the size of 20 to 23 nm and the high-density particles reaching sizes of 18 to 20nm only [47].

Peripheral cells express the LDL receptor for their uptake whenever they need cholesterol. Peripheral cells require cholesterol for the build-up, growing or repair of cell membranes. Excessive LDL, if not precipitated, is returned to the liver, which also expresses LDL receptors, where it is dismounted.

Modified LDL, such as oxLDL, plays a role in pathological processes [82]. The exact mechanism of LDL oxidation is still unknown [83]. As described in chapter 1.1.1, LDL and oxidized LDL (oxLDL) play a role in fatty streak and nanoplaque formation in atherosclerotic vessels [6, 78].

1.3.7. HDL

HDL is divided into three subclasses. The class with the lowest density consists of particles with 8 to 13 nm in size, while the class containing particles of intermediate density consists of particles with 7 to 8 nm in size. Pre-ß-HDL is the class with the highest density having a size of less than 7nm [47, 60]. In reverse cholesterol transport, HDL takes up excess cholesterol from periphery cells. Lipid-free apolipoprotein AI (apoAI), one of the main components of HDL, is produced and incorporated in pre-ß-HDL in the liver and the small intestine. From there, pre-ß-HDL finds its way to macrophages in the vessel walls to take up cholesterol. Pre-ß-HDL also originates from VLDL during the release of apoAI and phospholipids [26, 59]. It acts as the precursor of other HDL particles [47]. The formation of HDL particles out of pre-

HDL is catalysed by lecithin-cholesterol-acyltransferase (LCAT), which esterifies cholesterol. On its way through the circulatory system, HDL thereby enriches more and more cholesterol but also phospholipids via the phospholipid-transport-protein (PLTP) until it is taken up by the liver [26, 78]. Since HDL carries apoAI and apoAII, it presumably is an important factor when it comes to protective attributes concerning atherosclerosis and cardiovascular diseases [59, 64].

1.4. PML

PML is also known as MYL, RNF71, PP8675 and as TRIM19 [84-86]. It belongs to the TRIM/RBCC protein family and functions as a ubiquitin ligase. PML is a tumour suppressor protein and is expressed in most cells of vertebrates, where it is located in PML-NBs [87, 88].

1.4.1. Genetic background, structure, and isoforms of PML

The primary structure of PML features two B-boxes, an auto terminal RING domain (C4HC3) and an α-helical Ring-B-boxes-coiled-coil domain (RBCC) for homodimerization which contains a RBCC/TRIM motif [89, 90]. The RING domain itself is composed of four cysteine and histidine residues coordinating the crosswise binding of two zinc ions. This domain interacts with a small ubiquitin modifier (SUMO)-E2-conjugating enzyme, the so-called UBC9. This interaction causes PML to directly bind a SUMO (small ubiquitin-related modifier) ligase [91]. When it comes to phosphorylation and SUMOylation, PML passes through phosphorylation and SUMOylation as examples for posttranslational modifications [92]. SUMOylation is important, since the composition of PML-NBs is critical for their function [93]. Seven isoforms of PML are generated by alternative splicing [89] designated *PMLI, PMLII, PMLIII, PMLIV, PMLV*, *PMLVI* or *PMLVII* (*Figure 4*). Some of them appear in *a*, *b* and *c* variants. While their N-terminal region is identical in all isoforms, the C-terminal region varies [89] being responsible for the different functions of PML isoforms [94]. The PML gene itself consists of 9 major exons. The exons 7 to 9 most likely undergo alternative splicing. Condamine et al. [95] showed that PML isoforms are simultaneously expressed in different concentrations in various cell lines although the isoforms *PMLIII, PMLIV* and *PMLV* are less frequently demonstrated than *PMLI* and *PMLII*.

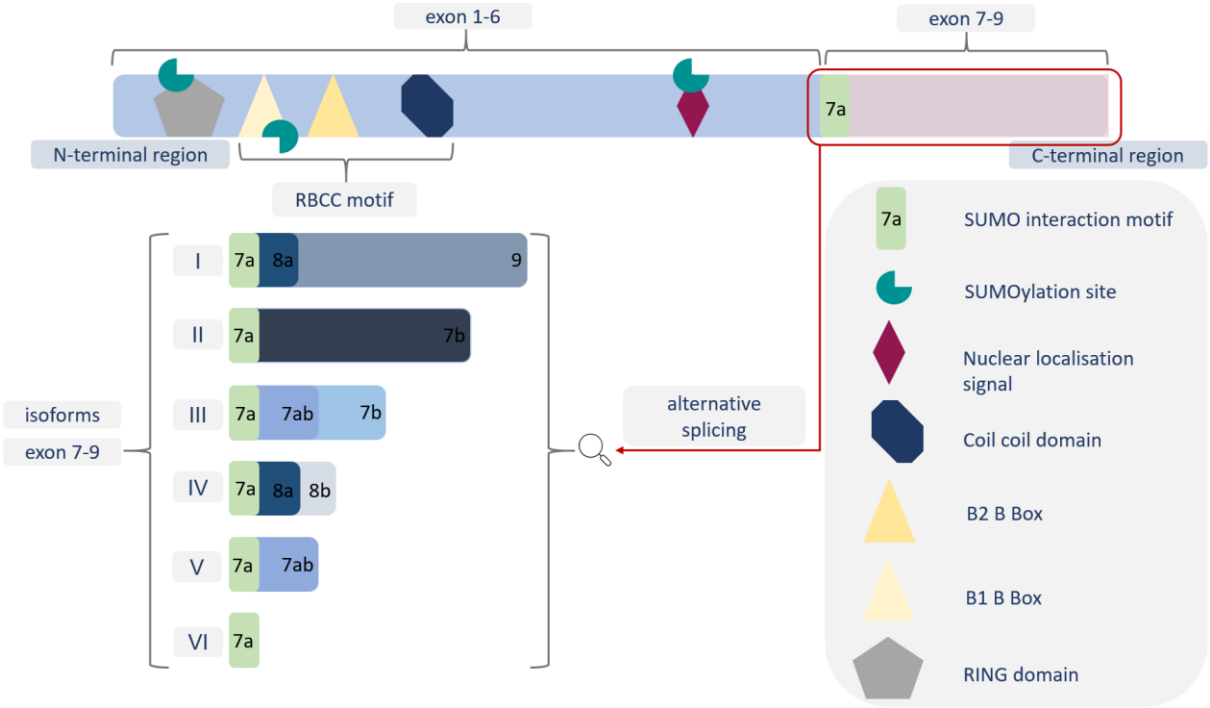

Figure 4. Schematic illustration of gene structure of PML isoforms, *which differ in the organisation of exons 7-9. Based on [88, 89, 94-96]. Created by the author.*

1.4.2. Functions of PML

The interferons α, β and γ, as well as p53 [97] induce PML gene transcription [98]. PML influences several physiological processes in the human organism. It plays a role in apoptosis and proteolysis as well as in renewal of stem cells, interferon response and senescence [99]. It also has an impact on gene regulation, tumour suppression, the elongation of telomeres, DNA repair, epigenetic regulation and antiviral responses [100, 101]. PML interacts with RelA/p65 to inhibit the transcription of nuclear factor "kappa-light-chain-enhancer" of activated B-cells (NFkB), which leads to an induction of apoptosis, while overexpression of NFkB prevents apoptosis induced by PML and TNF-α [102]. *PMLIV* is an isoform particularly necessary for apoptosis and senescence and, similarly to *PMLIII* and *PMLVI*, contributes to antiviral responses [95].

PML has pleiotropic functions in which the recruitment of several interaction partners within PML-NBs play a role [103]. Almost 50 % of PML interaction partners are SUMOylated, indicating that PML-NBs have a binding site for SUMOylated proteins [104]. In addition, PML organizes PML-NBs, which was proven by Ishov et al. [105] showing that constitutively expressed NB-associated proteins could not form PML-NB-alike structures when transfected in PML-negative cells. Interestingly, all PML isoforms in humans feature the possibility to form PML-NBs in PML-negative cells suggesting that they all are PML-NB organizers [88].

1.4.3. PML-NBs and their function

PML-NBs are present in almost every cellular nucleus [88]. They appear to be “doughnut-like in shape” (*Figure 5*) [106] and look like punctuate structures in immunofluorescence microscopy analysis [107]. PML starts oligomerization with its SUMO interaction motif (SIM) and the RBCC motif [93]. This process is mediated by the RBCC domain and leads to the formation of disulphide bonds. It comes to poly-SUMOylation reactions mediated by UBC9, followed by interactions of SUMO and SIM, which then both bind to their binding partners. The ultimate result of these processes is the self-organized formation of PML-NBs [93, 108-112]. About 10 to 30PML-NBs appear in one nucleus [113], but their actual number depends on the exposures and surroundings of the cells. Treatment with IFN for instance leads to larger numbers and bigger sizes of PML-NBs [107]. Different types of cell stress, such as damaged DNA, viral infection and moreover transformation and oxidative stress cause the PML-NB assemblage to disrupt and to release PML [114-116]. PML-NB formation is also affected by heat shock proteins and some heavy metals [117]. Even if there are strong indications to the organisation of PML-NB parts being necessary for physiological cell proliferation, the functions of PML-NBs have not yet been determined [107]. The PML-NBs influence DNA repair and the control of apoptosis [118]. They function as “hotspots” [104] for nuclear SUMOylation since both SUMO-specific proteases and SUMO E3-ligases of the protein inhibitor of activated signal transducer and activator of transcription (STAT) family exist within PML-NBs [119]. The degradation of PML protein itself and p53 are executed at a protein degradation site of the PML-NBs [111]. Accordingly, ring finger protein 4 (RNF4) targets PML to induce proteasome-mediated degradation by the addition of polyubiquitin chains to the SUMO moieties conjugated to PML (*Figure 6*) [120].

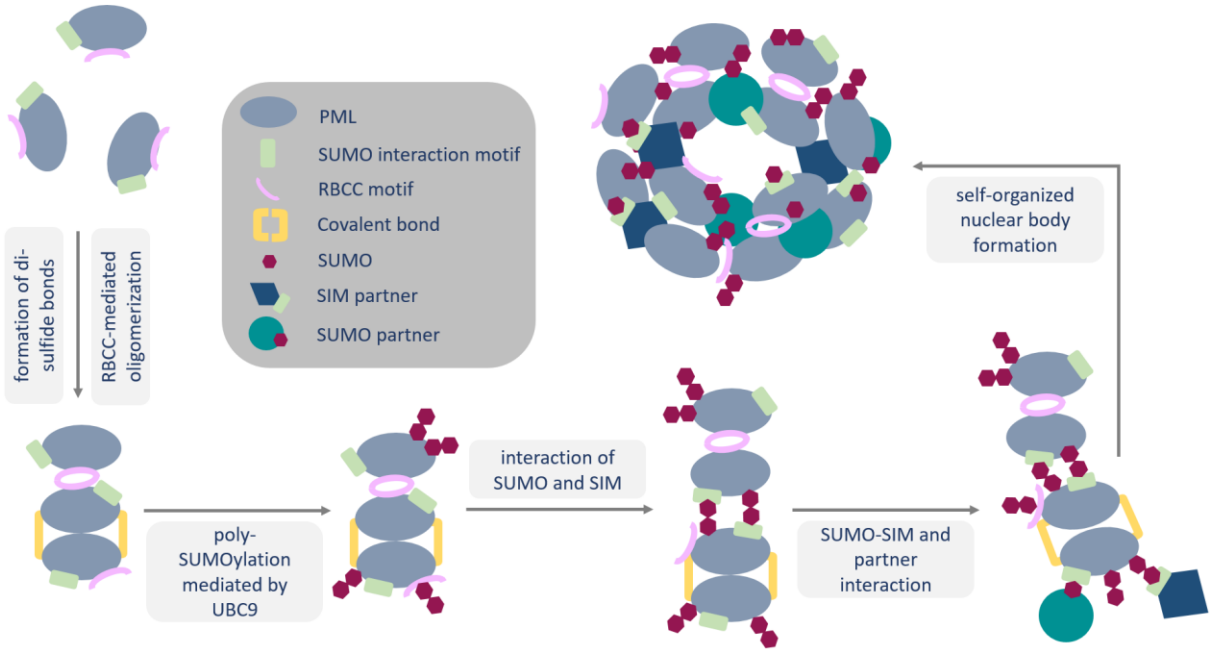

Figure 5. Schematic illustration of PML nuclear body formation. *PML with its SUMO interaction motif (SIM) and its RBCC motif oligomerizes mediated by RBCC and forms disulphide bonds. It comes to UBC9-mediated poly-SUMOylation and interactions of SUMO and SIM, which then interact with their binding partners. The following nuclear body formation is self-organized and leads to PML-NBs with a ring-like shape. Based on [93, 108-112]. Created by the author.*

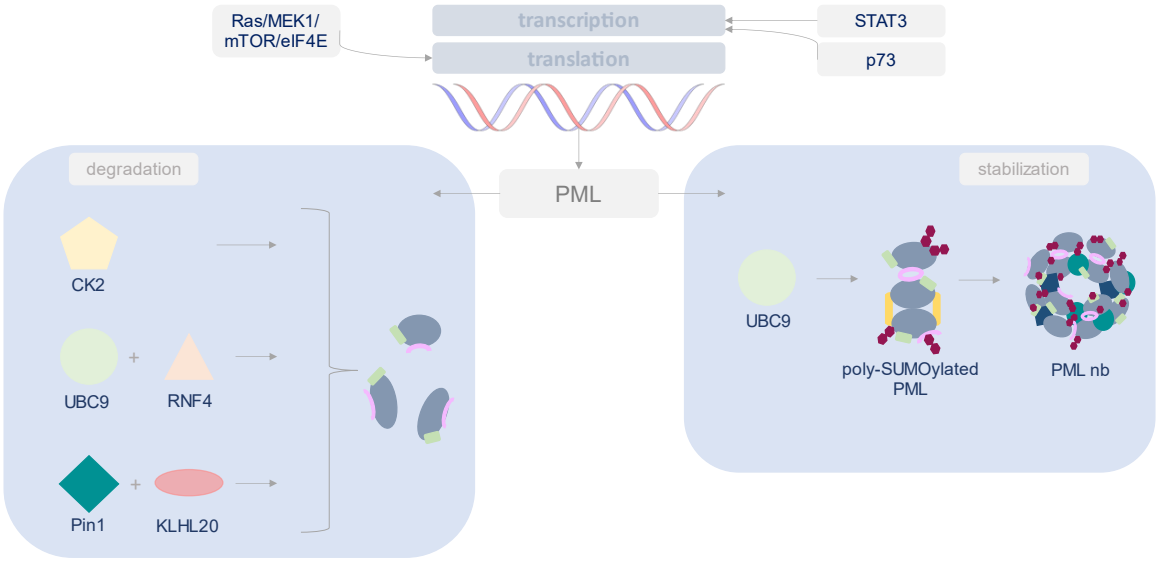

Figure 6. Degradation and stabilization of PML. *Stabilization occurs via SUMOylation, whereas casein kinase 2 (CK2), UBC9 and RNF4 as well as peptidyl-prolyl cis-trans isomerase NIMA-interacting 1(Pin1) and Kelch-like protein 20 (KLHL20) are responsible for the degradation of PML-NB. Based on [104, 111, 120-122]. Created by author.*

1.4.4. PML in atherosclerosis and AD

PML plays a role in atherosclerosis and AD. Just recently, Karle et al. found that high levels of PML appeared in arteries with atherosclerotic lesions [123]. However, PML is not involved in these pathologies alone, since SUMO1 and PML were both found in PML-NBs in vascular smooth muscle cells (VSMC) in atherosclerotic plaques [124]. SUMOylation of PML is responsible for more cell proliferation and de-differentiation in VSMC, whereas PML

overexpression does not exert the same effect [124], suggesting that the SUMOylation pathway is a potential target in the treatment of atherosclerosis.

PML is involved in the development of AD as well, since APP induces and triggers the interaction of p53 and PML [125]. Furthermore, PML-NB formation was activated dependent on APP and APP gene expression active in the PML-NBs [125].

1.5. The role of interleukin-6 and interleukin-8 in atherosclerosis and AD and their involvement with PML

1.5.1. The function and activation of IL-6

IL-6 is a multifunctional cytokine that is omnipresent in the human organism [126]. Several cell types produce it, e.g. monocytes and macrophages, fibroblasts, keratinocytes, endothelial cells and more. Whenever the organism experiences infection or inflammation, sepsis, lymphoma or an autoimmune disease and transplant rejection, IL-6 levels increase [127, 128]. IL-6 is active in immune response and hematopoietic processes [126].

The IL-6 receptor system is crucial for the function of IL-6 due to its impact on activating cell growth and differentiation [126, 127, 129]. The extracellular part of this receptor binds to IL-6, the other, gp130, acts as a signal transducer [129]. The binding of IL-6 causes homodimerization of the receptor complex [127], which activates JAK. The activated JAK then induces phosphorylation of gp130 at specific tyrosine residues, leading to the recruitment of other proteins, e.g. STAT (*Figure 11*) and Src homology region 2 domain-containing phosphatase-2 (SHP-2), initiating both the JAK/STAT pathway and the SHP-2/ERK MAPK pathway [127, 129].

1.5.2. The function and activation of IL-8

IL-8 is a proinflammatory cytokine that is secreted by several cell types. In contrast to IL-6 it is target specific for neutrophil granulocytes, thus acting as a chemoattractant in areas of inflammation [130, 131]. IL-8 is upregulated by cells sending off inflammatory signals. When IL-8 levels are increased in the circulatory system for a long time, tissue damage occurs [131]. After binding to its receptor the cytokine causes induction of MAP kinase expression and also triggers tyrosine phosphorylation of different cellular proteins leading to activation of STAT3 (*Figure 7*) [132, 133].

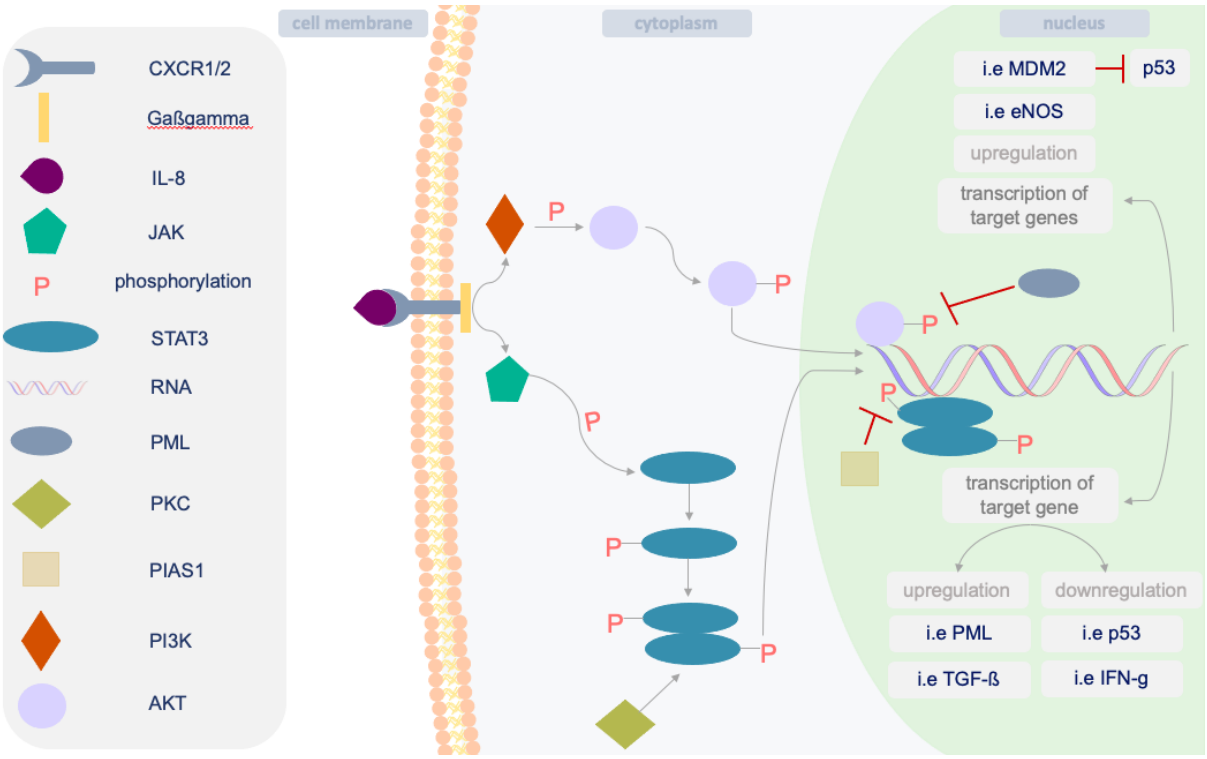

Figure 7. Schematic depiction of IL-8-induced cascades. *After binding to its receptor, the PI3K/AKT pathway, the JAK/STAT pathway and mitogen-activated protein kinase (MAPK) (not shown) are induced, leading to e.g. upregulation of MDM2 and eNOS via the PI3K/AKT pathway as well as to upregulation of e.g. PML and TGF-ß and downregulation of e.g. p53 and IFN-g via the JAK/STAT pathway. PML is capable of inhibiting AKT in the PI3K/AKT pathway, whereas PKC and PIAS1 inhibit STAT3 in the JAK/STAT pathway [131-133]. Created by the author.*

1.5.3. IL-6, IL-8 and their involvement with PML

One molecular mechanism to induce PML transcription is the activation of the JAK/STAT pathway, which links IL-6 and PML levels (*Figure 11*) [134]. PML and its PML-NBs are upregulated by increased IL-6 levels or phosphorylated - and thereby activated- STAT3 levels increase [135]. In multiple myeloma cells with PML knockout, IL-6 levels are lowered as well, underlining the link between the two proteins [136].

In prostate cancer patients IL-8 was proven to trigger the STAT3/AKT/NFkB pathway [137] which may indicate an indirect link between PML and STAT3 (chapter 1.7.3). In contrast, IL-8 is a target of STAT3 in glioblastoma cells. STAT3 antagonizes IL-8 transcription by blocking the IL-8 promoter, causing the repression of cell proliferation of glioblastoma cells [138].

1.5.4. IL-6 and IL-8 in atherosclerosis and AD

IL-6 plays a role in the development of atherosclerosis [139], where it is mostly found in fatty streaks. Seino et al. discovered IL-6 gene transcripts within these lesions [140]. When IL-6 was

induced in mice, the lesions turned out to grow up to 5.1-fold bigger than without IL-6 input [139].

IL-8 plays a role in atherosclerosis as well [141]. It was shown that oxidized phospholipids upregulated IL-8 levels [142]. In macrophages isolated from atherosclerotic plaques, IL-8 levels were enhanced 123-fold compared to the levels of monocyte-derived macrophages. IL-8 levels were also 7-times higher than in macrophages which were isolated from the circulatory system [143]. Additionally, Liu et al. showed that IL-8 levels in atherosclerotic tissue correlate with the progression of the disease [143].

IL-6 and IL-8 gene transcripts are present in the arterial atherosclerotic wall [144]. As the complement system is activated in these arterial atherosclerotic walls, the expression of IL-6 and IL-8 provides evidence towards their involvement in inflammation and atherosclerotic development [144].

In AD, the relevance of IL-6 was shown when it correlated with neuronal degeneration, as hyperphosphorylated tau protein appeared in neurons after IL-6 treatment [145]. In patients with AD, increased levels of IL-6 are possibly involved in the reduction of cognitive functions [146]. Additionally, IL-6 caused an increase in APP levels [147] and faster degradation of cultured astrocytes than cells producing lower levels of IL-6 [147].

Alsadany et al. performed a study with 25 patients diagnosed with AD and 25 age-matched control participants. They showed that patients diagnosed with AD produced significantly higher concentrations of IL-8 than the control participants related to the results of cognitive tests [148]. Regarding the increase of proinflammatory processes in AD, *in vitro* tests showed that IL-8 is of relevance [149] and amyloid β1-42 (Aβ1-42) appeared to even dose-dependently enhance the cytokine levels [150].

1.6. Protein kinase C and its role in atherosclerosis and AD in the human organism

Protein kinase C (PKC) is a calcium-phospholipid-activated threonine/serine kinase bearing important regulatory functions in signal transduction [151, 152].

1.6.1. Structure, isoforms and activation of PKC

PKC is a single polypeptide with an N-terminal and a C-terminal catalytic domain which has 4 conserved functional regions (C) as well as 5 variable modulatory regions (V). The N-terminal half consists of V1, C1, V2, C2 and V3 regions and is labeled as the regulatory domain, whereas the C-terminal half consists of C3, V4, C4 and V5 domains and thus forms the catalytic domain [152]. The C1 region of PKC contains two zinc finger-like regions, rich in cysteine, required for activation via diacylglycerol (DAG) or phorbol esters. It is divided into the regions C1A and C1B. C2 is capable of binding Ca^{2+}. The C3 region has a binding motif for ATP, whereas the C4 region is the region that interacts with the PKC substrates. The enzyme also has a pseudosubstrate binding site located at the N-terminus, right after the V1 region [152, 153]. Regardless of the initial activation factor, PKC activation is dependent on either Ca^{2+} or phosphatidylserine and DAG in a PKC isoform-specific way [154]. More than ten isoforms of PKC divided into three subclasses of PKC isoforms based on their differences in activation substrates and structures [155] exist (*Figure 8*):

1. Conventional PKCs (cPKC): *PKCα, PKCβI, PKCβII, PKCγ*
2. Novel PKCs (nPKC): *PKCδ, PKCε, PKCη, PKCθ*
3. Atypical PKCs (aPKC): *PKCζ, PKCι/λ*

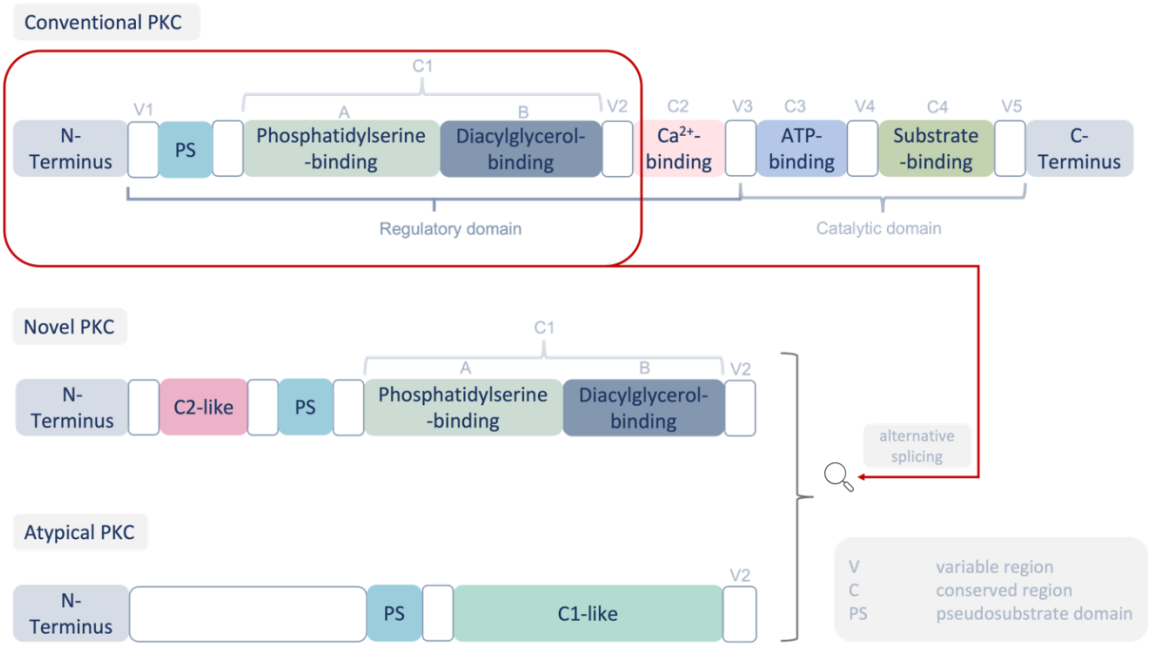

Figure 8. Schematic depiction of the different subclasses of PKCs. *The different subclasses of PKC differ in the regulatory domain. Based on [153-156]. Created by the author.*

'Conventional PKCs' (cPKC) are activated by phosphatidylserine and DAG and function Ca^{2+}-dependently. Included isoforms are PKC α, βI, βII and γ.'Novel PKCs' (nPKC) act Ca^{2+}-independently but are still regulated by DAG and phosphatidylserine and include the isoforms δ, ε, η and θ. Finally, 'atypical PKCs' (aPKC) are neither, Ca^{2+}-dependent, nor need DAG to be activated (phosphatidylserine is still necessary for their regulation). PKC isoforms of this group are PKC ζ and ι/λ [154, 157] (*Figure 9*).

Before activation, the pseudosubstrate domain blocks the actual substrate binding. When the pseudosubstrate domain disconnects from the substrate domain, it is sterically accessible for actual substrates. Once the substrate did bind to its domain, PKC phosphorylates the substrate by transferring a phosphate residue from ATP [151, 153-156, 158, 159] leading to its translocation from the cytosol to the membrane.

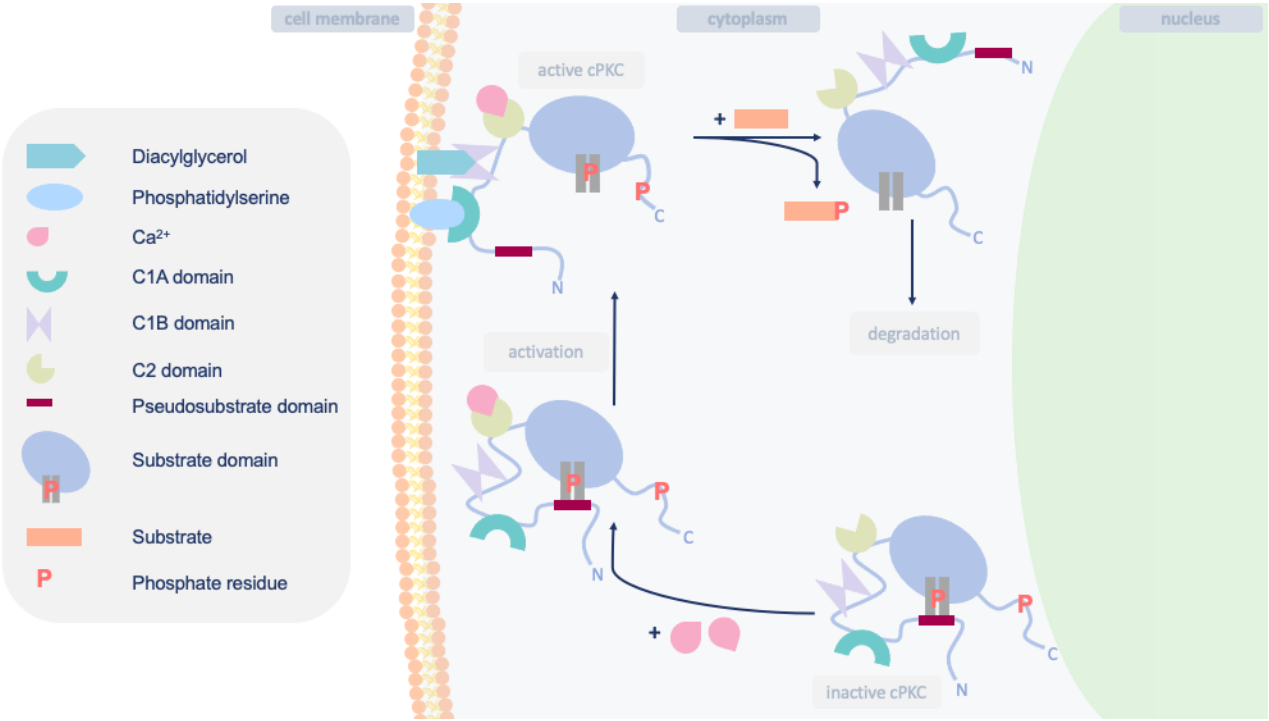

Figure 9. Schematic depiction of the activation of a cPKC. *The cPKC is kept inactive by its own pseudosubstrate domain. Activation requires binding of Ca^{2+} to the C2 domain and binding of phosphatidylserine to the C1A and DAG to the C1B domain. The cPKC substrate domain is now free for any PKC substrate, to which the cPKC provides a phosphate residue. After provision of the phosphate residue, the cPKC is degraded. Based on [151, 153-156, 158]. Created by the author.*

1.6.2. Roles and functions of PKC

Active PKC takes part in cellular signal transduction, in cell growth and proliferation. Through activation, PKC triggers several processes in the organism, such as lipid and glucose metabolism, gene expression and contraction of smooth muscle cells [152, 160-162]. Although PKC is omnipresent in the human organism, some PKC isoforms are more excessively expressed in some cells [154, 158]. PKCs have different functions. For instance, PKCε possibly plays a role in the cardiovascular protection of patients with ischaemic preconditions, whereas overexpression of PKCα contributes to tumor proliferation. Overexpression of PKCβII is involved in heart failure, cardiovascular complications and cardiomyopathy [154, 163, 164].

1.6.3. Molecular interactions between PKC and LDL

Treatment of HUVECs or human coronary artery endothelial cells (HCAECs) with either LDL or oxLDL triggered PKCβ translocation [165] to increase PAI-1 expression. These effects were observed in a dose-dependent manner and the effect of oxLDL was stronger than the effect of native LDL [165]. Treatment of macrophage-like cells with oxLDL and acetylated LDL led to higher PKC activity, while oxLDL effects on PKC activation were inhibited [166]. A similar effect was observed in HCAECs after oxLDL treatment, where it caused the cells to undergo

apoptosis [157]. oxLDL also had an impact on coronary vasoconstriction via activating PKCα and PKCε [167].

1.6.4. PKC in atherosclerosis and AD

Several molecular and functional links between atherosclerosis and PKC were observed [168]. PKCα is involved in the process of hepatic LDL degradation and in oxidation of LDL by monocytes in the endothelium, which is also catalyzed by PKCζ [169-174]. The PKC isoforms α, β and ε attract monocytes [175, 176]. PKCβ and PKCδ are involved in macrophages taking up oxLDL and forming foam cells [177], while PKCα, PKCβ, PKCε and the PKC isoforms δ and ζ are most likely engaged in plaque formation [168].

Alkon et al. [156] suggest that PKC plays a role in AD-related memory loss, since PKC pathways are important in neurodegeneration. PKC was found in the brain and fibroblasts of Alzheimer's patients [156, 178-180].

1.7. The role of STAT3 in atherosclerosis and AD of humans

STAT3 belongs to the STAT protein family of transcription factors and is a protein of 89 kDa with six different functional domains [181-183]. They all express an Src Homology 2 domain (SH2 domain), a DNA-binding domain and a tyrosine kinase domain [183].

1.7.1. Activation of STAT3

STAT3 is activated by the JAK/STAT signalling pathway. In this pathway (*Figure 10* and *Figure 11*), Janus kinases (JAKs) activate different STATs. JAK1, JAK2 and Tyk2 (tyrosine kinase 2) have a kinase-like domain and a bona fide kinase domain in their C-terminal facilitating them to phosphorylate and thus activate STATs [184, 185]. STAT3 is phosphorylated at the tyrosine residue in the SH2 domain [186], which leads to dimerization and relocation to the nucleus, where the activated STAT3 binds to its promoter sites to induce changes in the transcription rates of target genes [187-192].

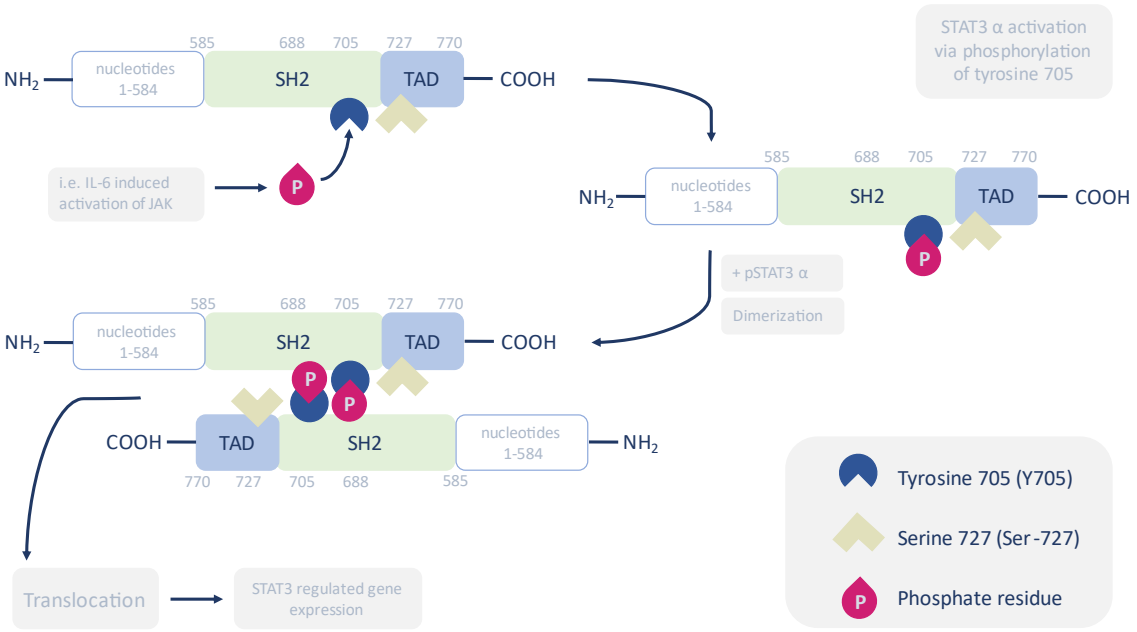

Figure 10. Schematic depiction of the activation of STAT3 via phosphorylation on tyrosine 705. *After phosphorylation on tyrosine 705, phosphorylated STAT3 (pSTAT3) dimerizes with another pSTAT3 molecule, before it is translocated into the nucleus, where it regulated gene expression. Based on [189-192]. Created by the author.*

STAT3 is also activated via phosphorylation on Ser-727, caused by PKC δ. This PKC/STAT3 pathway is stimulated by IL-6 and acts in various cell types *in vivo* as well as *in vitro* by a downregulation of STAT3 DNA binding and transcriptional activity [193-195]. When activated, STAT3 binds the p53 promoter *in vitro* and *in* vivo to inhibit p53 expression associated by uncontrollable cell growth of tumour cells and thereby cancerogenesis [196].

STAT3 undergoes several post-translational modifications, e.g. acetylation and phosphorylation, but also methylation and ubiquitination, which have an impact on its functionality [197]. In human aortic endothelial cells (HAECs), STAT3 is activated via the IL-6 receptor through phosphorylation. Saura et al. showed that STAT3 binds to a specific complex in the eNOS promoter causing downregulation of eNOS expression. PKC δ activity leads to Ser-727 phosphorylation of STAT3, which triggers binding to the eNOS promoter site [198, 199].

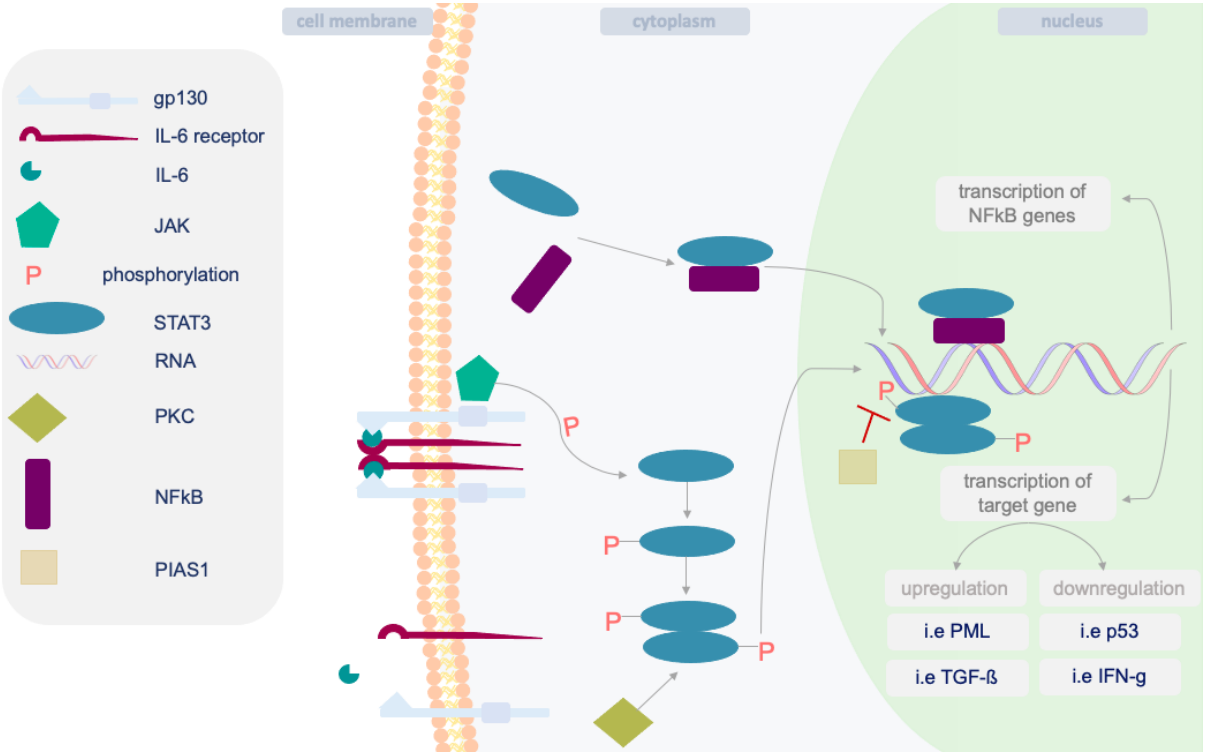

Figure 11. Schematic depiction of the activation of STAT3 via the JAK/STAT pathway and the PKC/STAT pathway activated by IL6 and the interaction of STAT3 and NFkB. *After IL-6 binds its receptor, the gp130 subunit is responsible for the activation of JAK, which causes STAT3 to dimerise and to be transphosphoylated and thereby activated. The activated STAT3 relocates to the nucleus where it functions as a transcription factor for the upregulation of e.g., PML and TGF-ß (transforming growth factor beta) and the downregulation of e.g., p53 and IFN-g. The activated STAT3 can either be inhibited by PKC in the cytoplasm or by PIAS1 in the nucleus. The interaction of NFkB and STAT3 leads to the transcription of NFkB genes. Based on [185-188, 193, 197-203]. Created by the author.*

1.7.2. The functions of STAT3

The most common and functional isoform of STAT3 is STAT3α, commonly referred to as STAT3. STAT3ß is a less active variant [181]. STAT3 mainly functions as a transcription factor [201]. It participates in several cell processes, such as cell growth and apoptosis, it regulates inflammation and is omnipresent in the human organism [204, 205]. For instance, STAT3 was shown to play a role as an acute phase response factor (APRF) and as an "inducible DNA binding protein" [183]. In this role, STAT3 binds to the IL-6-responsive element located in the hepatic acute-phase protein promoter [206]. STAT3 also participates in the repression of TGF-

ß-induced apoptosis [207] and exerts anti-inflammatory functions, such as the repression of insulin-like growth factor-binding protein 5 (IGFBP-5), which is responsible for the induction of apoptosis [208].

1.7.3. The interaction between STAT3 and PML

According to PML, STAT proteins 1, 2 and 3 all have an impact on angiogenesis. Especially STAT1 and STAT3 regulate the activity of several genes, which are also controlled by PML [209]. This activity profile underlines the relevance of PML in STAT1 and STAT3 activation. STAT3 and PML interact in a negative feedback loop, in which STAT3 activates PML and PML suppresses STAT3 phosphorylation and consequentially the repression of IL-6- mediated gene expression [203, 209, 210], especially when it comes to the inhibition of angiogenesis [209]. IL-6 is relevant in the interplay between PML and STAT3 in hepatoma cells, since it is responsible for PML deSUMOylation [210]. This process is induced by IL-6 activating SENP1, which is a SUMO-specific peptidase, whose wild-type is in charge of keeping the negative feedback loop of STAT3 and PML running by facilitating the repression of STAT3 via PML [210].

1.7.4. STAT3 in atherosclerosis and AD

Nuclear and mitochondrial STAT3 enhances endothelial dysfunction- and inflammation to accelerate atherosclerosis [211]. The endothelial dysfunction was induced by the phosphorylation of STAT3 *in vitro*, while endothelial dysfunction *in vivo* is a high risk factor for atherosclerosis, promoting the disease through lipid accumulation and inflammation [211]. After IL-6-exposure, STAT3 is a crucial factor for inhibiting the cell growth of neural stem cells by methylating or demethylating DNA. This process is less severe when the JAK2/STAT3 pathway is blocked [212]. However, blockage of the whole JAK2/STAT3 axis by amyloid β in hippocampal neurons leads to a dysfunction in the cholinergic system pre- and postsynaptically [213], a process causing deterioration of memory in AD patients [213].

1.8. The interaction of PML and p53 in the human organism

1.8.1. The function of p53 in the human organism

The tumour suppressor gene p53 is in some sort of "transcriptional control" [214] and is not only relevant in cancerogenesis, but also in inflammation, e.g. in atherosclerosis and AD. The p53 protein is involved in the response after DNA damage or hypoxia [215, 216]. It binds to DNA promoter sequences as a tetramer and causes induction or repression of the expression of different genes [217], in particular of those causing cell cycle arrest or DNA repair [218]. Because p53 reduces gene expression of e.g. microtubule-associated protein 4 (MAP4) [219] which encodes for a protein involved in microtubule stabilization, p53 activation causes apoptosis. In a fully functional organism, its apoptotic and inhibitory influences on cell growth are strictly controlled within the cells [220]. In atherosclerosis p53 is activated in plaques, whereas its absence causes progression of the disease [221, 222]. In AD monomer and dimer levels of p53 are increased [223], which is relevant in neuronal cell death and the influence of oxidative stress [224].

1.8.2. Activation and repression of p53

When activated, p53 protein levels rise rapidly through its protein stabilization and DNA binding [215]. Activation of p53 occurs via several modifications. For example, phosphorylation at sites within the C- and N-termini by protein kinases caused p53 activation. Ashcroft et al. showed that phosphorylation was important for p53 stabilization, but not essential for its biological functions [215]. p53 is also activated by acetylation, which involves several proteins [225].

Mouse double minute 2 homolog (MDM2) is the most important antagonist in p53 repression. It downregulates p53 expression through direct binding making it to a target for the so-called 'ubiquitin-dependent proteolytic pathway' [226, 227] (*Figure 12*). This impact of MDM2 on p53 activity is relevant for retaining lower p53 levels in cells [228]. Additionally, ubiquitination is of relevance for p53 degradation [225].

1.8.3. PML and p53

PML and p53 are linked in their stability and destabilization. Both *in vitro* and *in vivo*, p53 is present in PML-NB. p53 acts in a PML-dependent apoptosis pathway induced by DNA damage

[229]. PML gathers p53 protein in its PML-NBs to increase p53 levels. PML recruits p53, but also is a target of p53 accelerating cell growth. PML contains p53 binding sites to modulate oncogenesis and DNA damaging through chemotherapeutics. These findings are underlined by the fact that PML knockdown cells underwent apoptosis after activation with p53 [97].

„PML/p53-induced cellular senescence" [230] is antagonized by Sirtuin 1 (Sirt1), an enzyme responsible for deacetylation of various proteins in humans. Sirt1 is integrated in PML-NBs in PML overexpression in human cells and deacetylates p53 to and inhibit its activation. Sirt1 also inhibits cellular senescence by acting as an antagonist for PML-induced p53 acetylation in mice [230].

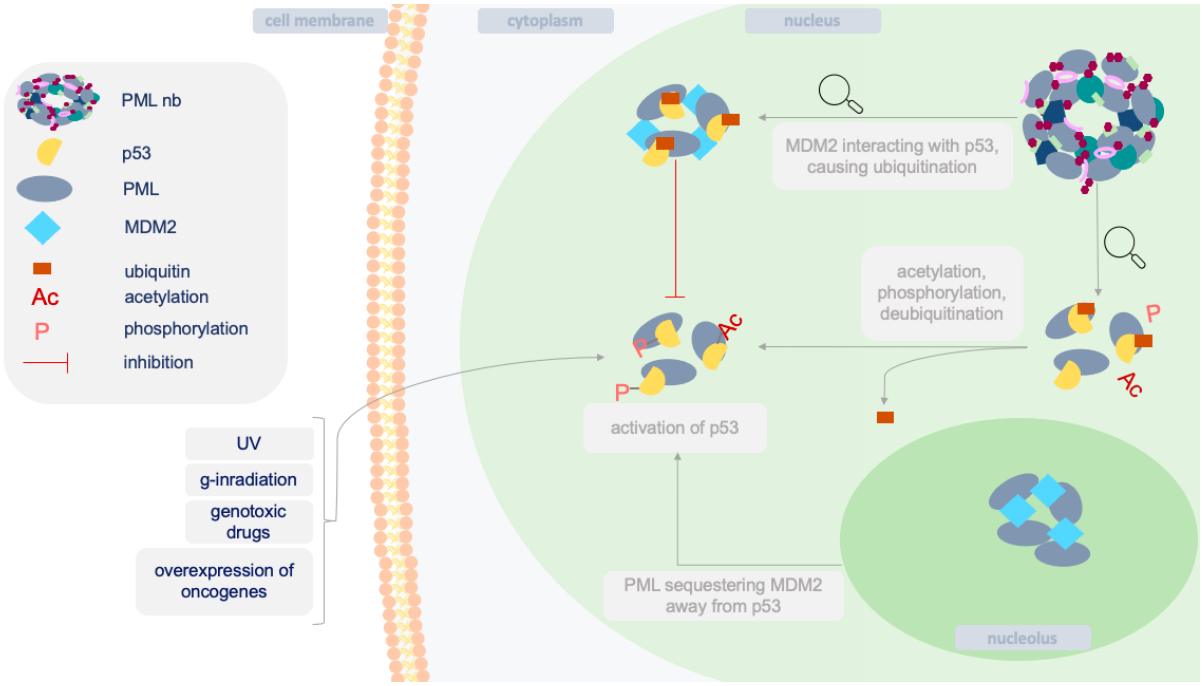

Figure 12. Schematic depiction of p53 activation and repression. *Cellular stress such as UV radiation, γ irradiation, chemotherapeutics or the overexpression of oncogenes leads to p53 activation. p53 is shifted into the nucleus to PML-NBs, where it gets phosphorylated or acetylated for activation. Deubiquitination also leads to p53 activation. MDM2 can inhibit p53 activation but can be hindered in interacting with p53 by PML. P53 activation leads to cell cycle arrest and apoptosis. Not shown: Sirt1 antagonization of p53 or PML. Based on the references [215, 225, 229, 230]. Created by the author.*

1.9. Physiology and pathophysiology of endothelial nitric oxide synthase (eNOS)

The homodimer eNOS is preferentially expressed in endothelial cells, where it catalyses the formation of nitric oxide (NO) and L-citrulline from L-arginine [231, 232]. Since NO is relevant for blood pressure regulation, eNOS is particularly crucial for this process [233]. Both eNOS subunits undergo myristoylation as well as palmitoylation [234].

1.9.1. Structure and function of eNOS

eNOS is a multi-domain enzyme. Heme, L-arginine and tetrahydrobiopterin (BH_4) are bound to specific binding sites at its N-terminal oxygenase domain, whereas its C-terminal reductase domain has binding sites for flavin mononucleotide (FMN), flavin adenine dinucleotide (FAD), nicotinamide adenine dinucleotide phosphate (NADPH) and calmodulin (CaM) [231, 235].
Interaction of eNOS with other proteins and membrane phospholipids, but also serine phosphorylation by specific kinases contribute to the regulation of eNOS activity [234]. Co-, and post-translational lipid modifications as well as protein-protein interactions play a role in the regulation of eNOS activity [236, 237]. The enzymatic activity of eNOS is furthermore reduced through binding to caveolae [231], small microdomains in the plasma membrane, which are rich in caveolin-1 protein [238, 239]. Its activation can be traced even further, since vascular endothelial growth factor (VEGF), sphingosine 1-phosphate, bradykinin and also oestrogen bind to their receptors which leads to activation of the PI3K/Akt pathway upstream of eNOS [231].
For the oxidation of L-arginine to the intermediate OH-L-arginine which, after second oxidation leads to the formation of nitric oxide and L-citrulline, eNOS uses molecular oxygen and also electrons from NADPH (*Figure 13*) [231, 232]. eNOS activity is pH-dependent, as alterations from 6.7 to 7.4 change eNOS activity [234]. eNOS function is relevant for the formation of NO, an endogenous gas causing vasodilation. It is in charge of regulating the blood vessel diameter continually but is also anti-proliferative and anti-apoptotic environment for the cells of the vessel wall [231].

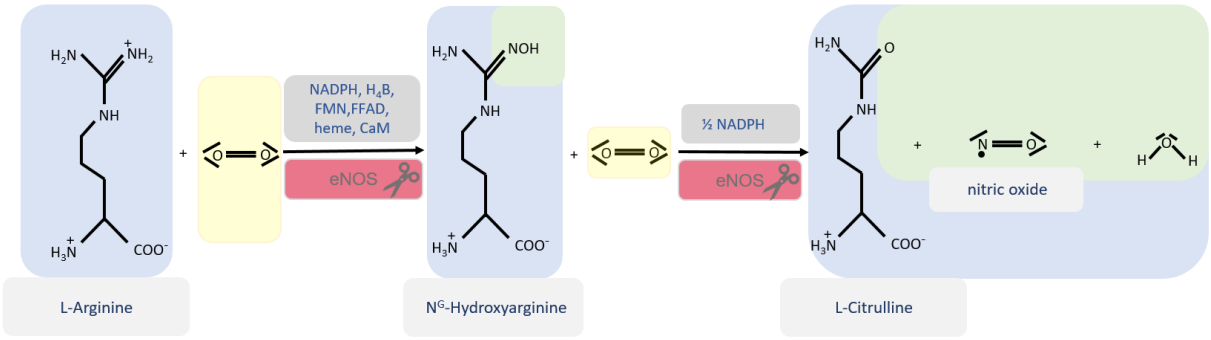

Figure 13. eNOS-mediated oxidation of L-arginine into the intermediate OH-L-arginine and following its oxidation to L-citrulline and nitric oxide. *Based on [231, 232]. Created by the author.*

When eNOS causes oxidation of L-arginine to form NO in endothelial cells, NO diffuses in a paracrine manner to adjacent cells e.g. smooth muscle cells, where it leads to the formation of the second messenger cGMP out of GTP leading to vascular smooth muscle relaxation resulting in vascular dilatation (*Figure 14*) [240].

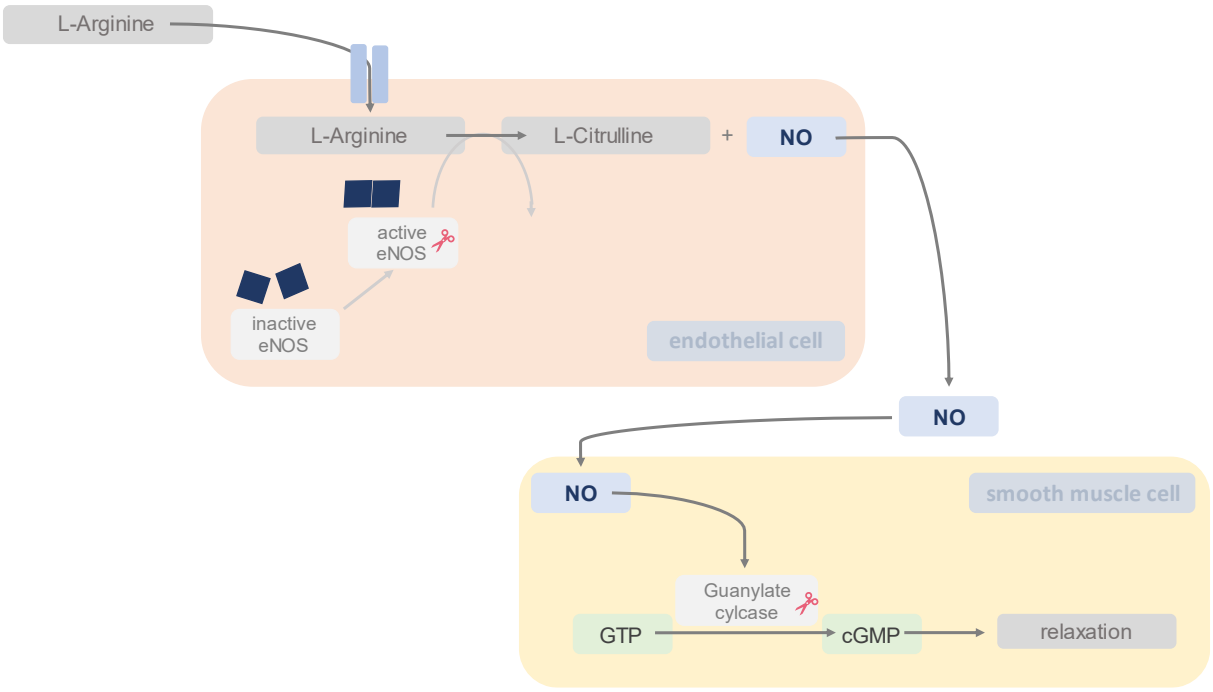

Figure 14. Schematic illustration of the eNOS pathway, the formation of nitric oxide and its impact on smooth muscle cells. *When L-arginine enters the endothelial cell, activated eNOS catalyses its oxidation to L-citrulline and nitric oxide. Nitric oxide is set free and diffuses into surrounding smooth muscle cell, where it activates the guanylate cyclase, an enzyme catalysing the transformation of GTP into cGMP and thereby leading to vessel relaxation via protein kinase G (PKG). Based on [240]. Created by the author.*

The endothelium produces NO, which regulates various vascular functions [231]. NO-release occurs in response to increases in shear stress and changes in the intracellular Ca^{2+}-concentration caused by agonists [241]. While active eNOS maintains various functions of the vascular system, dysfunctional eNOS causes damage to the organism due to the formation of

reactive oxygen species (ROS). As a consequence, NO synthesis and oxygen reduction are uncoupled, procuring eNOS to act proatherosclerotic by producing superoxide, which gives it a role as a so-called “Janus-faced” enzyme [242]. Sirtuin 1 (Sirt1), an enzyme responsible for e.g. preventing cell death via deacetylation or complexation, is activated by eNOS-derived NO and antagonizes PML [243]. Sirt1 also deacetylates p53 leading to the inhibition of senescence induced by p53 and PML [230].

1.9.2. eNOS in atherosclerosis and AD

eNOS is involved in endothelial dysfunction (chapter 1.10.3) and thus plays a direct role in atherosclerosis [241, 244]. In addition, an interaction of eNOS with lipoproteins is of relevance in hypercholesterolemia metabolism as a major risk factor for atherosclerosis. Andrews et al. showed that high cholesterol levels blunt eNOS phosphorylation and reduce calcium response by capacitive calcium entry (CCE) inhibition [241]. Additionally, cholesterol enrichment inhibits eNOS phosphorylation and shear stress-induced production of NO. With the study “Impact of Lifestyle Intervention on HDL-Induced eNOS Activation and Cholesterol Efflux Capacity in Obese Adolescent” [245], Wesnigk et al. demonstrated that HDL had a great impact on eNOS modulation and was protective against the development of atherosclerotic processes [245].

Experiments in mice showed that eNOS deficiency enhanced levels of APP and amyloid β. These findings suggest that the lack of eNOS directly promotes AD development [246].

1.10. The influence of lipoproteins on human endothelial cells

1.10.1. Endothelial cells

The human endothelium is omnipresent in the human body, lining the vascular and the lymphatic system [247]. Endothelial cells are widely engaged in pathophysiological states of various diseases, as they are involved in or cause pathological modifications or suffering from damage by diseases. Physiologically, endothelial cells are in charge of the vasomotor tone and function in haemostatic balance, leukocyte adhesion and transmigration, angiogenesis, apoptosis and antigen presentation and have barrier functions [247]. In healthy tissue, endothelial cells maintain blood fluidity, regulate the blood flow, control vessel wall permeability and exclude circulating leukocytes [248]. The resulting phenotype in cellular senescence is proinflammatory, proatherosclerotic and prothrombotic [249, 250]. Since the vascular endothelium is relevant for the initiation and regulation of haemostasis, it is also involved in bacterial infection. Additionally, it plays a role in non-bacterial infections, which links it to atherosclerosis, where inflammatory processes were determined in the disease itself and in its development [250, 251].

1.10.2. Endothelial activation

Endothelial cell activation is involved in inflammatory processes amongst pathological events [252, 253]. This occurrence is distinguished by its expression of cell-surface adhesion molecules, for instance VCAM-1 and ICAM-1 [254] and therefore is used to characterize a phenotypic response of endothelial cells to an inflammatory stimulus under specific conditions [247]. IL-6, IL-1, INF- γ and TNF-α induce endothelial cell activation, which links them directly to inflammatory processes [255]. Through the initiation of endothelial activation, circulating leukocytes are recruited and attached to the vessel wall [254]. Endothelial cell activation triggers the rapid recruitment of neutrophil granulocytes in acute inflammation [248]. In this state, endothelial cells also participate in inducing cardinal inflammatory signs, such as rubor and dolour, stemming from an increased local blood flow and leakage of plasma-protein-rich exudate into the tissue [248].

1.10.3. Endothelial dysfunction

Endothelial dysfunction is a process that occurs locally in atherosclerosis and systematically occurring during sepsis [247]. The term is used synonymously with “functional deficiency of eNOS and secondary abnormalities in endothelial-mediated vasorelaxation of atherosclerotic arteries” [256]. The functional phenotype includes many varieties and thus affects the regulation of haemostasis, thrombosis, local vascular tone and redox balance. It has an impact on the orchestration of both chronic and acute inflammatory events within the arterial wall [256]. The main attribute of endothelial dysfunction is the reduced production and thus availability of NO. In early-stage atherosclerosis, endothelial dysfunction might be a “hallmark” of the disease [241, 244]. Besides the decrease of eNOS activity, an increase of cholesterol accumulation in the vessel wall due to the reduction of reverse cholesterol transport [245] is relevant in endothelial dysfunction, which is strongly connected to cholesterol levels [257].

1.11. Human coronary arteries and their role in atherosclerosis

1.11.1. Anatomy and physiology of human coronary arteries

As shown in Figure 15, the human heart has a left (*Arteria coronaria sinistra)* and a right coronary artery (*Arteria coronaria dextra*) which provide it with oxygen-rich blood. The *Arteria coronaria dextra* becomes the *Ramus interventricularis posterior*, which runs to the back side of the heart to supply the right ventricle and a major part of the posterior left ventricle with oxygen. The *Arteria coronaria sinistra* divides into the *Ramus interventricularis*, which continues to the front of the heart, and into the *Ramus circumflexus*, which runs between the atrium sinister and the ventricle sinister to the back side of the heart. The *Arteria coronaria sinistra* provides oxygen to the septum and to the left and parts of the right ventricle. The coronary arteries collect extraordinarily oxygenated blood during ventricular diastole. Their function is essential for a well-functioning heart and thus for the maintenance of the entire organism [26, 258-261].

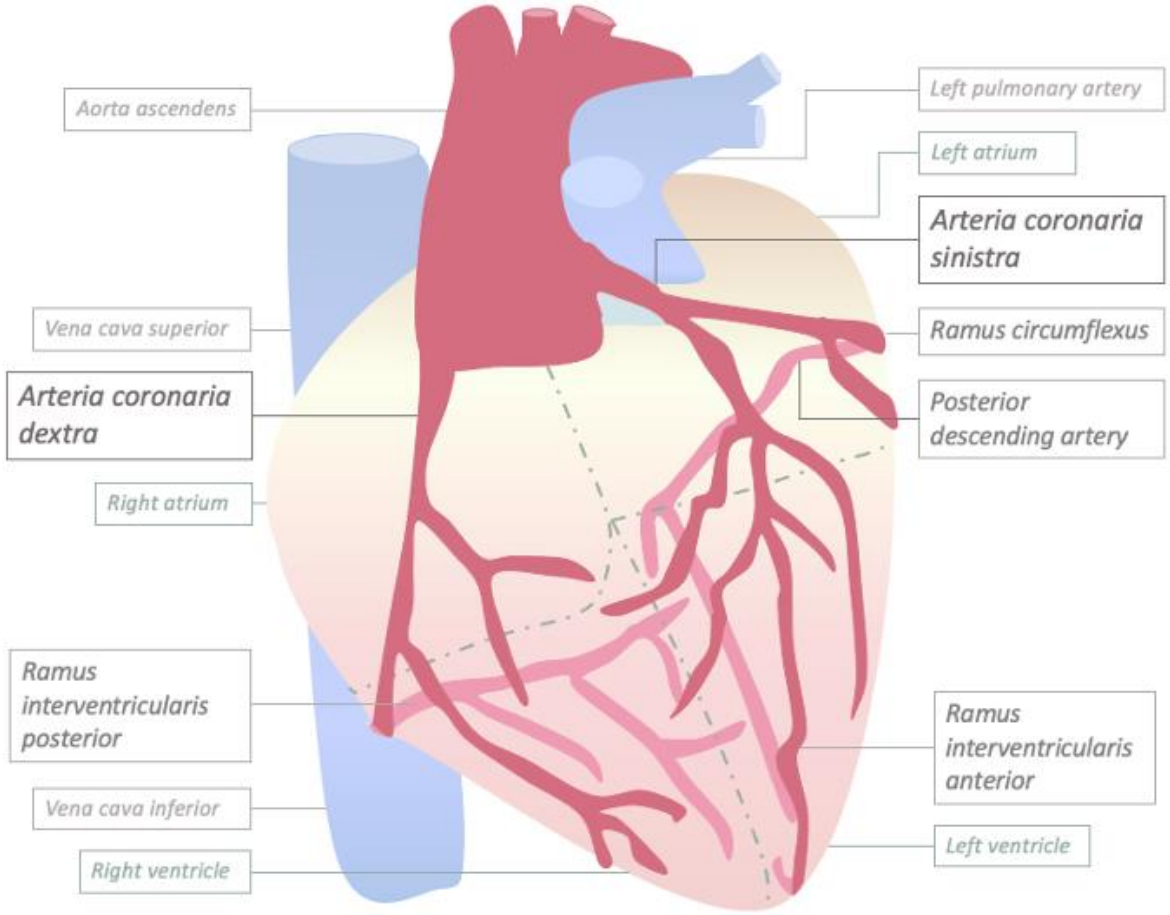

Figure 15. Schematic depiction of the coronary arteries in a human heart shown in a frontal view. *Coronary arteries on the front of the heart are displayed in dark pink, while the coronary arteries on the back of the heart are displayed in lighter pink. The dashed lines displayed in green give an idea of the atria and ventricles. Arteries and veins of the pulmonary circulation are displayed in blue. Based on [6, 26, 258-260, 262]. Created by the author.*

1.11.2. Pathophysiology of coronary arteries and their involvement in atherosclerosis

Coronary (heart) artery disease (CAD) affects the coronary arteries and occurs frequently. It is a disorder that usually develops due to atherosclerotic changes in the vascular system. Corresponding to the information provided in chapter 1.1.1, atherosclerotic lesions form in the lumen of the coronary arteries long time before any symptoms are noticed [26, 263, 264]. This leads to a loss in artery elasticity, reduces their ability to dilate and causes their vessel lumen to narrow [6, 26, 263]. Aside from the permanently ongoing inflammation in the affected areas it thereby comes to a functional constriction of the arteries and a reduction in blood flow, consequentially leading to a lack of oxygen delivery in the heart. This causes painful symptoms and reaches critical endpoints such as sudden cardiac death or acute coronary syndrome, including myocardial infarction [26, 263-265]. Coronary thrombi detach from the arteries under the permanently given blood flow. If a thrombus does not dissolve, it can grow or is built into the artery wall or the lumen, in both cases causing the vessel to narrow and in the end - as the

thrombus invades the smaller branches of the coronary arteries – also cause fatal cardiac events. However, there can be noticeable symptoms for the patient before it comes to severe or fatal cardiac events, such as acute angina pectoris. Symptomatic occlusion of the coronary arteries happens often, as plaque rupture and at least a beginning of coronary occlusion can be observed in most of the fatal thrombotic coronary events [6, 26, 263-265].

1.11.3. Flow dependent regulation of coronary arteries and how it is influenced by lipoproteins

The ability of coronary arteries to adjust their vessel lumen via dilation or constriction is important for their function, as the tonus of intact coronary arteries is adapted by flow changes [266]. There are different mechanisms driving these changes: on one hand, it was observed that an increase in blood flow causes vessels dilation due to an increase in eNOS expression and activity [46, 267], whereas on the other hand, an increase in blood pressure caused constriction of the vessel lumen, described as the 'Bayliss-effect' [46, 268, 269]. As hypertension and narrowing of the vessel lumen occur in atherosclerosis (chapter 1.11.2), intact flow-dependent regulation of coronary arteries plays a role in the development of the disease [270].
It has previously been shown that the different classes of lipoproteins exert specific effects on the flow-dependent vasodilation of coronary arteries [271]. LDL does not only impair flow-dependent vasodilation in coronary arteries, but also causes vasoconstriction [271]. IDL and VLDL impair flow-dependent vasodilation. ApoE4-homozygous VLDL induces a strong vasoconstriction as well as apoE0/E0 (patient with a apoE 'knockout') IDL [10, 49, 271, 272]. Only HDL contributes to flow-dependent vasodilation as it significantly increases dilation in response to higher NO availability. It also has a higher affinity to HS-PG receptors than LDL. These receptors are expressed on the endothelium of coronary arteries and function as a sensor for the extent of blood flow and thus take part in the regulation of flow-dependent vasodilation [10, 46, 240, 273].

1.12. Hypotheses and aims of this thesis

Atherosclerosis and AD frequently break out many years before symptoms occur, which complicates their treatment. Therefore, basic research in areas of their mechanisms and pathophysiology is highly relevant to get closer to find treatment opportunities or come closer to curing the diseases or preventing their outbreak.

This thesis aims to contribute to the fundamental understanding of atherosclerosis and AD to determine and better understand mechanisms of their development.

The focus of the experimental work is the research about the impact of lipoproteins, i.e. isolated or in defined compositions, on the expression profiles of PML and PKC in cultured endothelial cells, which are known to contribute to atherosclerosis and AD. For a better understanding of these interactions, *Figure 16* shows a schematic depiction of established activation and inhibition pathways of the molecular targets.

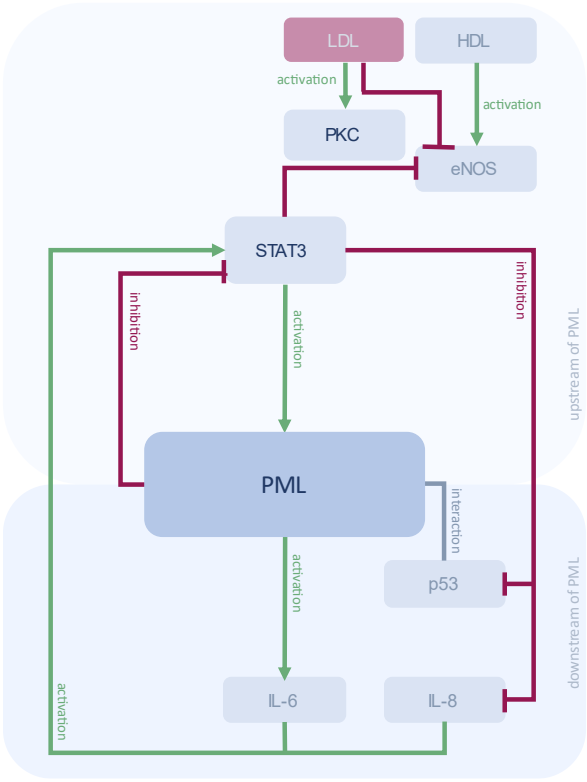

Figure 16. Schematic depiction of known mechanisms regarding the immunomodulatory effect of PML. *LDL activates PKC and inhibits eNOS expression. STAT3 is capable of inhibiting eNOS expression when activated via phosphorylation on Ser-727 by PKC. STAT3 further enhances PML expression and inhibits IL-8 and p53 expression, whereas PML is activated by STAT3 via IL-6 and IL-8. It interacts with p53 and enhances IL-6 secretion. PML and STAT3 act in a negative feedback loop, as PML inhibits STAT3 activation.* Based on *[123, 125, 139, 141, 145, 149, 156, 168, 169, 171, 176, 211, 213, 222, 224, 232, 233, 244, 245] Created by the author.*

The major hypothesis (Figure 17) of this study is that defined lipoproteins, especially LDL, act upstream of PML, while IL-6, IL-8 and p53 are expected to act downstream of PML. If the

hypothesis is validated, the question would raise what the upstream mechanism of PML upregulation via lipoproteins is and if it also enhances the expression of the PML targets IL-6, IL-8 and p53. Since LDL causes activation of PKC, it is also hypothesized that PKC is mechanistically involved in PML activation. STAT3 is potentially involved in lipoprotein-induced upregulation of PML, since it upregulates PML (Figure 17). Based on the knowledge that IDL, VLDL and LDL cause vasoconstriction in coronary arteries, while HDL causes vasodilation and upregulates eNOS expression [245], eNOS could act downstream of PML and be downregulated by LDL.

To validate the hypotheses and to get closer insights into the pathological mechanisms of atherosclerosis and AD, several experiments were conducted. To characterize the link between AD and atherosclerosis, most of the experiments were performed with a pooled lipoprotein fraction and with apoE4-homozygous lipoproteins.

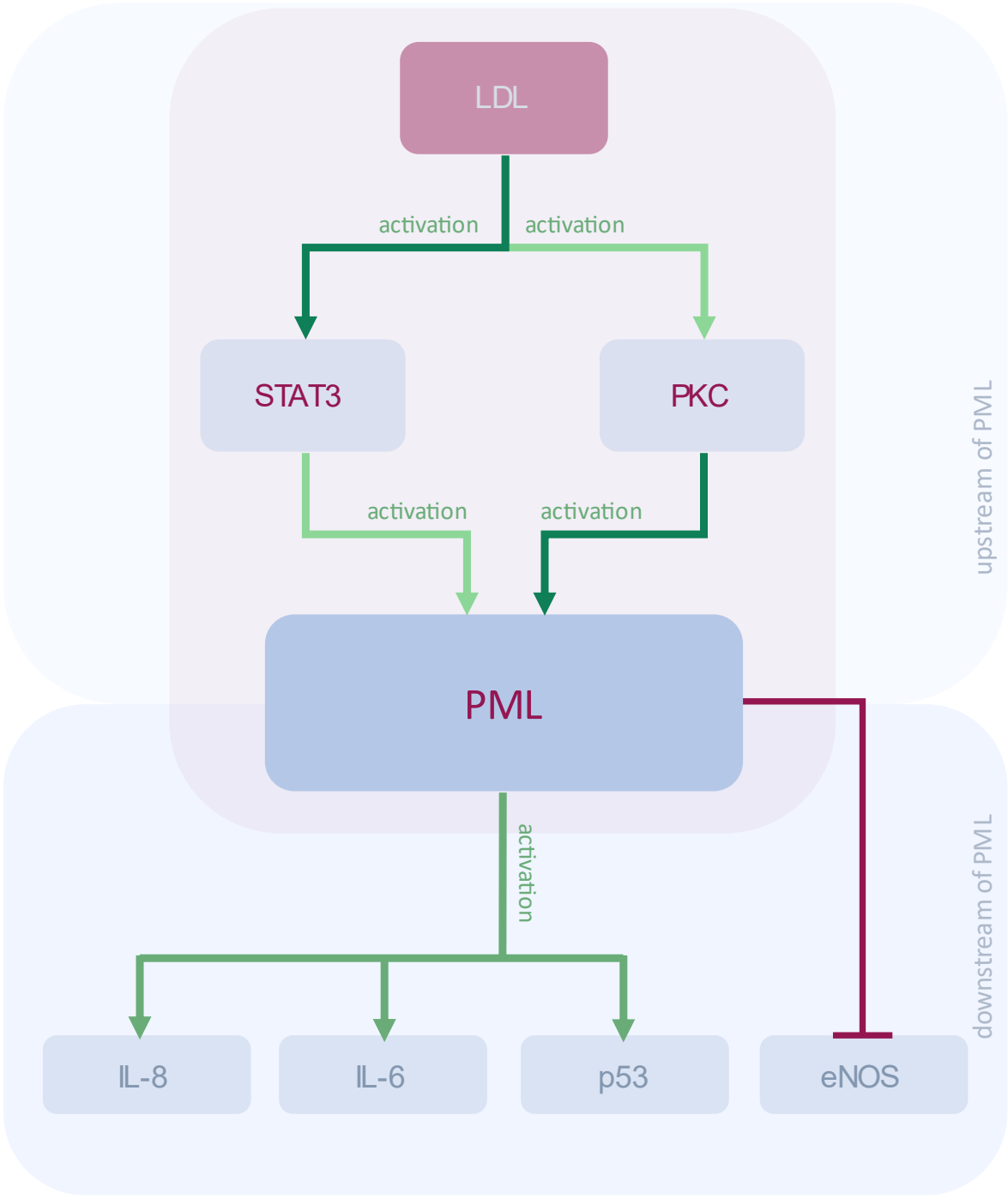

Figure 17. Schematic depiction of the working hypothesis. *This major hypothesis of this thesis involves activation of PKC and STAT3 via LDL, leading to enhanced PML activation, which further causes eNOS expression to be inhibited, while IL-6, IL-8 and p53 expression is increased. Created by the author.*

2. Materials and methods

2.1. Solutions, buffers and media

2.1.1. Krebs-Solution

Krebs-Henseleit-Solution (Krebs-Solution) was used to replace blood for the transport of the blood lipoproteins and as a control medium.
Krebs-Solution consists of different cations: 151.16 mmol/L sodium-ions (Na^+); 4.69 mmol/L potassium-ions (K^+); 2.52 mmol/L calcium-ions (Ca^{2+}) and 1.1 mmol/L magnesia-ions (Mg^{2+}) and anions: 145.40 mmol/L chloride-ions (Cl^-); 16.31 mmol/L hydrogen carbonite (HCO_3^-) and 1.38 mmol/L dihydrogen phosphate ($H_2PO_4^-$) supplemented with 7.77 mmol/L glucose [274].

2.1.2. PBS-Buffer

Phosphate-buffered saline (PBS) solution was used in blood lipid isolation and protein concentration determination. One litre of PBS contains 8.0 g NaCl; 0.2 g KCl; 1.42 g Na_2HPO_4 or 1.78 g Na_2HPO_4 x $2H_2O$ and 0.27 g KH_2PO_4 [275, 276].

2.1.3. DMEM

Dulbecco's Modified Eagle's Medium was used for EA.hy926 cells. It contains 200.00 mg/L $CaCl_2$; 0.10 mg/L $Fe(NO_3)_3$ x 9 H_2O; 400.00 mg/L KCl; 97.67 mg/L $MgSO_4$; 6400.00 mg/L NaCl; 125.00 mg/L NaH_2PO_4 x H_2O; 3700.00 mg/L $NaHCO_3$, 4500.00 mg/L D-Glucose, 15.00 mg/L Phenol red and 110.00 mg/L Sodium pyruvate (according to the manufacturer: Life Technologies™ Gibco® (Carlsbad, CA, USA)). Furthermore, it contains amino acids (*Table 3*) and vitamins (*Table 4*).

Amino acid	*Concentration (mg/L)*
L-Arginine HCl	84.00
L-Cystine 2HCl	63.00
L-Glutamine	584.00
L-Glycine	30.00
L-Histidine HCl H_2O	42.00
L-Isoleucine	105.00
L-Leucine	105.00
L-Lysine HCl	146.00
L-Methionine	30.00
L-Phenylalanine	66.00
L-Serine	42.00
L-Threonine	95.00
L-Tryptophan	16.00
L-Tyrosine 2Na x 2H_2O	104.33
L-Valine	94.00

Table 3. Composition of DMEM according to the manufacturer*: amino acids and their concentrations in mg/dL.*

Vitamin	*Concentration (mg/L)*
D-Calcium pantothenate	4.00
Choline chloride	4.00
Folic acid	4.00
i-Inositol	7.20
Niacinamide	4.00
Riboflavin	0.40
Thiamine HCl	4.00

Table 4. Composition of DMEM according to the manufacturer*: Vitamins and their concentrations in mg/dL.*

2.1.4. Opti-MEM

opti-MEM from Life Technologies™ Gibco® (Carlsbad, CA, USA) was used as a culture medium for the transfection of cells (chapter 2.5). According to the manufacturer, the medium consists of hypoxanthine, sodium pyruvate and L-glutamine, thymidine, growth factors and trace elements.

2.2. Lipid isolation and lipoprotein compositions

Blood lipoproteins were isolated in collaboration with Prof. Dr. Britta Eickholt from the Institute of biochemistry at Charité Universitätsmedizin Berlin and Prof. Dr. Michael Walter from the Institute for Clin Chem Lab Med at University of Rostock. The lipoproteins were isolated according to the methods mentioned by Chisari et al. [277], Leonhardt et al. [278] and Baumstark [279]. Blood samples were taken from several healthy volunteers not under medication or dietary supplements. All of them were starving for at least 10 hours. By pooling the blood samples, it was ensured that the lipoproteins represent the bigger part of the population. The blood was collected into ethylene diamine tetraacetate tubes (EDTA-tubes). For transport and storage, the samples were kept at 2-8°C.

For the preparation of lipoproteins, the samples were centrifuged for 5 mins. The lipoproteins remained in the supernatant.

The blood plasma was ultra-centrifuged for 24 hours at 40000 rpm at 4°C, using a Fixed-Angle Titanium Rotor TI-45 by Beckman Coulter (Indianapolis, IN, USA). The supernatant contained VLDL, which was pipetted off, sterile-filtered with a 0.2 µm filter and stored at 2-8°C for further use. The remaining plasma was mixed and mingled with potassium bromide in saline solution. This solution was ultra-centrifuged for 48 hours. After 48 hours, the supernatant was pipetted off, sterile-filtered, stored at 2-8°C. This step was repeated for every lipoprotein isolated, always a potassium bromide-saline solution-mix corresponding to the density of the lipoprotein.

For determining the concentrations of lipoproteins, the Pierce BCA Protein Assay Kit by Thermo Fisher Scientific (Waltham, MA, USA) was used. The quantification was done with a photometer at a wavelength of 562 nm.

Before using the blood lipoproteins in experimental procedures, EDTA and potassium bromide were replaced with Krebs-Solution using an ion-exchange technique. A sample of the used compositions and single lipoproteins was frozen at -80°C to later perform an oxLDL ELISA (*Figure 20*).

Different mixtures of lipoproteins in Krebs-solution were used in the experiments, their different compositions are shown in *Table 5*. In the first composition ($comp\_{LDL50}$), LDL levels are lowered and mixed with the same HDL concentrations, creating an LDL/HDL ratio of 1, whereas the second composition ($comp\_{LDL200}$) represents a pathophysiological development with increased LDL levels (LDL/HDL ratio = 4). The third composition ($comp\_{LDL100}$) represents the physiological concentrations of lipoproteins in the human organism (LDL/HDL

ratio = 2). Isolated LDL was used in two concentrations, 200 mg/dL and 50 mg/dL and isolated HDL was used in 100 mg/dL and 25 mg/dL. apoE4-homozygous LDL and HDL were used in the same concentrations and were prepared by Prof. Dr. Karl Winkler from the Institute for Clin Chem Lab Med at University of Freiburg.

Lipoprotein	*Lipoprotein concentration (mg/dL) in comp_LDL50*	*Lipoprotein concentration (mg/dL) in comp_LDL200*	*Lipoprotein concentration (mg/dL) in comp_LDL100*
VLDL	30	30	30
IDL	10	10	10
LDL	50	200	100
HDL	50	50	50

Table 5. Composition of lipoproteins used in the experiments. *Concentrations of isolated lipoproteins used in experiments not shown. Created by the author.*

2.3. Cell culture

EA.hy926 cells (Elabscience, Biotechnology Inc., Houston, TX, USA) are an immortalized human vascular endothelial cell line, generated by fusion of HUVECs and A549/8 cells, a lung cancer cell line. EA.hy926 cells grow adherently and bear typical functions of endothelial cells (information according to the manufacturer). EA.hy926 cells were treated according to the manufacturer's guidelines.

If the cells were not to be used immediately, they were kept in liquid nitrogen at -196°C. When prepared for use, the cells were thawed rapidly to 37°C, resuspended and transferred into cell culture flasks in a new cell growth medium. EA.hy926 cells were cultured in DMEM containing 10 % foetal calf serum (FCS, Growth Medium) as well as penicillin (50 units/mL) and streptomycin (50 µg/mL). For passaging or expanding the culture, the cells were detached from culture plates using trypsin, diluted in growth medium and then transferred into new cell culture flasks. The cells were incubated at 37°C in a humidified atmosphere with 5 % CO_2 and handled under aseptic conditions at all times.

The umbilical cords for the isolation of HUVECs were received from PD Dr. Thorsten Braun from the Department of Obstetrics at Charité – Universitätsmedizin Berlin. Consent according to the Declaration of Helsinki was given by the mothers for the use of the umbilical cords. The

Ethics Committee of Charité- Universitätsmedizin Berlin, Germany approved the isolation of the cells (EA4/107/17).

The umbilical cords were transported in PBS at pH 7.4, washed and disinfected with ethanol (70 %) before the vein was washed through with PBS. Following, the umbilical cord was sealed with a sterile clip and the vein was filled with collagenase. The other end of the umbilical cord was also sealed with a sterile clip, followed by a 10- to 15-min-long incubation in sterile aqua dest. at 37°C. To assure the cells detach from the vein and transit into the collagenase solution, the umbilical cord was massaged for some moments and disinfected. Afterwards, the sealed part was cut off and the cells were collected. The umbilical vein was then washed with 20 mL of PBS, which were collected as well. After isolation, HUVECs were centrifuged at 220 x g and cultured in Endothelial Cell Growth Medium (PromoCell, Heidelberg, Germany). They were incubated at 37°C in a humidified atmosphere with 5% CO_2 and always handled under aseptic conditions.

2.4. Endothelial cell measurements

EA.hy926 cells (Elabscience Biotechnology Inc. Houston, TX, USA) or HUVECs were seeded into 12 well plates, covered with medium or with a mixture of lipoproteins (*Table 5*), with or without previous transfection (chapter 2.5).

Cell harvesting was done after 3 or 24 hours of incubation. Therefore, the supernatant of the cells was immediately frozen at -80°C. For analysing RNA, a buffer from the GeneMATRIX Universal RNA Purification kit by EURx (Gdansk, Poland) was used. 300 µL per well were added to the sample for 1 min, the cells were detached and frozen at -80°C immediately. To isolate protein samples from cells, 100 µL of RIPA-buffer from Santa Cruz (Dallas, TX, USA), which contained 20 mM N-ethylmaleimide and protease inhibitors, both from Sigma-Aldrich (St. Louis, MO, USA) was added to the cells and incubated for 15 mins. The total lysates of the cells were then frozen at -80°C.

2.5. Transfection of EA.hy926 cells with PML expression vector or small interfering RNA

To transiently transfect full-length PML IV into EA.hy926 cells, the human expression plasmid pEGFP-C1-PML-IV was used, a vector that was gifted by PD Dr. Peter Hemmerich (Fritz

Lipmann Institute, Jena, Germany) [280]. To create reliable control samples, EA.hy926 cells were transfected with a corresponding empty vector that did not contain specific gene insert.
Furthermore, siRNA was used to create a PML knockdown as it is directed against specific PML nucleotide sequences. The siRNA mixture contained a total of four different siRNAs with a final concentration of 25 nM and was purchased from Dharmacon (Lafayette, CO, USA).
For transfection 'TurboFect' by Thermo Fisher Scientific (Waltham, MA, USA) was used according to the manufacturer's guidelines. EA.hy926 cells were transfected when they were about 70 % confluent. Therefore, 1.5 µL of TurboFect and 1 µg of DNA were diluted in 100 µL opti-Mem and incubated at room temperature before administration of the cells. Transfection happened at 37°C with a 5 % CO_2 atmosphere for 4 hours. The efficiency of transfection was tested 24 hours after incubation according to the experiments by reverse transcription quantitative PCR (RT-qPCR) and immunoblotting.

2.6. Inhibition and activation of PKC and inhibition of STAT3 in incubation of endothelial cells

2.6.1. Inhibition and activation of PKC

The PKC-peptide inhibitor called sc-3088 by Santa Cruz Biotechnology (Dallas, TX, USA) is thirteen amino acids long and inhibits PKC competitively. Sc-3088 binds specifically to the catalytic domain of PKC, and thus inhibits every isoform of PKC (information provided by Santa Cruz Biotechnology). A concentration of 1 µM of sc-3088 proved to be sufficient for inhibiting PKC.
To activate PKC, phorbol 12-myristate 13-acetate (PMA) purchased from LC Laboratories (Woburn, MA, USA) was used in a concentration of 80 nM. PMA only activates DAG-dependent PKC, since the molecule itself is a surrogate of DAG [281].
Sc-3088 and PMA were dissolved in DMSO and diluted in cell growth medium. DMSO alone served as a negative control.

2.6.2. Inhibition of STAT3

A small molecule named STATTIC (STAT three inhibitory compound, 6-nitro-benzo*(b)*thiophene-1,1-dioxide 1) purchased from Cayman Chemical (Ann Arbor, MI, USA) was used for the inhibition of STAT3 activity. STATTIC selectively inhibits phosphorylation in the tyrosine residue of the STAT3 SH2 region *in vitro* leading to an inhibition of pSTAT3

dimerization [186, 188]. STATTIC was used in a concentration of 5 µM. For incubation, STATTIC was diluted in cell growth medium.

2.7. RNA Isolation, Reverse Transcription, and RT-qPCR

The GeneMATRIX Universal RNA Purification kit from EURx (Gdansk, Poland) was used for isolating RNA according to the manufacturers protocol. A kit from Thermo Fisher Scientific (Waltham, MA, USA) was used to transcribe 0.5 µg of mRNA into complementary DNA (cDNA). For semi-quantitative RT-qPCR the QuantStudio 5 system by Applied Biosystems (Foster City, CA, USA) was used, paired with the GoTaq qPCR Master Mix from Promega Corporation (Madison, WI, USA) and specific primer pairs, whose sequences, annealing temperatures and product sizes are shown in *Table 6*. Samples without templates and non-RT samples served as negative controls in every experiment. Melting curve analysis was conducted to verify the production of a single transcript. GAPDH was used as a reference gene for mRNA levels. To quantify mRNA levels, the comparative C_T ($2^{-\Delta\Delta C_T}$) calculation method was applied.

Template	*Annealing temperature*	*Product size*	*Forward primer*	*Reverse primer*
PML	56°C	90 bp	5´ CCG CAA GAC CAA CAA CAT CTT 3′	5´ CAG CGG CTT GGA ACA TCC T 3′
STAT3	62°C	174 bp	5´ GCT TTT GTC AGC GAT GGA GT 3´	5´ATT TGT TGA CGG GTC TGA AGT T 3´
eNOS	62°C	181 bp	5´ CGG GTC CTG TGT ATG GAT GA 3´	5´ AAC TCT TGT GCT GTT CCG GC 3
IL-6	56°C	90 bp	5´ TGC CAG CCT GCT GAC GAA G 3′	5´ AGC TGC GCA GAA TGA GAT GAG 3′
IL-8	60°C	292 bp	5´ ATG ACT TCC AAG CTG GCC GTG GC 3´	TCT CAG CCC TCT TCA AAA ACT TCT C 3´
GAPDH	60°C	200 bp	5´ ATG ACC TTG CCC ACA GCC TT 3′	5´ AAC TGC TTA GCA CCC CTG GC 3′

Table 6. Primers and their annealing temperature, product size and sequences used for RT-qPCR. *All primers were purchased from BioTeZ Berlin-Buch GmbH (Berlin, Germany). Based on information provided by the manufacturer and [282, 283]. Created by the author.*

2.8. Immunoblotting

Total cell lysates of EA.hy926 cells were centrifuged for 5 min at 14.000 g. Subsequently, the protein concentration was determined using microtiter plates performing an assay with the Pierce™ BCA Protein Assay Kit by Thermo Fisher Scientific (Waltham, MA, USA). The results of the assay were read in UV-VIS spectroscopy at 562 nm using the Tecan Sunrise microplate reader and the Magellan V 7.2 software (Tecan Group AG, Männedorf, Switzerland).

For immunoblotting, 10 µg of protein were loaded to a self-made gel of 10 %, they were resolved by SDS-PAGE gel electrophoresis (Sodium dodecyl sulfate polyacrylamide gel electrophoresis) and subsequently transferred to nitrocellulose membranes (GE Healthcare, Chicago, IL, USA) in a semidry system. The following different types of primary and peroxidase-conjugated secondary antibodies in different dilutions were used for immunoblotting (*Table 7* and *Table 8*):

Antibody	*Molecule size (kDa)*	*Dilution*	*Manufacturer*
Anti-PML	117	1:2000 or 1:1000	Novus Biologicals (Littleton, CO, USA)
Anti-p53	53	1:500	Santa Cruz (Dallas, TX, USA)
Anti-eNOS	133	1:1000	Novus Biologicals (Littleton, CO, USA)
Anti-STAT3	91; 86	1:500	Santa Cruz (Dallas, TX, USA)
Anti-pSTAT3	79; 86	1:1000	Cell Signaling Technology (Danvers, MA, USA)
Anti-GAPDH	37	1:10.000	Proteintech (Rosemont, IL, USA)

Table 7. Primary antibodies used for immunoblotting. *Molecule size, dilutions used, and manufacturer shown. Created by the author.*

Secondary Antibody	*Dilution*	*Company*
Anti-mouse igG	1:10.000	Santa Cruz (Dallas, TX, USA)
Anti-rabbit igG	1:10.000	Santa Cruz (Dallas, TX, USA)

Table 8. Secondary antibodies used for immunoblotting. *Dilutions used and manufacturer shown. Created by the author.*

Anti-GAPDH was used as a housekeeping gene. To visualize signals on the nitrocellulose membranes, a chemiluminescence kit (Clarity Max^{TM} Western ECL Substrate, Bio-Rad, Hercules, CA, USA) was used. The public-domain program imageJ [284] was used for the quantification of immunoblotting.

2.9. Immunofluorescence analysis

For immunofluorescence, cells were grown on conventional cover slips added to the well and fixed using paraformaldehyde in PBS (4 %) at pH 7.4 for a duration of 15 min at room temperature. After fixation the cells were permeabilized with PBS and a primary antibody (anti-PML antibody by Santa Cruz, Dallas, TX, USA) diluted 1:50 or 1:100 in a blocking buffer of 10 % FCS (diluted with PBS). Additionally, an anti-alpha-tubulin antibody by Santa Cruz (1:100; Dallas, TX, USA) in blocking buffer was used. The cover slips were incubated with the primary antibody overnight at 4°C and washed with PBS afterwards. Phalloidin (568 nm; 1:200) was added to detect the actin structures of the cells and incubated for a few hours at room temperature. Subsequently, the cells were incubated for 1 hour with the corresponding secondary antibodies conjugated to Alexa Fluor (Life Technologies, Carlsbad, CA, USA) in a blocking buffer which furthermore contained 5 µM Draq5 (Thermo Fisher Scientific, Waltham, MA, USA) for labelling the nucleus. A fluorescence mounting medium by Agilent (1:2000, Santa Clara, CA, USA) was added to the cover slips. Negative controls were done by adding non-binding primary igG antibodies, which were isotype-matched and the same species and concentration as the specific primary antibodies used.

For analysis, a confocal laser microscope (Leica DMI 6000, Wetzlar, Germany) equipped with a 20x and 63x oil immersion lens, a single-photon argon laser as well as a solid -state laser and a helium-neon laser (excitation HeNe, 633 nm; detection PMT, 400-800 nm) was used. For the processing of digital images and to determine the mean fluorescence intensity (MFI), the software “Leica LAS AF Lite” was used. To analyse the images and to quantify the MFI, identical optical settings were used for all images. To determine the MFI, 20 regions of interest

(ROIs) were examined in every experiment. Therefore, ROIs were measured in the cytoplasm and the nucleus, whereas a region without fluorescence was used as a background MFI and subtracted from those in the ROIs analysed.

2.10. ELISA analysis

To determine the concentrations of IL-8 and IL-6 protein within the supernatants of the cells, Enzyme-linked immunosorbent assay (ELISA) was performed using the kit “Invitrogen” from Thermo Fisher Scientific (Waltham, MA, USA). To quantify PML protein, an ELISA kit purchased from Aviva Systems Biology (San Diego, CA, USA) was used on total cell lysates. PKC activity was quantified using an ELISA kit purchased from Abcam (Cambridge, UK). For the PKC activity ELISA, cell lysates were obtained, and protein concentrations were quantified according to chapter 2.8. To determine the concentrations of oxLDL in the mixtures of lipoproteins, an oxLDL ELISA kit from Elabscience Biotechnology Inc. (Houston, TX, USA) was used. The ELISAs were carried out according to the protocols of the manufacturers and read via UV-VIS spectroscopy at 450 nm.

2.11. Preparation of coronary arteries

The coronary arteries were obtained in collaboration with Prof. Dr. Christoph Knosalla from Deutsches Herzzentrum Berlin. Consent for the use of the arteries was given by the patients. The human heart providing the coronary arteries was kept in cooled isotonic saline solution or Ringer solution before the arteries were abstracted.

The arteries were kept in Krebs-Solution at pH 7.35 and 37°C and gassed with 5 % CO_2 and 95 % oxygen for all preparations necessary. For creating a piece of artery fitting into the name of equipment, a small piece of artery was cut out of a fine prepared coronary artery and opened lengthwise. The flat piece measured about 0.5 cm x 1.5 cm. To equilibrate the preparations, they were kept at pH 7.35 and 37°C for at least two hours. During the experimental procedure, it was assured that none of the instruments or machines touched any of the endothelium, to ensure an undamaged endothelium.

2.12. Flow-dependent vasodilation measurements

By clamping the cut-off ends to the movable end of the device, the coronary artery pieces were fixed into the measuring chamber, the endothelial side showing upwards. The fixation of the artery piece was done in Krebs-Solution under a flow of 3 mL/min. As shown in *Figure 19*, the left fastener was fixed to the machine, while the right one was movable and tied to a force transducer (KWS 522.C, K 52 C by Hottinger-Baldwin, Darmstadt, Germany), which was linked to a digital measuring amplifier connected to a computer, transforming the measurements into evaluable data. The tension was measured as an axial tension [10, 46]. 10 minutes prior to the experiment, the preparation was mechanically pre-stretched (400mg per min for 5 min) and adjusted to an initial value of 2.00 g (the value mimics the arterial blood pressure of 100 mmHG [285]). Afterwards, the preparation was left still for five mins to adjust to the value. The tension was measured computer-aided constantly and taken manually every 5 min. As even a maximum shortening of the preparation only caused a maximum change of 1 % of the preparation's length compared to the starting length, the measurements can be seen as nearly isometric [46, 285-287]. Therefore, a relaxation of the vessel corresponds to a lower pull to the force transducer and thereby a reduction of the registered tension.

A flow regulator attached to the measuring chamber was used to increase the flow rate every 10 min. The different flow rates of the test solution were 3 mL/min, 5 mL/min, 20 mL/min, 40 mL/min and 100 mL/min (*Figure 18* and *Figure 19)*. It was ensured that the whole preparation was fully covered by test solution and that the flow rate was stable during the whole test run. Once a test run was finished, the preparation was covered in tin foil and immediately frozen in liquid nitrogen for later experiments. A sample of the test solution containing blood lipoproteins kept at -80°C for determination of oxLDL levels using ELISA.

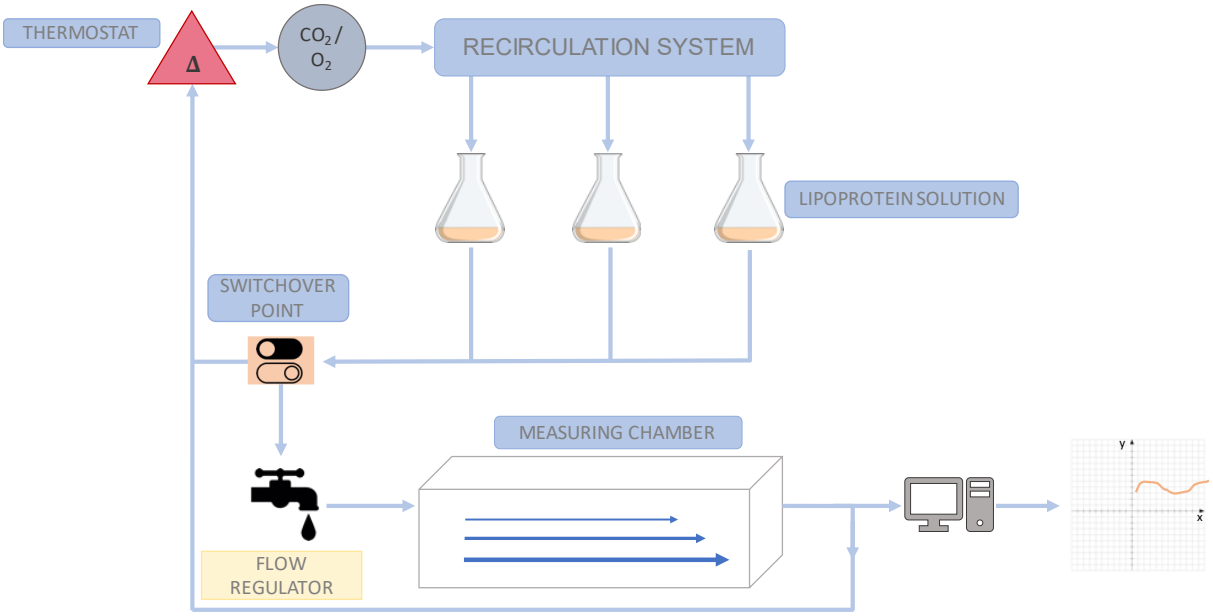

Figure 18. Schematic depiction of the test setup. *The test solution being used either recirculates within the recirculation system, permanently being heated up to 37° Celsius and gassed with 5 % CO_2 and 95 % of oxygen. The switchover point allows the executor of the experiments to either let the solution recirculate without getting to the measuring chamber or, by redirecting the flow of the test solution to get into the measuring chamber, crossing the flow regulator, allowing to set any wanted flow rate. The data collected from the force transducer linked to the measuring chamber is transferred to a computer. After crossing the measuring chamber, the test solution runs back to the thermostat und thus getting back into the recirculation system, ensuring the solution is permanently at the right temperature and gassed with carbogen at any time. Created by the author.*

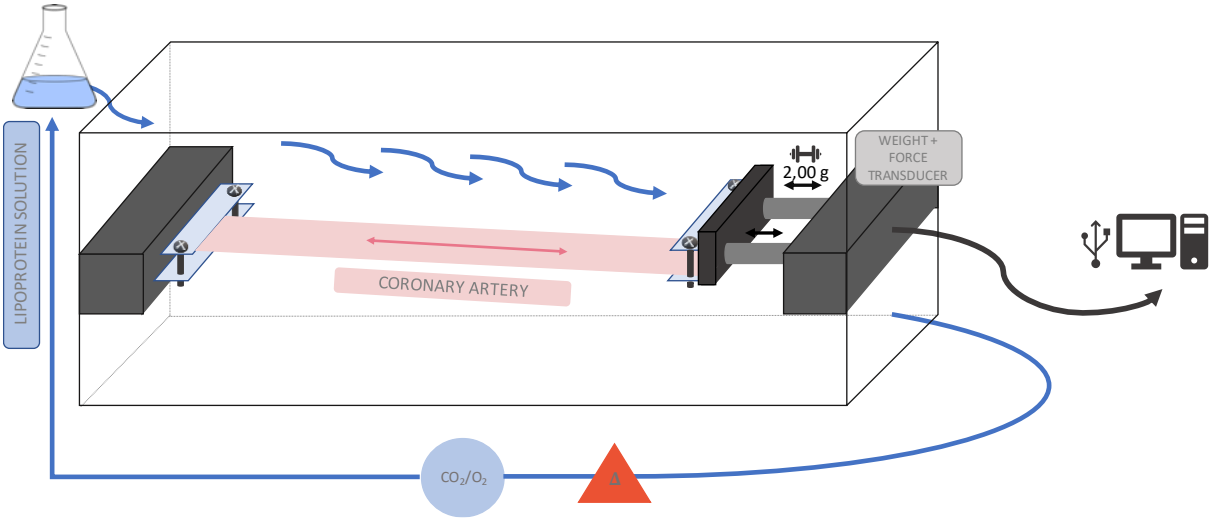

Figure 19. Schematic depiction of the measuring chamber. *The preparation of the coronary artery is being clamped into the fixed side of the holding device, the endothelial side showing upwards. As the test solution reaches the measuring chamber through the flow regulator (not shown) at the right flow rate, the unfixed side of the holding device is able to move according to the reaction of the preparation to the test solution. If the preparation contracts, the holding device is pulled more strongly into direction of the opposite side of the measuring chamber, causing the tension that is permanently measured by a force transducer and sent to a computer to increase. Likewise, if it comes to a relaxation of the preparation, a lower pull is registered and thereby the tension reduces. When leaving the measuring chamber, the test solution floats back to a recirculation system, where it is tempered to 37°C and gassed with carbogen. Created by the author.*

2.13. Statistical analysis

Statistical analysis was performed using the software GraphPad Prism (version 9.3.1; GraphPad Software, San Diego, CA, USA). The experiments were performed independently of each other (the number of times the experiment was executed is provided in the figure legends). The results of the experiments are shown as their mean values ±SD.

Shapiro-Wilk test was performed on all data to ensure normality of distribution. Grubbs's test was used to detect outliers in the data sets. Brown-Forsythe test was used to test the equality of variance. Statistical significance is shown as follows in all figures:

Symbol as it appears in the graphs	*p-value*
*	$p < 0.05$
**	$p < 0.01$
***	$p < 0.001$
****	$p < 0.0001$

Table 9. Symbols used to specify the p-value in the results. *Created by the author.*

To calculate statistical significance, the following tests were used: one-way ANOVA post hoc Dunnett's test or Tukey's test, two-way ANOVA post hoc Tukey's test or Šidák correction (both for more than two groups) as well as a 2-tailed unpaired Student's t-test (for two groups). Significances and the statistical tests used are specified in the figure legends.

3. Results

Since most of the experiments were conducted using LDL in either compositions or as single blood lipoproteins in different concentrations, an oxLDL ELISA was performed to ensure that the concentration of oxLDL was low enough to not affect the experiments. All lipoprotein compositions used for the experiments contained physiological concentrations of VLDL, IDL and HDL, but varying concentrations of LDL. These concentrations were either 50 mg/dL, 100 mg/dL or 200 mg/dL of LDL. The single lipoproteins, either with genetically pooled apoE or apoE4-homozygous, were HDL in the concentrations of 25 and 100 mg/dL and LDL in concentrations of 50 and 200 mg/dL. For this ELISA, the used lipoprotein solutions were immediately frozen at -80°C after using them for each experiment and later thawed to perform the ELISA. As seen in Figure 20, the highest oxLDL levels were determined in comp_$_{LDL100}$. This composition contains $1.1x10^{-7}$ % of oxLDL, while isolated LDL with a concentration of 200 mg/dL only contains $1x10^{-8}$ % of oxLDL. apoE4-homozygous LDL solutions did not contain any detectable oxLDL (data not shown). All in all, the concentrations of oxLDL determined in the lipoprotein solutions used for the experiments do not interfere with the results of the experiments regarding their low levels and the fact that there are no significant differences in the oxLDL levels of the solutions tested.

Figure 20

A

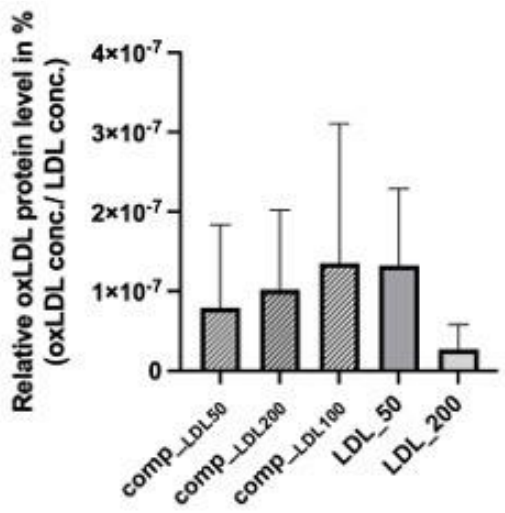

Figure 20. Relative oxLDL protein levels in compositions and single lipoproteins that were used for the experiments are low enough to not interfere with LDL experiments. *To quantify relative oxLDL protein levels, a specific ELISA was performed on the single lipoproteins and lipoprotein compositions used for all experiments. Expression values relative to LDL concentrations n=4 (n = 8 for comp$_{LDL100}$), oxLDL levels for apoE4-homozygous lipoproteins not shown, since no oxLDL was detected. p > 0.99 in two-way ANOVA. All Graphs shown as mean ± SD.*

3.1. LDL upregulates PKC-induced PML expression and its immunomodulatory effect in EA.hy926 cells

3.1.1. LDL upregulates PML expression and its targets IL-6 and IL-8

To investigate whether blood lipoproteins have an influence on PML expression in endothelial cells, EA.hy926 cells were incubated with one of three lipoprotein compositions. After incubation, relative PML mRNA levels were measured using RT-qPCR. Cells incubated without lipoprotein treatment served as a control. Treatment with the lipoprotein compositions for 3 hours (Figure 21A) increased PML mRNA expression in EA.hy926 cells dose-dependently on LDL. Physiological LDL concentrations caused an increase of +134 % ($p < 0.01$) compared to the control. A composition with 200 mg/dL of LDL caused relative PML mRNA levels to increase +251 % ($p < 0.05$) compared to the control. After 24 hours of incubation with the lipoprotein compositions (Figure 21B), relative PML mRNA levels were increased after incubation with $comp_{\_LDL100}$ (+128 %, $p < 0.05$) and $comp_{\_LDL200}$ (+289 %, $p < 0.05$). Apparently, physiological and high levels of LDL lead to a dose-dependent increase in PML mRNA expression after 3 and 24 hours of incubation.

Figure 21

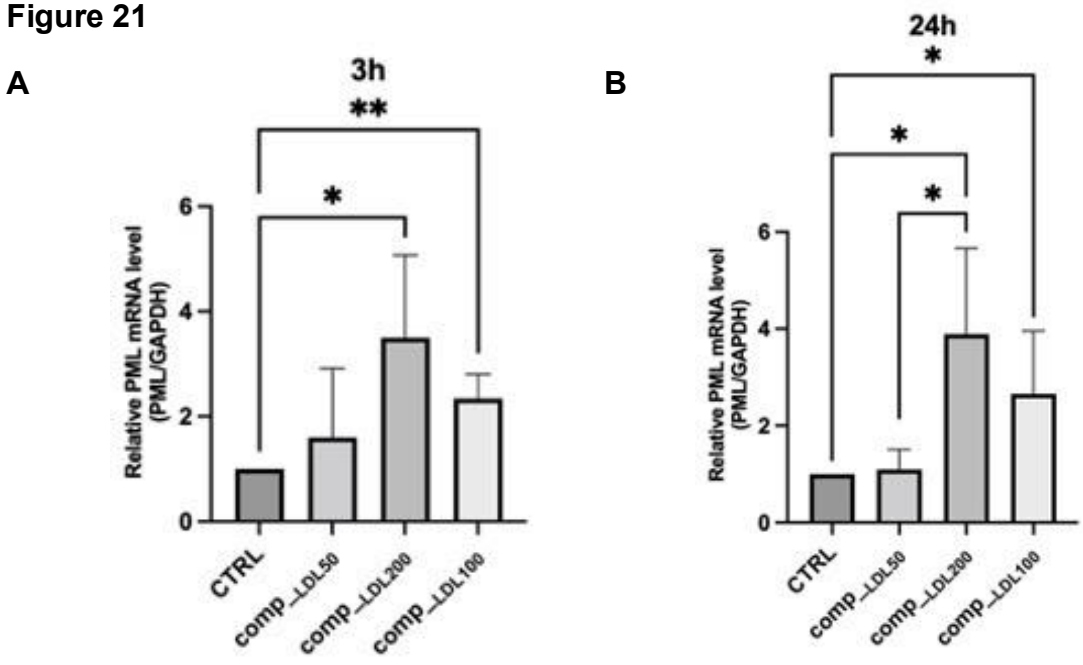

Figure 21. Lipoprotein compositions with different LDL concentrations enhance PML mRNA expression in endothelial cells dose-dependently. *To quantify PML mRNA levels, RT-qPCR was performed on EA.hy926 cells incubated with lipoprotein compositions with LDL concentrations varying from 50 mg/dL to 200 mg/dL for 3h (A) or 24h (B). Expression values relative to control (CTRL, no lipoprotein supplement). n=4, * p < 0.05, ** p < 0.01 in one-way ANOVA. All Graphs shown as mean ± SD.*

To determine the impact of lipoprotein compositions on relative PML protein levels, immunoblotting was performed on total cell lysates of EA.hy926 cells after 3 or 24 hours of

incubation without lipoproteins (control) or with one of the lipoprotein compositions. After incubation for 3 hours (Figure 22A), incubation with comp_$_{LDL50}$ caused relative PML protein levels to rise +161 % ($p < 0.001$) compared to the control, incubation with comp_$_{LDL100}$ even led to an increase of +201 % ($p < 0.0001$). The highest increase in relative PML protein levels was observed after incubation with comp_$_{LDL200}$, which caused PML protein levels to increase +223 % ($p < 0.0001$) compared to the levels of the control. When incubated for 24 hours (Figure 22B), incubation with comp_$_{LDL100}$ led to an increase of +189 % ($p < 0.05$) in PML protein levels. Incubation with comp_$_{LDL200}$ again led to the highest increase in relative PML protein levels (+520 %; $p < 0.0001$) compared to the control. Incubation for 24 hours with comp_$_{LDL200}$ led to higher PML protein levels than it did after 3 hours of incubation. Obviously, lipoprotein compositions with physiological and high LDL concentrations enhance PML protein levels.

Figure 22

A

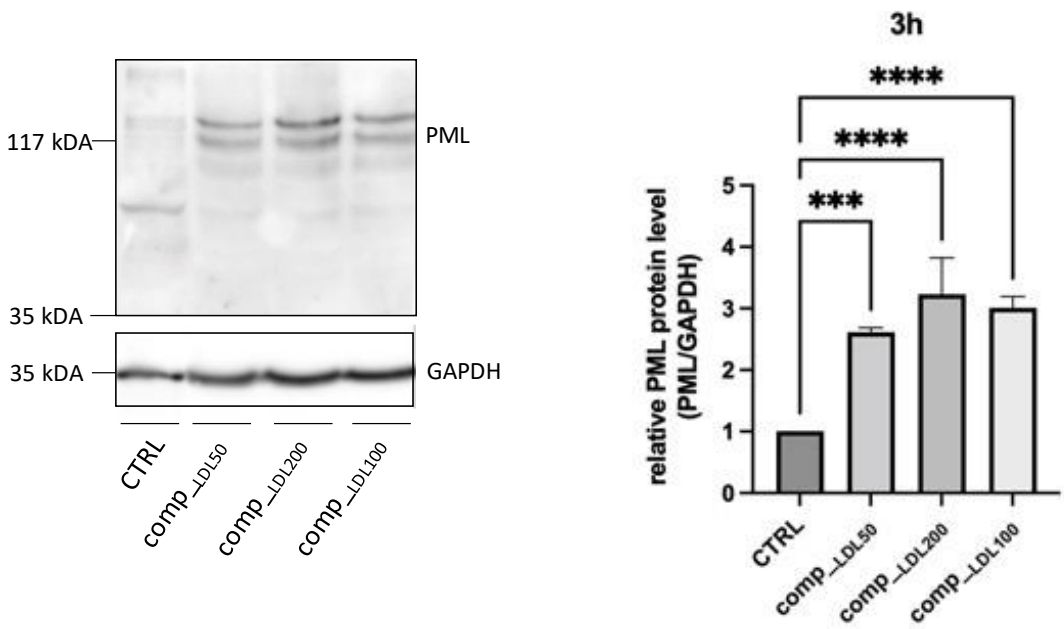

B

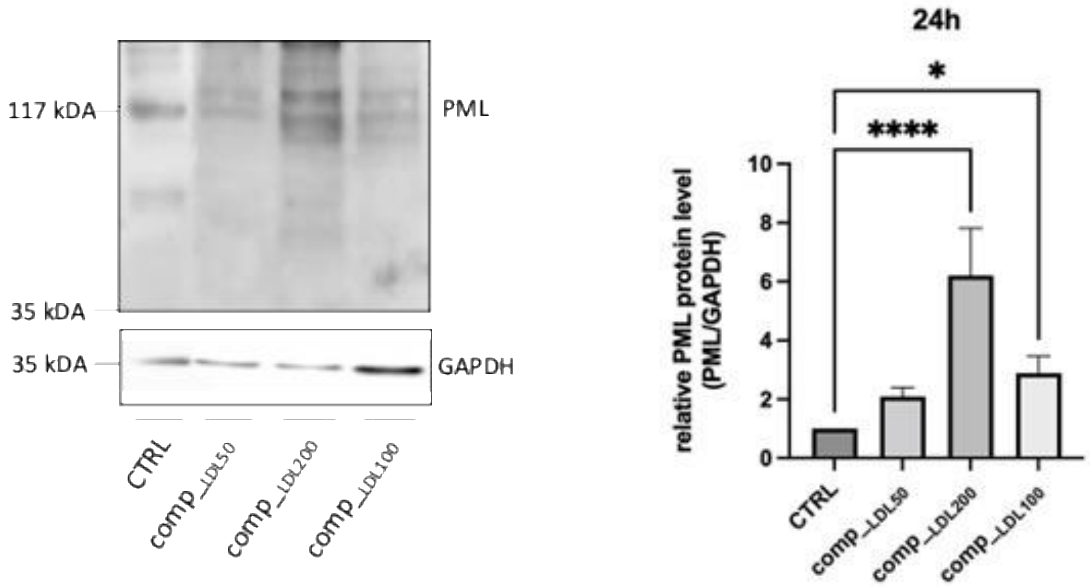

Figure 22. Lipoprotein compositions with different LDL concentrations enhance PML protein expression in endothelial cells. *Immunoblotting for the quantification of PML protein levels in total lysates of EA.hy926 cells incubated with three different lipoprotein compositions with LDL concentrations from 50 mg/dL to 200 mg/dL for 3h (A) and 24h (B). Expression values relative to control (CTRL, no lipoprotein supplement). Representative immunoblots of n=4, * p < 0.05, *** p < 0.001, **** p < 0.0001 performing one-way ANOVA. All Graphs shown as mean ± SD.*

Relative PML protein levels were also determined by performing a PML-specific ELISA analysis of total cell lysates of EA.hy926 cells after incubation with different lipoprotein compositions. Cells incubated without lipoproteins served as a control. Although the ELISA did not show significant results, the results were similar to those of the immunoblot analyses: Incubation for 3 hours (Figure 23A) and 24 hours (Figure 23B) caused relative PML protein levels to increase after treatment with comp$_{_LDL50}$ and with comp$_{_LDL100}$, while treatment with comp$_{_LDL200}$ led to the highest PML protein expression with compared to the control. Incubation of the cells for 24 hours led to higher relative PML protein levels than incubation for 3 hours did.

Figure 23

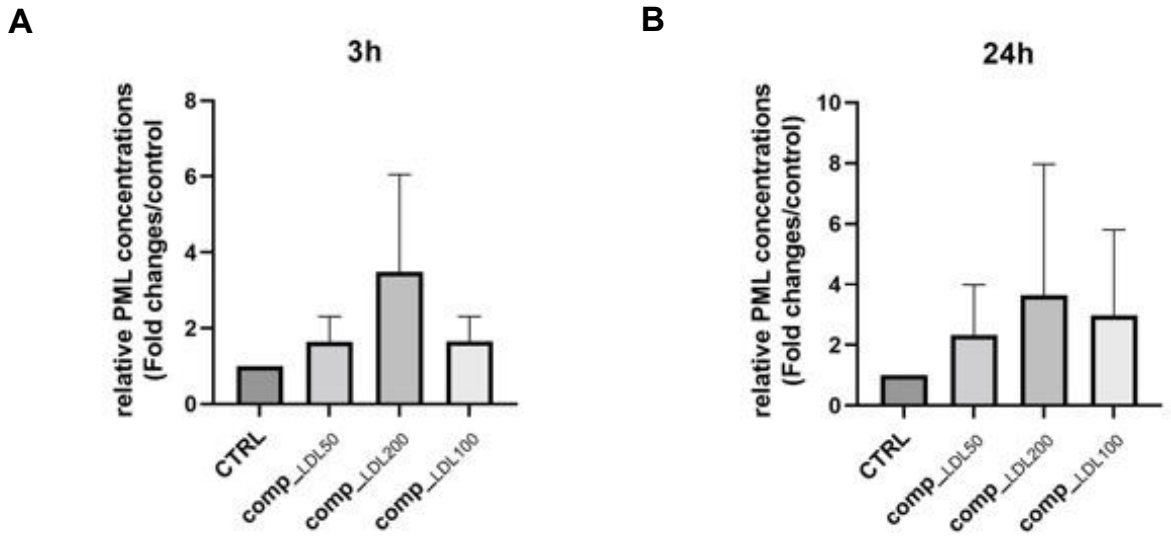

Figure 23. Lipoprotein compositions with different LDL concentrations increase PML protein expression in endothelial cells. *ELISA for the determination of PML protein levels in the lysates EA.hy926 cells incubated with lipoprotein compositions with LDL concentrations varying from 50 mg/dL to 200 mg/dL for 3h (A) or 24h (B). Expression values relative to control (CTRL, no lipoprotein supplement). n=3 (A), n=4 (B), p < 0.9 using one-way ANOVA. All Graphs shown as mean ± SD.*

To investigate whether lipoprotein compositions have an impact on the number of PML-NBs per nucleus, EA.hy926 cells were incubated with the lipoprotein compositions and PML-NBs were detected and quantified using immunofluorescence analysis (Figure 24H, Figure 24I). Control cells (Figure 24A) were incubated without lipoproteins and contained 8.4 PML-NBs on average. The number of PML-NBs in EA.hy926 cells incubated with comp$_{_LDL200}$ for 3 hours increased (Figure 24D) to 17.7 PML-NBs on average (+111 %; **** $p < 0.0001$). Expanding the incubation period to 24 hours (Figure 24E) led to 19.6 PML-NBs per nucleus on average (+133 %; * $p < 0.05$). Incubation of EA.hy926 cells with comp$_{_LDL100}$ for 3 hours (Figure 24F) increased PML-NB numbers to an average of 14.8 PML-NBs per nucleus (+ 76 %; ** $p < 0.01$). Incubation of EA.hy926 cells with comp$_{_LDL100}$ for 24 hours (Figure 24G) increased PML-NB numbers by 96 % (16.5 PML-NBs per nucleus; * $p < 0.05$). As shown in Figure 24K, immunofluorescence was also performed on HUVECs incubated with comp$_{_LDL100}$ for 3 hours which increased the number of PML-NBs from 11.3 PML-NBs on average in the control cells (Figure 24J) to 15.9 PML-NBs per nucleus on average (+41 %; $p < 0.0001$, Figure 24M). When HUVECs were incubated with comp$_{_LDL100}$ for 24 hours before undergoing immunofluorescence analysis (Figure 24L), the number of PML-NBs increased from 11.3 PML-NBs per nucleus (control) to an average of 18.3 PML-NBs per nucleus (+62 %; $p < 0.0001$, Figure 24N). Obviously, lipoprotein compositions, especially with high LDL

concentrations, increase the number of PML-NBs per nucleus in endothelial cells.

Figure 24

A

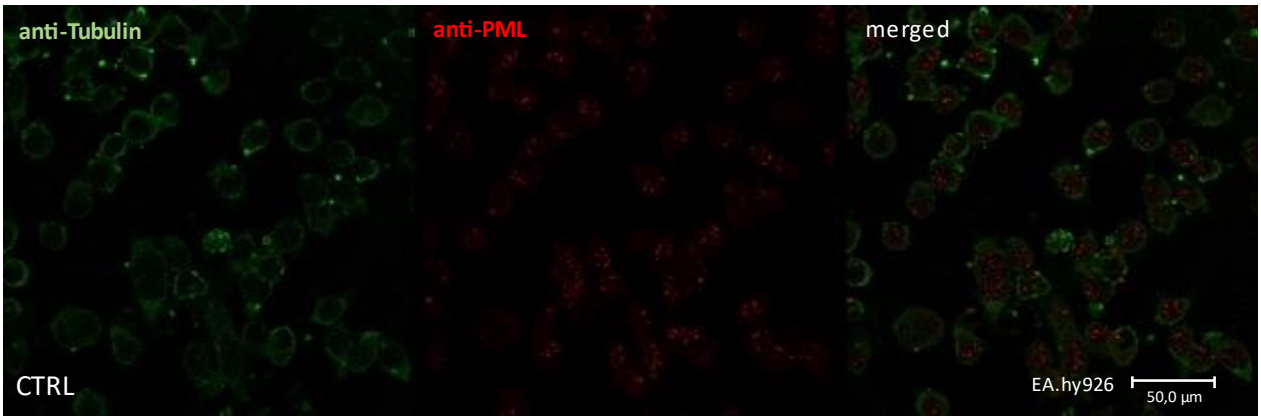

B

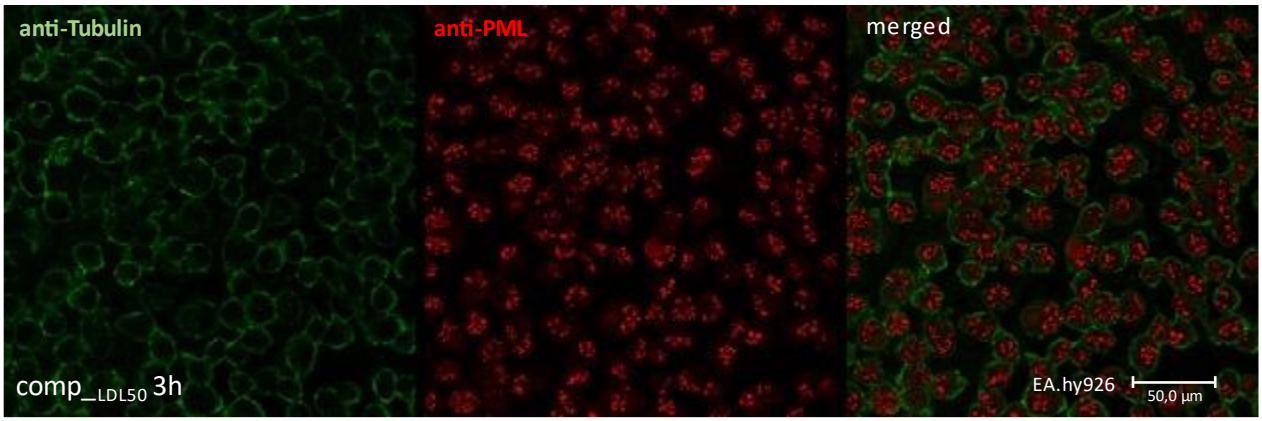

C

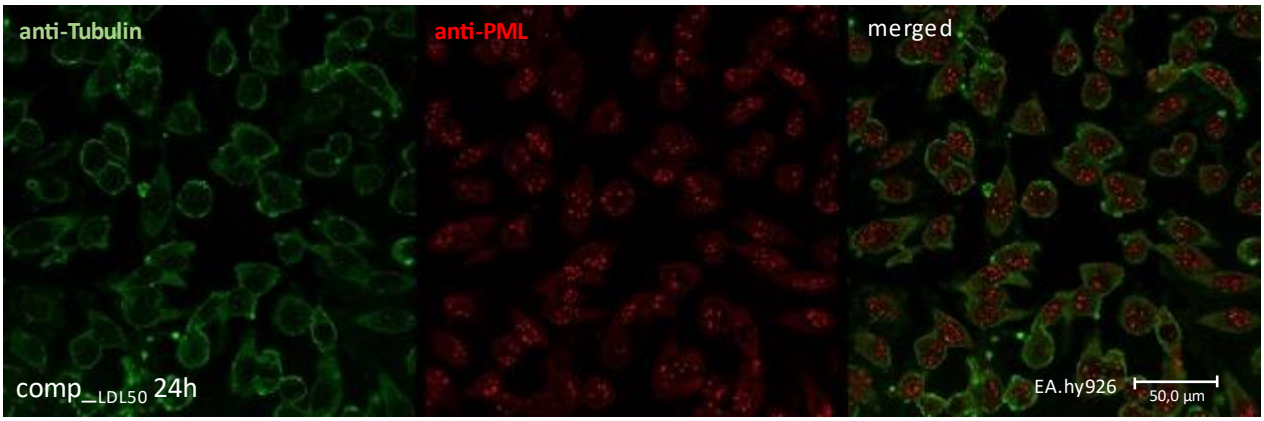

D

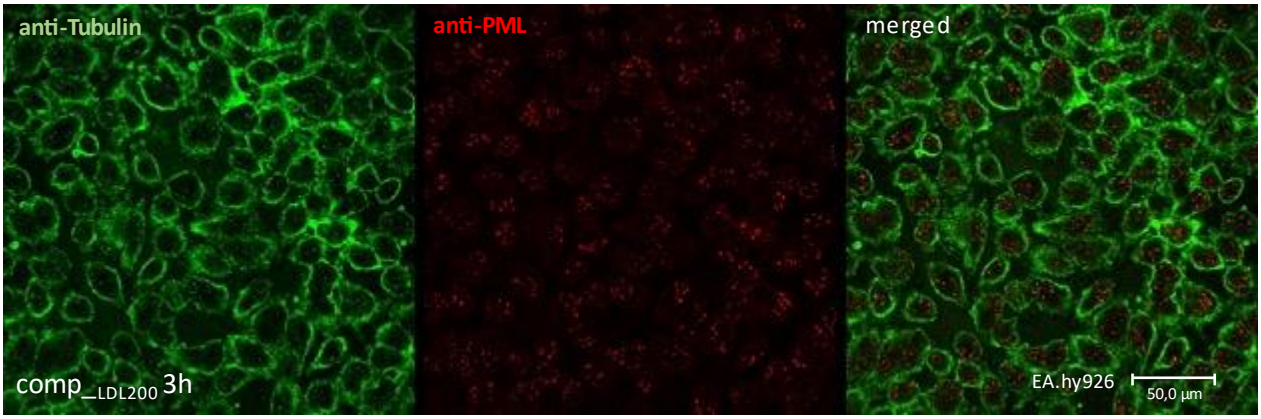
anti-Tubulin
anti-PML
merged
comp_LDL200 3h
EA.hy926
50,0 µm

E

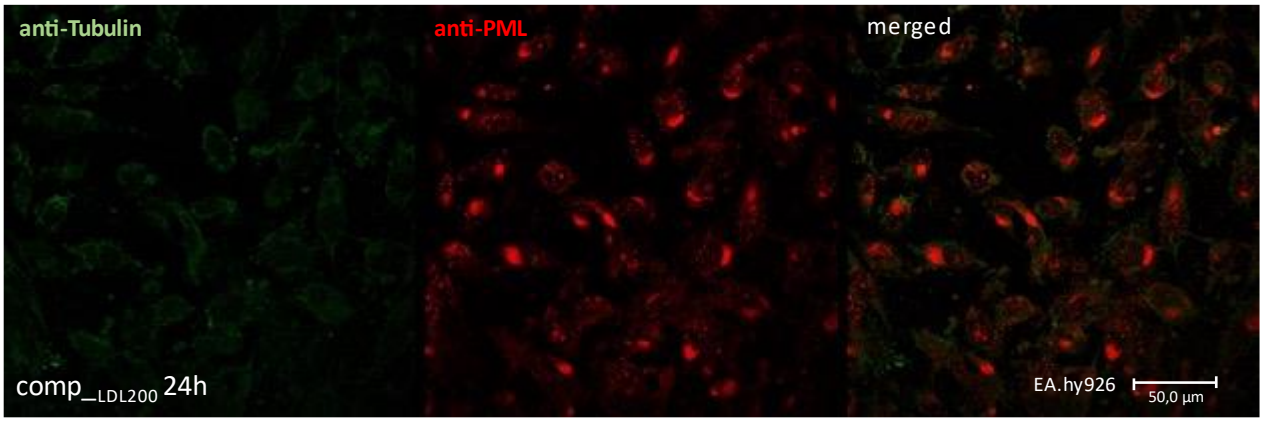
anti-Tubulin
anti-PML
merged
comp_LDL200 24h
EA.hy926
50,0 µm

F

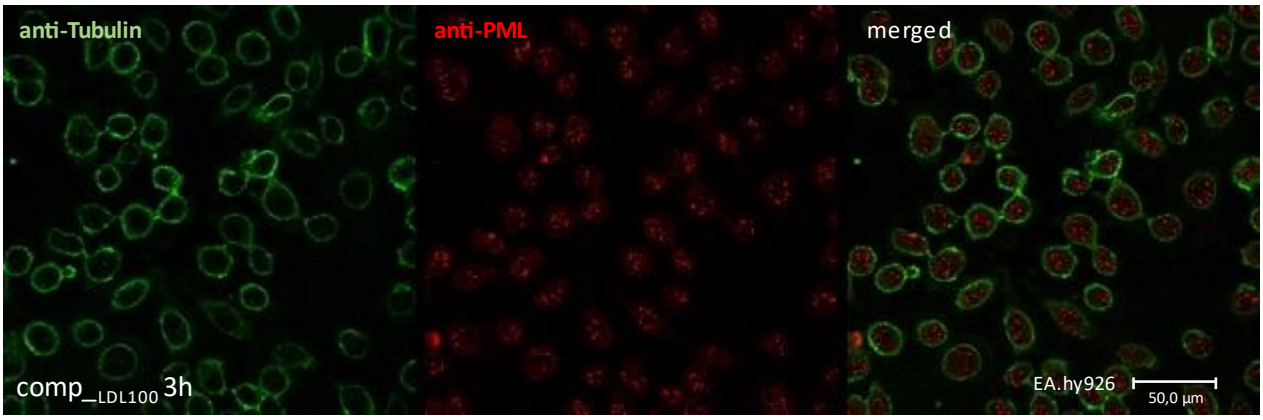
anti-Tubulin
anti-PML
merged
comp_LDL100 3h
EA.hy926
50,0 µm

G

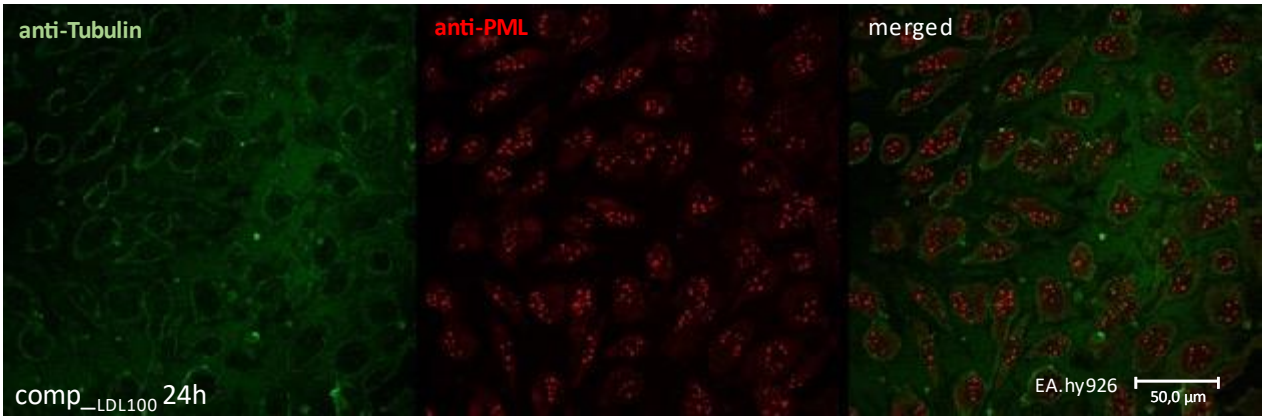
anti-Tubulin
anti-PML
merged
comp_LDL100 24h
EA.hy926
50,0 µm

H

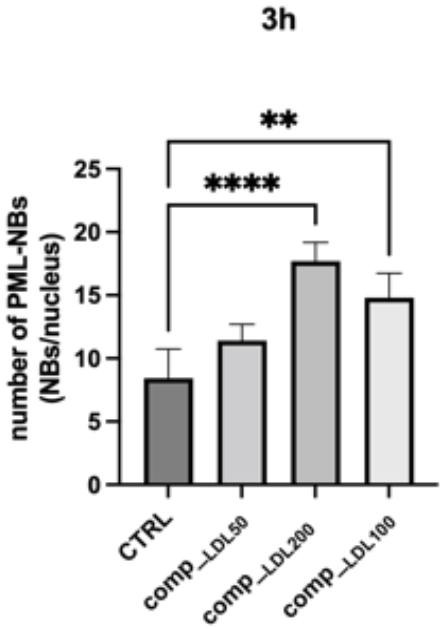
3h
number of PML-NBs (NBs/nucleus)
**
****
0
5
10
15
20
25
CTRL
comp_LDL50
comp_LDL200
comp_LDL100

I

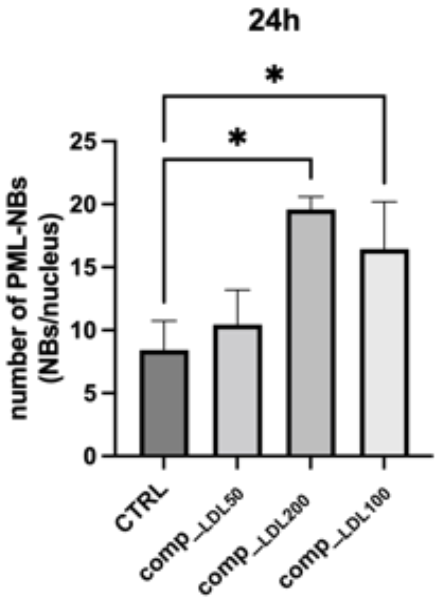
24h
number of PML-NBs (NBs/nucleus)
*
*
0
5
10
15
20
25
CTRL
comp_LDL50
comp_LDL200
comp_LDL100

J

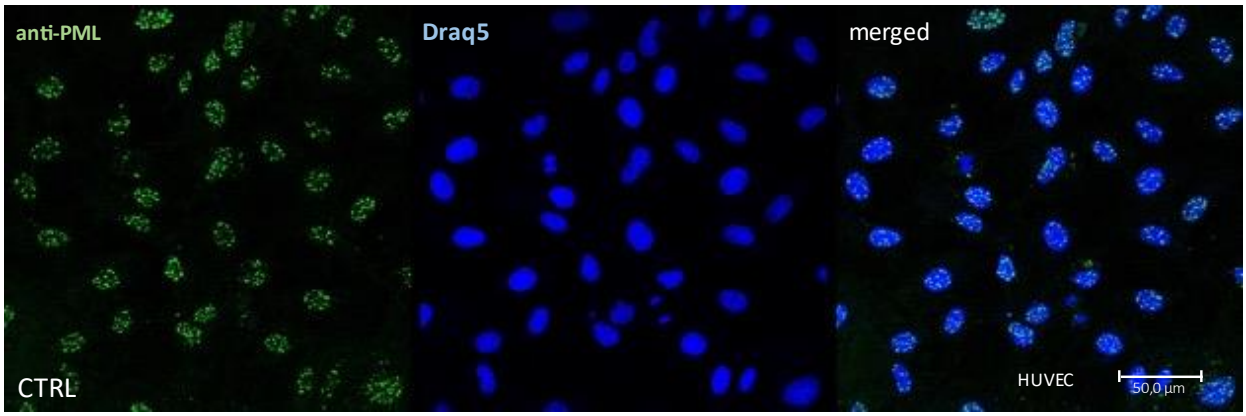
anti-PML
Draq5
merged
CTRL
HUVEC
50,0 µm

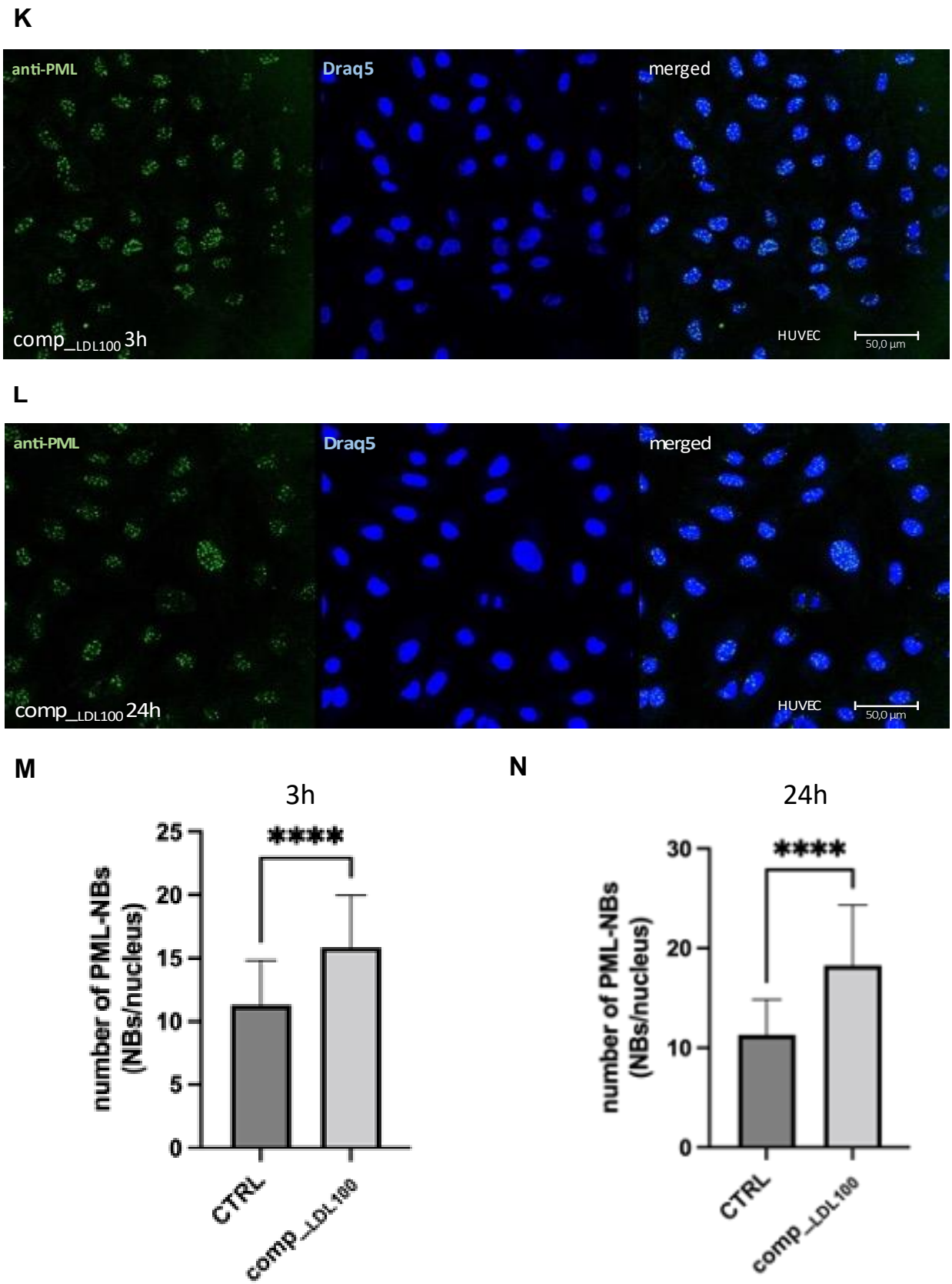

Figure 24. Lipoprotein compositions with different LDL concentrations increase the number of PML-NBs in endothelial cells. *Immunofluorescence of EA.hy926 cells with an anti-PML antibody (red) to determine the number of PML-NBs (H, I) after incubation without lipoprotein supplement (A; CTRL) or with lipoprotein compositions with LDL concentrations of 50 mg/dL for 3h (B) or 24h (C), 200 mg/dL for 3h (D) or 24h (E) or 100 mg/dL for 3h (F) or 24h (G). anti-Tubulin (green) was used to highlight the cell structure. Draq5 was used to highlight the nuclei (data not shown). Images shown are representative of n=4*

*(for 3h of incubation) and n=2 (for 24h of incubation) experiments with 40-60 cell nuclei analysed. ** p < 0.01, **** p < 0.0001 (3h of incubation), * p < 0.05 (24h of incubation) using one-way ANOVA. Immunofluorescence was performed on HUVEC with anti-PML (green) and anti-tubulin (data not shown) to determine the number of PML-NBs after incubation with a lipoprotein composition with physiological lipoprotein concentrations for 3 hours (K, M) or 24 hours (L, N). Control cells were left untreated (J). Draq5 was used to highlight the nuclei (blue). Images shown are representative of n=1 with 60 nuclei analysed. **** p < 0.0001 using Student's t-test. All Graphs shown as mean ± SD.*

These experiments were also conducted with lipoprotein solutions that contained only one specific lipoprotein in different concentrations. Cells were incubated for 3 or 24 hours. Cells incubated without lipoproteins served as a control. Relative PML mRNA levels were determined performing RT-qPCR. Figure 25A shows the results of incubation with the single blood lipoproteins after an incubation period of 3 hours. Incubation with HDL in low concentrations of 25 mg/dL caused relative PML mRNA levels to decrease to only 21 % ($p < 0.0001$) of the levels of the control cells. Treatment with 100 mg/dL of HDL caused a decrease in PML mRNA levels (-68 %, $p < 0.001$) as well. Incubation with 200 mg/dL of LDL enhanced relative PML mRNA levels +175 % ($p < 0.05$) compared to the control. After 24 hours of incubation (Figure 25B), cells treated with both concentrations of HDL had lower PML mRNA levels than the control cells. Incubating the cells with 200 mg/dL of LDL led to an increase of PML mRNA expression of +171 % ($p < 0.001$) compared to the control. Clearly, high concentrations of LDL increase PML mRNA expression in EA.hy926 cells.

Figure 25

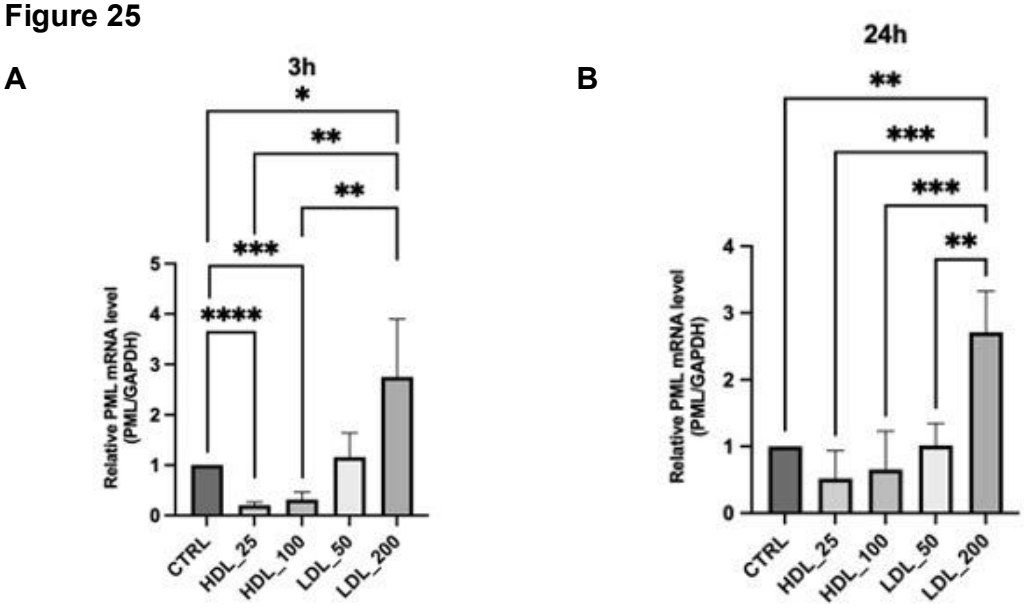

Figure 25. LDL enhances PML mRNA expression in endothelial cells. *RT-qPCR was performed on EA.hy926 cells incubated with 25 mg/dL or 100 mg/dL of HDL and 50 mg/dL or 200 mg/dL of LDL for 3h (A) or 24h (B) to determine PML mRNA levels. Expression values relative to an untreated control. n=3 (A) and n=4 (B), * p < 0.05, ** p < 0.01, *** p < 0.001, **** p < 0.0001 in two-way ANOVA. All Graphs shown as mean ± SD.*

To investigate the impact on single blood lipoproteins on PML protein expression, relative PML protein levels were determined using total cell lysates of EA.hy926 cells for immunoblotting after incubation with single blood lipoproteins. Control cells were incubated without lipoprotein

supplement. After 3 hours of incubation (Figure 26A), 50 mg/dL of LDL caused PML protein levels to increase (+104 %; $p < 0.05$). Incubation with 200 mg/dL of LDL even led to an increase of 173 % ($p < 0.001$) compared to the levels of the control cells. After a 24 hour period of incubation (Figure 26B), incubating EA.hy926 cells with 100 mg/dL of HDL caused an increase of +124 % ($p < 0.01$) and incubation with 50 mg/dL of LDL led to an increase of PML protein expression (+ 115 %; $p < 0.01$). The highest PML protein expression was determined after incubation with 200 mg/dL of LDL (+180 %; $p < 0.0001$) compared to the control. After 24 hours of incubation, cells incubated with LDL showed higher relative PML protein levels than cells incubated for 3 hours did. Obviously, PML protein levels in EA.hy926 cells increase when incubated with different concentrations of LDL.

Figure 26

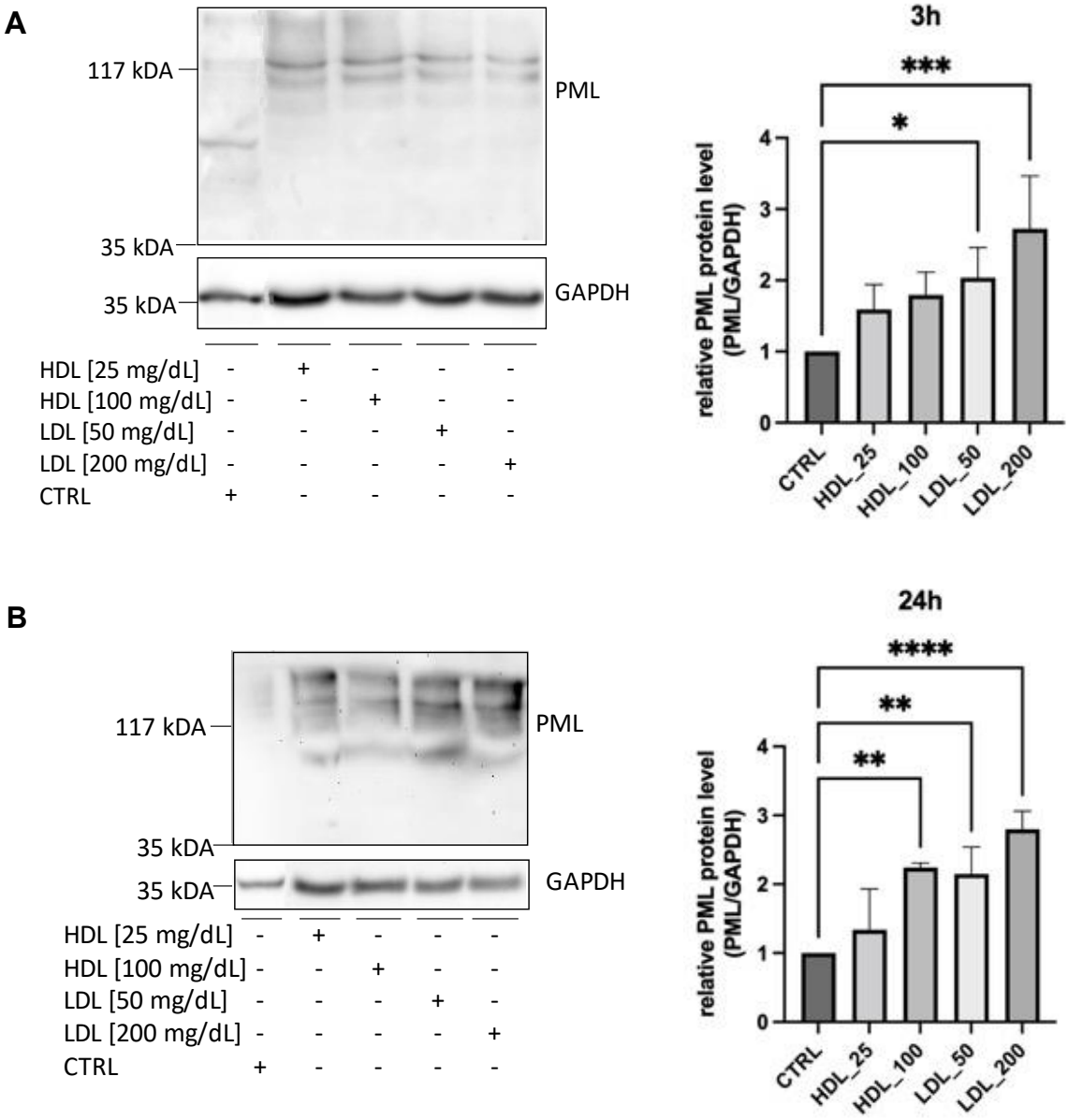

Figure 26. LDL enhances PML protein expression in endothelial cells. *Immunoblotting of total lysates of EA.hy926 cells incubated with 25 mg/dL or 100 mg/dL of HDL and 50 mg/dL or 200 mg/dL of LDL for 3h (A) or 24h (B) to quantify PML protein levels. Expression values relative to an untreated control. Representative immunoblots of n=4, * p < 0.05, ** p < 0.01, *** p < 0.001, **** p < 0.0001 in two-way ANOVA. All Graphs shown as mean ± SD.*

In order to investigate the impact of single blood lipoproteins of different concentrations on PML protein expression, relative PML protein levels of total lysates of EA.hy926 cells incubated with single blood lipoproteins for 3 or 24 hours were additionally determined performing ELISA. Again, no significant results were obtained. When incubated for 3 hours (Figure 27A) and 24 hours (Figure 27B) incubation with any of the lipoproteins caused the endothelial cells to express higher PML protein levels compared to the control, with 200 mg/dL of LDL causing the highest relative PML protein levels.

Figure 27

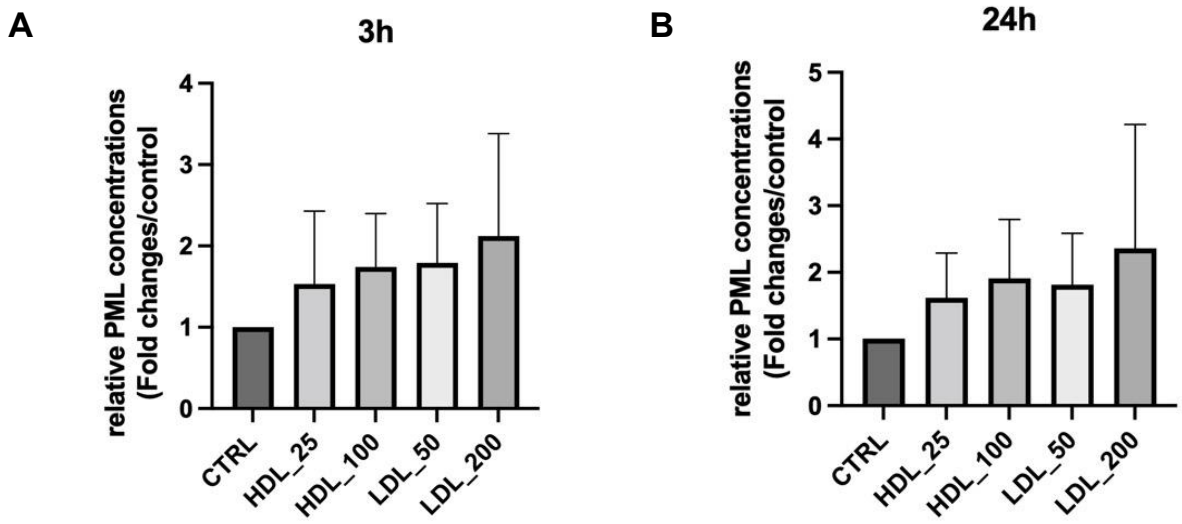

Figure 27. LDL increases PML protein expression in endothelial cells. *ELISA to determine PML protein levels in the lysates EA.hy926 cells incubated with 25 mg/dL or 100 mg/dL of HDL and 50 mg/dL or 200 mg/dL of LDL for 3h (A) or 24h (B) Expression values relative to control (CTRL, no lipoprotein supplement). n=3 (A), n=4 (B), p < 0.9999 using two-way ANOVA. All Graphs shown as mean ± SD.*

To investigate the impact of single blood lipoproteins on the number of PML-NBs per nucleus after incubation of EA.hy926 cells for 3 or 24 hours, immunofluorescence was performed. Control cells were incubated without lipoprotein supplement. Results of highlighting and determining PML-NBs in immunofluorescence (Figure 28) show that after an incubation period of 3 hours, compared to the control sample (Figure 28A; 8.4 PML-NBs on average), incubation with 200 mg/dL of LDL (Figure 28H) enhanced the number of PML NBs (14.2 PML-NBs per nucleus on average, +69 %; * $p < 0.05$; Figure 28J). Incubation of EA.hy926 cells with 200 mg/dL of LDL for 24 hours (Figure 28I) increased PML-NB numbers to an average of 16.0 PML-NBs per nucleus (+90 %; * $p < 0.05$; Figure 28K). PML-NB numbers in EA.hy926 cells

were generally higher after 24 hours of incubation than after 3 hours of incubation. Clearly, incubation with high concentrations of LDL leads to elevated numbers of PML-NBs.

Figure 28

A

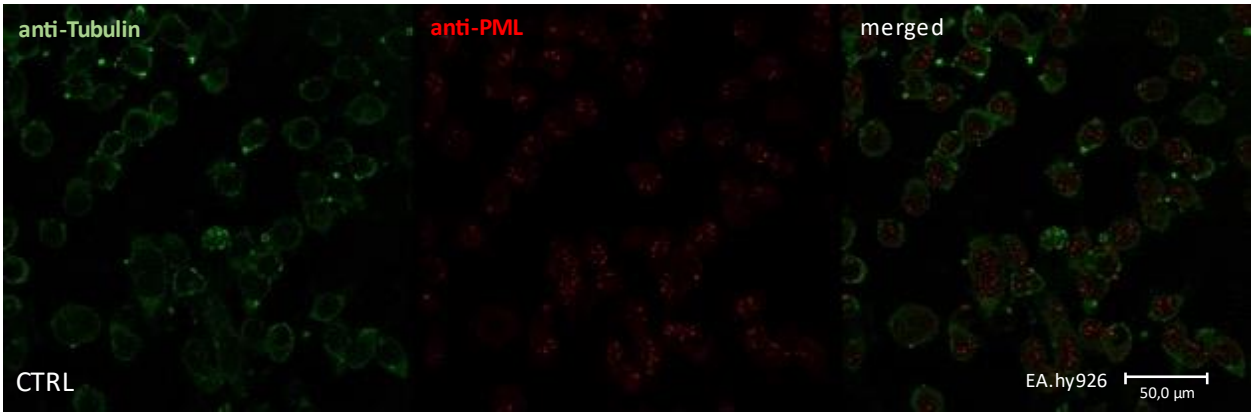

B

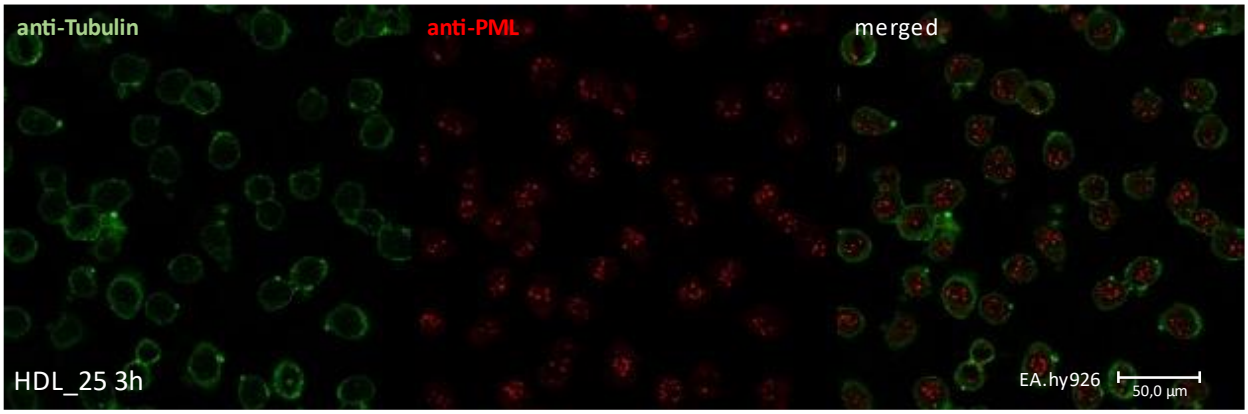

C

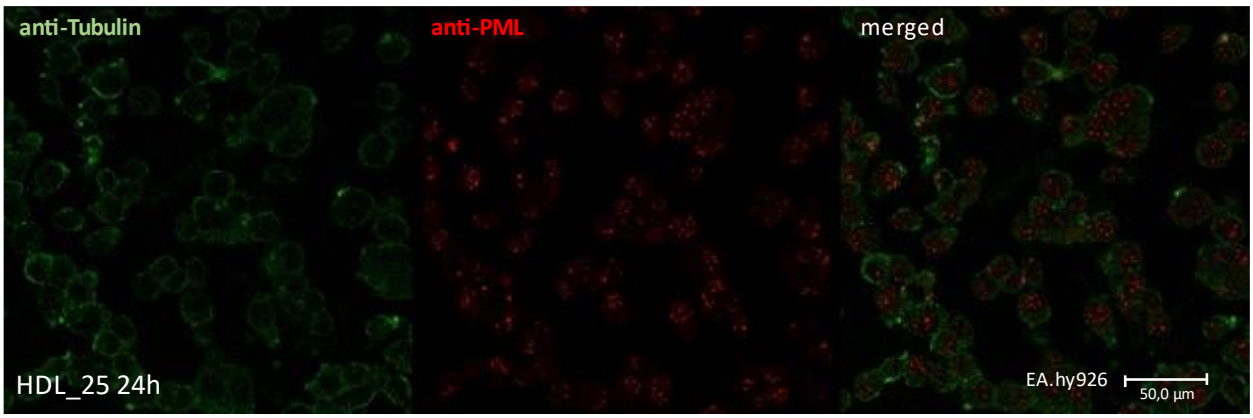

D

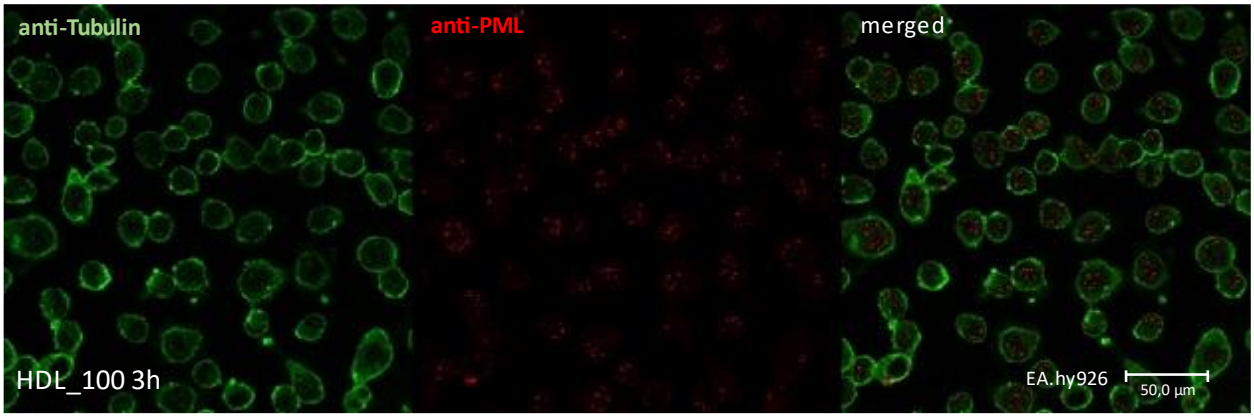
anti-Tubulin
anti-PML
merged
HDL_100 3h
EA.hy926
50,0 µm

E

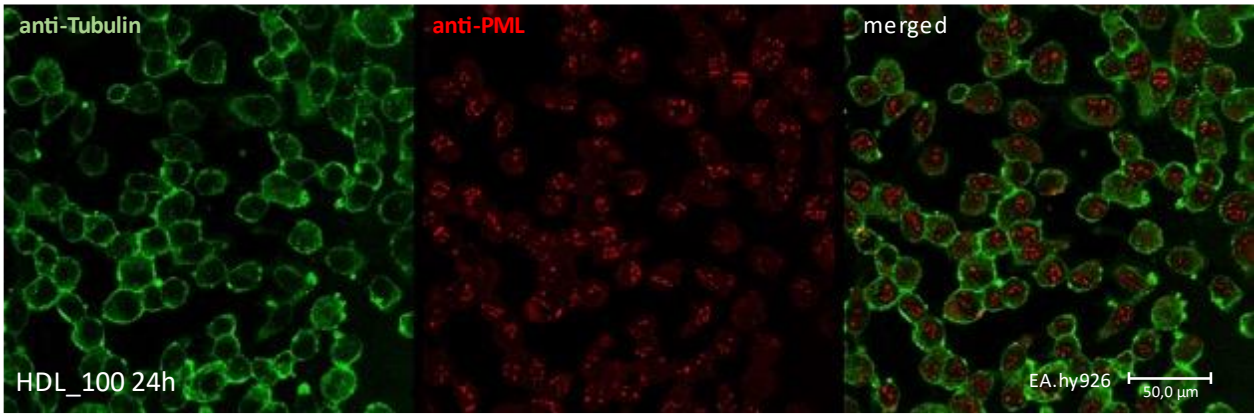
anti-Tubulin
anti-PML
merged
HDL_100 24h
EA.hy926
50,0 µm

F

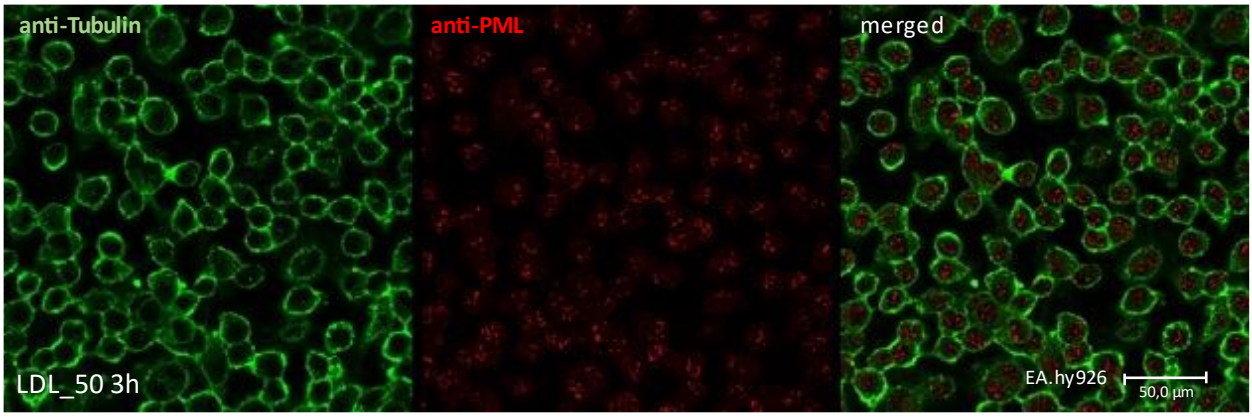
anti-Tubulin
anti-PML
merged
LDL_50 3h
EA.hy926
50,0 µm

G

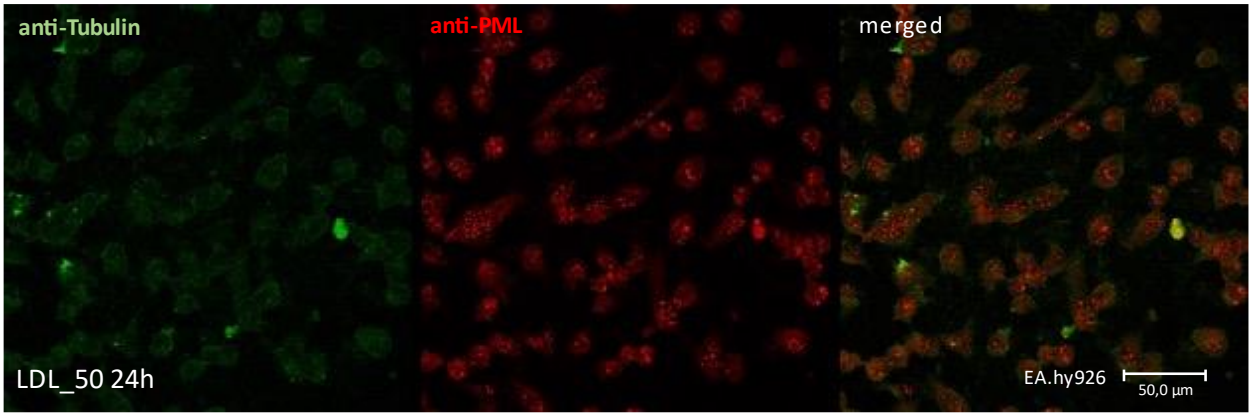
anti-Tubulin
anti-PML
merged
LDL_50 24h
EA.hy926
50,0 µm

H

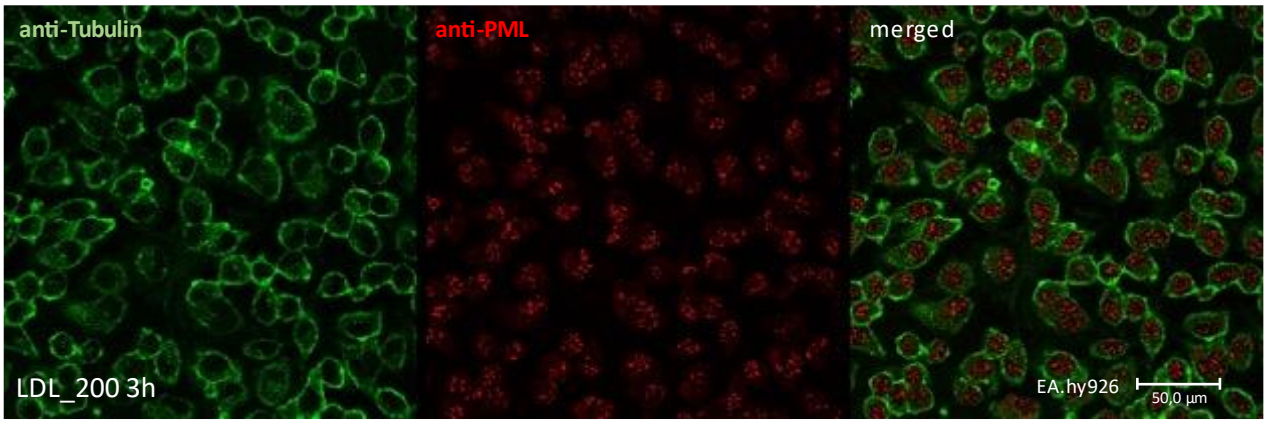
anti-Tubulin
anti-PML
merged
LDL_200 3h
EA.hy926
50,0 µm

I

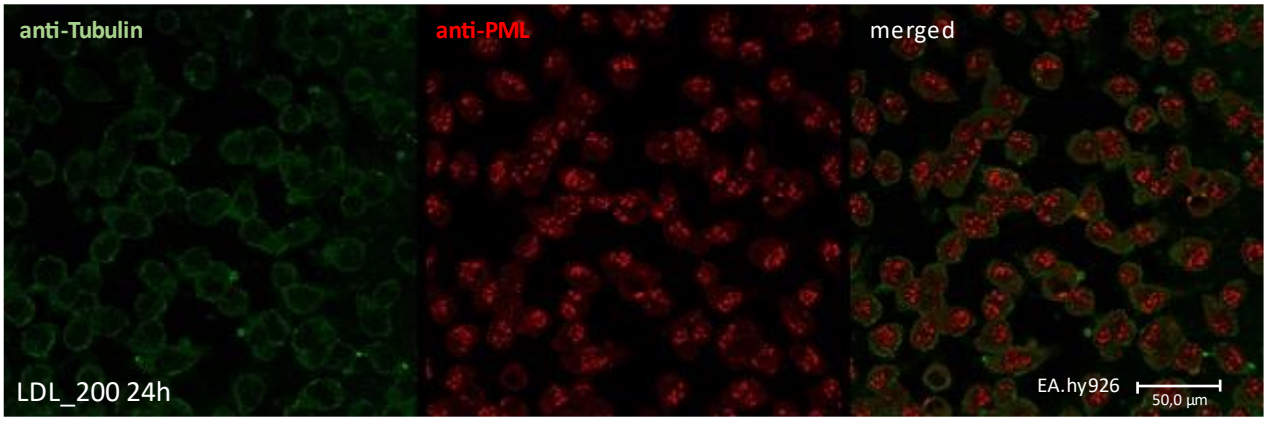
anti-Tubulin
anti-PML
merged
LDL_200 24h
EA.hy926
50,0 µm

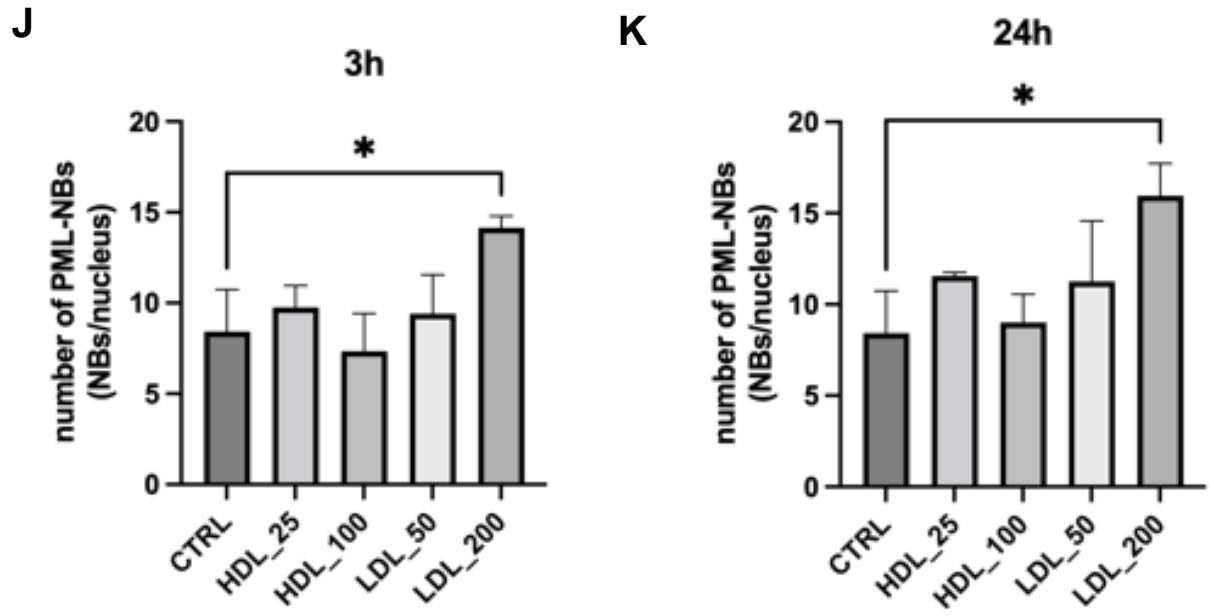

Figure 28. LDL enhances the number of PML-NBs in endothelial cells. *To determine the number of PML-NBs (J, K), Immunofluorescence of EA.hy926 cells with anti-PML (red) and anti-Tubulin (green) was performed after incubation without lipoprotein supplement (A; CTRL) or with 25 mg/dL of HDL for 3h (B) or 24h (C), 100 mg/dL of HDL for 3h (D) or 24h (E), 50 mg/dL of LDL for 3h (F) or 24h (G) and with 200 mg/dL of LDL for 3h (H) and 24h (I). The cell nuclei were highlighted using Draq5 (data not shown). n=3 (for 3h of incubation), and n=2 (for 24 h of incubation) independent experiments with 40 – 60 nuclei evaluated, images shown are representatives. * p < 0.05 using one-way ANOVA. All Graphs shown as mean ± SD.*

EA.hy926 cells were incubated with single apoE4-homozygous blood lipoproteins for 3 or 24 hours. To determine relative PML mRNA levels after incubation with apoE4-homozygous lipoproteins, RT-qPCR was performed. Cells incubated without lipoprotein supplement served as a control. Figure 29A shows that compared to PML mRNA levels of a control, treatment for 3 hours with 25 mg/dL of apoE4-homozygous HDL decreases relative PML mRNA levels to only 24 % ($p < 0.05$). Yet, incubation with 200 mg/dL of apoE4-homozygous LDL causes relative PML mRNA levels to increase (+41 %). When incubated for a duration of 24 hours (Figure 29B), only incubation with 200 mg/dL of apoE4-homozygous LDL increased PML mRNA expression compared to the control (+181 %; $p < 0.05$). An incubation period of 24 hours caused relative PML mRNA levels to increase more than an incubation period of 3 hours. Apparently, incubation with high concentrations of apoE4-homozygous LDL increases PML mRNA expression.

Figure 29

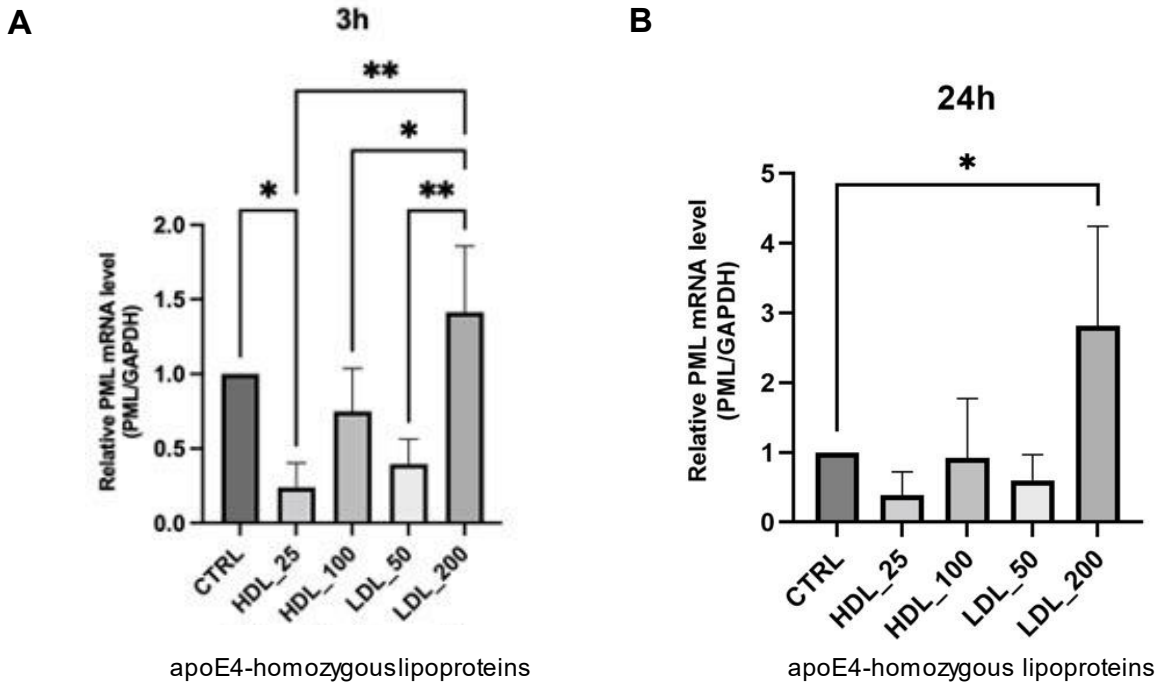

Figure 29. apoE4-homozygous LDL increases PML mRNA expression in endothelial cells. *For determination of PML mRNA levels, RT-qPCR was performed on EA.hy926 cells incubated with apoE4-homozygous 25 mg/dL or 100 mg/dL of HDL and 50 mg/dL or 200 mg/dL of LDL for 3h (A) or 24h (B). Expression values relative to a control without lipoprotein supplement. n=3 (A), n=4 (B) * p < 0.05, ** p < 0.01 performing two-way ANOVA. All Graphs shown as mean ± SD.*

Incubation of EA.hy926 cells either untreated (control) or with different concentrations of apoE4-homozygous lipoproteins for 3 and 24 hours was followed up by immunoblotting to determine relative PML protein levels of total cell lysates. As Figure 30A shows, incubation with 200 mg/dL of apoE4-homozygous LDL led to an increase in relative PML protein levels (+190 %, $p < 0.05$) compared to the control. When the incubation period was extended to 24 hours (Figure 30B), only treatment with high concentrations of apoE4-homozygous LDL led to an increase in relative PML protein levels (+113 %, $p < 0.05$) compared to PML protein levels of the control. Obviously, incubation with high concentrations of apoE4-homozygous LDL leads to enhanced PML protein levels.

Figure 30

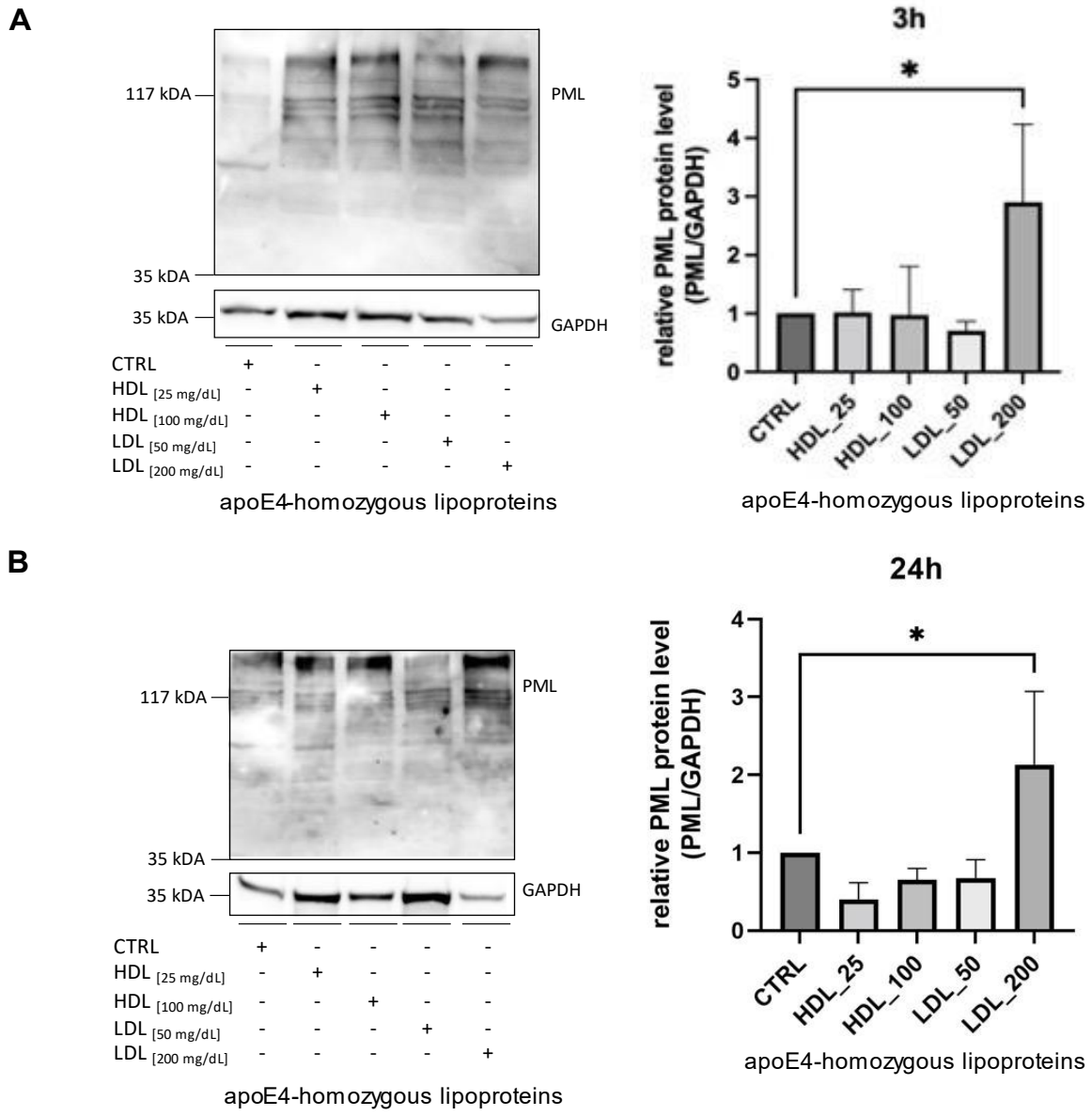

Figure 30. High concentrations of apoE4-homozygous LDL increase PML protein expression in endothelial cells. *PML protein levels were determined using immunoblotting on total lysates of EA.hy926 cells incubated with apoE4-homozygous 25 mg/dL or 100 mg/dL of HDL and 50 mg/dL or 200 mg/dL of LDL for 3h (A) or 24h (B). Expression values relative to an untreated control. Immunoblots are representative of n=4 independent experiments, * p < 0.05 (A), performing two-way ANOVA. All Graphs shown as mean ± SD.*

Since PML is known to have immunomodulatory properties, IL-6 and IL-8 concentrations in the supernatant of EA.hy926 cells incubated without (control) or with different lipoprotein compositions were determined performing ELISA. When the incubation period of the cells was 3 hours (Figure 31A), IL-6 concentrations of the control were 5.1 pg/mL of IL-6. Highest IL-6 concentrations were reached after incubation with comp_$_{LDL200}$, exhibiting 10.9 pg/mL, an enhance of +114 % ($p < 0.01$), followed by IL-6 levels after incubation with comp_$_{LDL100}$, which causes IL-6 concentrations to be slightly higher (7.0 pg/mL; +37 % compared to the control)

than after incubation with the composition with comp_$_{LDL50}$. After 24 hours of incubation (Figure 31B), the control cells exhibited an average of 9.4 pg/mL of IL-6, while again, incubation with comp_$_{LDL200}$ caused the highest IL-6 concentration in the supernatant of 31.7 pg/mL (+237 %; $p < 0.01$), followed by incubation with comp_$_{LDL50}$, which led to an average IL-6 concentration of 28.4 pg/mL (+202 %; $p < 0.05$) and incubation with the composition with physiological lipoprotein concentrations, which enhanced IL-6 concentrations to a total average of 26.4 pg/mL (+181 %; $p < 0.05$).

Besides IL-6, also IL-8 concentrations in the supernatant of EA.hy926 cells incubated without (control) or with lipoprotein compositions were determined after 3 and 24 hours of incubation. After 3 hours of incubation (Figure 31C) average IL-8 concentrations were lowest in the supernatant of the control (51.1 pg/mL), while they were highest after incubation with comp_$_{LDL200}$, reaching an IL-8 concentration of 384.5 pg/mL (+653 % compared to the control; $p < 0.01$). Second highest IL-8 concentrations were measured after incubation with comp_$_{LDL100,}$ reaching an average concentration of 142.6 pg/mL (+ 179 %). When the incubation period was extended to 24 hours (Figure 31D), highest concentrations of IL-8 were expressed in cells incubated with comp_$_{LDL200}$, obtaining an average concentration of 281.7 pg/mL (+516 %; $p < 0.01$), whereas IL-8 levels measured in the supernatants of the control cells had an average of 45.7 pg/mL. Incubation with comp_$_{LDL100}$ caused IL-8 concentrations to enhance to an average of 175.3 pg/mL (+284 %). Clearly, incubation with lipoprotein compositions with high LDL concentrations increases IL-6 and IL-8 protein concentrations in the supernatant of EA.hy926 cells.

Figure 31

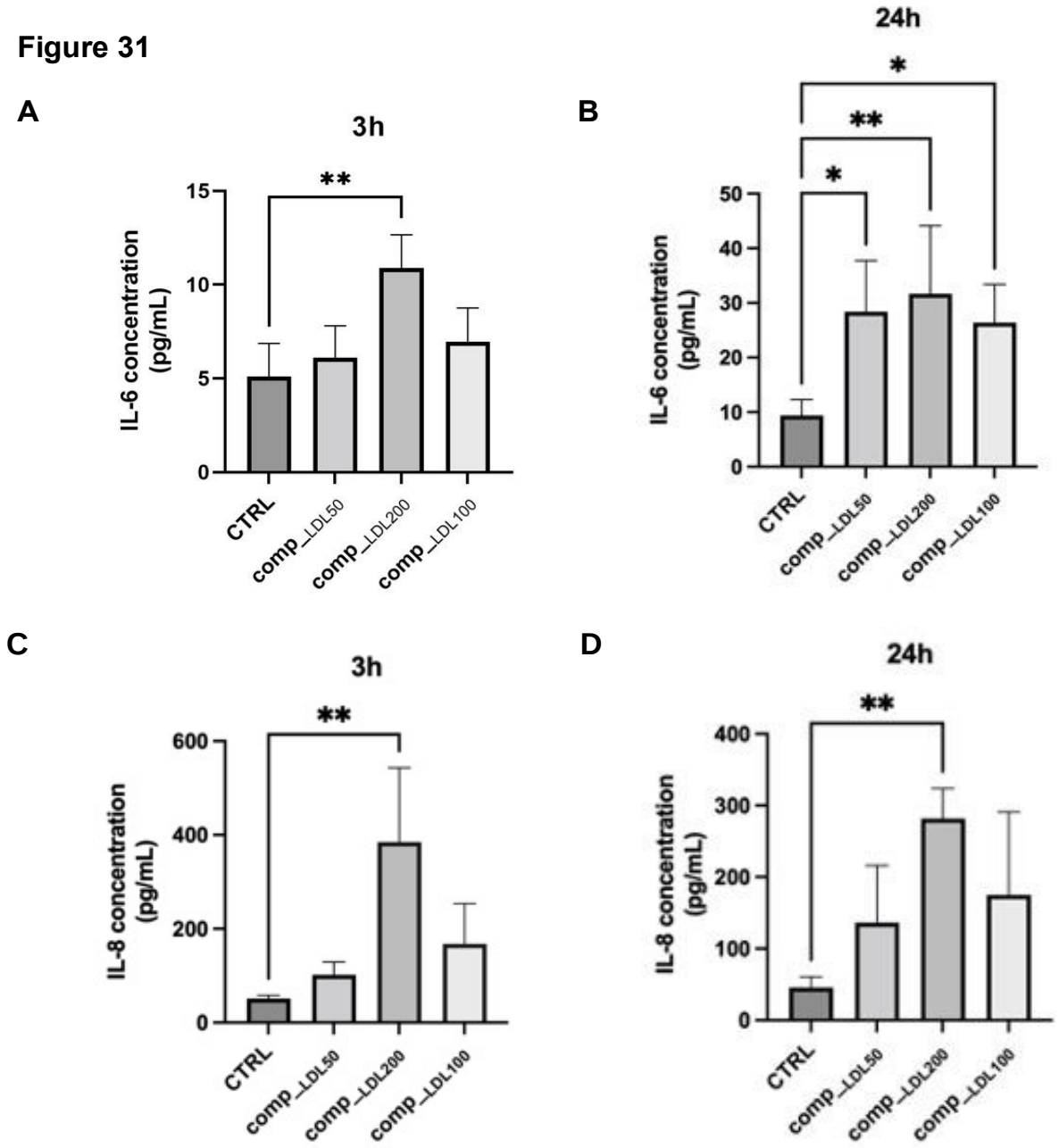

Figure 31. Protein levels of the PML targets IL-6 and IL-8 in endothelial cells increase after incubation with lipoprotein compositions with enhanced LDL concentrations. *(A, B) Determination of IL-6 protein concentrations using ELISA on the supernatant of non-treated EA.hy926 cells or after incubation with lipoprotein compositions with LDL concentrations varying from 50 mg/dL to 200 mg/dL for 3h (A) or 24h (B). n = 3 (A) n=4 (B), * p < 0.05, ** p < 0.01 in one-way ANOVA. (C, D) IL-8 protein concentrations quantified by using ELISA on the supernatant of either untreated EA.hy926 cells (CTRL) or EA.hy926 cells treated with lipoprotein compositions with varying LDL concentrations from 50 mg/dL to 200 mg/dL for 3h (C) or 24h (D). n=3 (C), n=4 (D), ** p < 0.01 using one-way ANOVA. All Graphs shown as mean ± SD.*

To investigate the influence of single lipoproteins on IL-6 and IL-8 secretion in EA.hy926 cells, the experiment was conducted with single blood lipoproteins of different concentrations as well. IL-6 concentrations in the supernatant of EA.hy926 cells incubated with pooled lipoproteins for 3 hours (Figure 32A) were especially high when incubated with 200 mg/dL of LDL. Here the concentration reached an average of 14.6 pg/mL (+186 %; $p < 0.01$), while the concentration measured in the supernatant of untreated control cells measures 5.1 pg/mL. After

incubating EA.hy926 cells for 24 hours (Figure 32B), the control measured an average of 12.5 pg/mL, whereas incubation with 200 mg/dL of LDL led to an average of 29.0 pg/mL (+132 %; $p < 0.05$), followed by incubation with 50 mg/dL of LDL, resulting in an IL-6 concentration of 28.9 pg/mL (+131 %; $p < 0.05$) compared to the control. IL-6 concentrations are higher after an extended incubation period of 24 hours of incubation than after 3 hours.

As executed with incubation with lipoprotein compositions, IL-8 concentrations were measured in the supernatants of EA.hy926 cells by ELISA after incubation with pooled lipoproteins for 3 or 24 hours. After incubating the cells for 3 hours the control sample measured 45.5 pg/mL of IL-8 (Figure 32C). Incubation with 200 mg/dL of LDL caused the highest IL-8 concentration in the supernatant, reaching 203.1 pg/mL (+346 %; $p < 0.05$). When extending the incubation period to 24 hours, the control cells expressed 45.7 pg/mL of IL-8 (Figure 32D). Treatment with 200 mg/dL of LDL enhanced IL-8 concentrations the most, reaching a concentration of IL-8 of 416.5 pg/mL (+811 % compared to control; $p < 0.05$).

Apparently, incubation with LDL causes IL-6 and IL-8 protein concentrations in the supernatant of EA.hy926 cells to enhance after 3 and 24 hours of incubation.

Figure 32

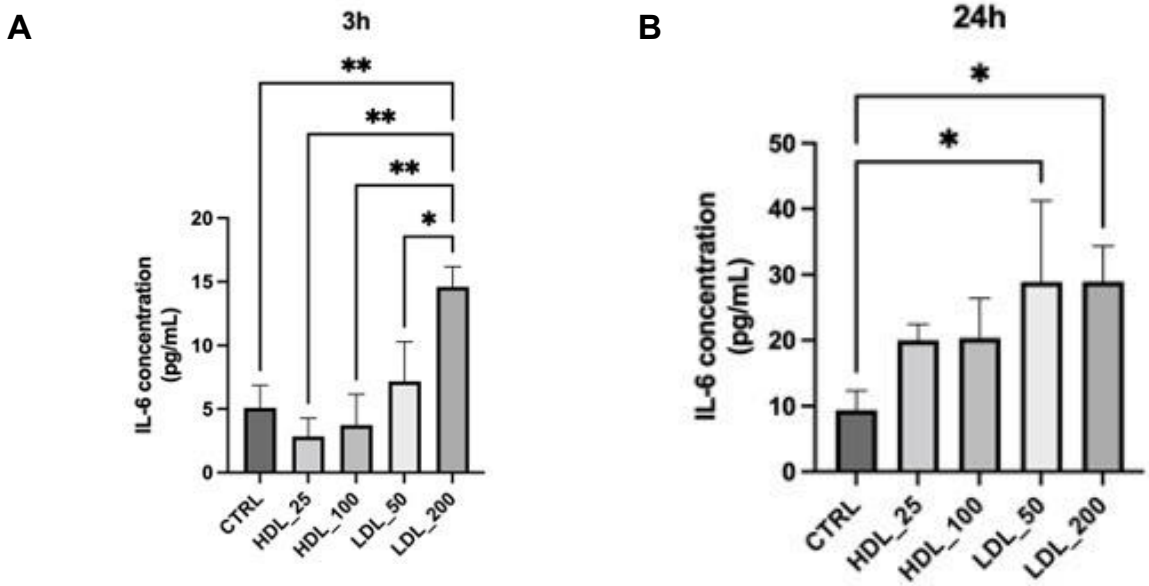

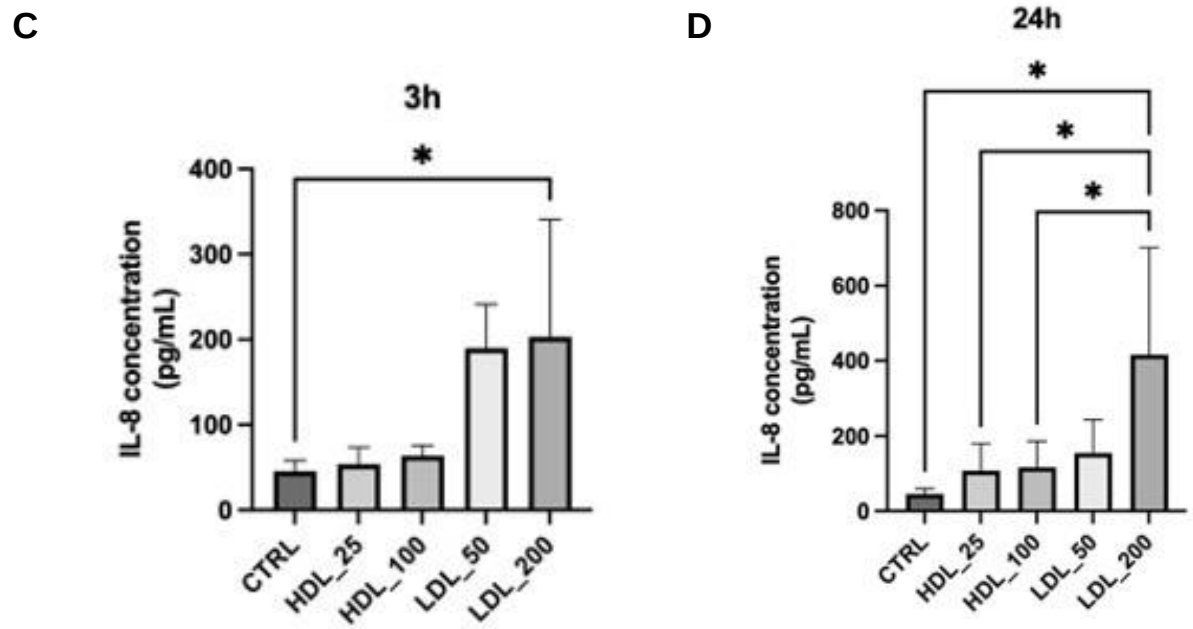

Figure 32. LDL enhances secretion of the PML targets IL-6 and IL-8 in endothelial cells. *(A, B) ELISA was performed to quantify IL-6 protein concentrations in the supernatant of EA.hy926 cells with either no treatment (CTRL) or after incubation with 25 mg/dL or 100 mg/dL of HDL and 50 mg/dL or 200 mg/dL of LDL for 3h (A) or 24h (B). n=3 (A), n=4 (B), * p < 0.05, ** p < 0.01 using one-way ANOVA. (C, D) Quantification of IL-8 protein concentrations using ELISA on the supernatant of either untreated EA.hy926 cells (CTRL) or EA.hy926 cells treated with 25 mg/dL or 100 mg/dL of HDL and 50 mg/dL or 200 mg/dL of LDL for 3h (C) or 24h (D). n=3 (C), n=4 (D) independent experiments, * p < 0.05 performing two-way ANOVA. All Graphs shown as mean ± SD.*

To determine the impact of apoE4-homozygous lipoproteins on IL-6 and IL-8 protein concentrations in the supernatant of EA.hy926, ELISA was performed after 3 or 24 hours of incubation with the apoE4-homozygous lipoproteins. When incubated with apoE4-homozygous lipoproteins for 3 hours (Figure 33A), relative IL-6 protein concentrations were highest when incubated with 200 mg/dL of apoE4-homozygous LDL. While the control cells express a mean of 6.0 pg/mL of IL-6, cells treated with 200 mg/dL of apoE4-homozygous LDL expressed 121 % more IL-6, a total mean of 13.2 pg/mL ($p < 0.05$). The results of incubating the cells for 24 hours and determining IL-6 levels in the supernatants is shown in Figure 33B. IL-6 concentrations in an untreated control were at 15.5 pg/mL. Incubation with 200 mg/dL of apoE4-homozygous LDL again led to the highest IL-6 concentrations measured, 35.7 pg/mL (+130 %; $p < 0.01$). After an incubation period of 24 hours, IL-6 levels enhanced more than after 3 hours of incubation.

EA.hy926 cells were incubated with apoE4-homozygous lipoproteins for 3 or 24 hours before IL-8 levels were determined performing ELISA. When incubated for 3 hours (Figure 33C), untreated cells (control) expressed 351.7 pg/mL of IL-8, whereas treatment with 200 mg/dL of apoE4-homozygous LDL led to IL-8 concentrations of 675.5 pg/mL (+92 %; $p < 0.05$), highest concentrations measured in this experiment. After extending incubation to 24 hours (Figure 33D), IL-8 concentrations measured in the supernatant of control cells were 55.9 pg/mL.

Incubation with 200 mg/dL of apoE4-homozygous LDL again increased IL-8 concentrations the most, reaching concentrations of 979.8 pg/mL (+1653 %, $p < 0.01$). All in all, incubation with high concentrations of LDL causes EA.hy926 cells to express enhanced levels of IL-6 and IL-8 protein.

Figure 33

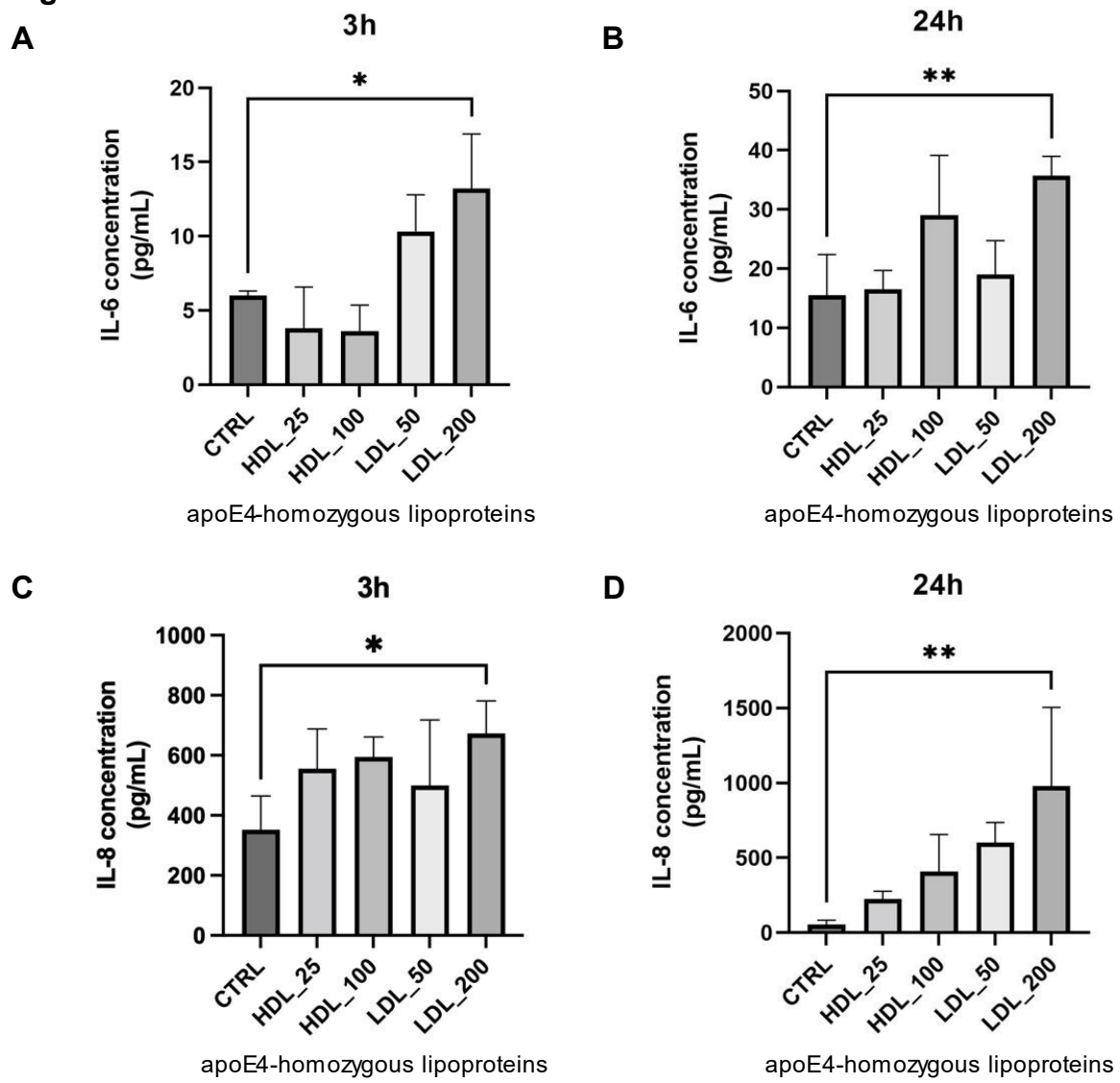

Figure 33. apoE4-homozygous LDL enhances secretion of the PML targets IL-6 and IL-8 in endothelial cells. *(A, B) Quantification of IL-6 protein concentrations in the supernatant of EA.hy926 cells using ELISA after either no treatment (CTRL) or after incubation with 25 mg/dL or 100 mg/dL of apoE4-homozygous HDL and 50 mg/dL or 200 mg/dL of apoE4-homozygous LDL for 3h (A) or 24h (B). n=3 (A), n=4 (B), * p < 0.05, ** p < 0.01 using one-way ANOVA. (C, D) IL-8 protein concentrations were quantified using ELISA on the supernatant of either untreated EA.hy926 cells (CTRL) or EA.hy926 cells treated with 25 mg/dL or 100 mg/dL of apoE4-homozygous HDL and 50 mg/dL or 200 mg/dL of apoE4-homozygous LDL for 3h (C) or 24h (D). n=4, * p < 0.05, ** p < 0.01 in one-way ANOVA. All Graphs shown as mean ± SD.*

To find out whether the LDL-induced increase in IL-6 and IL-8 expression is dependent on PML expression, relative IL-6 and IL-8 mRNA expression were determined using RT-qPCR. EA.hy926 cells transfected with a vector without the specific gene insert served as a control.

Furthermore, EA.hy926 cells were transfected with a pEGFP-C1-PML-IV-vector (PML↑) and incubated for 24 hours, either without or with comp_$_{LDL100}$ supplement. Relative IL-6 mRNA levels (Figure 34A) were 920 % ($p < 0.05$) higher in PML↑ cells than the levels determined in the control cells. Relative IL-6 mRNA levels in PML↑ cells incubated with comp_$_{LDL100}$ expressed were more than 13-fold higher (+1261 %; $p < 0.01$) than the levels of the control. Figure 34B displays relative IL-8 mRNA levels after transfection without or with incubation with comp_$_{LDL100}$ for 24 hours. PML↑ cells showed an increase of +1109 % ($p < 0.05$) in relative IL-8 mRNA levels compared to the control cells. PML↑ cells that were incubated with comp_$_{LDL100}$ for 24 hours even expressed 1160 % ($p < 0.05$) more IL-8 mRNA than the control cells. Taken together, the results indicate that PML cells exhibit higher IL-6 and IL-8 mRNA levels than corresponding cells, which cannot be further increased by additional incubation with blood lipoproteins.

Figure 34

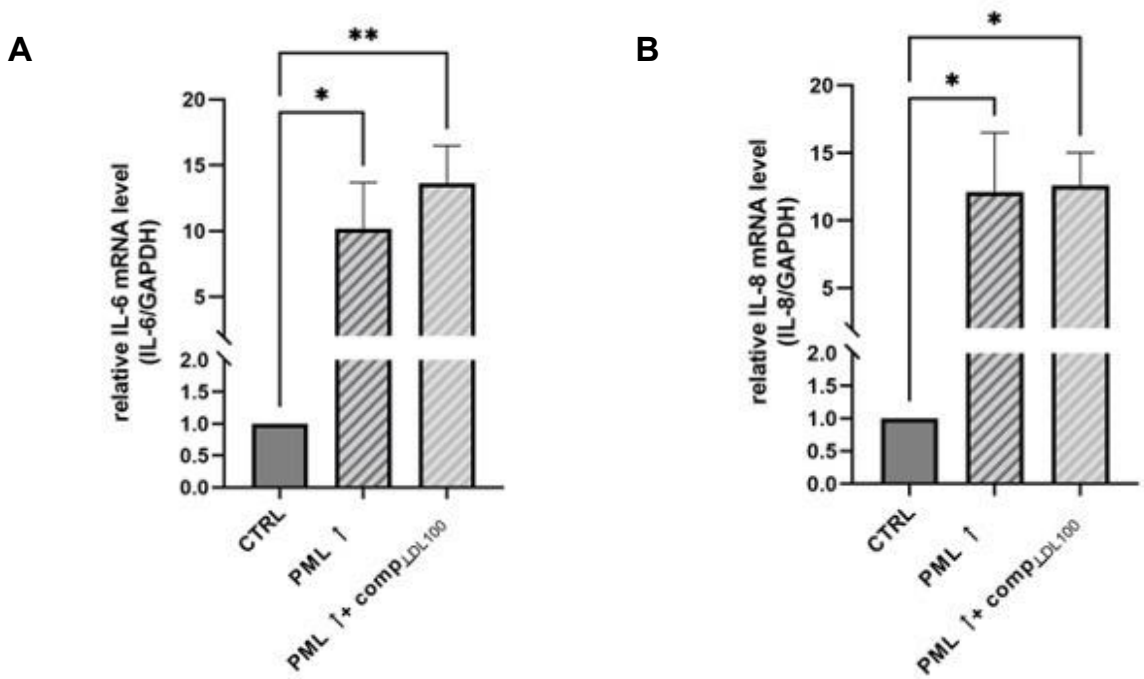

Figure 34. PML overexpression itself or in combination with a lipoprotein composition leads to an increase in IL-6 and IL-8 mRNA expression. *(A) Quantification of IL-6 mRNA levels of EA.hy926 cells transfected with a vector without a specific gene insert, a pEGFP-C1-PML-IV-vector (PML↑) or cells transfected with pEGFP-C1-PML-IV and further incubated with the lipoprotein composition containing 100 mg/dL of LDL for 24h. n=3, * p < 0.05, ** p < 0.01 using two-way ANOVA. (B) Quantification of IL-8 mRNA levels of EA.hy926 cells transfected with a pEGFP-C1-PML-IV-vector (PML↑) or cells transfected with pEGFP-C1-PML-IV and further incubated with the lipoprotein composition containing 100 mg/dL of LDL for 24h. Control cells were transfected with a vector without a specific gene insert n=3, * p < 0.05 using two-way ANOVA. All Graphs shown as mean ± SD.*

3.1.2. LDL-induced upregulation of PKC causes upregulation of PML

To prove that lipoproteins, especially LDL, are capable of increasing PKC activity, a PKC activity ELISA was performed on total cell lysates of EA.hy926 cells after incubation with lipoprotein compositions with different LDL concentrations or with single blood lipoproteins of different concentration. Untreated EA.hy926 cells served as a control. As seen in Figure 35A, incubation with comp_$_{LDL100}$ caused PKC activity to elevate by 65 % ($p < 0.01$). When incubated with comp_$_{LDL200}$, relative PKC activity levels increased (+171 %; $p < 0.001$) compared to the levels measured in the control cells. When incubated with single blood lipoproteins of different concentrations (Figure 35B), incubation with 200 mg/dL of LDL caused the highest relative PKC activity (+90 %; $p < 0.01$). HDL in both concentrations used did not lead to an increase in relative PKC activity levels. Clearly, incubation with lipoprotein compositions with physiological and high LDL levels or single LDL in high concentrations increases PKC activity in EA.hy926 cells.

Figure 35

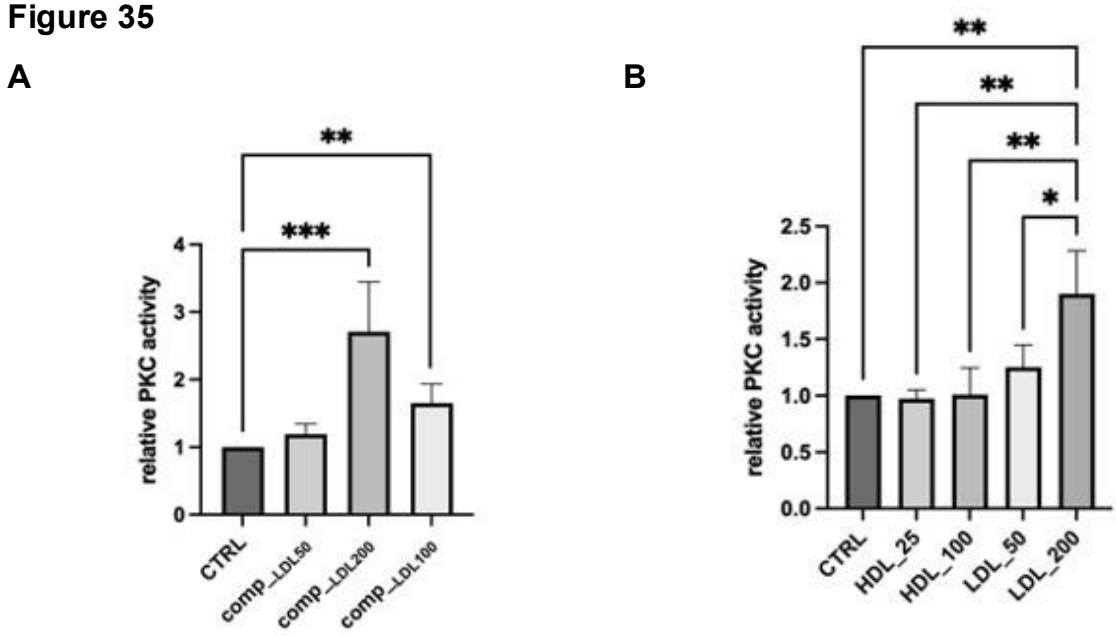

Figure 35. High LDL concentrations increase PKC activity in endothelial cells. *(A) Semi-quantitative detection of levels of activated PKC via ELISA of total cell lysates of EA.hy926 cells incubated with lipoprotein compositions with LDL concentrations varying from 50 mg/dL to 200 mg/dL for 24h. Expression values relative to an untreated control. n=3, ** p < 0.01, *** p < 0.001 using one-way ANOVA. (B) Semi-quantitative detection of levels of activated PKC performing ELISA of total cell lysates of EA.hy926 cells incubated either 25 mg/dL or 100 mg/dL of HDL or with 50 mg/dL or 200 mg/dL of LDL for 24h. Expression values relative to an untreated control. n=3, * p < 0.05, ** p < 0.01 using two-way ANOVA. All Graphs shown as mean ± SD.*

To prove the inhibitory effect of the PKC inhibitor sc-3088, a PKC activity ELISA was performed on total cell lysates of either untreated EA.hy926 cells (control) or on cells that were incubated with sc-3088 for 24 hours (Figure 36A). Compared to the relative levels of active PKC in the control cells, active PKC levels were decreased by 37 % ($p < 0.01$) when incubated

with sc-3088. This experiment was also performed with an activator of PKC, PMA (Figure 36B). EA.hy926 cells that were incubated with PMA for 24 hours showed an increase in relative PKC activity levels of 36 % ($p < 0.0001$) compared to the control.

In addition, the PKC activity ELISA was performed on total cell lysates of untreated EA.hy926 cells (control), or on lysates of EA.hy926 cells either incubated with $comp_{\_LDL100}$ or with sc-3088 in addition to $comp_{\_LDL100}$ (Figure 36C). Compared to the control cells incubation with $comp_{\_LDL100}$ led to an increase in PKC activity of 30 % ($p < 0.05$), while incubation with both, sc-3088 and $comp_{\_LDL100}$ led to a decrease in PKC activity of 30 % ($p < 0.01$) compared to the PKC activity measured in cells incubated with $comp_{\_LDL100}$ only.

When EA.hy926 cells were either incubated without or with $comp_{\_LDL100}$ or PMA in addition to $comp_{\_LDL100}$ (Figure 36D), cells incubated with $comp_{\_LDL100}$ showed an increase in PKC activity of 30 % ($p < 0.01$), while cells incubated with the combination of the composition and PMA showed an increase in relative PKC activity levels of 107 % ($p < 0.001$) compared to the levels measured in the control cells and an increase of 59 % ($p < 0.001$) compared to the levels measured in the cells that were incubated with $comp_{\_LDL100}$ only. As assumed, sc-3088 inhibits (LDL-induced) PKC activity, while PMA increases PKC activity.

Figure 36

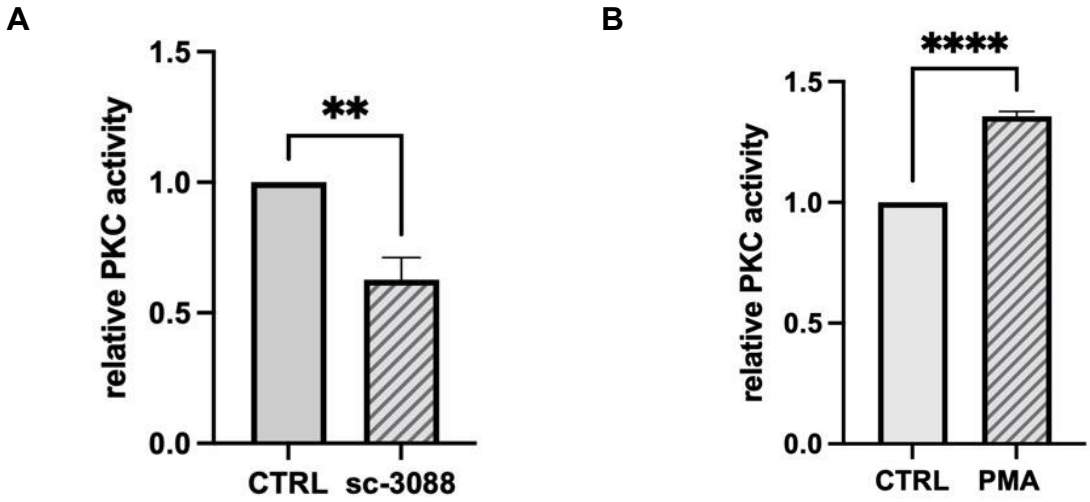

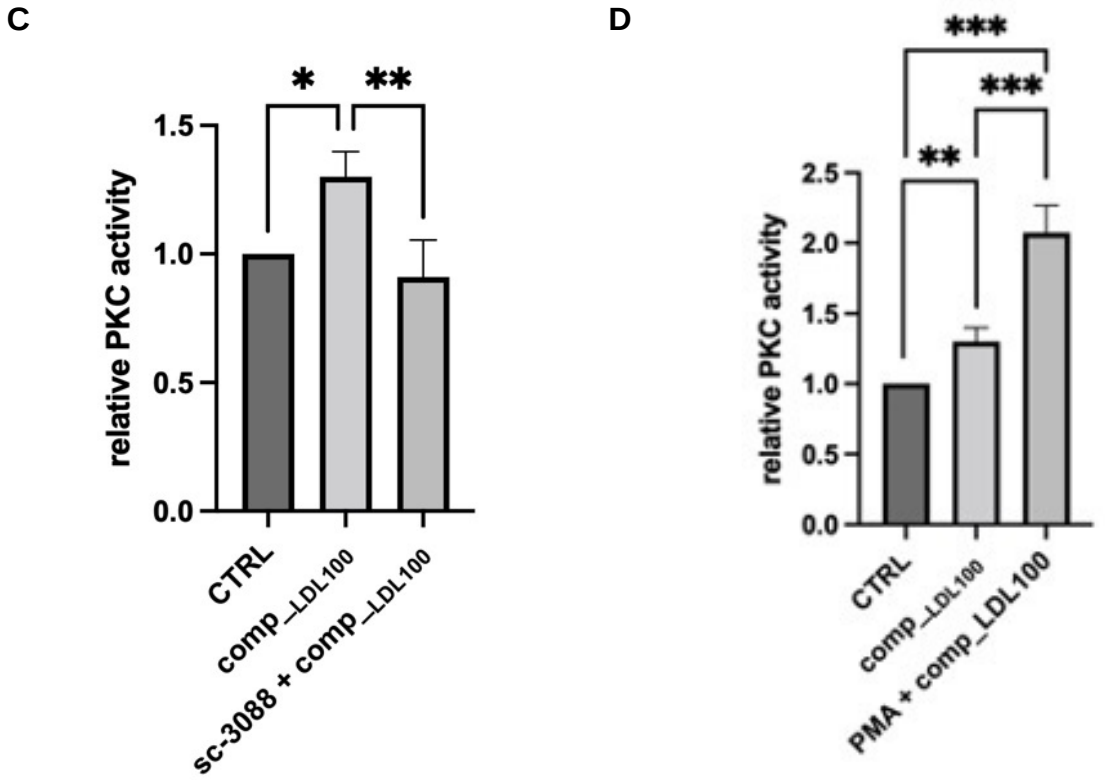

Figure 36. (LDL-induced) activation of PKC in endothelial cells is inhibited by sc-3088, but increased by PMA. *(A) Semi-quantitative detection of levels of activated PKC via ELISA of total cell lysates of EA.hy926 cells incubated with sc-3088 for 24h. Expression values relative to an untreated control. n=3, ** p < 0.01 using Student's t-test. (B) Semi-quantitative detection of levels of activated PKC via ELISA of total cell lysates of EA.hy926 cells incubated with PMA for 24h. Expression values relative to an untreated control. n=3, **** p < 0.0001 using Student's t-test. (C) Activated PKC levels were detected via ELISA in total lysates of EA.hy926 cells after incubation with either the lipoprotein composition with physiological lipoprotein concentrations or with sc-3088 in addition to the composition for 24h. Expression values relative to a control that was not treated. n=3, * p < 0.05, ** p < 0.01 using one-way ANOVA. (D) Active PKC was measured in total cell lysates of EA-hy926 cells after incubation for 24h with either the physiologically concentrated lipoprotein composition or with both, the composition and PMA combined. Untreated cells incubated with medium only served as a control. Expression values relative to the control. n=3, ** p < 0.01, *** p < 0.001. All Graphs shown as mean ± SD.*

To determine whether PML expression is linked to PKC activity, RT-qPCR was performed on EA.hy926 cells that were incubated without (control) or with sc-3088 for 24 hours to detect relative PML mRNA levels (Figure 37A). Cells incubated with sc-3088 showed a decrease in relative PML mRNA levels of 94 % ($p < 0.0001$) compared to the control.

To secure the assumption that PML expression is influenced by PKC activity, EA.hy926 cells were transfected with a vector lacking specific gene insert (control), or with a pEGFP-C1-PML-IV-vector (PML↑), and incubated without (control) or with sc-3088 (Figure 37B). Relative PML mRNA levels were detected performing RT-qPCR. PML↑ cells showed an increase in relative PML mRNA levels of 10511 % ($p < 0.001$) compared to the levels measured in the control cells, while incubation of PML↑ cells with sc-3088 caused PML mRNA levels to decrease (-87 %; $p < 0.001$) compared to the PML↑ cells. These experiments were conducted with PMA as well. As shown in Figure 37C, incubation of EA.hy926 cells with PMA for 24

hours led to elevated relative PML mRNA levels (+ 329 %; $p < 0.05$) compared to the levels detected in the control. Furthermore, as shown in Figure 37D, PML↑ cells showed an increase in relative PML mRNA levels of 10511 % ($p < 0.001$) compared to the control (transfected with an empty vector), whereas in PML↑ cells incubated with PMA enhanced relative PML mRNA levels of 19211 % ($p < 0.05$) were detected.

Immunoblotting was performed on total cell lysates of EA.hy926 cells either left untreated (control) or incubated with sc-3088 for 24 hours to determine relative PML protein levels (Figure 37E). When incubated with sc-3088, relative PML protein decreased by 66 % ($p < 0.01$) compared to the relative PML protein levels in the control cells. Immunoblotting was further performed on PML↑ cells either incubated without or with sc-3088 to determine relative PML protein levels. Control cells were transfected with a vector that did not have any specific gene insert. PML↑ cells expressed 4 times as much PML protein as the control cells (+ 307 %; $p < 0.05$), while PML↑ cells that were incubated with sc-3088 showed decreased relative PML protein levels by 70 % ($p < 0.05$) compared to untreated PML↑ cells.

In order to investigate the influence of sc-3088 or PMA on the number of PML-NBs, immunofluorescence was performed on EA.hy926 cells incubated without treatment to serve as a control (representative image shown in Figure 37G) or on EA.hy926 cells incubated with sc-3088 for 24 hours (representative image shown in Figure 37H). As shown in Figure 37J, control cells showed an average of 14.4 PML-NBs per nucleus, whereas after incubation with sc-3088 for 24 hours, PML-NB expression was decreased to 9.3 PML-NBs per nucleus (-35 %; $p < 0.01$). When incubated with PMA (Figure 37I), the number of PML-NBs increased from an average of 13.5 PML-NBs per nucleus in the control to 19.9 PML-NBs per nucleus (+47 %; $p < 0.0001$, Figure 37K). When immunofluorescence analysis was performed on HUVECs incubated with sc-3088 for 24 hours or left untreated (control) (Figure 37L and M), treatment with sc-3088 caused a decrease in the number of PML-NBs from 11.3 PML-NBs in the control cells to an average of 7 PML-NBs per nucleus (-38 %; $p < 0.0001$, s. Figure 37O). When incubated without or with PMA for 24 hours (Figure 37L and N), incubation of HUVEC with PMA led to an increase in PML-NB numbers from an average of 11.3 PML-NBs in the nuclei of the control cells to 17.2 PML-NBs (+52 %; $p < 0.0001$, s. Figure 37P).

All in all, sc-3088 decreases PML mRNA and protein expression as well as the number of PML-NBs in EA.hy926 cells, whereas PMA increases PML mRNA, protein and the number of PML-NBs.

Figure 37

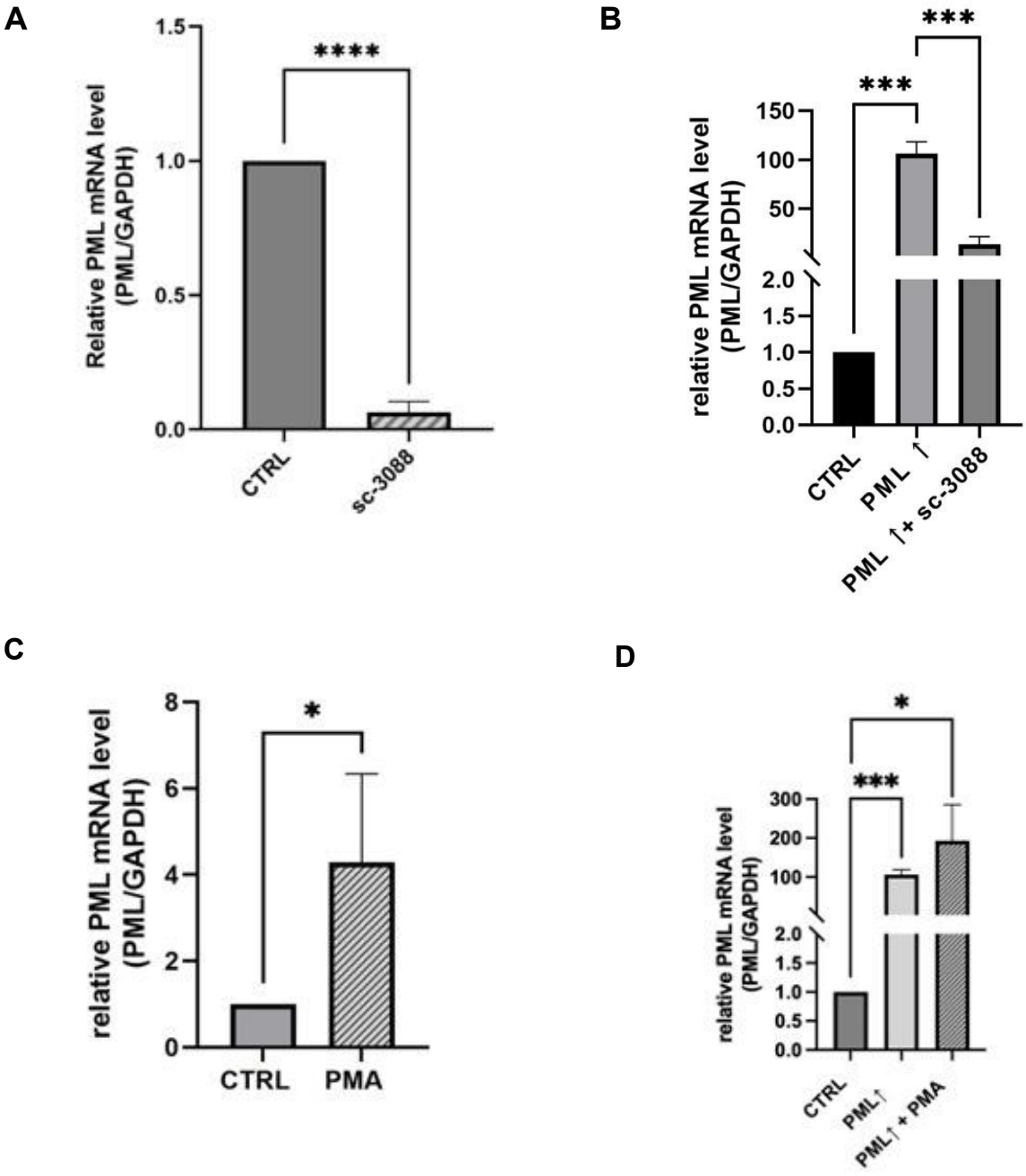
A
Relative PML mRNA level (PML/GAPDH)
1.5
1.0
0.5
0.0
****
CTRL
sc-3088
B
relative PML mRNA level (PML/GAPDH)
***
***
150
100
50
2.0
1.5
1.0
0.5
0.0
CTRL
PML ↑
PML ↑+ sc-3088
C
relative PML mRNA level (PML/GAPDH)
8
6
4
2
0
*
CTRL
PMA
D
relative PML mRNA level (PML/GAPDH)
*
***
300
200
100
2.0
1.5
1.0
0.5
0.0
CTRL
PML↑
PML↑ + PMA

E

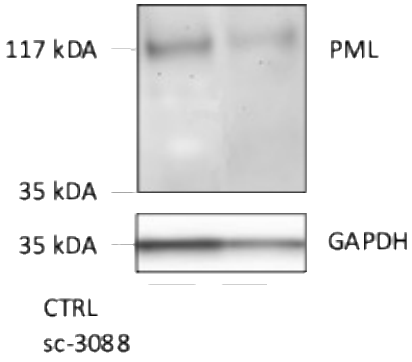
117 kDA
PML
35 kDA
35 kDA
GAPDH
CTRL
sc-3088

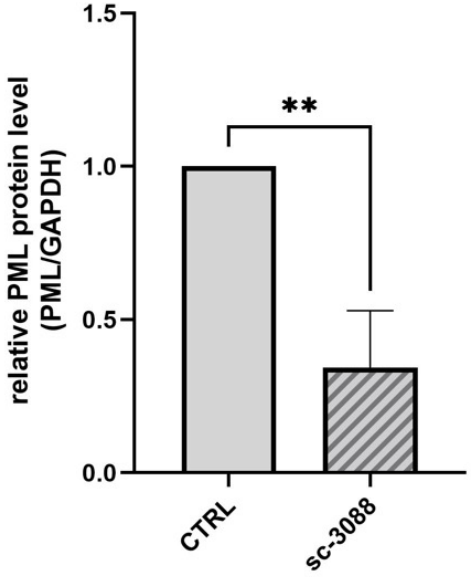
relative PML protein level (PML/GAPDH)
1.5
1.0
0.5
0.0
**
CTRL
sc-3088

F

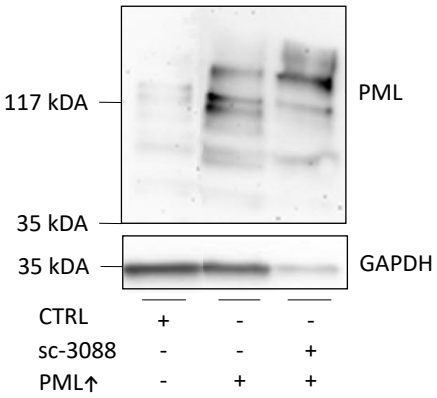
117 kDA
PML
35 kDA
35 kDA
GAPDH
CTRL + - -
sc-3088 - - +
PML↑ - + +

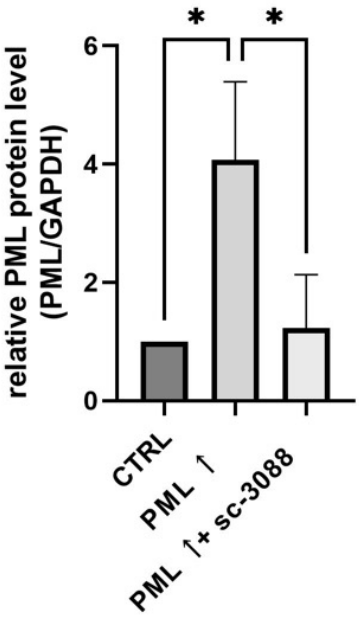
relative PML protein level (PML/GAPDH)
6
4
2
0
* *
CTRL
PML ↑
PML ↑+ sc-3088

G

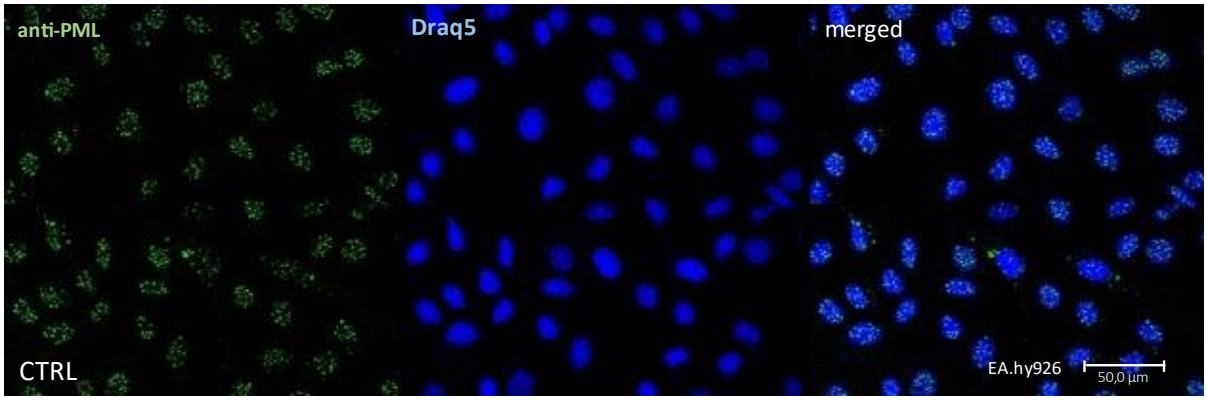
anti-PML
Draq5
merged
CTRL
EA.hy926
50,0 µm

H

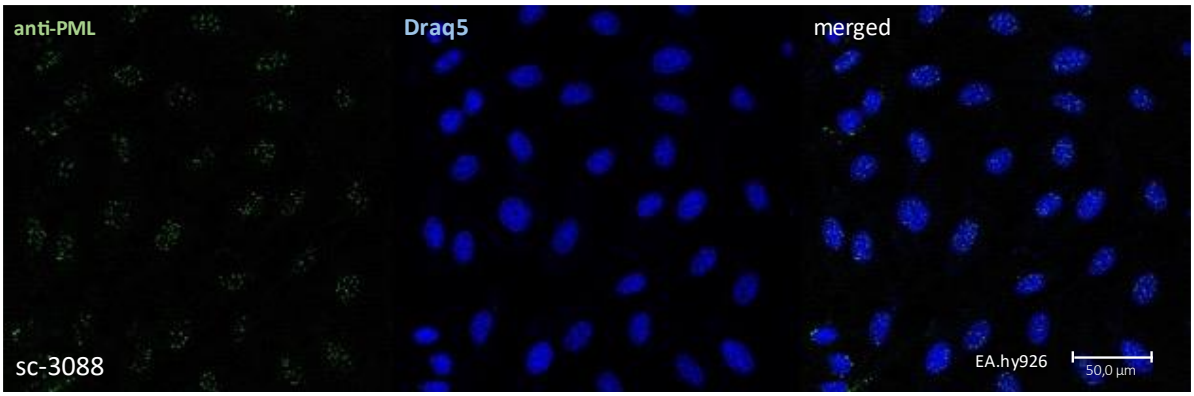
anti-PML
Draq5
merged
sc-3088
EA.hy926
50,0 µm

I

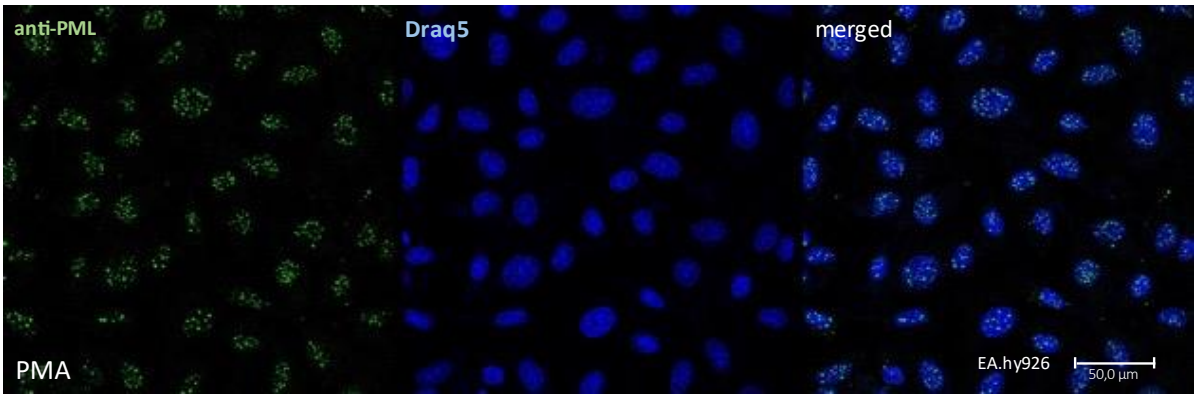
anti-PML
Draq5
merged
PMA
EA.hy926
50,0 µm

J

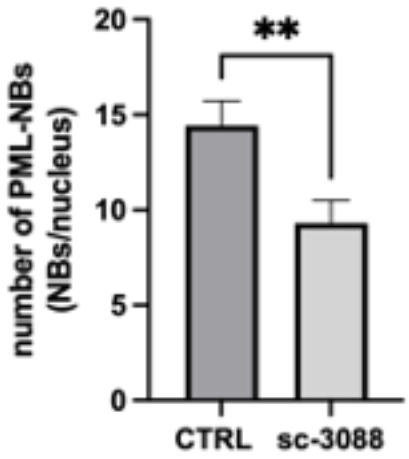
number of PML-NBs
(NBs/nucleus)
20
15
10
5
0
**
CTRL
sc-3088

K

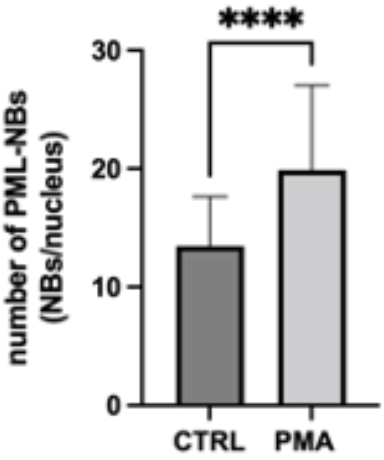
number of PML-NBs
(NBs/nucleus)
30
20
10
0
****
CTRL
PMA

L

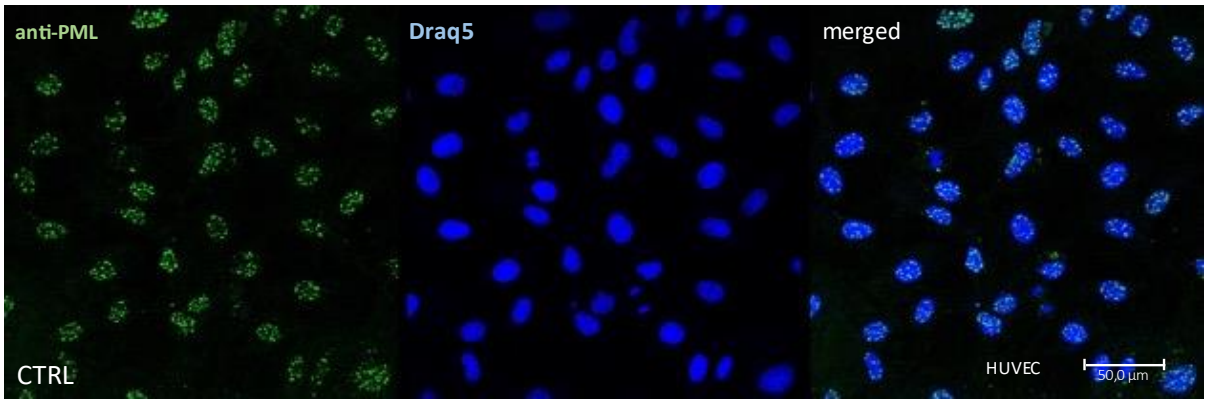
anti-PML
Draq5
merged
CTRL
HUVEC
50,0 µm

M

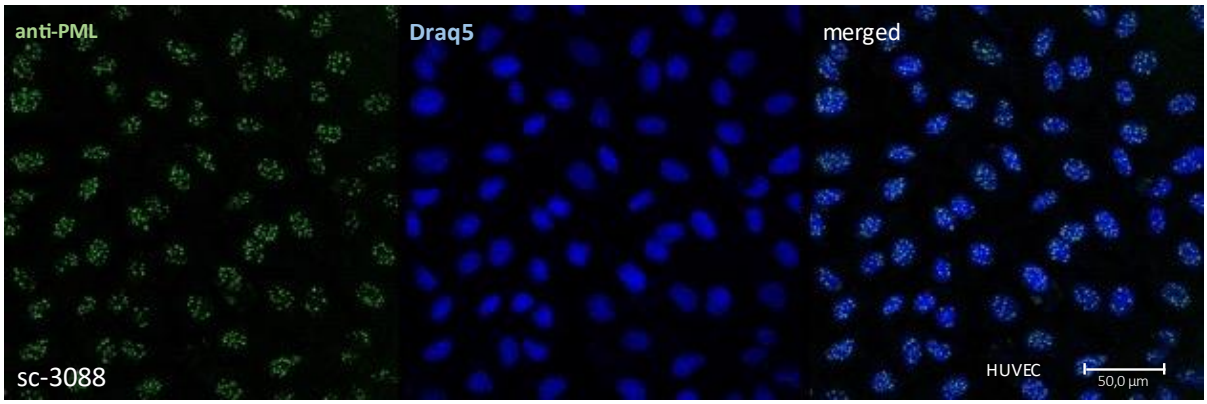
anti-PML
Draq5
merged
sc-3088
HUVEC
50,0 µm

N

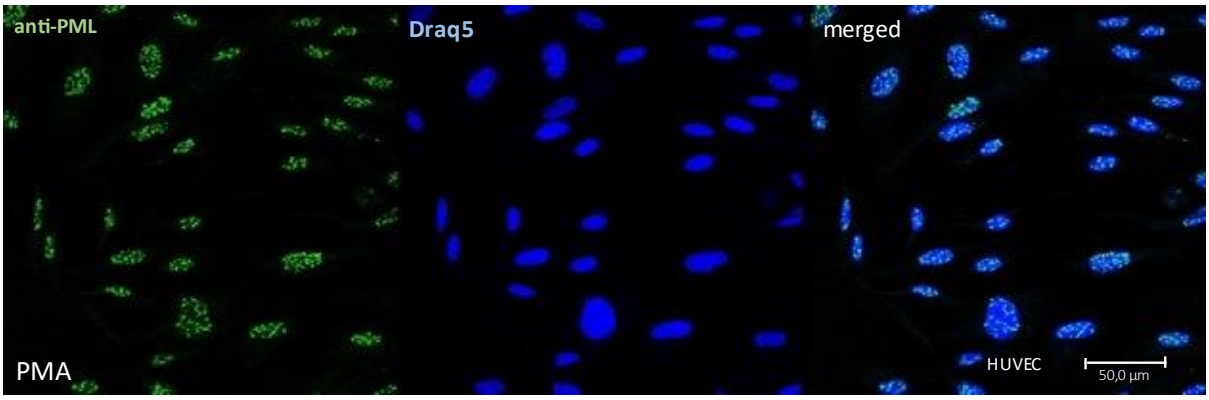
anti-PML
Draq5
merged
PMA
HUVEC
50,0 µm

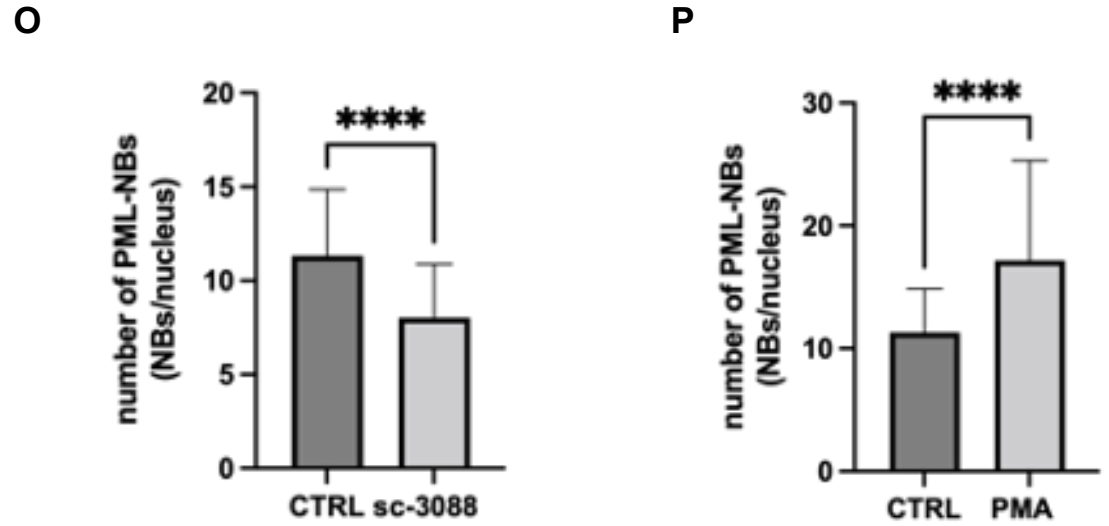

Figure 37. The PKC inhibitor sc-3088 significantly decreases PML mRNA and protein expression and lowers the number of PML-NBs in endothelial cells, the PKC activator PMA enhances PML mRNA levels and the number of PML-NBs in endothelial cells. *(A) PML mRNA levels were determined performing RT-qPCR on EA.hy926 cells incubated with the PKC-peptide inhibitor sc-3088 for 24h. Expression values relative to control (CTRL, no lipoprotein supplement). n=3, **** p < 0.0001 using Student's t-test. (B) Quantification of PML mRNA levels of EA.hy926 cells transfected with a vector without a specific gene insert, a pEGFP-C1-PML-IV-vector (PML↑) or cells transfected with pEGFP-C1-PML-IV and further incubated with sc-3088 for 24h. n=3, *** p < 0.001 using two-way ANOVA. (C) PML mRNA levels were determined performing RT-qPCR on EA.hy926 cells incubated with the PKC-peptide activator PMA for 24h. Expression values relative to control (CTRL, no lipoprotein supplement). n=3, * p < 0.05 using Student's t-test. . (D) Quantification of PML mRNA levels of EA.hy926 cells transfected with a vector without a specific gene insert, a pEGFP-C1-PML-IV-vector (PML↑) or cells transfected with pEGFP-C1-PML-IV and further incubated with PMA for 24h. n=3, * p < 0.05 using two-way ANOVA. (E) Immunoblotting to quantify PML protein levels in the total lysates of EA.hy926 cells incubated with sc-3088 for 24h. Expression values relative to an untreated control (CTRL). Representative immunoblot of n=3, ** p < 0.01 using Student's t-test. (F) Immunoblotting for the determination of PML protein levels of total lysates of EA.hy926 cells after transfection with a vector without a specific gene insert, a pEGFP-C1-PML-IV-vector (PML↑) or cells after transfection with pEGFP-C1-PML-IV and incubation with sc-3088 for 24h. n=3, representative immunoblot shown, * p < 0.05 using two-way ANOVA. (J) Immunofluorescence of EA.hy926 cells with an anti-PML (green) antibody was performed to determine the number of PML-NBs after incubation without supplement (CTRL, G) or with sc-3088 (H) for 24h. The cell nuclei were accentuated using Draq5 (blue). n=3 independent experiments with 40 – 60 nuclei evaluated; images shown are representatives. ** p < 0.01 using Student's t-test. (I, K) Immunofluorescence was performed on EA.hy926 cells after incubation with PMA for 24 hours. Anti-PML (green) and anti-tubulin (not shown) were used to determine the number of PML-NBs per nucleus. Draq5 was used to highlight the nuclei (blue). Control cells were left untreated. Representative image of n=1 with 60 nuclei analysed shown, **** p < 0.0001 using Student's t-test. Immunofluorescence was performed on HUVEC with anti-PML (green) and anti-tubulin (not shown) to determine the number of PML-NBs after incubation with sc-3088 (M, O) or PMA (N, P). Control cells (L) were left untreated. Draq5 was used to highlight the nuclei (blue). Images shown are representative of n=1 with 60 nuclei analysed. **** p < 0.0001 using Student's t-test. All Graphs shown as mean ± SD.*

To examine whether PKC has an impact on the LDL-induced increase of relative PML mRNA levels, EA.hy926 cells were incubated without (control) treatment, with comp_$_{LDL100}$ alone, or with comp_$_{LDL100}$ and sc-3088 together (Figure 38A). To detect relative PML mRNA levels, RT-qPCR was used. Incubation with comp_$_{LDL100}$ enhanced relative PML mRNA levels more than 3-fold (+266 %; $p < 0.01$) compared to the control cells, whereas cells incubated with both, comp_$_{LDL100}$ and sc-3088 combined expressed decreased PML mRNA levels compared to cells incubated with comp_$_{LDL100}$ only (-81 %; $p < 0.01$). To determine if PKC activity modulates (LDL-induced) PML mRNA expression, cells were incubated without treatment, incubated with comp_$_{LDL100}$ or with both, comp_$_{LDL100}$ and PMA (Figure 38B). In contrast to the control cells, cells incubated with the composition showed elevated relative PML mRNA levels, while

treatment with the composition and PMA combined elevated PML mRNA levels more than 3-fold (+227 %; $p < 0.05$) compared to the control.

Additionally, immunoblotting was performed to detect relative PML protein levels. As depicted in Figure 38C, EA.hy926 cells were incubated without treatment (control), treated with sc-3088 or comp_$_{LDL100}$ alone or with the two of them combined for a 24 hour period. When incubated with sc-3088, relative PML protein levels lowered to 34 % ($p < 0.01$) of the protein levels detected in the control cells, whereas incubation with comp_$_{LDL100}$ caused the endothelial cells to express increased PML protein levels (+54 %; $p < 0.05$). When treated with the combination of sc-3088 and comp_$_{LDL100}$, PML protein expression in cells incubated with the combination even reduced by 65 % ($p < 0.01$) compared to cells incubated with comp_$_{LDL100}$ alone. Immunoblotting was executed for PML↑ cells as well (Figure 38D). PML↑ cells were incubated without treatment, incubated with comp_$_{LDL100}$ or with sc-3088 and comp_$_{LDL100}$ together for 24 hours. EA.hy926 cells transfected with a vector lacking specific gene insert served as a control. Incubation of PML↑ cells with comp_$_{LDL100}$ led to an increase in PML protein levels (+218 %; $p < 0.01$). Treating PML↑ cells with a combination of sc-3088 and comp_$_{LDL100}$ led to lower relative PML protein levels (-83 %; $p < 0.01$) compared to PML↑ cells treated with comp_$_{LDL100}$ only. Obviously, PKC appears to be an important link in the LDL-induced upregulation of PML in endothelial cells.

Figure 38

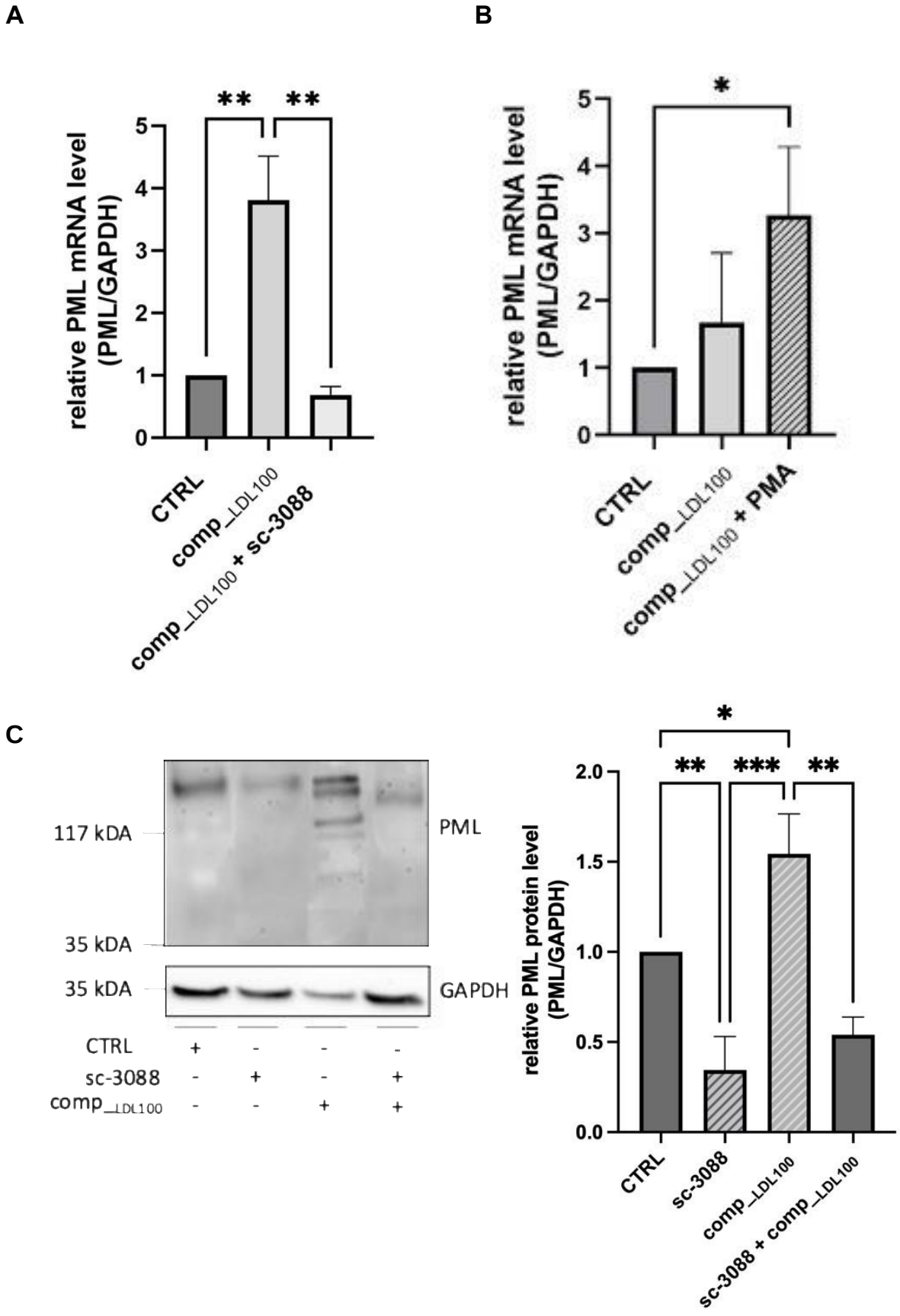
A
B
C
relative PML mRNA level (PML/GAPDH)
**
**
CTRL
comp_LDL100
comp_LDL100 + sc-3088
*
comp_LDL100 + PMA
117 kDA
35 kDA
PML
GAPDH
CTRL
sc-3088
comp_LDL100
relative PML protein level (PML/GAPDH)
***
sc-3088 + comp_LDL100

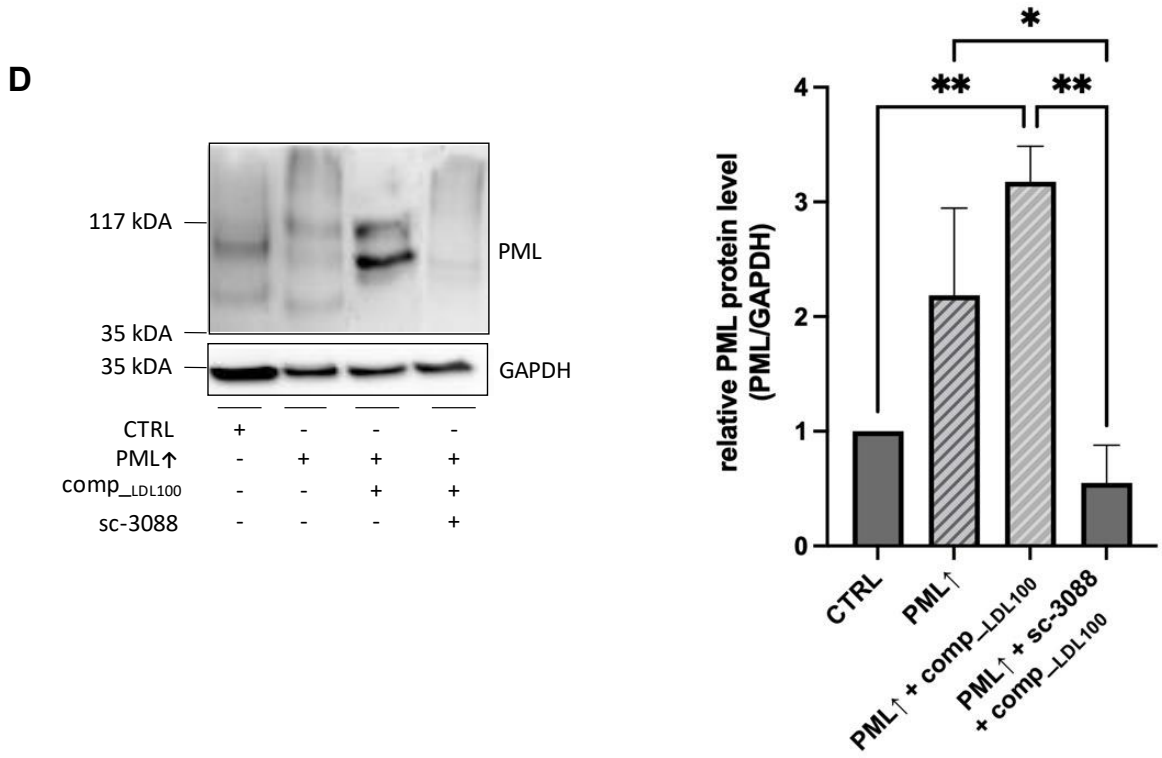

Figure 38. sc-3088 decreases LDL-induced PML mRNA and protein expression in endothelial cells. *(A) RT-qPCR was performed on EA.hy926 cells to quantify PML mRNA levels after incubation with lipoprotein composition with 100 mg/dL of LDL or with the composition and sc-3088 combined for 24h. Expression values relative to control (CTRL, no lipoprotein supplement). n=3, ** p < 0.01 in one-way ANOVA. (B) RT-qPCR was performed on EA.hy926 cells to quantify PML mRNA levels after incubation with lipoprotein composition with 100 mg/dL of LDL or with the composition and PMA combined for 24h. Expression values relative to control (CTRL, no lipoprotein supplement). n=3, * p < 0.05 in one-way ANOVA. (C) To quantify PML protein levels, immunoblotting was used on EA.hy926 cells incubated with lipoprotein composition with 100 mg/dL of LDL or with the composition and sc-3088 combined for 24h. Expression values relative to an untreated control. Representative immunoblot of n=3 is shown, * p < 0.05, ** p < 0.01, *** p < 0.001 using one-way ANOVA. (D) Immunoblotting was used to quantify PML protein levels on EA.hy926 after transfection with a pEGFP-C1-PML-IV-vector (PML↑), cells after transfection with pEGFP-C1-PML-IV and incubation with the lipoprotein composition containing 100 mg/dL of LDL, or cells that were incubated with sc-3088 and the composition combined for 24h after transfection with pEGFP-C1-PML-IV. Expression values relative to control (transfection with vector without a specific gene insert). Representative immunoblot of n=3, * p < 0.5, ** p < 0.01, *** p 0.001 performing two-way ANOVA. All Graphs shown as mean ± SD.*

3.1.3. The LDL-induced increase in STAT3 affects PML mRNA expression

To determine the influence of lipoprotein compositions on STAT3 mRNA and protein expression, RT-qPCR and immunoblotting were performed. Relative STAT3 mRNA levels were determined after incubating EA.hy926 cells with different concentrated lipoprotein compositions for 3 hours (Figure 39A). STAT3 mRNA levels did not significantly change after this incubation period. When extending the duration of incubation from 3 to 24 hours and detecting relative PML mRNA levels (Figure 39B), incubation with comp_$_{LDL200}$ increased relative PML levels the most (+132 %; $p < 0.05$). All measurements were compared to the relative PML mRNA levels detected in the untreated control cells.

Relative STAT3 protein levels were detected using immunoblotting on EA.hy926 cells that were incubated with lipoprotein compositions of different concentrations. Untreated cells

served as a control. As shown in Figure 39C, lowest levels were detected in cells incubated with comp_$_{LDL50}$ (-65 %; $p < 0.01$), followed by the levels that were measured after treatment with comp_$_{LDL100}$ (-61 %; $p < 0.01$). Incubation with comp_$_{LDL200}$ caused the least decrease in relative PML protein levels compared to the levels measured in the control cells (-48 %; $p < 0.05$). When the incubation span was extended to 24 hours of incubation (Figure 39D), incubation with comp_$_{LDL200}$ for 24 hours caused an increase in relative PML protein levels (+108 %; $p < 0.05$).

Besides relative STAT3 protein levels, relative protein levels of phosphorylated STAT3 (pSTAT3) were detected to determine the impact of lipoprotein compositions on the activation of STAT3. When EA.hy926 cells were incubated with different concentrated lipoprotein compositions for 3 hours (Figure 39E), an increase in relative pSTAT3 levels was measured in EA.hy926 cells incubated with comp_$_{LDL200}$ (+156 %;$p < 0.05$). As before, the incubation period was extended to 24 hours (Figure 39F). Elevated pSTAT3 levels were detected after EA.hy926 cells were incubated with comp_$_{LDL200}$ (+143 %; $p < 0.05$). Obviously, incubation with lipoprotein compositions with high LDL levels for 24 hours leads to an increase in STAT3 mRNA and protein expression and its activation.

Figure 39

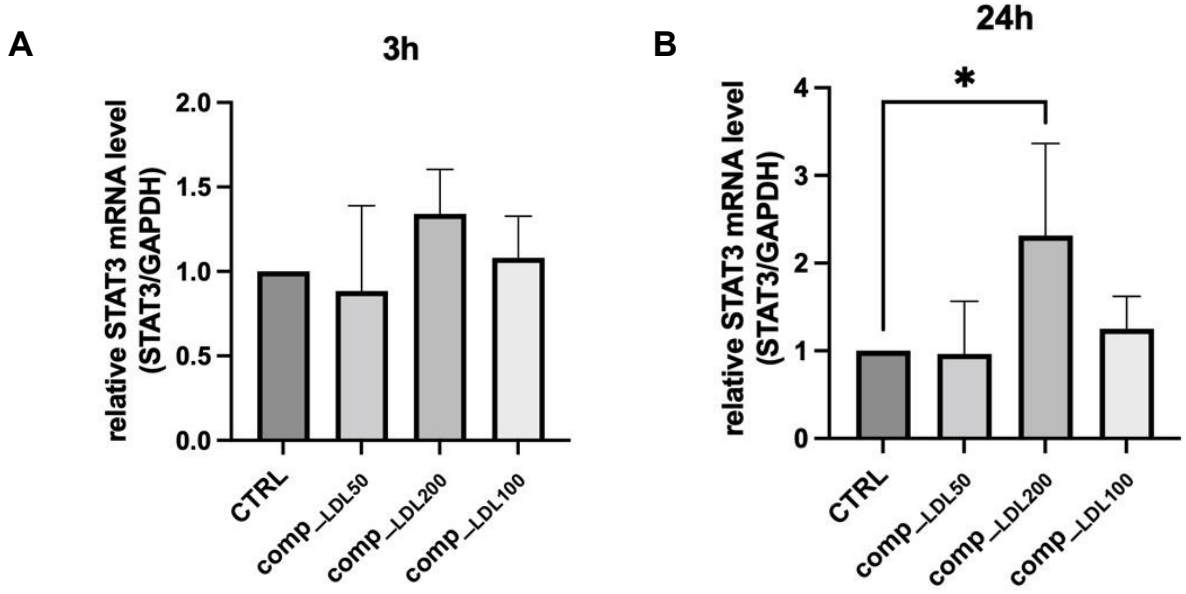

C

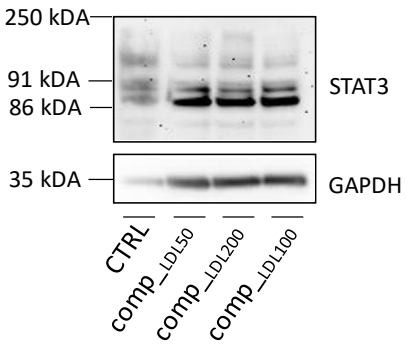
250 kDA
91 kDA
86 kDA
STAT3
35 kDA
GAPDH
CTRL
comp_LDL50
comp_LDL200
comp_LDL100

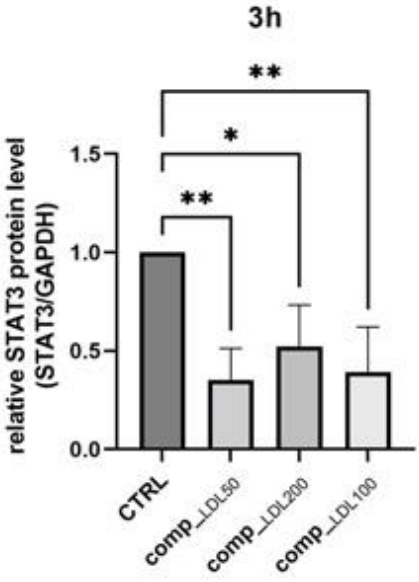
3h
**
*
**
relative STAT3 protein level (STAT3/GAPDH)
1.5
1.0
0.5
0.0
CTRL
comp_LDL50
comp_LDL200
comp_LDL100

D

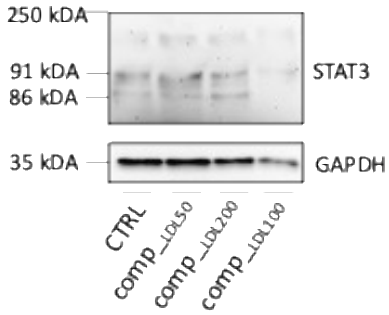
250 kDA
91 kDA
86 kDA
STAT3
35 kDA
GAPDH
CTRL
comp_LDL50
comp_LDL200
comp_LDL100

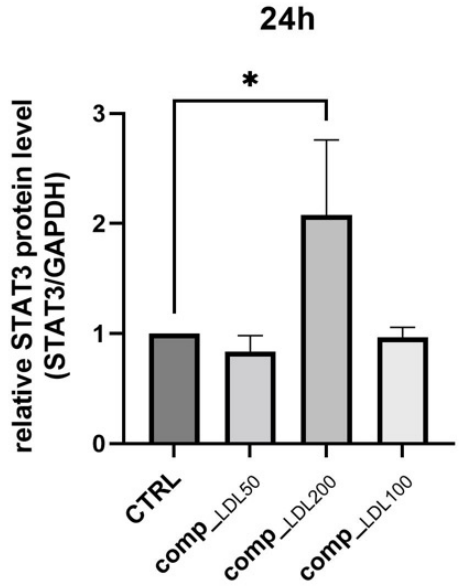
24h
*
relative STAT3 protein level (STAT3/GAPDH)
3
2
1
0
CTRL
comp_LDL50
comp_LDL200
comp_LDL100

E

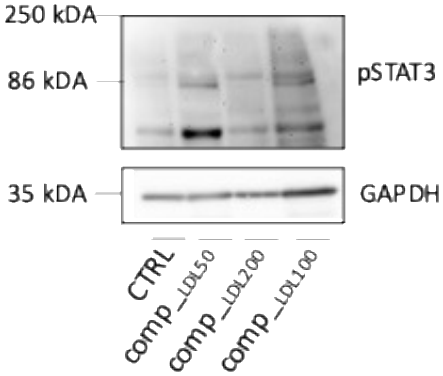
250 kDA
86 kDA
pSTAT3
35 kDA
GAPDH
CTRL
comp_LDL50
comp_LDL200
comp_LDL100

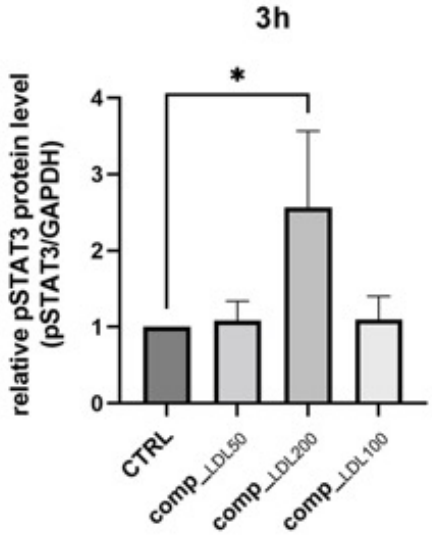
3h
*
relative pSTAT3 protein level (pSTAT3/GAPDH)
4
3
2
1
0
CTRL
comp_LDL50
comp_LDL200
comp_LDL100

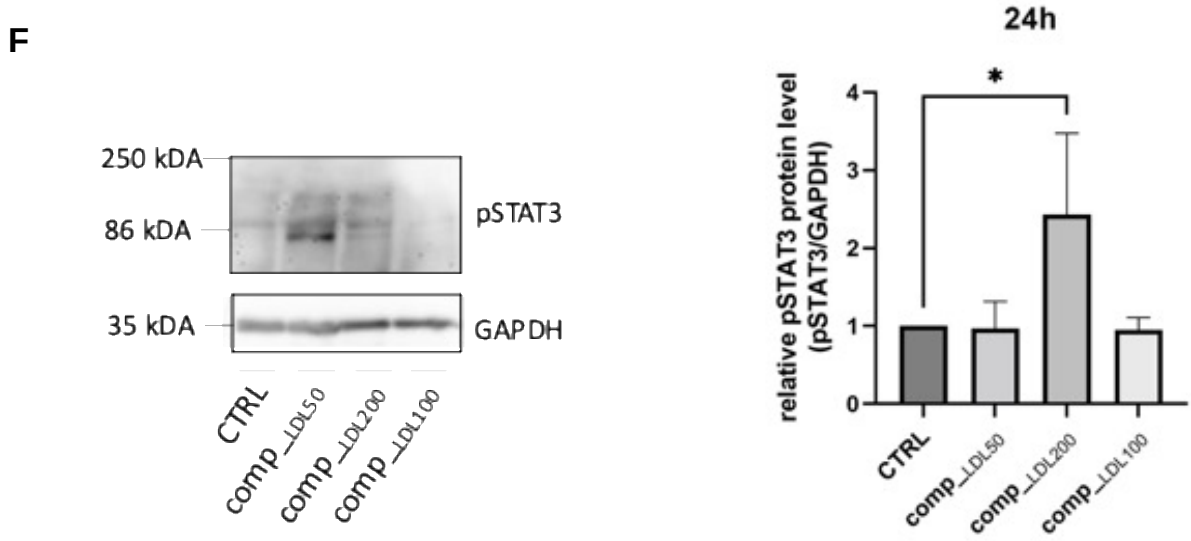

Figure 39. Lipoprotein compositions with high LDL concentrations lead to an increase in STAT3 and pSTAT3 expression in endothelial cells. *Quantification of STAT3 mRNA levels using RT-qPCR on EA.hy926 cells incubated with lipoprotein compositions with LDL concentrations varying from 50 mg/dL to 200 mg/dL for 3h (A) or 24h (B). Expression values relative to an untreated control. n=4, p < 0.99 (A), * p < 0.05 (B) using one-way ANOVA. (C, D) Immunoblotting used for determination of STAT3 protein concentrations on total lysates of untreated EA.hy926 cells or after incubation with lipoprotein compositions with LDL concentrations varying from 50 mg/dL to 200 mg/dL for 3h (C) or 24h (D). Representative immunoblot of n=3, * p < 0.05, ** p < 0.01 in one-way ANOVA. (E, F) pSTAT3 protein concentrations quantified by immunoblotting of total lysates of EA.hy926 cells treated with lipoprotein compositions with varying LDL concentrations from 50 mg/dL to 200 mg/dL for 3h (E) or 24h (F). Expression values relative to control without lipoprotein supplement, representative immunoblot of n=3, * p < 0.05, using one-way ANOVA. All Graphs shown as mean ± SD.*

To examine the influence of the inhibitor STATTIC on relative STAT3 and pSTAT3 protein levels of EA.hy926 cells, the cells were either left untreated (control) or incubated with STATTIC for 24 hours. Relative STAT3 protein levels were determined performing immunoblotting (Figure 40A). No effect was determined compared to the control. Relative pSTAT3 protein levels after 24 hours of incubation with STATTIC (Figure 40B) were decreased by 51 % ($p < 0.05$) compared to the levels of the control cells. Apparently STATTIC causes a decrease in active STAT3 levels.

Figure 40

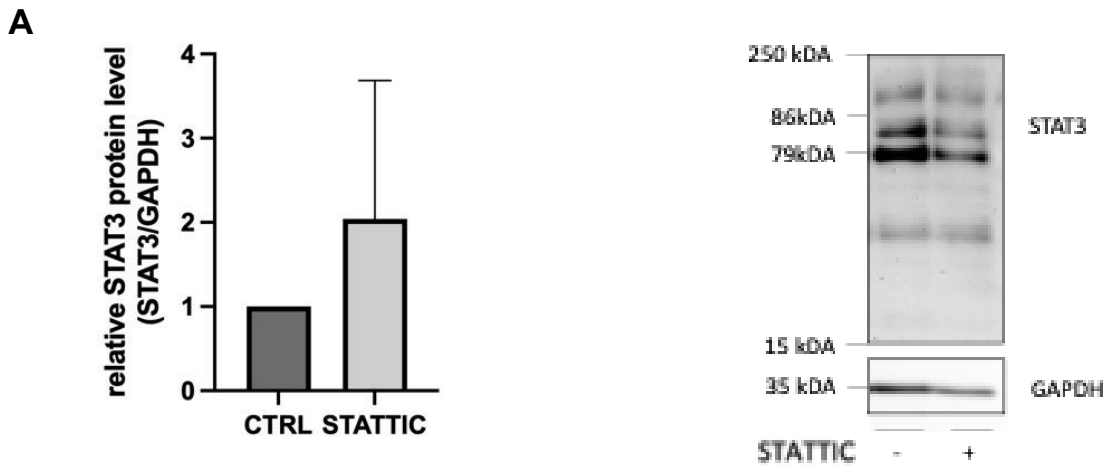

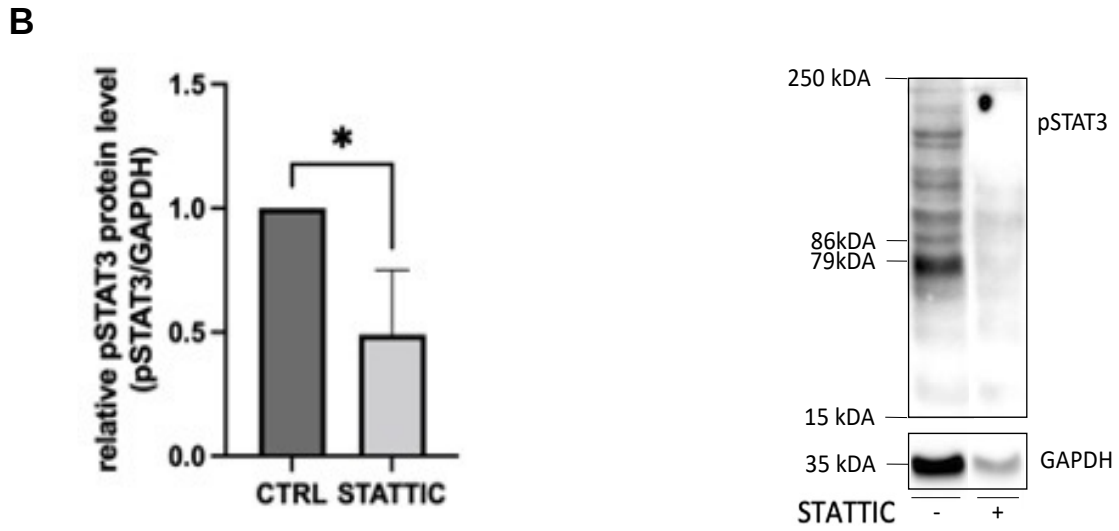

Figure 40. The inhibitor STATTIC inhibits STAT3 activation in endothelial cells. *(A) Quantification of STAT3 protein levels using immunoblotting on total lysates of EA.hy926 cells incubated with STATTIC for 24h. Expression values relative to an untreated control. Representative immunoblot of n=3, p = 0.335 using Student's t-test. (B) Immunoblotting for determination of pSTAT3 protein levels of EA.hy926 cells incubated with STATTIC for 24h. Expression values relative to an untreated control, n=3, * p < 0.05 using Student's t-test. All Graphs shown as mean ± SD.*

To determine whether or not STAT3 has an influence on PML expression, EA.hy926 cells were either left untreated to serve as a control or incubated with STATTIC for 24 hours and analysed performing RT-qPCR, immunoblotting and immunofluorescence. As seen in Figure 41A, incubation with STATTIC led to a decrease in relative PML mRNA levels (-65 %; $p < 0.05$). When incubated with STATTIC, relative PML protein levels (Figure 41B) slightly decreased compared to the control cells. Immunofluorescence was performed and as shown in Figure 41C and Figure 41E, control cells counted 14.4 PML-NBs on average per cell. Treatment with STATTIC for 24 hours (representative images shown in Figure 41D) only caused a slight decrease of PML-NBs (12.5 PML-NBs on average, -13.2 %). Immunofluorescence was performed on HUVECs either left untreated (control, Figure 41F) or incubated with STATTIC for 24 hours (representative images shown in Figure 41G). As shown in Figure 41H, incubation with STATTIC led to a decrease in the number of PML-NBs (-35 %; $p < 0.0001$) from 11.3 PML-NBs per nucleus in the control cells to 7.3 PML-NBs per nucleus counted in the cells incubated with STATTIC. Apparently, incubation with STATTIC leads to a decrease in PML mRNA, protein and PML-NBs.

Figure 41

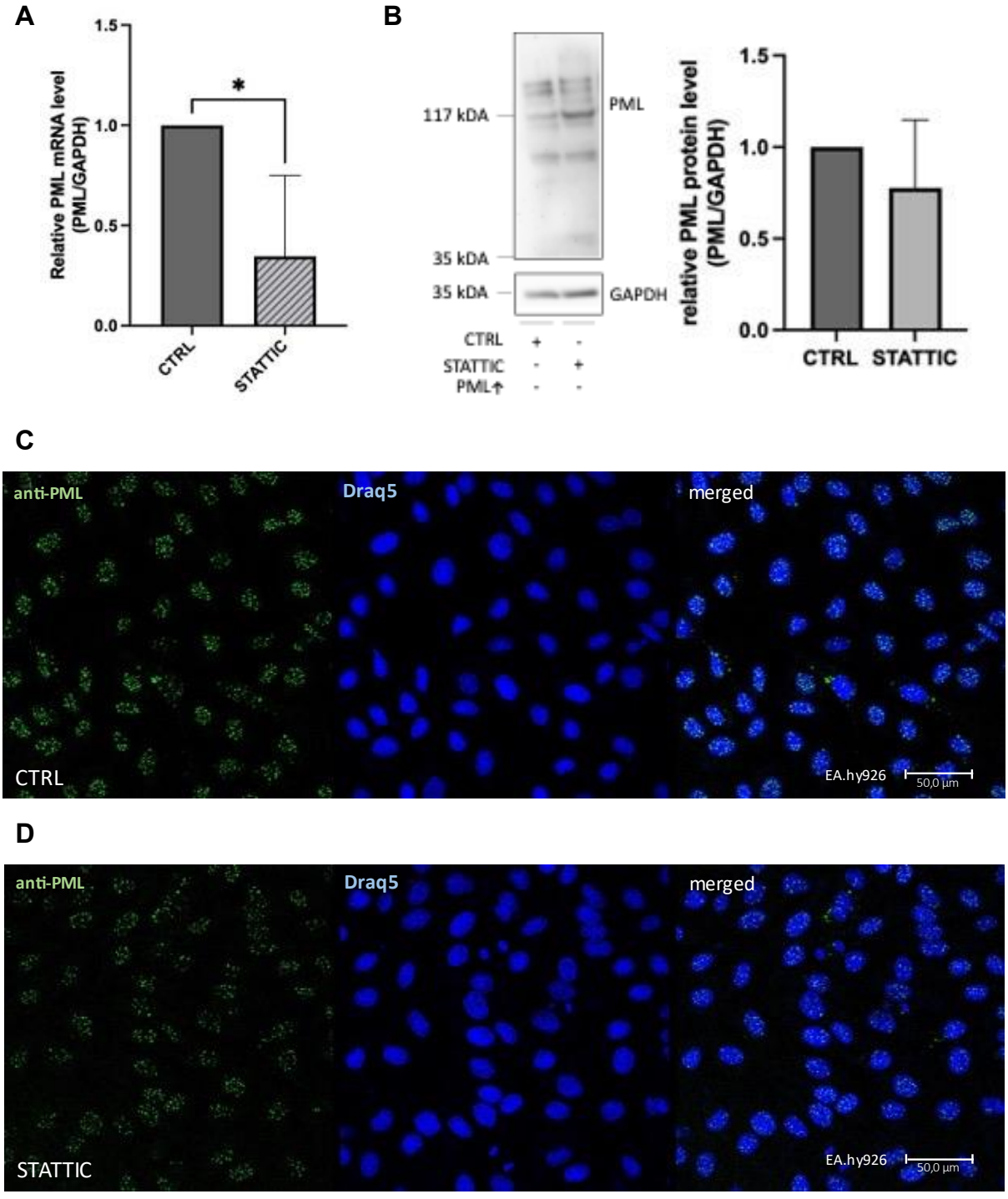
A
Relative PML mRNA level (PML/GAPDH)
1.5
1.0
0.5
0.0
*
CTRL
STATTIC
B
117 kDA
PML
35 kDA
35 kDA
GAPDH
CTRL + -
STATTIC - +
PML↑ - -
relative PML protein level (PML/GAPDH)
1.5
1.0
0.5
0.0
CTRL STATTIC
C
anti-PML
Draq5
merged
CTRL
EA.hy926
50,0 µm
D
anti-PML
Draq5
merged
STATTIC
EA.hy926
50,0 µm

E

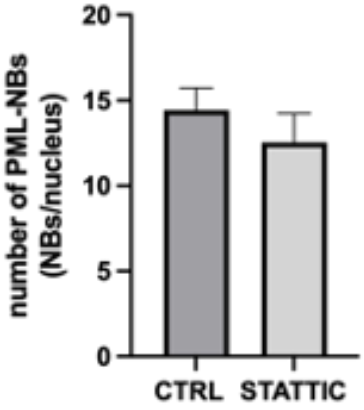
number of PML-NBs
(NBs/nucleus)
20
15
10
5
0
CTRL
STATTIC

F

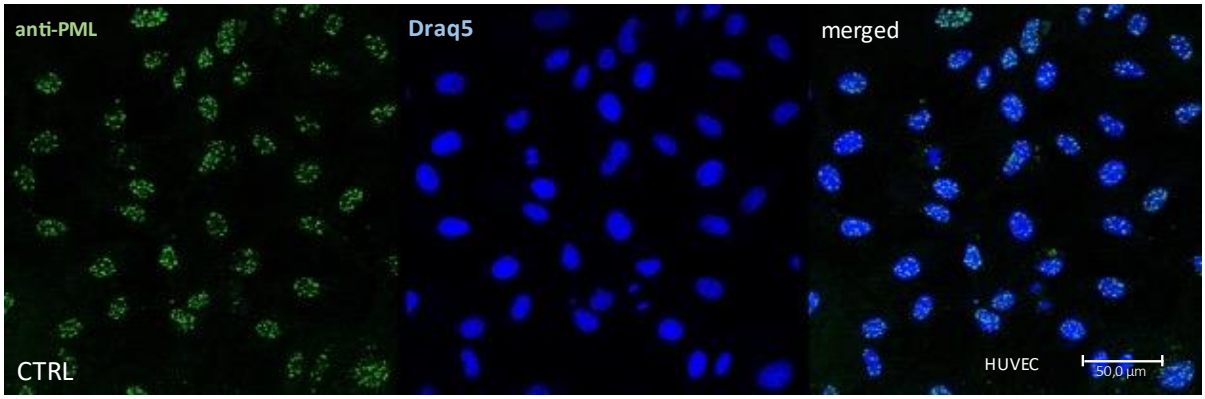
anti-PML
Draq5
merged
CTRL
HUVEC
50,0 µm

G

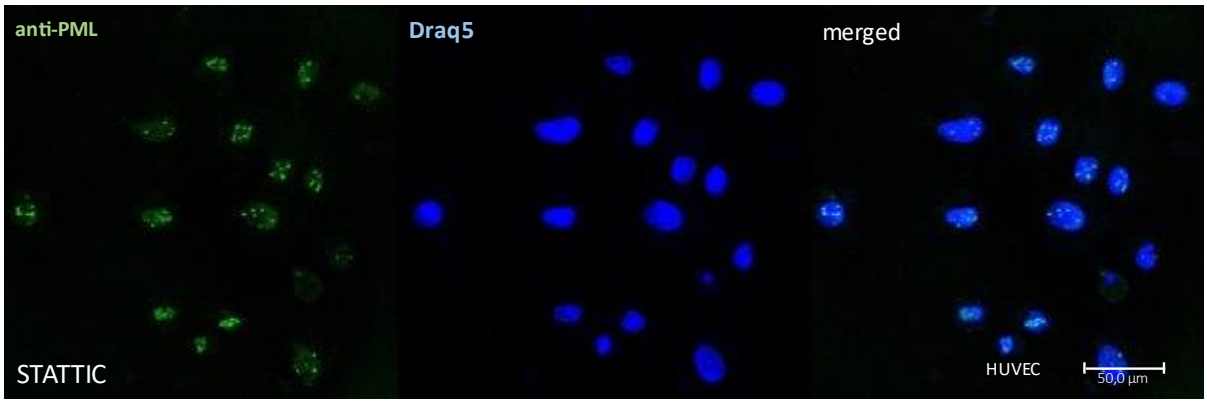
anti-PML
Draq5
merged
STATTIC
HUVEC
50,0 µm

H

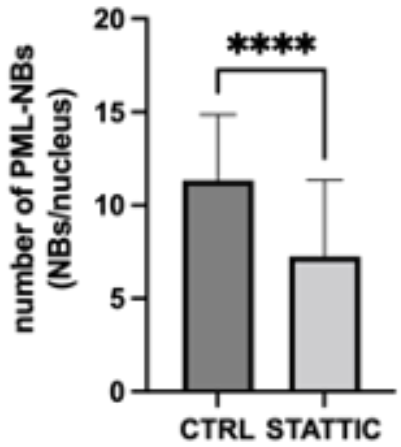

Figure 41. STATTIC leads to a decrease in PML mRNA expression and lowers the number of PML-NBs in endothelial cells. *(A) RT-qPCR to quantify PML mRNA levels of EA.hy926 cells incubated with STATTIC for 24h. Expression values relative to an untreated control, n=3, * p < 0.05, using Student's t-test. (B) Immunoblotting to determine PML protein levels of EA.hy926 cells incubated with STATTIC for 24h. Expression values relative to an untreated control, n=3, p = 0.37 using Student's t-test. (E) Immunofluorescence of EA.hy926 cells with anti-PML (green) and anti-Tubulin (not shown) antibodies was performed to determine the number of PML-NBs after incubation without supplement (CTRL, C) or with STATTIC (D) for 24h. The cell nuclei were highlighted using Draq5 (blue). images shown are representatives of n=3 independent experiments with 40 – 60 nuclei evaluated. p = 0.1964 using Student's t-test. Immunofluorescence was performed on HUVEC either non-treated (control, F) or incubated with STATTIC for 24 hours (G). To determine the number of PML-NBs (H), anti-PML (green) and anti-tubulin (not shown) were used to highlight the corresponding cell structure. Draq5 was used to highlight the nucleus (blue). n=1, 28 (STATTIC) to 60 (CTRL) nuclei were analysed. p < 0.0001 using Student's t-test. All Graphs shown as mean ± SD.*

To investigate if LDL-induced upregulation of PML is mediated by STAT3, PML expression was determined after treatment with STATTIC. To examine relative PML mRNA levels, RT-qPCR was performed on EA.hy926 cells incubated with STATTIC, comp_$_{LDL100}$ or both of them combined (Figure 42A). Relative PML mRNA levels of untreated EA.hy926 cells served as control. Incubation with comp_$_{LDL100}$ caused relative PML mRNA to increase (+394 %; $p < 0.05$) compared to the levels of the control cells. When incubated with the combination of STATTIC and the composition, relative PML mRNA levels decreased compared to the mRNA levels of the cells incubated with comp_$_{LDL100}$ alone. Figure 42B displays relative PML protein levels determined in EA.hy926 cells either left untreated (control), incubated with STATTIC, comp_$_{LDL100}$ or the two of them combined. Treatment with comp_$_{LDL100}$ led to an increase of PML protein levels of 373 % ($p < 0.01$). Treatment of the cells with the combination of STATTIC and the lipoprotein composition caused relative PML protein levels to decrease compared to the cells incubated with comp_$_{LDL100}$. As seen in Figure 42C, EA.hy926 cells were transfected with a pEGFP-C1-PML-IV-vector (PML↑). Relative PML protein levels were evaluated using immunoblotting. EA.hy926 cells transfected with an empty vector served as control. PML↑ cells were either incubated without treatment or incubated with comp_$_{LDL100}$ or with a combination of comp_$_{LDL100}$ and STATTIC for a duration of 24 hours. PML↑ cells expressed relative PML protein levels of 219 % and treatment of PML↑ with comp_$_{LDL100}$ also

led to a slight increase in relative PML protein levels compared to the control cells. Treatment with the combination of the lipoprotein composition and STATTIC decreased PML protein levels in comparison to PML↑ cells treated with comp_$_{LDL100}$. To investigate whether PML itself has an influence on STAT3 and pSTAT3 expression, PML↑ cells or cells with specific siRNAs to knockdown PML expression (siPML) were used. EA.hy926 cells transfected with an empty vector served as control cells. As seen in Figure 42D, RT-qPCR was performed to detect relative STAT3 mRNA levels. PML↑ cells showed an increase in relative STAT3 mRNA levels (+637 %; $p < 0.01$), whereas siPML cells expressed lower relative STAT3 mRNA levels than the control cells did. As shown in Figure 42E, immunoblotting was performed on transfected EA.hy926 cells to investigate the influence of PML on relative STAT3 protein levels. PML↑ cells showed an increase in relative STAT3 protein levels (+160 %; $p < 0.05$). Further, relative pSTAT3 protein levels were measured using immunoblotting on transfected EA.hy926 cells. PML↑ cells showed elevated relative pSTAT3 levels (+99 %), whereas siPML cells showed a decrease in relative pSTAT3 protein levels compared to the control cells. Apparently, treatment with STATTIC slightly decreases LDL-induced PML mRNA and protein expression, while PML has an increasing effect on STAT3 and pSTAT3 expression.

Figure 42

A

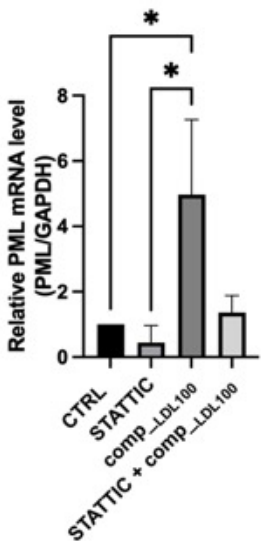

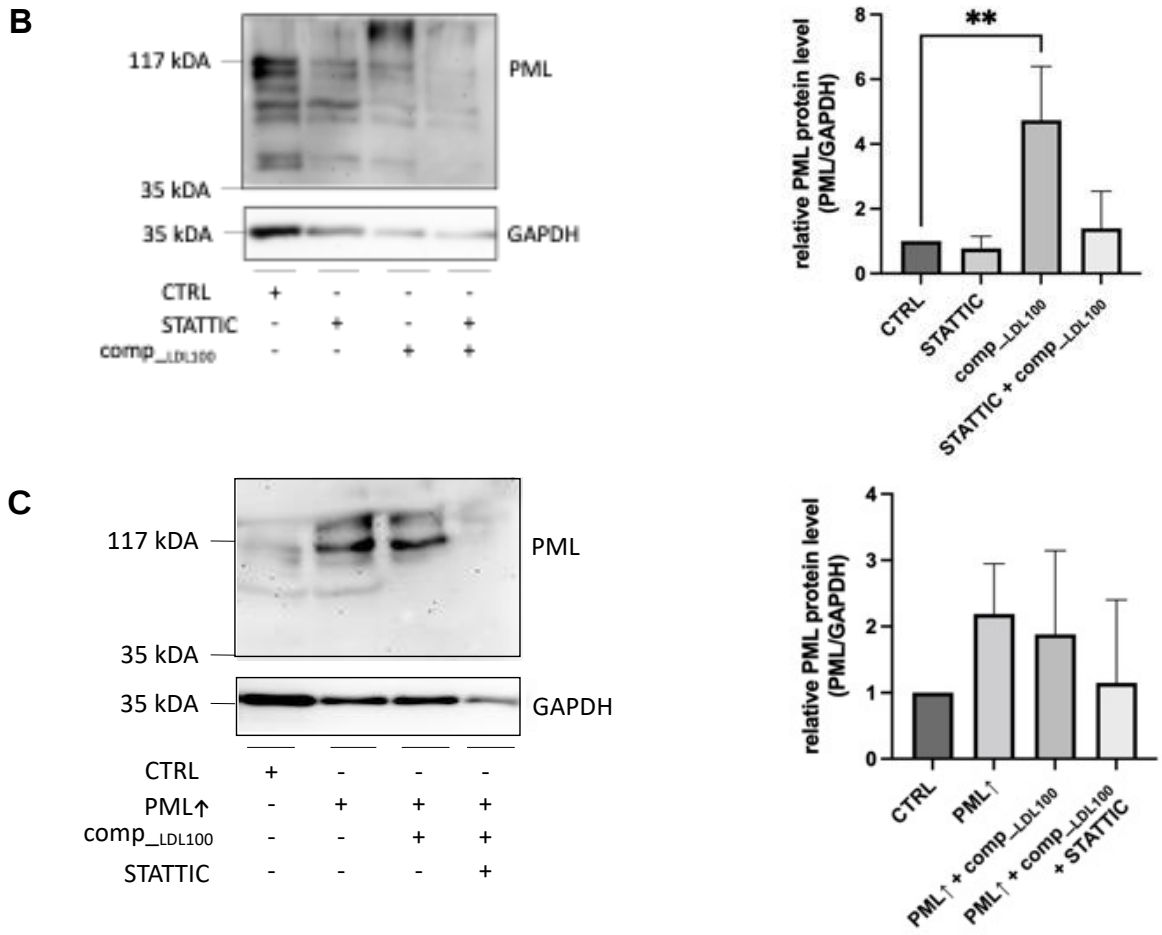
B
117 kDA
PML
35 kDA
35 kDA
GAPDH
CTRL + - - -
STATTIC - + - +
comp_LDL100 - - + +
relative PML protein level (PML/GAPDH)
**
CTRL
STATTIC
comp_LDL100
STATTIC + comp_LDL100
C
117 kDA
PML
35 kDA
35 kDA
GAPDH
CTRL + - - -
PML↑ - + + +
comp_LDL100 - - + +
STATTIC - - - +
relative PML protein level (PML/GAPDH)
CTRL
PML↑
PML↑ + comp_LDL100
PML↑ + comp_LDL100 + STATTIC
D
relative STAT3 mRNA level (STAT3/GAPDH)
**
**
CTRL
PML↑
siPML
E
relative STAT3 protein level (STAT3/GAPDH)
*
CTRL
PML↑
siPML

F

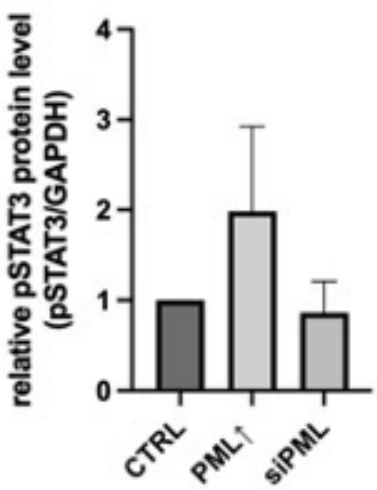

Figure 42. STATTIC slightly decreases LDL-induced PML mRNA and protein expression in endothelial cells, while overexpression of PML increases STAT3 and pSTAT3 expression. *(A) RT-qPCR was performed on EA.hy926 cells to determine PML mRNA levels after incubation with either STATTIC, the lipoprotein composition with 100 mg/dL of LDL or with the composition and STATTIC in combination for 24h. Expression values relative to an untreated control. n=3, * p < 0.05 in one-way ANOVA. (B) PML protein levels were quantified using immunoblotting on EA.hy926 cells incubated with STATTIC, the lipoprotein composition with 100 mg/dL of LDL or with the composition and STATTIC combined for 24h. Expression values relative to an untreated control. Representative immunoblot of n=3, ** p < 0.01, using one-way ANOVA. (C) Immunoblotting was used to quantify PML protein levels on EA.hy926 after transfection with a pEGFP-C1-PML-IV-vector (PML↑), cells after transfection with pEGFP-C1-PML-IV and incubation with the lipoprotein composition containing 100 mg/dL of LDL, or cells that were transfected with pEGFP-C1-PML-IV and afterwards incubated with STATTIC and the composition combined for 24h. Expression values relative to control (transfection with vector without a specific gene insert). Representative immunoblot of n=3, p < 0.999 using two-way ANOVA. (D) To determine relative STAT3 mRNA levels, RT-qPCR was performed on EA.hy926 cells transfected with a pEGFP-C1-PML-IV-vector or treated with siRNA. Expression values relative to control (transfection with vector without a specific gene insert). n=3, ** p < 0.01 using two-way ANOVA. (E) Immunoblotting was performed of EA.hy926 cells transfected with a pEGFP-C1-PML-IV-vector or siRNA to determine relative STAT3 protein levels. Expression values relative to control (transfection with vector without a specific gene insert). Representative immunoblot of n=3, * p < 0.05 using two-way-ANOVA. (F) To determine relative pSTAT3 protein levels, immunoblotting of EA.hy926 cells transfected with a pEGFP-C1-PML-IV-vector or siRNA was performed. Expression values relative to control (transfection with vector without a specific gene insert). Representative immunoblot of n=3, p < 0.99, using two-way-ANOVA. All Graphs shown as mean ± SD.*

3.1.4. Inhibition of PKC leads to a decrease in STAT3 expression and activation, whereas inhibition of STAT3 increases PKC activity

To determine whether STAT3 influences PKC activity, relative PKC activity was determined using ELISA after incubating EA.hy926 cells with STATTIC for 24 hours (Figure 43A). Untreated EA.hy926 cells served as control cells. After incubation with STATTIC, the cells showed increased PKC activity (+73 %; $p < 0.0001$) in comparison to the control cells. As shown in Figure 43B, PKC activity levels enhanced slightly when treated with comp_$_{LDL100}$ (+30 %; $p < 0.01$) compared to the activity detected in the control cells. Treatment with both, comp_$_{LDL100}$ and STATTIC led to an increase of 271 % ($p < 0.05$) compared to PKC activity measured in total cell lysates of the control cells. To figure out a possible impact of PKC on STAT3 protein expression, immunoblotting was performed on EA.hy926 either left untreated (control) or incubated with sc-3088 for 24 hours (Figure 43C). Compared to the relative STAT3

protein levels detected in the total lysates of the control cells, cells incubated with sc-3088 for 24 hours showed a decrease in relative STAT3 protein levels (-41 %; $p < 0.01$). To detect relative pSTAT3 protein levels, immunoblotting was performed on total cell lysates of EA.hy926 cells incubated with sc-3088 for 24 hours (Figure 43D). Untreated EA.hy926 cells served as a control. When incubated with sc-3088, relative pSTAT3 protein levels lowered to 37 % ($p < 0.01$) of the levels that were determined in the total lysates of the control cells. Apparently, incubation of EA.hy926 with STATTIC causes PKC activity to increase, whereas incubation with sc-3088 leads to a decrease in STAT3 and pSTAT3 protein levels.

Figure 43

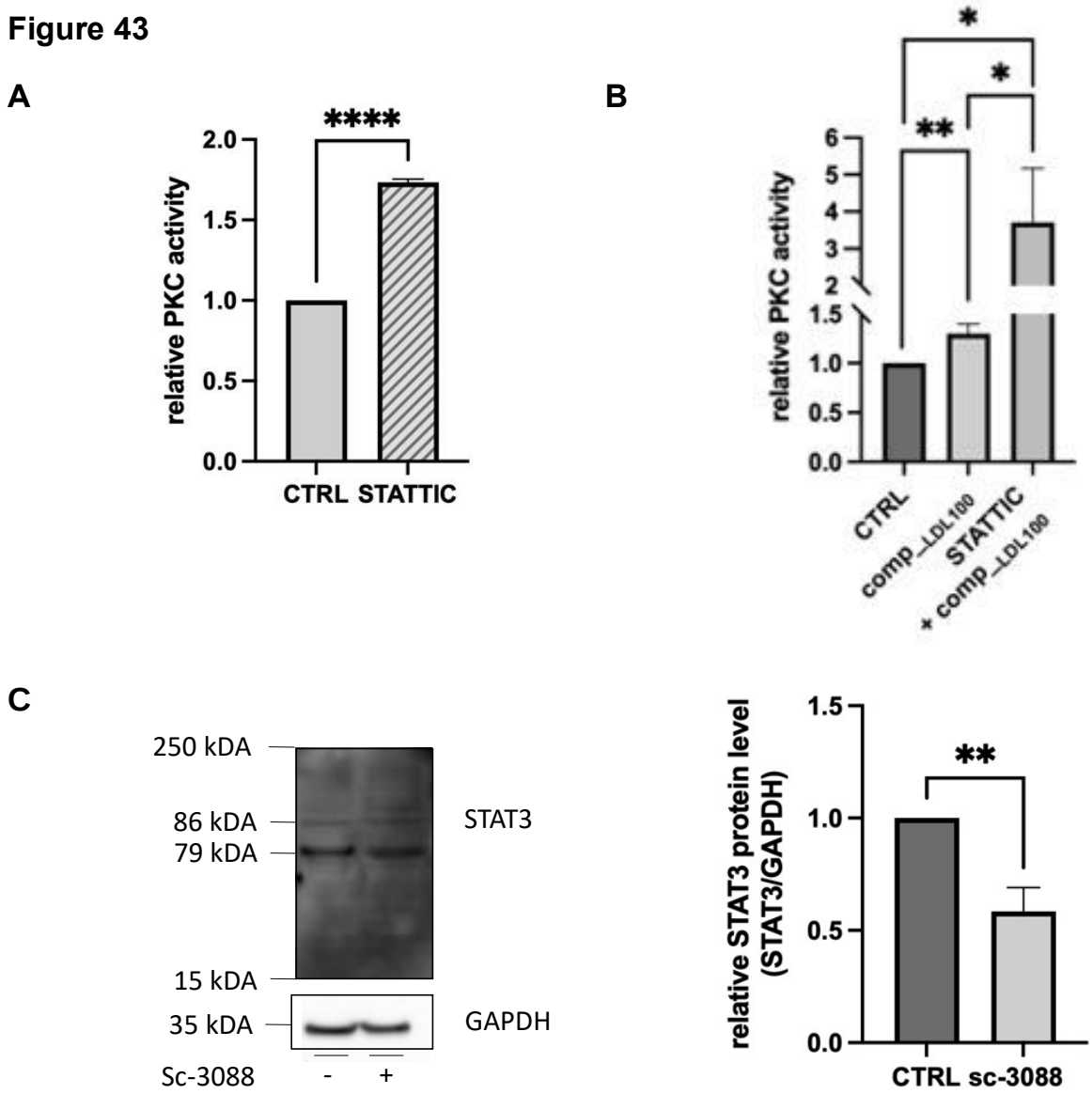

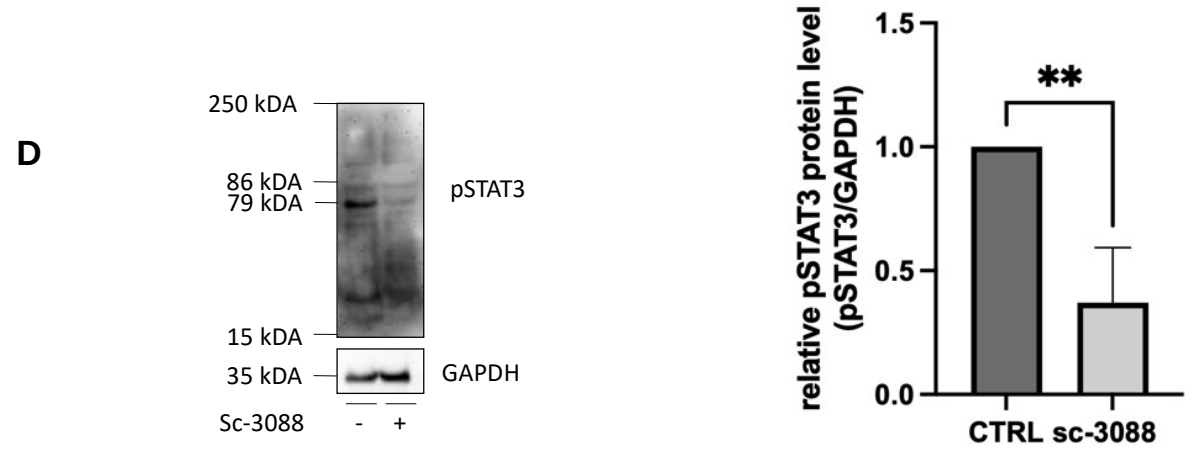

Figure 43. STATTIC increases (LDL-induced) PKC activation, whereas sc-3088 decreases STAT3 and active STAT3 protein expression in endothelial cells. *(A) Semi-quantitative detection of active PKC of total cell lysates of EA.hy926 cells via ELISA after incubation with STATTIC for 24h. Expression values relative to an untreated control. n=3, **** p < 0.0001 using Student's t-test. (B) To measure active PKC levels in total lysates of EA.hy926 cells, an ELISA was performed after incubation with either the physiologically concentrated lipoprotein composition or with the composition and STATTIC combined for 24h. Expression values relative to a control that remained untreated. n=3, * p < 0.05, ** p < 0.01 using one-way ANOVA. (C) Determination of STAT3 protein levels of totally lysates of EA.hy926 cells incubated with sc-3088 for 24h. Expression values relative to an untreated control. Representative immunoblot of n=3, ** p < 0.01 using Student's t-test. (D) Immunoblotting to quantify pSTAT3 protein levels in the total lysates of EA.hy926 cells incubated with sc-3088 for 24h. Expression values relative to a control (untreated). Representative immunoblot of n=3, ** p < 0.01 using Student's t-test. All Graphs shown as mean ± SD.*

3.1.5. (LDL-induced) upregulation of PKC leads to an increase in the expression of the PML targets IL-6 and IL-8, upregulation of STAT3 leads to a decrease in expression of the cytokines

To ensure the detected effect of PKC on PML expression in endothelial cells, the expression of the identified PML target IL-6 was also examined. RT-qPCR was performed on EA.hy926 cells that were either treated with sc-3088 or comp_$_{LDL100}$ or the two of them together for 24 hours to evaluate their influence on relative IL-6 mRNA levels (Figure 44A). sc-3088 caused relative IL-6 mRNA levels to decrease by 71 % ($p < 0.05$) compared to the control. However, incubation with comp_$_{LDL100}$ led to an increase of relative IL-6 mRNA levels (+77 %; $p < 0.05$). Incubation with the combination of comp_$_{LDL100}$ and sc-3088 led to a decrease in relative IL-6 mRNA levels of 79 % ($p < 0.01$) in comparison to cells incubated with comp_$_{LDL100}$ only. Relative IL-6 mRNA levels were determined using RT-qPCR after EA.hy926 cells were treated for 24 hours, whereas control cells remained untreated (Figure 44B). The strongest increase of relative IL-6 mRNA levels compared to the levels measured in the control cells were expressed by cells incubated with the combination with PMA and comp_$_{LDL100}$ (+127 %; $p < 0.01$). To further detect whether the impact of sc-3088 on relative IL-6 mRNA levels is connected to PML, EA.hy926 cells were transfected with a pEGFP-C1-PML-IV-vector (PML↑) and incubated without or with sc-3088 for 24 hours (Figure 44C). PML↑ cells expressed increased relative IL-6 mRNA levels (+8521 %; $p < 0.05$) compared to the levels of the control cells. Compared to

PML↑ cells, IL-6 mRNA levels decreased by 94 % ($p < 0.05$) when additionally incubated with sc-3088.

To get more insights about STAT3's influence on (LDL-induced) IL-6 expression, EA.hy926 cells were incubated with STATTIC, comp_$_{LDL100}$ or STATTIC and comp_$_{LDL100}$ together for 24 hours (Figure 44C). To detect relative IL-6 mRNA levels, RT-qPCR was performed. Control cells were incubated for 24 hours without further treatment. Incubation with STATTIC led to an increase in relative IL-6 mRNA levels (+ 914 %; 0.001) compared to the IL-6 mRNA levels of the control. Incubation with comp_$_{LDL100}$ led to an increase as well. Incubation with the combination of comp_$_{LDL100}$ and STATTIC led to the highest increase in relative IL-6 mRNA levels detected in this experiment (+1710 %; $p < 0.0001$). As presented in Figure 44D, to learn more about the connection between STATTIC, IL-6 and PML the experiment was conducted with PML↑ cells as well. Control cells were transfected with a vector lacking specific gene insert. PML↑ cells were incubated without or with STATTIC. PML↑ cells already expressed increased relative IL-6 mRNA levels (+916 %) compared to the levels detected in the control cells. This effect was even higher when PML↑ cells were incubated with STATTIC (+1999 %; $p < 0.05$). Clearly, sc-3088 decreases the (LDL-induced) increase in IL-6 mRNA levels, whereas PMA and STATTIC increase it.

Figure 44

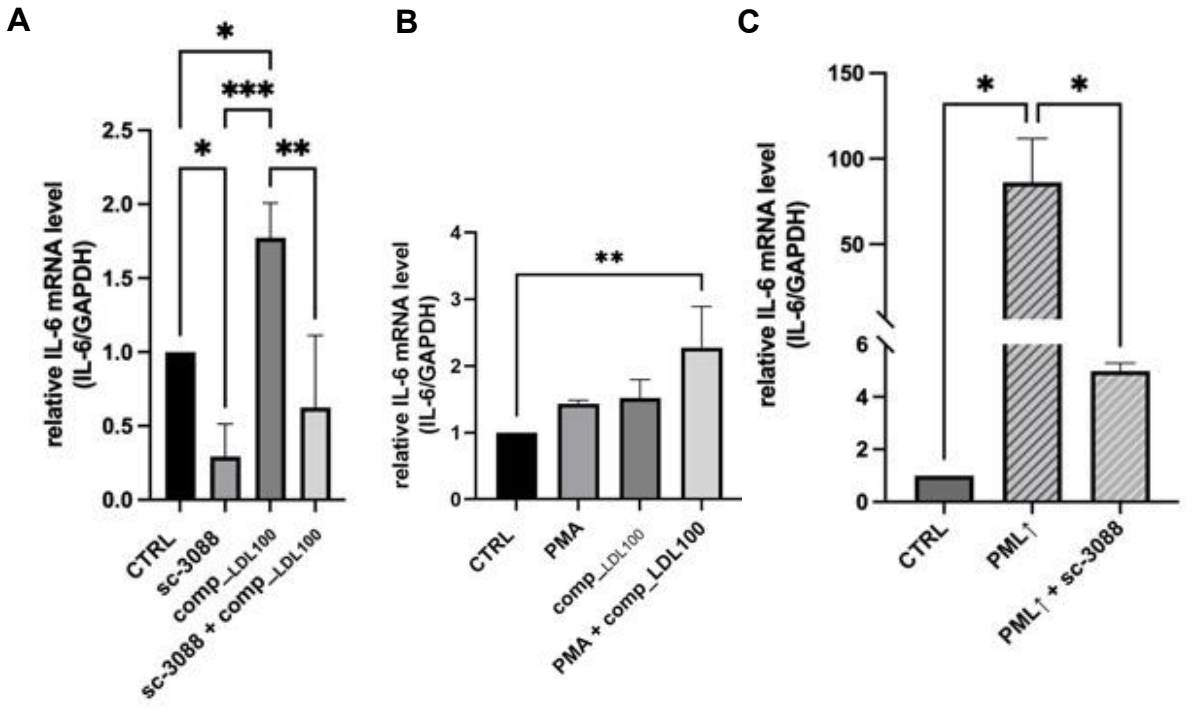

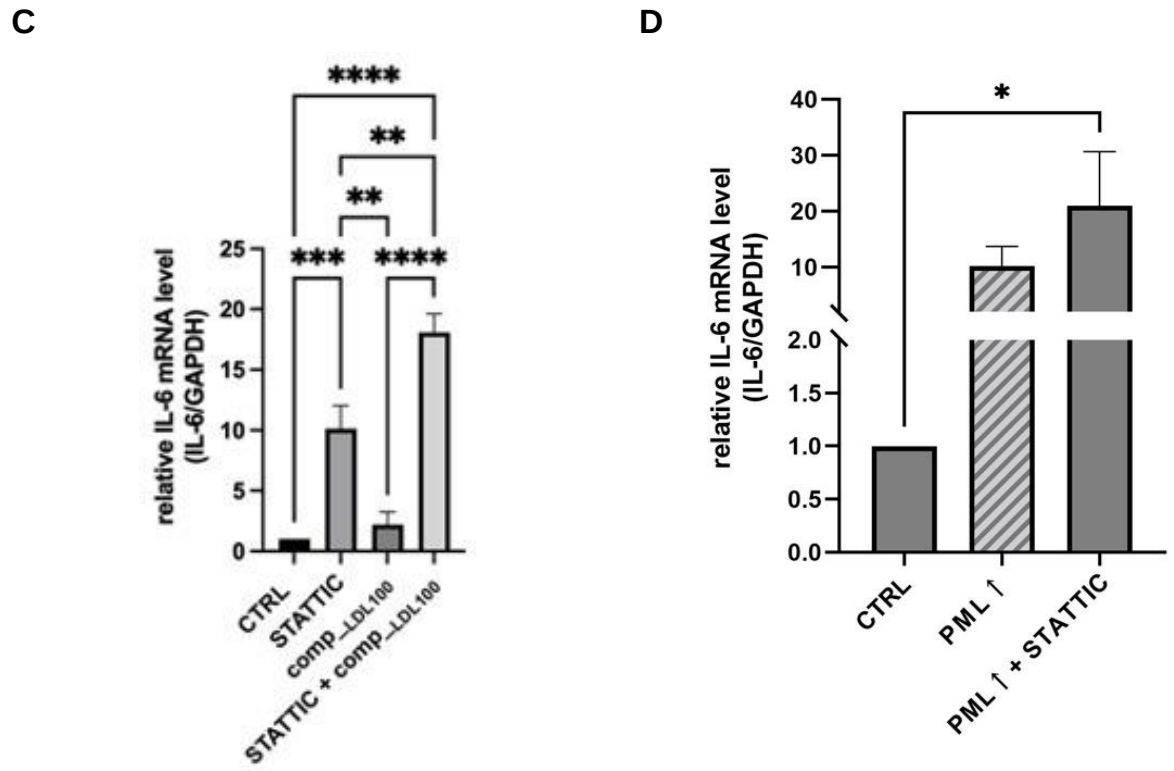

Figure 44. sc-3088 decreases (LDL-induced) expression of the PML target IL-6 mRNA in endothelial cells, whereas PMA and STATTIC increase it. *(A) IL-6 mRNA levels were determined using RT-qPCR on EA.hy926 cells incubated with either sc-3088, the lipoprotein composition with 100 mg/dL of LDL or sc-3088 and the composition combined. Expression values relative to an untreated control. n=3, * p < 0.05, ** p < 0.01, *** p < 0.001 using one-way ANOVA. (B) Determination of IL-6 mRNA levels using RT-qPCR on EA.hy926 cells transfected with a vector lacking gene insert (CTRL), with a pEGFP-C1-PML-IV-vector (PML↑) or incubated with sc-3088 after transfection with pEGFP-C1-PML-IV. n=3, * p < 0.05 in two-way ANOVA. (C) RT-qPCR was used to quantify IL-6 mRNA levels in EA.hy926 cells incubated with STATTIC, the lipoprotein composition with 100 mg/dL of LDL or a combination of STATTIC and the composition. Expression values relative to an untreated control. n=3, ** p < 0.01, *** p < 0.001, using one-way ANOVA. (D) IL-6 mRNA levels were determined using RT-qPCR on EA.hy926 cells transfected with a pEGFP-C1-PML-IV-vector (PML↑) or incubated with STATTIC after transfection with pEGFP-C1-PML-IV. Expression values relative to a control transfected with a vector lacking gene insert. n=3, * p < 0.05 in two-way ANOVA. All Graphs shown as mean ± SD.*

To ensure the detected effect of PKC on PML expression in endothelial cells, the expression of the identified PML target IL-8 was examined. Relative IL-8 mRNA levels were investigated via RT-qPCR. As seen in Figure 45A, EA.hy926 cells were treated with sc-3088, comp$_{_LDL100}$ or with sc-3088 and comp$_{_LDL100}$ together for 24 hours. Control cells were left untreated. When incubated with sc-3088 for 24 hours, relative IL-8 mRNA levels were 73 % ($p < 0.01$) lower than levels in the control cells. Incubation with comp$_{_LDL100}$ nonetheless caused relative IL-8 mRNA levels to increase by 226 % ($p < 0.01$). When incubated with sc-3088 and comp$_{_LDL100}$ together, IL-8 mRNA levels decreased compared to both, the control cells (-70 %; $p < 0.01$) and cells incubated with comp$_{_LDL100}$ only (-91 %; $p < 0.001$). To determine the connection between IL-8, PML and PKC, EA.hy926 cells were transfected with a pEGFP-C1-PML-IV-vector (PML↑) and incubated without or with sc-3088 for 24 hours. (Figure 45B). EA.hy926 cells transfected with a vector lacking specific gene insert served as control cells. Relative IL-8 mRNA levels in PML↑ cells strongly increased (+6895 %; $p < 0.05$) compared to the levels

of the control cells. When incubating PML↑ cells with sc-3088, relative IL-8 mRNA levels decreased compared to PML↑ cells (-89 %; $p < 0.05$).

To investigate the connection between STAT3 and IL-8, the experiments described above were conducted with STATTIC as well. Figure 45C depicts relative IL-8 mRNA levels in EA.hy926 cells either left untreated to serve as a control, incubated with STATTIC, comp_$_{LDL100}$ or the two of them combined for 24 hours. Treatment with both, STATTIC and comp_$_{LDL100}$ led to the strongest increase determined in this experiment (+1694 %; $p < 0.0001$). Clearly, incubation with sc-3088 leads to a decrease of the (LDL-induced) increase in IL-8 mRNA levels, while incubation with STATTIC causes IL-8 mRNA levels to increase.

Figure 45

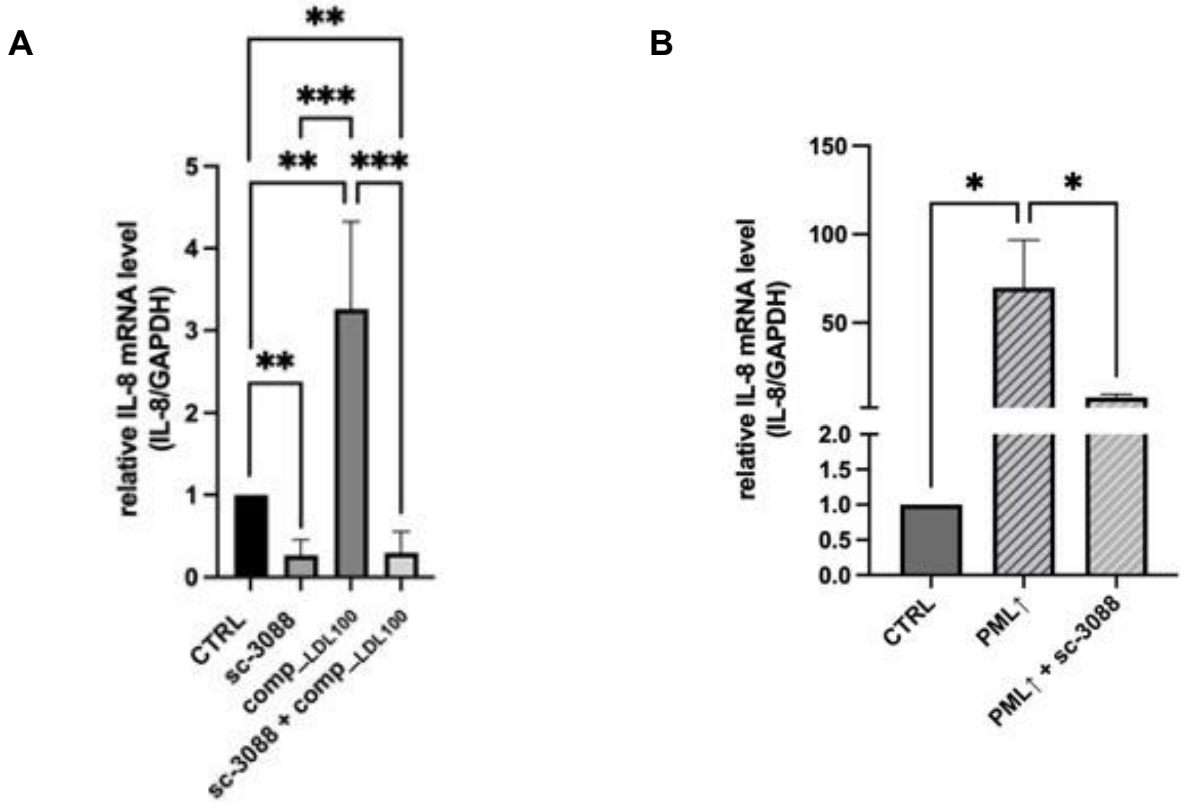

C

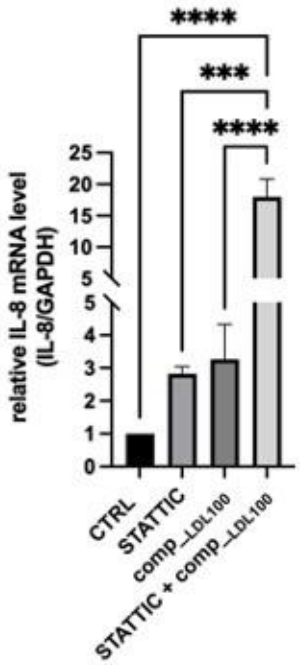

Figure 45. (LDL-induced) mRNA expression of the PML target IL-8 decreases after incubation of endothelial cells with sc-3088, whereas it increases after incubation with STATTIC. *(A) IL-8 mRNA levels were determined using RT-qPCR on EA.hy926 cells incubated with either sc-3088, the lipoprotein composition with 100 mg/dL of LDL or sc-3088 and the composition combined. Expression values relative to an untreated control. n=3, * p < 0.05, ** p < 0.01, *** p < 0.001 using one-way ANOVA. (B) Determination of IL-8 mRNA levels using RT-qPCR on EA.hy926 cells transfected with a pEGFP-C1-PML-IV-vector (PML↑) or incubated with sc-3088 after transfection with pEGFP-C1-PML-IV. Expression values relative to a control transfected with a vector lacking gene insert. n=3, * p < 0.05 in two-way ANOVA. (C) RT-qPCR was used to quantify IL-8 mRNA levels in EA.hy926 cells incubated with STATTIC, the lipoprotein composition with 100 mg/dL of LDL or a combination of STATTIC and the composition. Expression values relative to an untreated control. n=3, ** p < 0.01, *** p < 0.001, using one-way ANOVA. All Graphs shown as mean ± SD.*

3.1.6. p53 protein expression is upregulated by LDL and PKC and is inhibited by STAT3

To determine the impact of different concentrated lipoprotein compositions on p53 expression, relative p53 protein levels were detected by measuring the signal intensity after immunoblotting of total cell lysates of EA.hy926 cells. After 3 hours of incubation, p53 protein levels enhanced most when incubated with the comp$_{_LDL200}$ (+217 %; $p < 0.001$) (Figure 46A). After an incubation period of 24 hours, highest relative p53 protein levels were again the result of incubation with comp$_{_LDL200}$ (+302 %; $p < 0.05$) (Figure 46B). When incubated with the lipoprotein compositions for 24 hours, relative p53 protein levels were higher than after an incubation period of 3 hours. As illustrated in Figure 46C, EA.hy926 cells were transfected with a pEGFP-C1-PML-IV-vector (PML↑) and incubated without or with comp$_{_LDL100}$ for 24 hours. Control cells were transfected with an empty vector. PML↑ cells expressed slightly

enhanced relative p53 protein levels compared to the levels detected in the control, while PML↑ cells incubated with comp_LDL100 for 24 hours even showed elevated relative p53 protein levels of +191 % ($p < 0.05$) compared to the levels of the control cells. Obviously, incubation with lipoprotein compositions, especially with high LDL concentrations, lead to an increase in p53 protein levels.

Figure 46

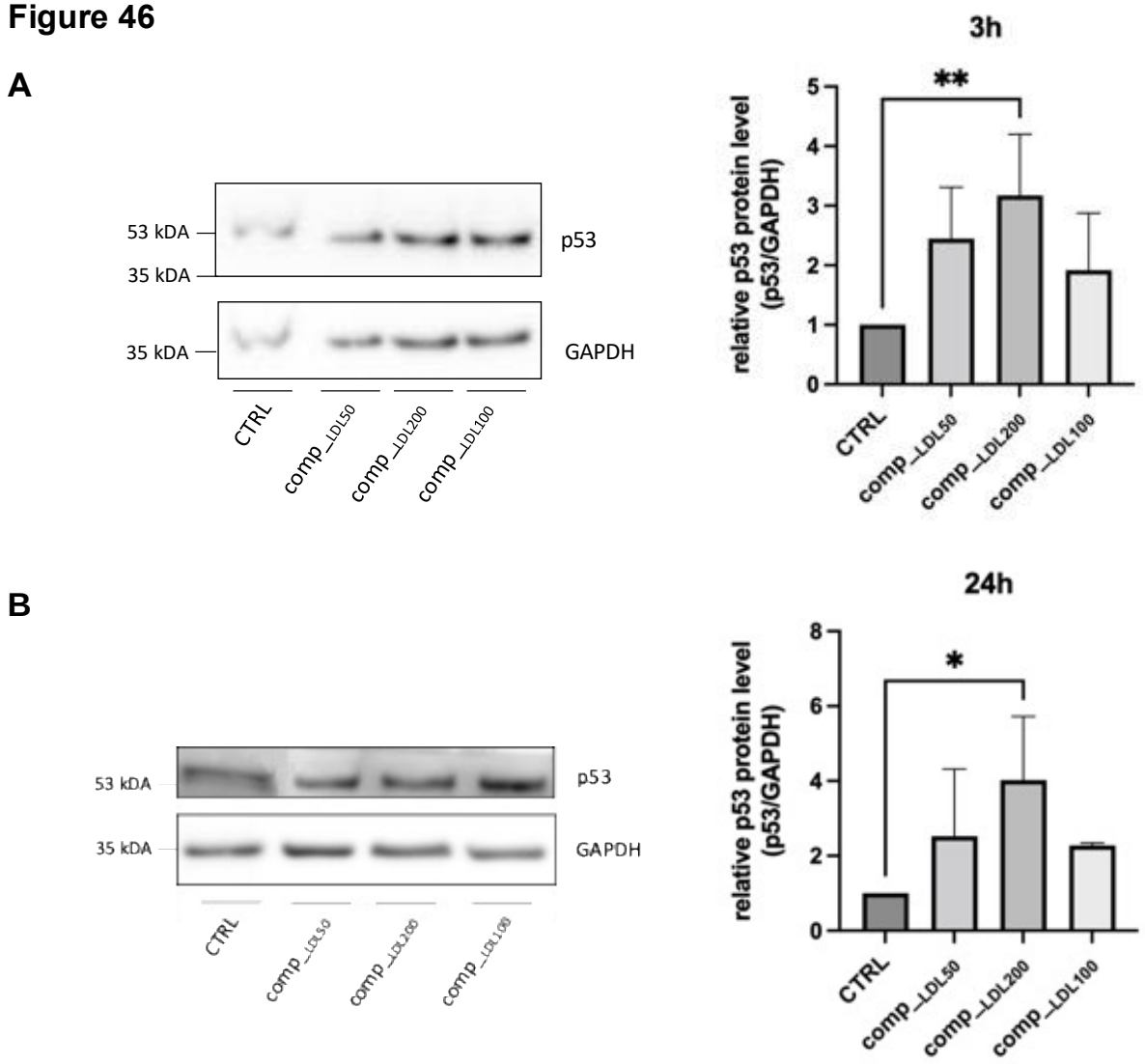

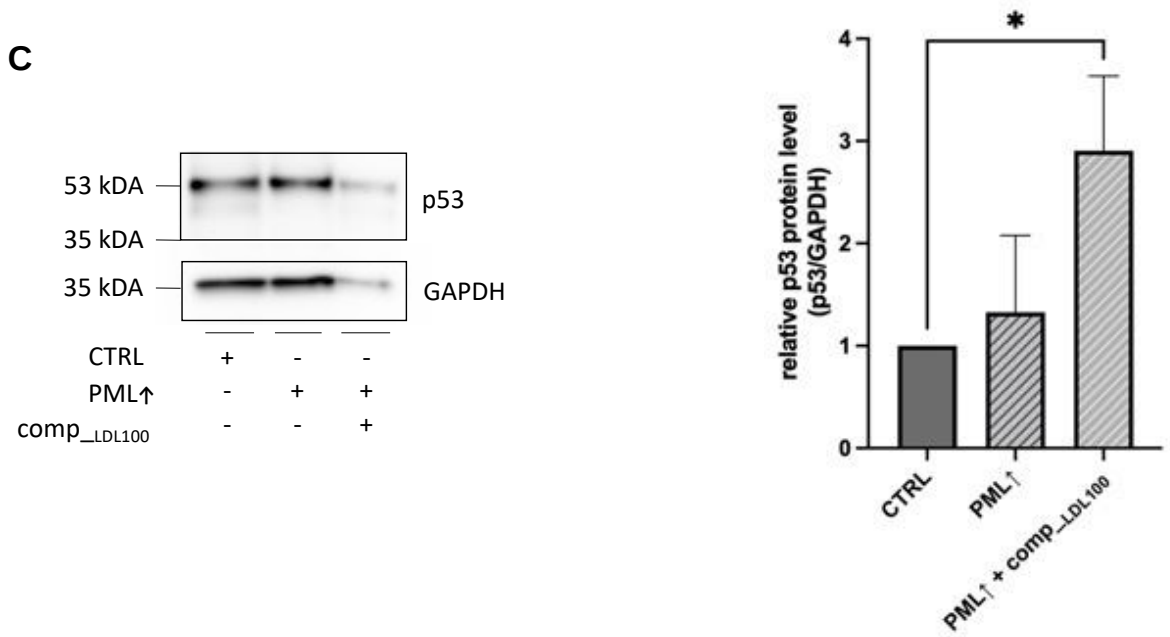

Figure 46. Lipoprotein compositions with different LDL concentrations enhance PML target p53 protein expression in endothelial cells. *To determine p53 protein levels, immunoblotting was performed on total lysates of EA.hy926 cells incubated with lipoprotein compositions with LDL concentrations varying from 50 mg/dL to 200 mg/dL for 3h (A) or 24h (B). Expression values relative to an untreated control. Representative immunoblots of n=4, ** p < 0.01, using one-way ANOVA. (C) Immunoblotting was used to quantify p53 protein levels of total lysates of EA.hy926 cells transfected with a vector without gene insert (CTRL), transfected with a pEGFP-C1-PML-IV-vector (PML↑) or incubated with the lipoprotein composition with 100 mg/dL of LDL after transfection with pEGFP-C1-PML-IV. Representative immunoblot of n=3, * p < 0.05 using two-way ANOVA. All Graphs shown as mean ± SD.*

To find out more about the connection between lipoproteins, PML and the PML target p53, immunoblotting was also performed on EA.hy926 cells that were incubated with single blood lipoproteins of different concentrations to detect relative p53 protein levels. Control cells were left untreated. When incubated for a duration of 3 hours (Figure 47A), highest relative p53 protein levels compared to those of the control were detected after treatment with 200 mg/dL of LDL (+188 %; $p < 0.01$). When the incubation span was extended to 24 hours (Figure 47B), treatment with 200 mg/dL of LDL increased p53 protein levels the most of all tested lipoproteins (258 %; $p < 0.05$) compared to the levels determined in the control cells. Apparently, high levels of LDL cause an increase in p53 protein levels.

Figure 47

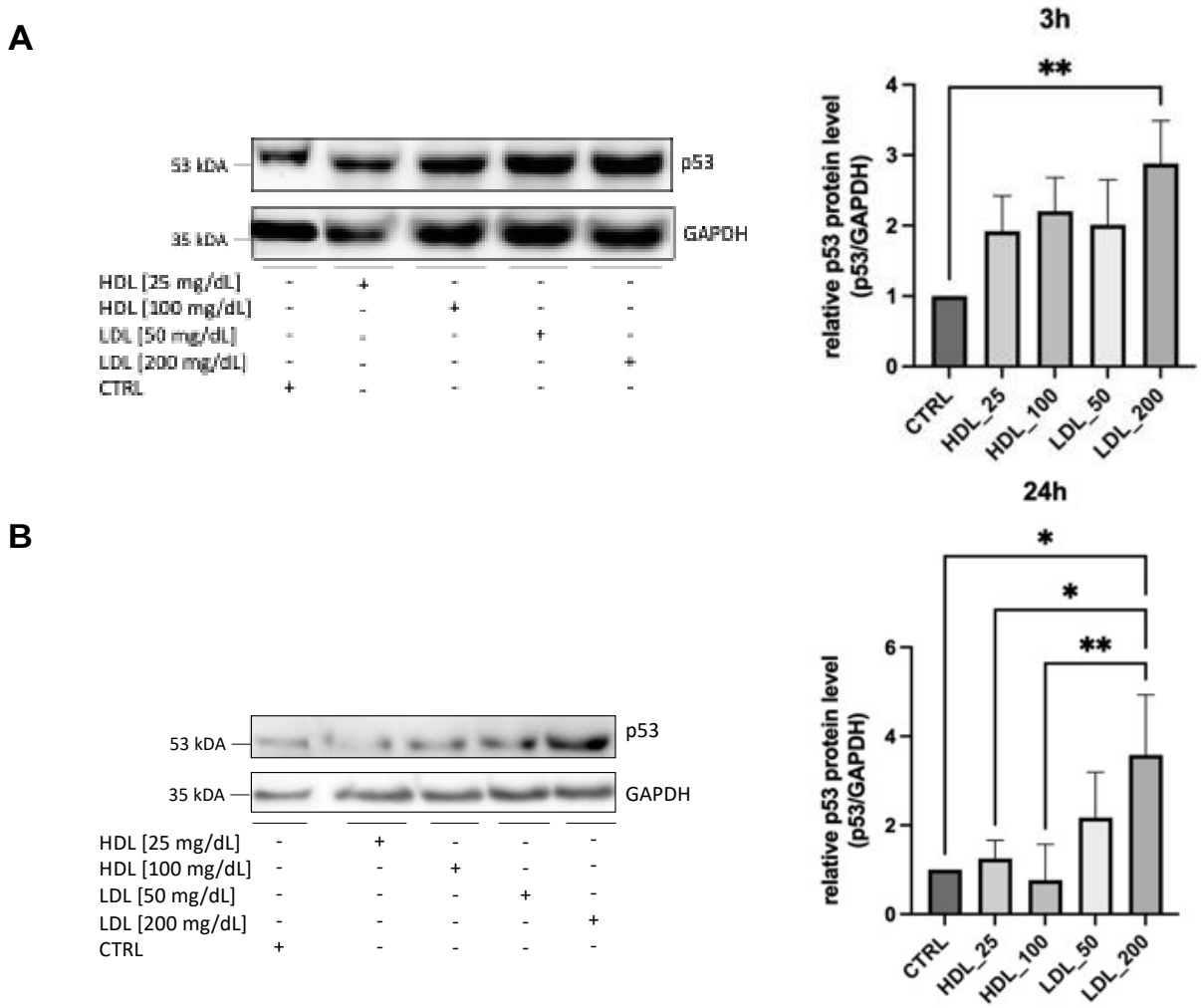

Figure 47. LDL increases PML target p53 protein expression in endothelial cells. *Immunoblotting was used to determine p53 protein levels of total lysates of EA.hy926 cells incubated with 25 mg/dL or 100 mg/dL of HDL and 50 mg/dL or 200 mg/dL of LDL for 3h (A) or 24h (B). Expression values relative to an untreated control. Representative immunoblots of n=3 (A), n=4 (B) independent experiments, * p < 0.05, ** p < 0.01, performing two-way ANOVA. All Graphs shown as mean ± SD.*

In order to investigate the impact of apoE4-homozygous lipoproteins on relative p53 protein levels, immunoblotting was performed on EA.hy926 cells incubated with different concentrated apoE4-homozygous lipoproteins. When incubated for 3 hours (Figure 48A), highest relative p53 protein levels compared to the levels of the control cells were detected in cells incubated with 200 mg/dL of LDL (+297 %). As shown in Figure 48B, extending the incubation to 24 hours led to increased relative p53 protein levels of cells incubated with 200 mg/dL of LDL (+179 %; $p < 0.05$) compared to control. Obviously, high levels of apoE4-homozygous LDL lead to an increase in p53 protein levels.

Figure 48

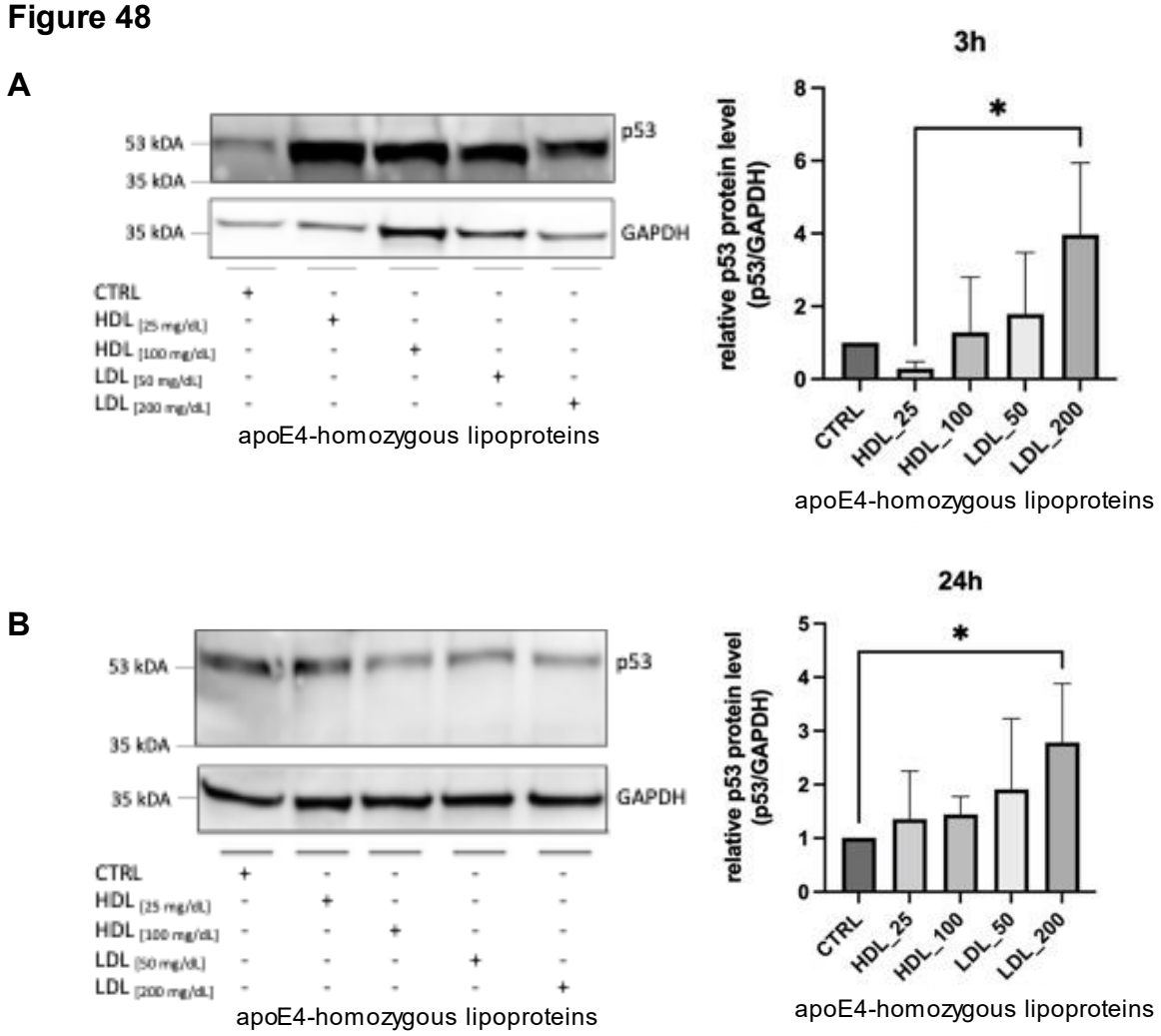

Figure 48. apoE4-homozygous LDL increases PML target p53 protein expression in endothelial cells. *To determine p53 protein levels, immunoblotting was used on total lysates of EA.hy926 cells after incubation with apoE4-homozygous 25 mg/dL or 100 mg/dL of HDL and 50 mg/dL or 200 mg/dL of LDL for 3h (A) or 24h (B). Expression values relative to an untreated control. Immunoblots are representative of n=3 (A), n=4 (B), * p < 0.05, using two-way ANOVA. All Graphs shown as mean ± SD.*

To investigate the influence of (LDL-induced) PKC and STAT3 activation and additionally a possible impact of PML on relative p53 protein levels, immunoblotting was performed on EA.hy926 cells incubated with the corresponding inhibitors, comp_$_{LDL100}$ for 24 hours or after transfection. As shown in Figure 49A, incubation with comp_$_{LDL100}$ for 24 hours led to an increase of relative p53 protein levels compared to the levels measured in the control cells (+127 %; $p < 0.05$). Treatment with a combination of sc-3088 and comp_$_{LDL100}$ caused relative p53 protein levels to decrease -64 % ($p < 0.05$) compared to the cells incubated with comp_$_{LDL100}$ alone. Figure 49B shows relative p53 protein levels of immunoblotting of EA.hy926 cells either transfected with an empty vector to serve as a control or transfected with a pEGFP-C1-PML-IV-vector (PML↑). PML↑ cells were incubated without or with sc-3088 for 24 hours. PML↑ cells did not significantly affect p53 protein levels compared to the control. Figure 49C shows

relative p53 protein levels of total cell lysates of EA.hy926 cells either incubated with STATTIC, comp_LDL100 or the two of them combined for 24 hours. Untreated EA.hy926 cells served as a control. Incubation with comp_LDL100 led to an increase in relative p53 protein levels (+127 %; $p < 0.0001$). Incubation of STATTIC and comp_LDL100 together also led to an increase in relative p53 protein levels compared to the levels of the control (+48 %; $p < 0.05$). As seen in Figure 49D, PML↑ cells were incubated without or with STATTIC for 24 hours. EA.hy926 cells transfected with a vector lacking specific gene insert were used as a control. Relative p53 protein levels in PML↑ cells remained the same as the levels detected in the control cells, whereas incubation of PML↑ cells with STATTIC led to a slight increase in relative p53 protein levels. Apparently, incubation with sc-3088 leads to a decrease in LDL-induced p53 protein levels, whereas incubation with STATTIC leads to an increase in p53 protein levels.

Figure 49

A

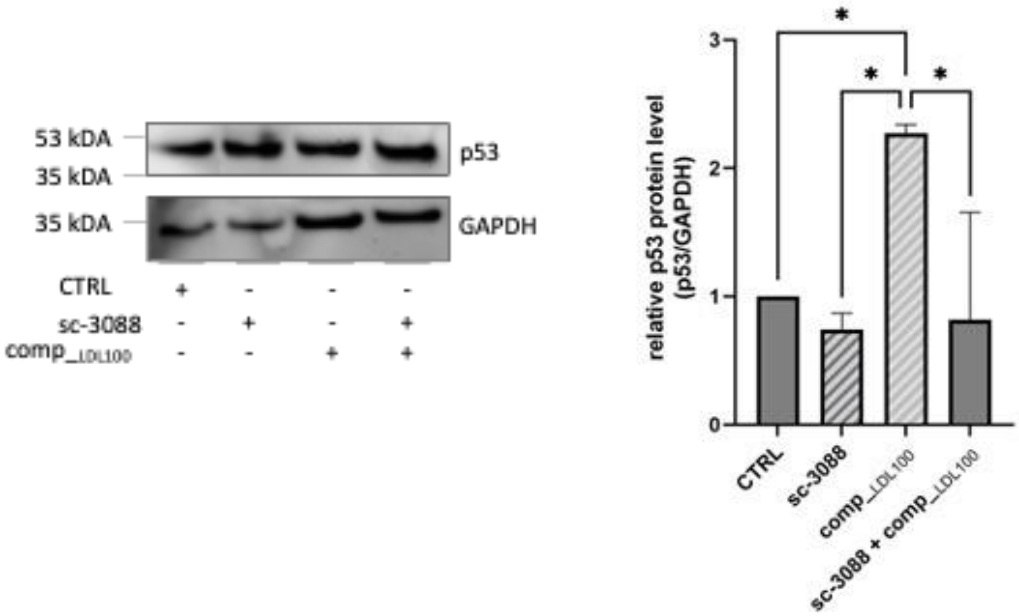

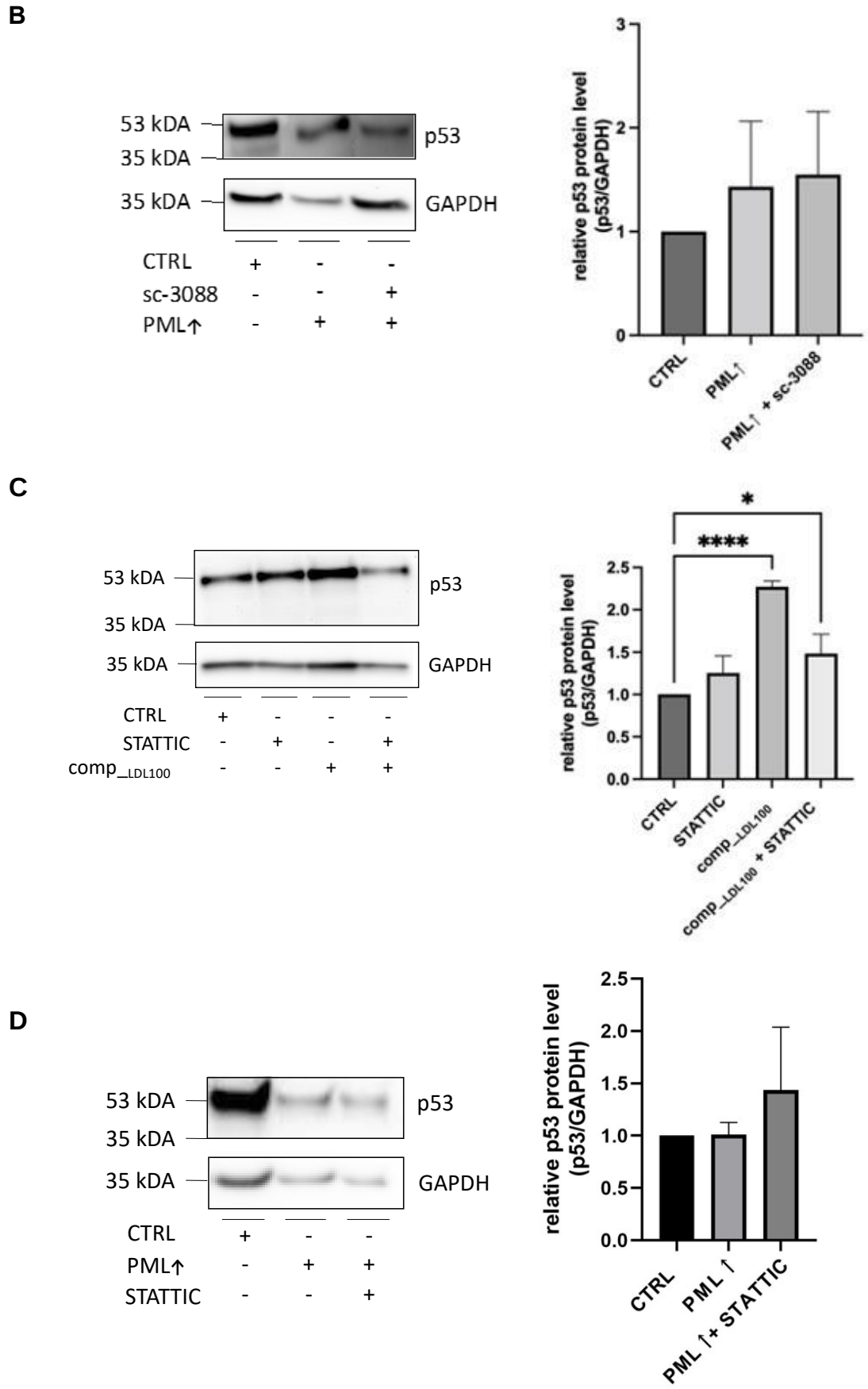

Figure 49. sc-3088 decreases LDL-induced PML target p53 protein expression in endothelial cells, whereas STATTIC enhances it. *(A) Immunoblotting was used on total lysates of EA.hy926 cells incubated with either sc-3088, the lipoprotein*

*composition with 100 mg/dL of LDL or sc-3088 and the composition combined to determine p53 protein levels. Expression values relative to an untreated control. n=3, * p < 0.05 using one-way ANOVA. (B) Immunoblotting of p53 protein levels of EA.hy926 cells transfected with a pEGFP-C1-PML-IV-vector (PML↑) or incubated with sc-3088 after transfection with pEGFP-C1-PML-IV. Control cells were transfected with a vector lacking gene insert. n=3, * p < 0.05, ** p < 0.01, using two-way ANOVA. (C) Immunoblotting of total EA.hy926 cell lysates after incubation with STATTIC, the lipoprotein composition with 100 mg/dL of LDL or STATTIC and the composition combined. The results are relative to an untreated control. n=3, * p < 0.05, **** p < 0.0001 (D) Immunoblotting of p53 protein levels of EA.hy926 cells transfected with a pEGFP-C1-PML-IV-vector (PML↑) or incubated with STATTIC after transfection with pEGFP-C1-PML-IV. Control cells were transfected with a vector lacking gene insert. n=3, p < 0.999. All Graphs shown as mean ± SD.*

3.1.7. HDL enhances eNOS expression, while PML, PKC and STAT3 cause eNOS levels to decrease

To find out about the influence of lipoprotein compositions with different LDL concentrations on eNOS mRNA expression in EA.hy926 cells, RT-qPCR was performed after treating the cells with lipoprotein compositions for 3 or 24 hours. Untreated EA.hy926 cells served as a control. As seen in Figure 50A, incubation of the cells with comp_$_{LDL50}$ for 3 hours led to the highest increase in relative eNOS mRNA levels (+303 %; $p < 0.01$) compared to the control. As shown in Figure 50B, relative eNOS mRNA levels were highest after incubation with comp_$_{LDL50}$ (+309 %; $p < 0.01$) for 24 hours. Compared to the levels detected in the control cells. Obviously, lipoprotein compositions with low LDL levels increase eNOS mRNA levels.

Figure 50

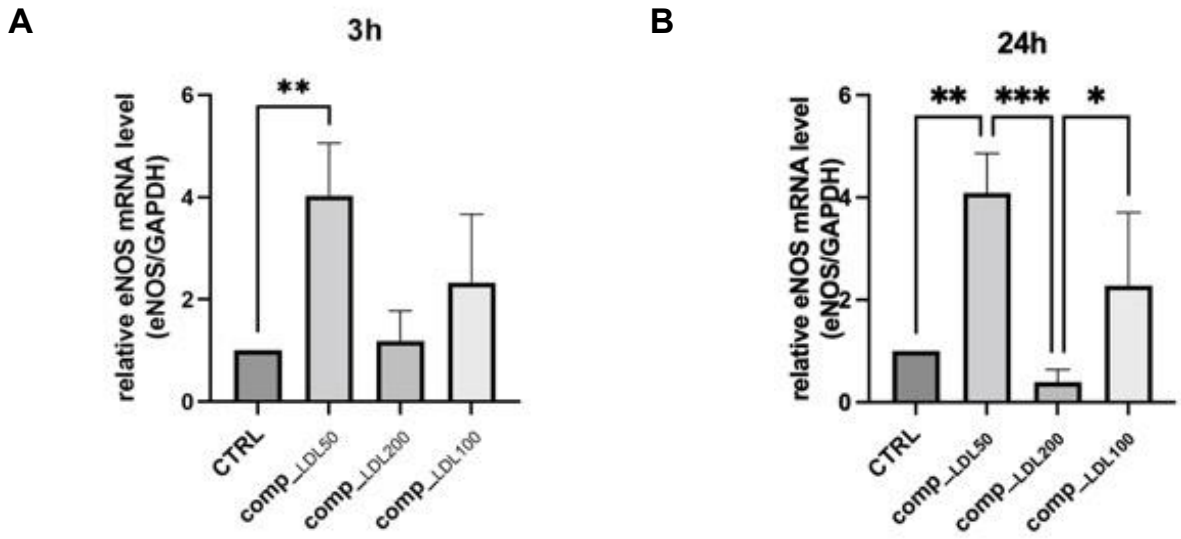

Figure 50. Lipoprotein compositions with low LDL concentrations but not with high LDL concentrations increase eNOS mRNA expression in endothelial cells. *To determine eNOS mRNA levels, RT-qPCR was performed on EA.hy926 cells incubated with lipoprotein compositions with LDL concentrations varying from 50 mg/dL to 200 mg/dL for 3h (A) or 24h (B). Expression values relative to control (CTRL, no lipoprotein supplement). n=4, * p < 0.05, ** p < 0.01, *** p < 0.001 using one-way ANOVA. All Graphs shown as mean ± SD.*

To investigate the impact of different concentrated lipoprotein compositions and PML on relative eNOS protein expression, immunoblotting was performed on EA.hy926 cells that were incubated for 3 or 24 hours. Untreated EA.hy926 cells served as a control. After incubating the

cells for 3 hours (Figure 51A), relative eNOS protein levels were highest when incubated with the composition with comp_$_{LDL50}$ (+97 %; $p < 0.05$). As seen in Figure 51B, incubation with the different compositions for 24 hours caused relative eNOS protein levels to be highest after incubation with comp_$_{LDL50}$ (+175 %; $p < 0.01$) compared to the control. Figure 51C shows relative eNOS protein levels of EA.hy926 cells transfected with a pEGFP-C1-PML-IV-vector (PML↑) and incubated without or with comp_$_{LDL100}$. EA.hy926 cells transfected with an empty vector served as control cells. PML↑ cells expressed decreased relative eNOS protein levels (-93 %; $p < 0.0001$) compared to the control. Apparently, lipoprotein compositions with low LDL levels enhance eNOS protein levels.

Figure 51

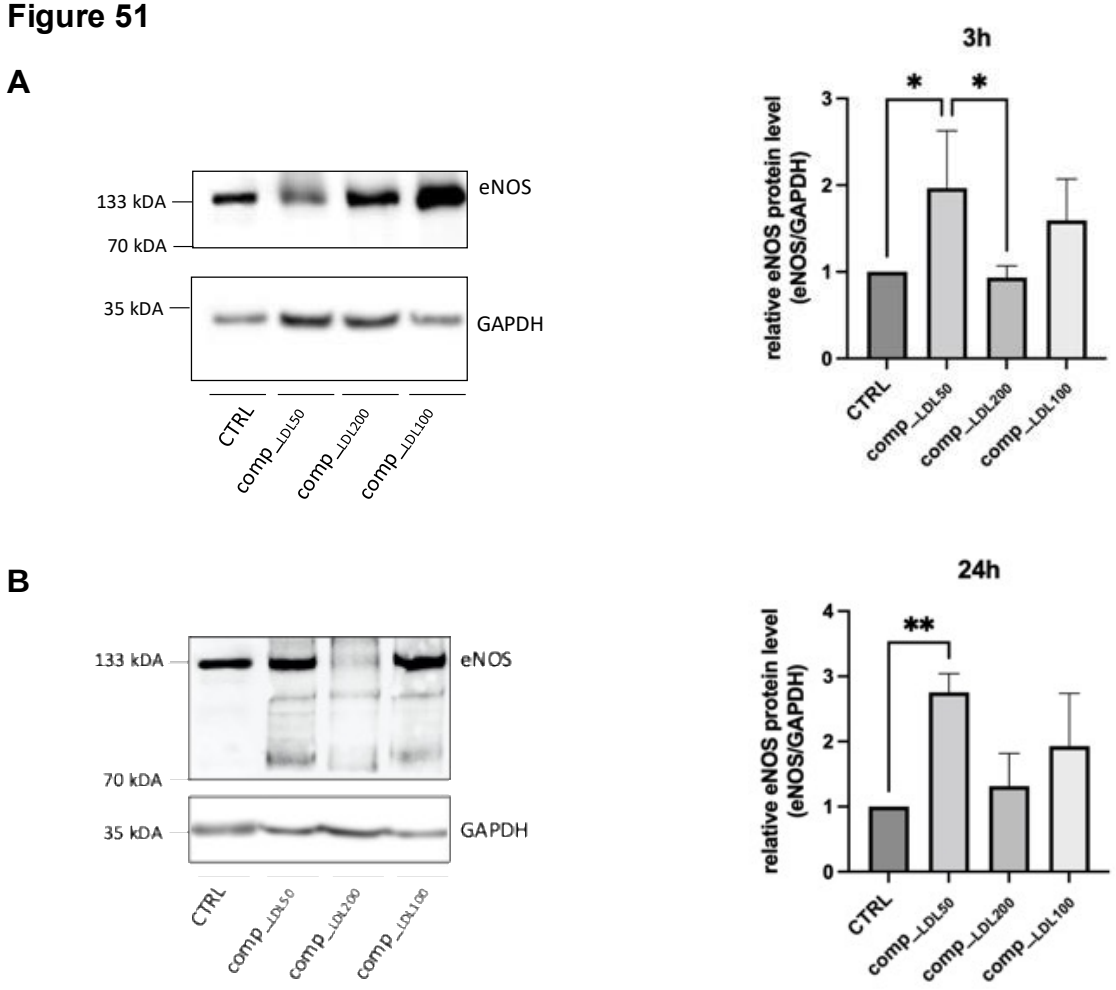

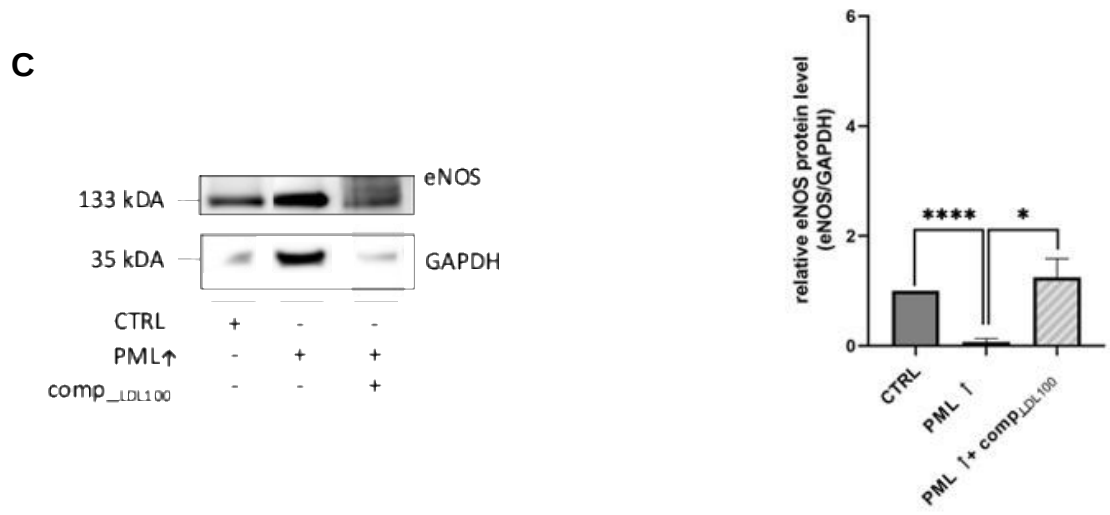

Figure 51. Lipoprotein compositions with low LDL concentrations but not with high LDL concentrations enhance eNOS protein expression in endothelial cells. *Immunoblotting was performed on total lysates of EA.hy926 cells to quantify eNOS protein levels after incubation with lipoprotein compositions with LDL concentrations varying from 50 mg/dL to 200 mg/dL for 3h (A) or 24h (B). Expression values relative to control (CTRL, no lipoprotein supplement). Representative immunoblots of n=4 (A), n=3 (B), * p < 0.05, ** p < 0.01, using one-way ANOVA. (C) eNOS protein levels were determined by performing immunoblotting on total lysates of EA.hy926 cells transfected with a vector without gene insert (CTRL), transfected with a pEGFP-C1-PML-IV-vector (PML↑) or incubated with the lipoprotein composition with 100 mg/dL of LDL after transfection with pEGFP-C1-PML-IV. Representative immunoblot of n=3, * p < 0.05, **** p < 0.0001 using two-way ANOVA. All Graphs shown as mean ± SD.*

To determine the impact of single blood lipoproteins on relative eNOS mRNA expression, RT-qPCR was performed after incubation of EA.hy926 cells with different concentrated lipoproteins for 3 or 24 hours. Untreated EA.hy926 cells served as a control. After 3 hours of incubation (Figure 52A), relative eNOS mRNA levels were highest in cells incubated with 100 mg/dL of HDL (+832 %; $p < 0.0001$). Incubation with 200 mg/dL of LDL caused relative eNOS mRNA levels decrease (-60 %) compared to the control. Figure 52B shows that when incubated for 24 hours, incubation with 100 mg/dL of HDL again led to the highest relative eNOS mRNA levels (+468 %). Apparently, HDL enhances eNOS mRNA levels.

Figure 52

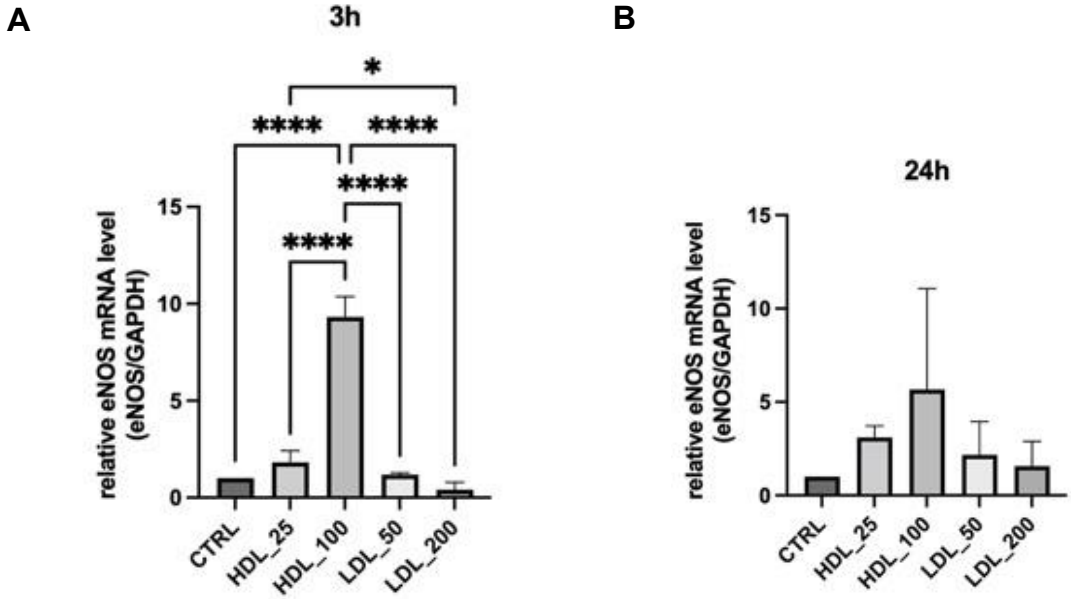

Figure 52. HDL but not LDL leads to an increase in eNOS mRNA expression in endothelial cells. *To determine eNOS mRNA levels in EA.hy926 cells incubated with 25 mg/dL or 100 mg/dL of HDL and 50 mg/dL or 200 mg/dL of LDL for 3h (A) or 24h (B), RT-qPCR was performed. Expression values relative to an untreated control. n=4 (A), n=3 (B) * p < 0.05, **** p < 0.0001 (A), p < 0.999 (B) in two-way ANOVA. All Graphs shown as mean ± SD.*

To investigate the influence of single blood lipoproteins on relative eNOS protein levels of EA.hy926 cells, immunoblotting was performed after an incubation period of 3 or 24 hours. Untreated EA.hy926 cells were used as a control. When incubated with single blood lipoproteins for 3 hours (Figure 53A) highest relative eNOS protein levels were expressed by cells incubated with 100 mg/dL of HDL (+214 %; $p < 0.01$) compared to the control, closely followed by the levels expressed by cells incubated with 25 mg/dL of HDL (+212 %; $p < 0.01$). As seen in Figure 53B, when the incubation span was extended to 24 hours, highest relative eNOS protein levels compared to the levels of the control cells were detected in EA.hy926 cells incubated with 25 mg/dL of HDL (+188 %; $p < 0.01$), closely followed by relative eNOS protein levels detected in cells incubated with 100 mg/dL of HDL (+182 %; $p < 0.01$). Incubation with 50 mg/dL of LDL enhanced relative eNOS protein levels a little less than HDL did (+168 %; $p < 0.05$). Obviously, incubation of EA.hy926 cells with HDL leads to enhanced eNOS protein levels.

Figure 53

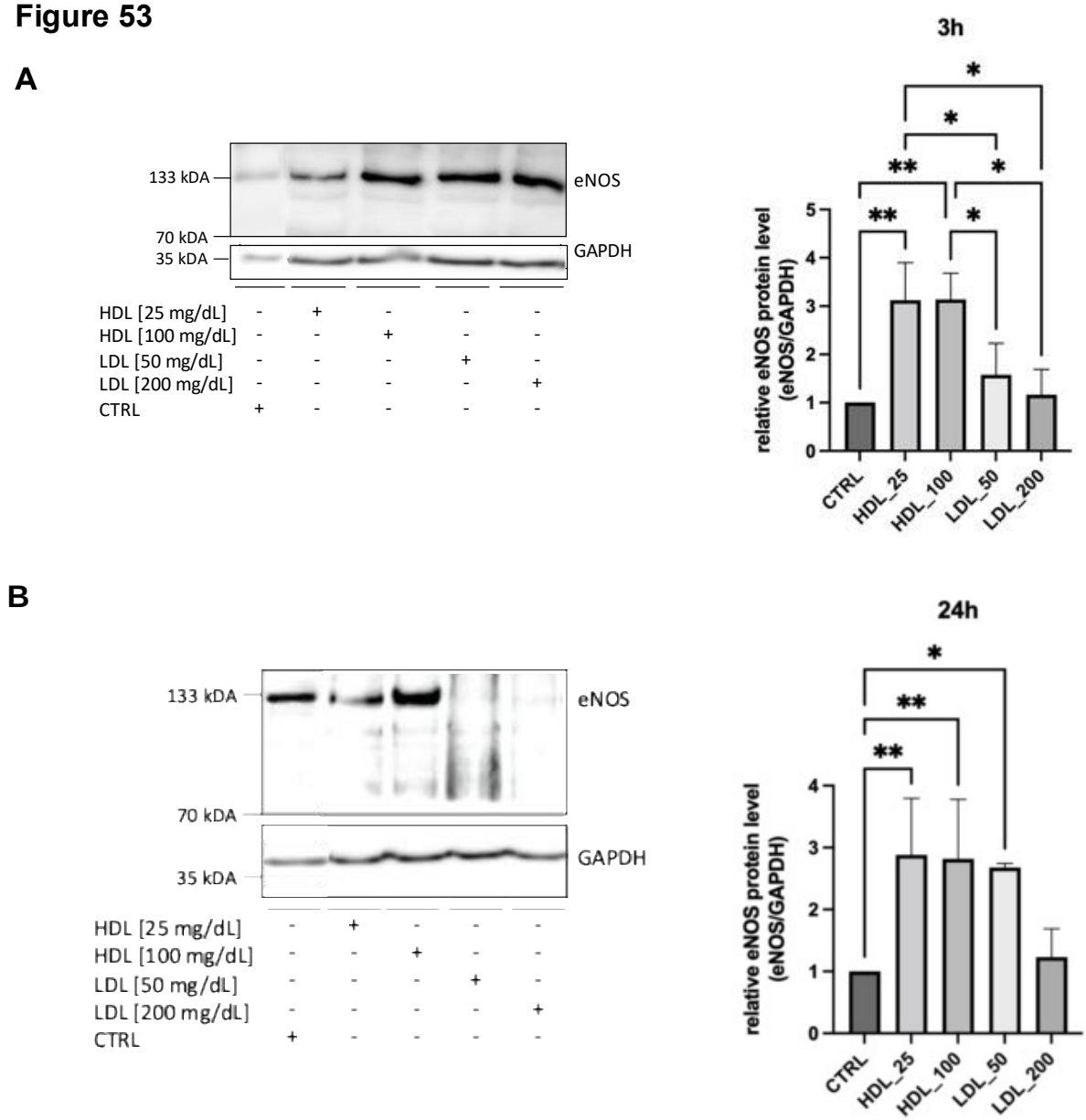

Figure 53. HDL but not high concentrations of LDL lead to an increase in eNOS protein expression in endothelial cells. *To determine eNOS protein levels of total lysates of EA.hy926 cells incubated with 25 mg/dL or 100 mg/dL of HDL and 50 mg/dL or 200 mg/dL of LDL for 3h (A) or 24h (B) immunoblotting was used. Expression values relative to an untreated control. Representative immunoblots of n=3 (A), n=4 (B), * p < 0.05, ** p < 0.01, performing two-way ANOVA. All Graphs shown as mean ± SD.*

In order to investigate whether or not apoE4-homozygous lipoproteins influence relative eNOS mRNA expression, RT-qPCR was performed after incubating EA.hy926 cells with e4/e4-poistive lipoproteins for 3 or 24 hours. As shown in Figure 54A, incubation with the lipoproteins for 3 hours caused relative eNOS mRNA levels to be highest after incubation with 100 mg/dL of apoE4-homozygous HDL compared to the control (+468 %; $p < 0.05$). Figure 54B shows relative eNOS mRNA levels after 24 hours of incubation with apoE4-homozygous lipoproteins. Incubation with 25 mg/dL of apoE4-homozygous HDL led to an increase of relative eNOS mRNA levels (+592 %; $p < 0.001$) compared to the control, as did incubation

with 100 mg/dL of apoE4-homozygous HDL (+532 %; $p < 0.01$). Relative eNOS mRNA levels increase from 3 hours of incubation with apoE4-homozygous lipoproteins to 24 hours of incubation. Obviously, apoE4-homozygous HDL causes an increase in eNOS mRNA expression.

Figure 54

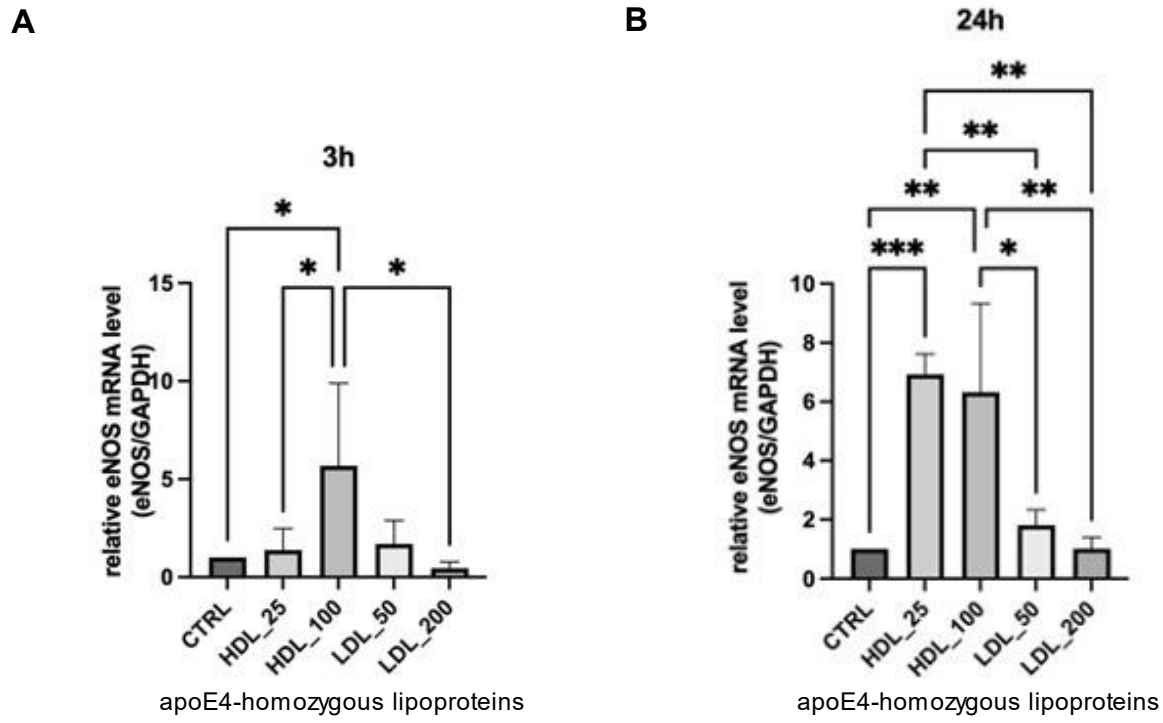

Figure 54. apoE4-homozygous HDL, but not LDL enhances eNOS mRNA expression in endothelial cells. *For determination of eNOS mRNA levels, RT-qPCR was performed on untreated EA.hy926 cells (CTRL) or EA.hy926 cells incubated with apoE4-homozygous 25 mg/dL or 100 mg/dL of HDL and 50 mg/dL or 200 mg/dL of LDL for 3h (A) or 24h (B). n=4 (A), n=3 (B), * p < 0.05, ** p < 0.01, *** p < 0.001, performing two-way ANOVA. All Graphs shown as mean ± SD.*

In order to determine relative eNOS protein levels, immunoblotting was performed on EA.hy926 cells incubated with different apoE4-homozygous lipoproteins for a duration of 3 or 24 hours. As shown in Figure 55A, when incubated for 3 hours, relative eNOS protein levels increase most after incubation with 25 mg/dL of apoE4-homozygous HDL compared to the control. When incubated for 24 hours (Figure 55B), relative eNOS protein levels in EA.hy926 cells were highest when incubated with 25 mg/dL of apoE4-homozygous HDL. Apparently, low levels of apoE4-homozygous HDL lead to enhanced eNOS protein levels.

Figure 55

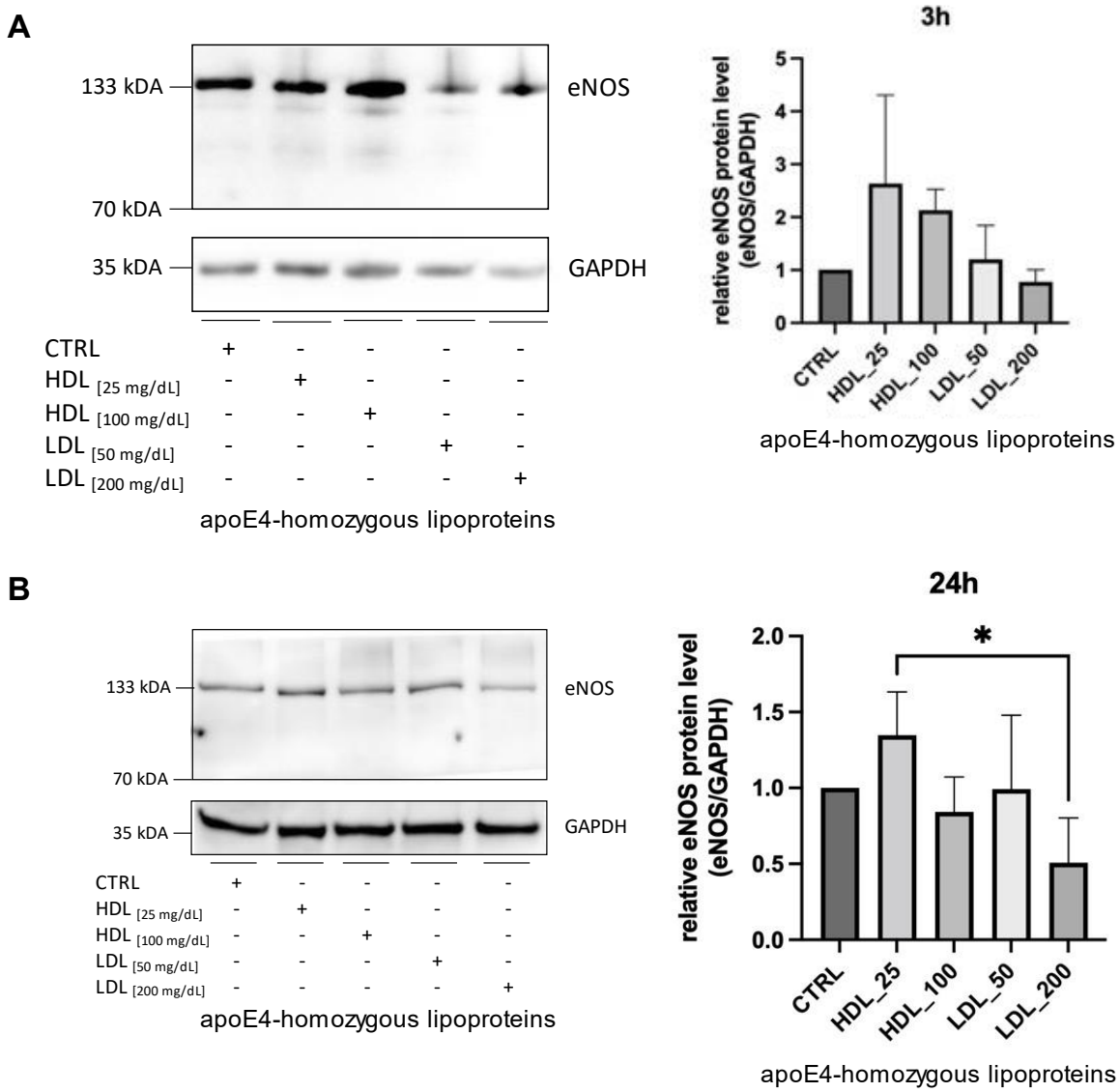

Figure 55. apoE4-homozygous HDL increases eNOS protein expression in endothelial cells, whereas high LDL concentrations decrease it. *Immunoblotting on total lysates of EA.hy926 cells was used to quantify eNOS protein levels after incubation with apoE4-homozygous 25 mg/dL or 100 mg/dL of HDL and 50 mg/dL or 200 mg/dL of LDL for 3h (A) or 24h (B). Expression values relative to an untreated control. Immunoblots are representative of n=3 independent experiments, p < 0.999, * p < 0.05 (B), performing two-way ANOVA. All Graphs shown as mean ± SD.*

To find out about the influence of (LDL-induced) PKC activity and STAT3 activity on eNOS protein expression, immunoblotting was performed on EA.hy926 cells incubated for 24 hours, or on cells transfected with a pEGFP-C1-PML-IV-vector. As shown in Figure 56A, EA.hy926 cells were either incubated with sc-3088, comp_$_{LDL100}$ or with both of them together for 24 hours before immunoblotting was performed. Untreated EA.hy926 cells served as a control. When the cells were incubated with sc-3088, relative eNOS protein levels increased (+49 %; $p < 0.05$). Figure 56B illustrates relative eNOS protein levels detected in EA.hy926 cells after transfection with a pEGFP-C1-PML-IV-vector (PML↑) and incubated without or with sc-3088

for 24 hours. EA.hy926 cells transfected with an empty vector served as control cells. Relative eNOS protein levels in PML↑ cells were decreased (-89 %; $p < 0.05$) compared to the control, whereas PML↑ cells incubated with sc-3088 for 24 hours expressed about the same eNOS protein levels that were determined in the control. When EA.hy926 cells were incubated with STATTIC and comp_LDL100 together (Figure 56C), relative eNOS protein levels increased compared to an untreated control. Apparently, incubation of EA.hy926 cells with sc-3088 causes relative eNOS protein levels to increase, whereas transfection with a pEGFP-C1-PML-IV-vector leads to a decrease in eNOS protein levels.

Figure 56

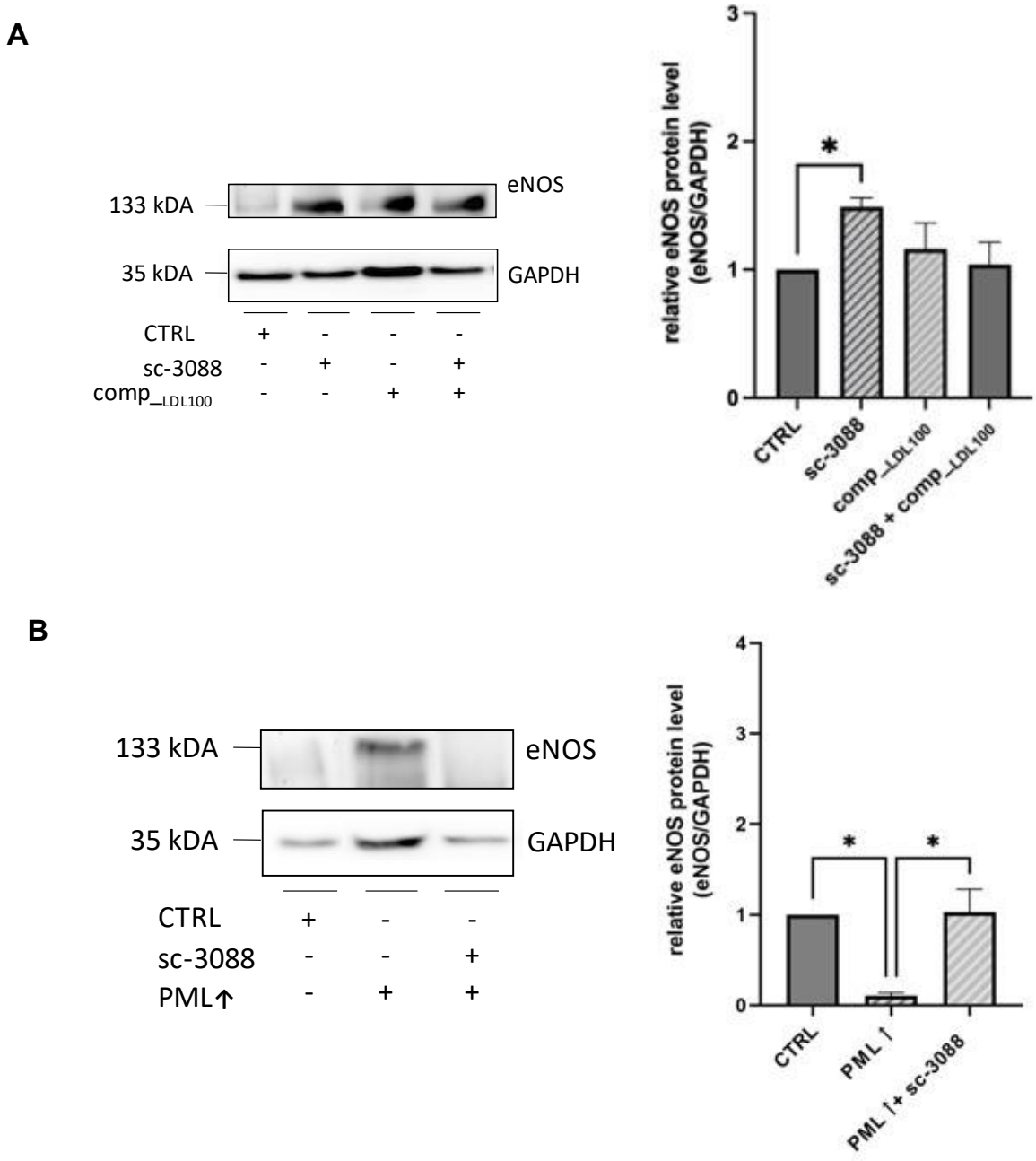

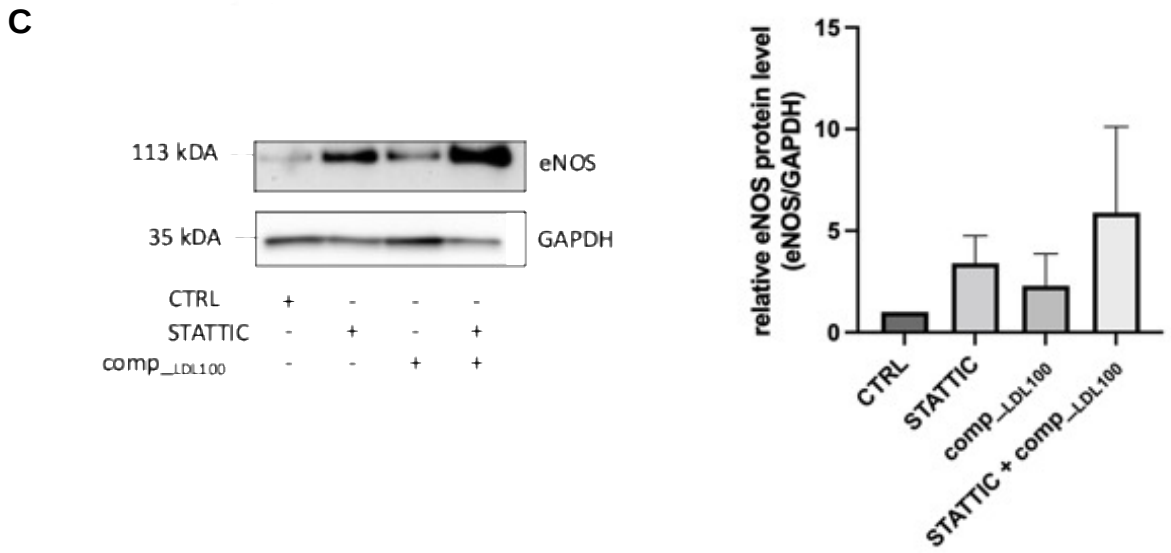

Figure 56. Incubation with sc-3088 and STATTIC enhances eNOS protein expression in endothelial cells. *(A) eNOS protein levels were determined using immunoblotting on EA.hy926 cells incubated with either sc-3088, the lipoprotein composition with 100 mg/dL of LDL or sc-3088 and the composition combined. Expression values relative to an untreated control. n=3, p < 0.99 using one-way ANOVA. (B) Immunoblotting of eNOS protein levels of EA.hy926 cells transfected with a pEGFP-C1-PML-IV-vector (PML↑) or incubated with sc-3088 after transfection with pEGFP-C1-PML-IV. Expression values relative to a control transfected with a vector lacking gene insert. n=3, * p < 0.05 in two-way ANOVA. (C) immunoblotting was used to quantify eNOS protein levels in EA.hy926 cells incubated with STATTIC, the lipoprotein composition with 100 mg/dL of LDL or a combination of STATTIC and the composition. Expression values relative to an untreated control. n=3, p < 0.85 using one-way ANOVA. All Graphs shown as mean ± SD.*

3.2. Lipoprotein compositions with physiological lipoprotein concentrations leave the flow-dependent vasodilation of coronary arteries unaffected

In order to investigate the impact of a lipoprotein composition with physiological lipoprotein concentrations on the flow-dependent vasodilation of human coronary arteries, an experiment was conducted, where comp_$_{LDL100}$ was tested on human coronary arteries with different flow rates. As seen in Figure 57, different flow rates of Krebs-solution were tested on the different pieces of coronary arteries as well and served as a control (displayed in grey). The results of testing different flow rates of comp_$_{LDL100}$ on the arteries are displayed in blue. When a flow rate of 3 mL/min was tested, Krebs-solution caused a tension of the arteries of 1.688 g, while comp_$_{LDL100}$ caused the arteries to have a tension of 1.709 g (+1 % compared to control). A flow rate of 5 mL/min caused the arteries in the control experiment to have a tension of 1.554 g. Testing with comp_$_{LDL100}$ caused a tension of 1.504 g (-3 % compared to the control). A flow rate of 20 mL/min caused the control to have a tension of 1.424 g, while comp_$_{LDL100}$ caused a slightly lower tension of 1.384 g (a decrease of 3 % compared to the tension of the control). When the flow rate was increased to 40 mL/min, the control showed a tension of 1.333 g. comp_$_{LDL100}$ caused a slight decrease in tension of the coronary arteries of 1.289 g (-3 % compared to the control). The fastest flow rate tested was a flow rate of 100 mL/min, which caused the control to have a tension of 1.262 g, while the coronary arteries treated with comp_$_{LDL100}$ at 100 mL/min had a tension of 1.222 g, representing a decrease of 3 % compared to the control.

These comparisons made above can be put in an absolute lipoprotein-dependent reduction in tonus and can be calculated as followed for every flow rate:

$\Delta T_{absolute} = T_{comp\_LDL100} - T_{Krebs\text{-}solution}$

'T' meaning the tension measured in the corresponding part of the experiment. $\Delta T_{absolute}$ for every flow rate is listed in *Table 10*.

Flow (mL/min)	*3*	*5*	*20*	*40*	*100*
$\Delta T_{absolute}$	0.021	-0.050	-0.040	-0.043	-0.041
p value	0.9998	0.9867	0.9952	0.9931	0.9950

Table 10. $\Delta T_{absolute}$ and p values for the experiments conducted to determine the impact of lipoprotein compositions on human coronary arteries.

When $\Delta T_{absolute}$ of all flow rates is combined, the mean change in absolute lipoprotein-dependent tonus reduction is -0.031, indicating a slight, yet not significant (*Table 10*) relaxation

of the coronary arteries when treated with comp_$_{LDL100}$. This effect itself is flow-dependent and measures its highest value at a flow rate of 100 mL/min and its lowest value at 3 mL/min, so that the actual tonus reduction that is mediated by the flow needs to be calculated as well, using the following equation:

$\Delta T_{flow} = T_{3mL/min} - T_{100\ mL/min}$

The flow-mediated reduction in tonus needs to be calculated for both, the control experiment and the experiment using comp_$_{LDL100}$ to investigate its influence on the flow-dependent vasodilation. ΔT_{flow} for the control equals 0.426, while ΔT_{flow} for comp_$_{LDL100}$ equals 0.487. Regarding these calculations, treatment with comp_$_{LDL100}$ led to an enhancement of the flow-dependent vasodilation of the tested coronary arteries of 0.061 g, which equals 14 % compared to the control.

Obviously, different flow rates of the lipoprotein composition with physiological lipoprotein compositions does not have an impact on the flow-dependent vasodilation of human coronary arteries.

Figure 57

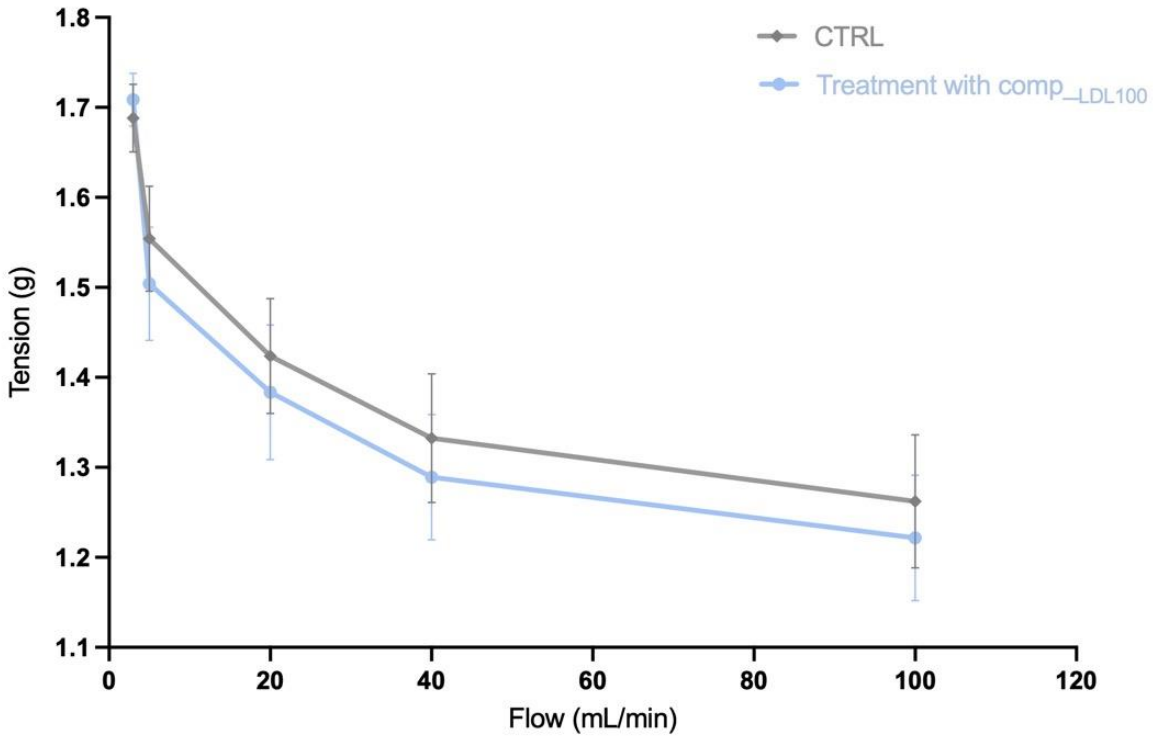

Figure 57. A composition of blood lipoproteins of physiological concentration leaves the flow-dependent vasodilation of human coronary arteries unaffected. *The flow-dependent vasodilation of human coronary arteries was determined via measuring tension while either Krebs-solution (displayed in grey, n=5) or a blood lipoprotein composition with physiological lipoprotein concentrations (displayed in blue, n=6 pieces of the coronary arteries of one patient) flowed through the arteries with flow rates varying from 3 mL/min to 100 mL/min. p > 0.9 (Table 10) performing two-way ANOVA. All Graphs shown as mean ± SD.*

4. Discussion

It was investigated in the present study whether a molecular module centring PML contributes to the lipoprotein-induced signal transduction of atherosclerosis and AD in endothelial cells. Initially, the upstream effect of lipoproteins on PML expression in EA.hy926 cells and HUVECs was evaluated, whereupon IL-6, IL-8, PKC, STAT3, p53 and eNOS expression in EA.hy926 cells were analysed to clarify their downstream connection to PML. Furthermore, the influence of lipoproteins on the flow-dependent vasodilation of human coronary arteries was assessed. Essentially, 9 major results were gained (Figure 58): 1. Exposure of EA.hy926 cells to LDL was associated with a higher PML expression, 2. LDL and PML caused an upregulation of IL-6 and IL-8 expression in EA.hy926 cells, 3. LDL caused higher PKC activity in EA.hy926 cells, 4. (LDL-induced) elevated PKC activity increased PML expression in Ea.hy926 cells and HUVECs, while PML induced PKC activity in EA.hy926 cells. 5. STAT3 expression in EA.hy926 cells increased due to LDL exposure, 6. (LDL-induced) PKC activity elevated IL-6 and IL-8 expression in EA.hy926 cells, 7. treatment of EA.hy926 cells with LDL led to an increase in p53 protein expression, and 8. HDL triggered higher eNOS expression in EA.hy926 cells, but eNOS expression decreased through PML and PKC activity. 9. The flow-dependent vasodilation of human coronary arteries was not affected by lipoproteins in physiological concentrations.

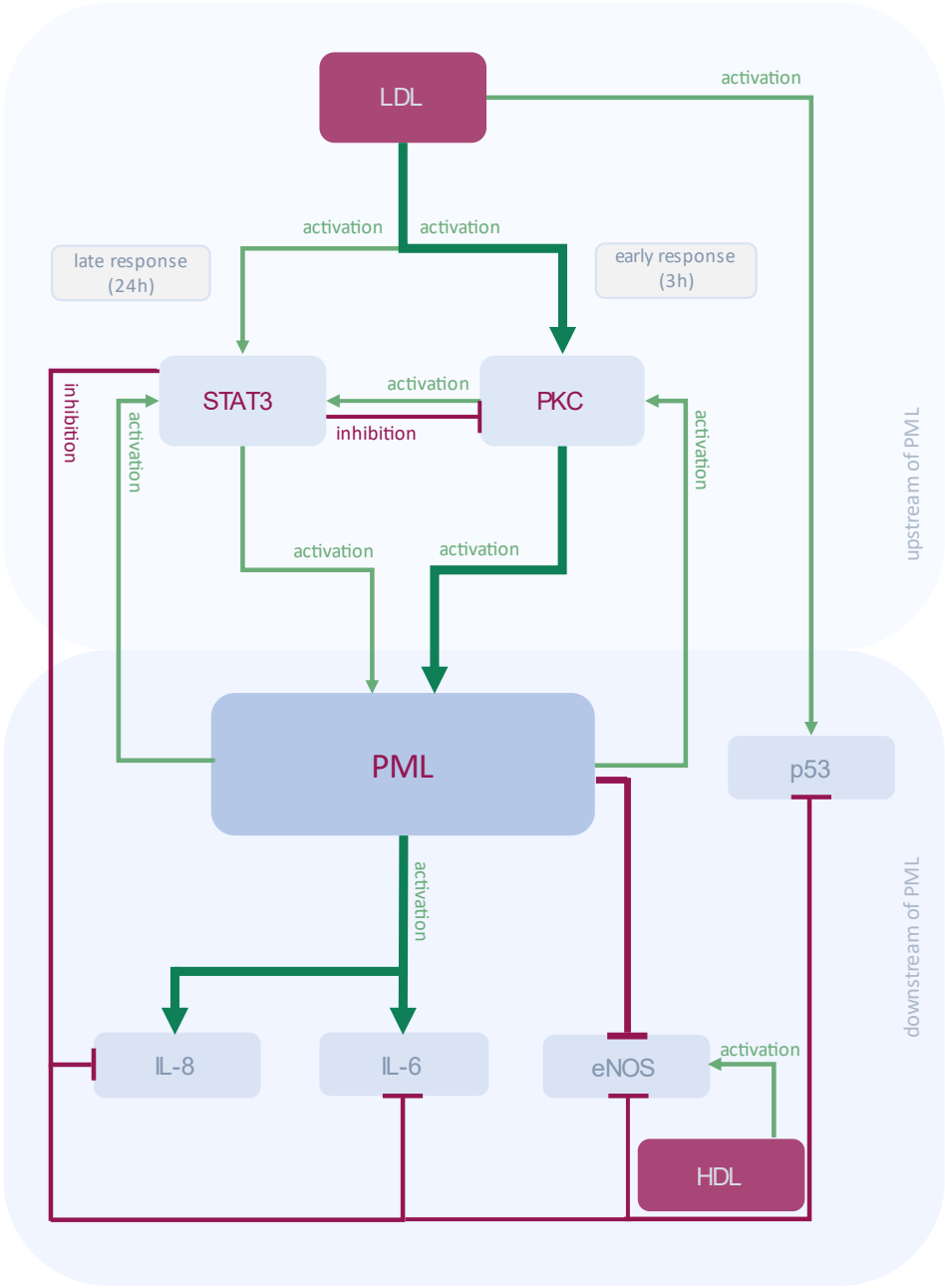

Figure 58. Schematic depiction of the major findings described in this thesis. *The results and their interpretation suggest the depicted molecular mechanisms. LDL activates PKC in an early response, which further leads to enhanced PML expression. This causes higher IL-6 and IL-8 expression and secretion levels to enhance and eNOS levels to decrease. LDL further activates STAT3 in a late response, which also has an increasing effect on PML. However, STAT3 activation leads to inhibition of IL-8, IL-6 and eNOS. eNOS is activated by HDL. LDL enhances p53 protein expression, which is inhibited by STAT3. Created by the author.*

4.1. Does oxLDL interference with the results of the study?

Several investigations already reported that oxLDL significantly influences endothelial cells, e.g. Cu^{2+} - oxidized LDL (Cu^{2+}-oxLDL) increased the adhesiveness of endothelial cells dose-dependently [288]. Binding of mildly oxidized LDL to endothelial cells led to the specific induction of three different colony stimulating factors (CSFs) [289]. Cytotoxicity is induced by

oxLDL in high concentrations [290]. Furthermore, oxLDL activates protein kinase C (PKC) and protein tyrosine kinase (PTK) in HCAEC [157] and mediates coronary vasoconstriction via activating PKCα and PKCε in single coronary smooth muscle cells [167]. These findings provide the opportunity that the results of this study are falsified by oxLDL. However, the oxLDL concentrations in the lipoprotein solutions, as measured by ELISA, were almost neglectable. It thus is concluded that oxLDL did not interfere with the outcome of the experiments.

4.2. The influence of lipoproteins on PML expression

As PML is involved in atherosclerosis and AD [123, 125], the impact of lipoproteins on PML expression was investigated. PML mRNA and protein expression as well as the number of PML-NBs per nucleus were increased dose-dependently when EA.hy926 cells and HUVECs were incubated with LDL alone or in lipoprotein compositions with different LDL concentrations in an early response. These findings suggest that PML is integrated in LDL-dependent inflammatory processes in atherosclerosis, such as TH1-proliferation [291]. This conclusion is in agreement with previous findings, which demonstrated PML to play a role in IFN-mediated immunomodulation [292] e.g. IFN-dependent PML-NB assembly [107, 293] and TNF-α-induced inflammatory responses in HUVECs [294]. However, as VLDL and IDL were components of the lipoprotein compositions (aside from LDL and HDL) used in the experiments, it is also possible that they positively influence PML expression. As VLDL stimulates plasminogen activator inhibitor-1 (PAI-1) in HUVECs and PAI-1 levels in endothelial cells were increased through TNF-α exposition [295], which stimulates PML expression in endothelial cells [296], the suggestion forms that VLDL also influences PML. Additionally, VLDL strongly enhances NFkB activation [297], which is linked to PML-NB assembly [298]. It would therefore be advisable to conduct similar experiments with VLDL as with IDL to gain more insights on the interaction of PML with lipoproteins.

Incubation with HDL alone led to a rapid decrease in PML mRNA expression. This was expected, as HDL has protective properties in inflammation, for example by protecting the cell via activation of the PI3K/AKT-pathway [299]. HDL furthermore has a protective effect on endothelial cells and apoA, which is a part of HDL [300], prevents ox-LDL-induced cytotoxicity [301]. Preincubation of HUVECs with HDL prior to addition of TNF-α led to the inhibition of the negative effects of TNF-α exposition, such as DNA-fragmentation [302]. Surprisingly, incubation with HDL did not lower PML protein expression nor the number of

PML-NBs. As ABCA1, which is involved in reversed cholesterol transport [303], is stabilized by the HDL component apoAI [300, 304], it is possible that additional posttranslational modifications cause stabilization of PML protein.

apoE4-homozygous LDL caused higher PML expression. As apoE4 increases the risk for developing AD [40], apoE4-homozygous LDL was expected to cause a stronger effect on PML levels than genetically pooled LDL did, which did not occur. Moreover, as Hoshino et al. reported that HDL negatively correlates with apoE4 concentrations [305], suggesting a promotion in the development of AD, it was expected that apoE4-homozygous HDL would increase PML expression, whereas incubation of endothelial cells with apoE4-homozygous HDL led to a decrease in PML expression.

4.3. The influence of lipoproteins on IL-6 and IL-8 secretion and expression

Several reports demonstrated that IL-6 and IL-8 act upstream of PML [134, 137, 306]. To assess if IL-6 and IL-8 also act downstream of PML in endothelial cells, it was investigated whether IL-6 and IL-8 secretion is affected by lipoproteins and PML. Actually, IL-6 and IL-8 secretion in the supernatants of EA.hy926 cells rapidly increased after incubation with LDL or lipoprotein compositions dose-dependently on LDL. The significant increase in IL-8 secretion through high LDL concentrations is in accordance with the findings of Ryoo et al. that revealed LDL to be capable of upregulating IL-8 expression in a dose-dependent manner [307]. HDL did not affect IL-6 and IL-8 secretion. Interestingly, Gomaraschi et al. showed that HDL lowered IL-6 levels via inhibition of p38 MAP kinase when induced by TNFα [308], suggesting that this mechanism of inhibition did not play a role in this study. Again, as VLDL and IDL were components of the lipoprotein compositions that were used in the experiments, it would be beneficial to investigate on their influence on the secretion of the cytokines, especially as it is known that IL-8 is upregulated by VLDL [309], which indicates an additive effect of LDL and VLDL on IL-8 secretion when incubated with the lipoprotein compositions.

IL-6 and IL-8 secretion increased after incubation with apoE4-homozygous LDL in a dose- and time-dependent manner, indicating that the cytokines could act as a risk factor for the development of AD, as it has already been reported that IL-6 levels in mouse macrophages treated with apoE4 express higher IL-6 levels compared to macrophages treated with apoE3 [310] and IL-8 levels are increased in patients with AD [148].

PML-overexpressing EA.hy926 cells showed a significantly higher expression of IL-6 and IL-8 mRNA levels, indicating that both of the cytokines act downstream of PML in endothelial

cells. This suggestion is underlined by the fact that IL-6 acts downstream of PML in mouse embryonic fibroblasts [306].These initially contradictory findings suggests a positive control loop with mutual upregulation of IL-6 and IL-8 by PML, which may be controlled by other molecular mechanisms, as it is already known that IL-6 interacts in a feedback loop with STAT3 and NFkB in myofibroblasts [311], while IL-8 is part of a positive feedback loop in breast cancer cells [312].

4.4. The impact of lipoproteins on PKC activity

PKC is activated by LDL [165] and plays a role in atherosclerosis and AD [156, 168]. Therefore, the impact of lipoproteins on PKC activity was investigated. PKC activity enhanced dose-dependently on LDL when EA.hy926 cells were treated with the lipoprotein compositions with physiological or high LDL concentrations for 24 hours. These data suggest that LDL directly triggers the increase of PKC activity in EA.hy926 cells, in agreement with the findings of Ren et al., which found LDL and oxLDL to be responsible for increased PKC activity in mesangial cells [165]. In contrast, treatment of the cells with the PKC-peptide inhibitor sc-3088 in presence of the physiological lipoprotein composition led to a decrease in PKC activity. As sc-3088 binds to the common catalytic domain of PKC, it inhibits activity of all PKC isoforms [152, 153]. Incubation with the PKC activator PMA in presence of the lipoprotein composition with physiological lipoprotein concentrations led to a higher increase in PKC activity than incubation with the lipoprotein composition alone. Interestingly, PMA is a derivative of DAG and thus only activates DAG-dependent PKCs [281], thus it remains to be investigated whether aPKCs, which function independent of DAG [154], are involved in this pathway as well, or if LDL only increases PKC activity of only one or multiple PKC isoforms, as oxLDL is known to increase PKCα and PKCε activity [167]. Furthermore, it would be interesting to know if LDL controls the expression patterns of PKC as well. As Lee et al. hypothesised that LDL activates PKC through binding to a specific receptor [313] and it is already known that PKC promotes mRNA expression of the LDL-receptor [314], it would be beneficial to figure out what molecular mechanism stands behind the increase of PKC activation through LDL.

4.5. The molecular relationship between PKC and PML

As PKC is activated by LDL (chapter 4.4), it was hypothesised that PKC plays a role in LDL-induced upregulation of PML (chapter 4.2). Therefore, it was tested whether PKC indeed

upregulates PML expression and if PKC activity is affected by PML. Incubation of EA.hy926 cells with sc-3088 for 24 hours significantly decreased PML mRNA and protein expression, thus it might not only be helpful to get closer insights on the molecular transcription mechanisms of PML induction via PKC, but also to investigate posttranslational interactions between PML and PKC. A posttranslational interaction that might occur between the two is SUMOylation. Sun et al. discovered that PKC is SUMOylated, as e.g. activation of kainate receptors triggered deSUMOylation of PKC [315]. Additionally, PML has a SUMO binding site [93] and about 50 % of PML interaction partners are SUMOylated [104], therefore investigating if SUMOylation plays a role in the interaction between PKC and PML would be beneficial.

Treatment of EA.hy926 cells and HUVECs with sc-3088 decreased the number of PML-NBs, whereas incubation with PMA enhanced the number of PML-NBs. Interestingly, PML-NBs were generally larger in HUVECs than in EA.hy926 cells, but lower in number, underlining the difference of PML-NB assembly in different cell types [96].

As incubation with the lipoprotein composition with physiological lipoprotein concentration in presence of sc-3088 significantly decreased and incubation with said lipoprotein composition, while incubation with PMA increased PML expression, it is assumed that the upregulation of PML via LDL-induced PKC activity is of relevance for PML expression in atherosclerosis and AD.

4.6. Molecular interaction between lipoproteins, STAT3, PML and PKC

STAT3 and PML are functionally linked as STAT3 upregulates PML via the JAK/STAT pathway and PML inhibits IL-6 mediated STAT3 activation [134, 203]. Therefore, it was determined whether STAT3 is upregulated by lipoprotein treatment. The analysis revealed that STAT3 mRNA and protein levels increased when incubated with the lipoprotein composition with high LDL concentrations. This effect has been detected only after 24 hours of incubation, suggesting this increase to occur as a late response, which is underlined by the fact that Ripperger et al. found STAT3 in rat liver cells to be expressed only in a late response after IL-6 treatment [316].

As phosphorylation on Tyr-705 and Ser-727 of STAT3 is crucial for its activation and thus for inducing the transcription of its target genes [186, 187, 193], the effect of lipoproteins on STAT3 activation was determined. The lipoprotein composition with high LDL concentrations caused pSTAT3 protein levels to increase. Accordingly, Jung et al. found that LDL induces the

STAT3 pathway in cancer cells [317]. STAT3 activation in EA.hy926 cells occurred after 3 hours of incubation, which is in accordance to the fact that in rat hepatoma cells, pSTAT3 appeared in an early response to IL-6 treatment [316].

When incubating EA.hy926 cells with STATTIC, a small-molecule inhibitor of STAT3 activation and dimerization, PML mRNA expression decreased. Interestingly, PML protein expression was not reduced under these conditions, raising the question if there is another interaction partner involved in the regulation of PML protein expression.

The number of PML-NBs did significantly change in HUVECS but not in EA.hy926 cells after treatment with STATTIC.

Since STAT3 and PML interact in a negative feedback loop [210], it would be beneficial to understand the molecular mechanism behind the PML and STAT3 interaction. It furthermore remains unclear why PML causes a decrease in STAT3 activity when, at the same time, it causes STAT3 mRNA and protein expression levels to be increased.

To investigate the interaction between STAT3 and PKC, EA.hy926 cells were incubated with STATTIC before PKC activity was determined. PKC activity in EA.hy926 cells increased after 24 hours of incubation with STATTIC, an effect that was further increased after additional treatment with the physiologically-concentrated lipoprotein composition. Additionally, EA.hy926 cells were incubated with sc-3088 before STAT3 and pSTAT3 expression were determined. Incubation of EA.hy926 cells with sc-3088 decreased STAT3 and pSTAT3 protein levels. These findings imply that active STAT3 inhibits PKC activation in general and also LDL-induced PKC activation, while PKC increases STAT3 and pSTAT3 protein expression.

Jain et al. already showed that PKCδ, together with IL-6, activates STAT3 through phosphorylation on Ser-727 in different cell lines [193]. Furthermore, Kwon et al. showed that PKCθ caused upregulation of STAT3 in mice [318]. These results suggest an interaction of PKC and STAT3 in a negative feedback loop including upregulation and activation of STAT3, which then decreases PKC activity. This molecular interaction would correspond to other STAT3-dependent feedback loops, e.g. the loop including miR-146b, NFkB and IL-6 [319]. Furthermore, it is possible that the LDL-induced upregulation of STAT3 is not directly mediated but is realised by the LDL-induced increase of PKC activity.

4.7. The influence of PKC and STAT3 on IL6- and IL-8 expression

IL-6 and IL-8 secretion was induced by LDL and the cytokines were shown to act downstream of PML (chapter 4.3). It was investigated whether these effects are dependent on (LDL-

induced) PKC or STAT3 activity. Incubation with sc-3088 decreased IL-6 and IL-8 mRNA expression in EA.hy926 cells, also when induced by LDL. Treatment with PMA in presence of the lipoprotein composition with physiological concentrations led to an additive effect on IL-6 mRNA expression. These findings point out the dependency of IL-6 and IL-8 mRNA expression on PKC activation and PML. This observation is in accordance to the findings made in skeletal muscle, where IL-6 is induced via a pathway involving PKC [320] and in bronchial epithelial cells, where PKC directly induced IL-8 and IL-6 secretion [321].

Surprisingly, LDL-induced STAT3 activity negatively affected IL-6 and IL-8 mRNA expression in non-transfected and PML-overexpressing EA.hy926 cells. Even though IL-6 and IL-8 are part of activating STAT3 (review chapters 1.5 and 1.7) [127, 133] and interact with STAT3 [311], the finding that STAT3 decreases both, IL-6 and IL-8 mRNA expression suggests them acting in a negative feedback loop.

4.8. The influence of lipoproteins, PKC, PML and STAT3 on p53 protein expression

p53 is co-localised with PML in PML-NBs [322]. It was therefore investigated if p53 also acts as a downstream target of PML in the proposed LDL-dependent pathway. It was found that p53 protein levels increased after incubation with all lipoprotein compositions or with high concentrations of single apoE-pooled or apoE4-homozygous LDL. These findings are promoted by the fact that p53-mediated apoptosis in EA.hy926 cells is induced by ox-LDL [323]. Interestingly, PML-overexpressing cells did not increase p53 protein expression. Accordingly, p53 is not a downstream target of PML.

Incubation with the lipoprotein composition with physiological concentrations in presence of sc-3088 resulted in a decrease of p53 protein levels, suggesting that the LDL-induced increase of p53 protein levels is caused by PKC, which is in accordance to the findings of Abbas et al., reporting that downregulation of PKCδ inhibits p53 mRNA expression in different cell types [324]. However, the assumption that the decrease of p53 protein expression is mediated through inhibition of PKC has to be experimentally validated as it might occur that MDM2-mediated p53 protein stability is influenced by PKC [325]. Furthermore, as PML-NBs play a role in the activation of p53 [326], it would be beneficial to investigate on p53 activation in context with LDL, PKC and PML.

As active STAT3 is known to bind to the p53 promoter and subsequently inhibit p53 expression [196], the finding that incubation of EA.hy926 with STATTIC did not lead to an increase in p53 protein levels was not in accordance to the literature.

4.9. The influence of lipoproteins, PKC, STAT3 and PML on eNOS expression

eNOS expression is promoted by HDL [245], but high cholesterol levels are known to have a negative influence on eNOS functionality [241]. Therefore, the influence of lipoproteins, PKC and PML on eNOS expression was investigated. eNOS mRNA and protein expression was only higher when EA.hy926 cells were incubated with the lipoprotein composition with low LDL concentrations or with HDL. The fact that eNOS mRNA and protein levels were increased after incubation with HDL supports the observation that HDL increases eNOS expression in general [245]. eNOS protein levels remained unaltered by incubation with LDL alone, contradicting the results of Gonnissen et al. who described LDL to decrease both, eNOS mRNA and protein expression [327]. As stated before, investigation of the influence of VLDL on eNOS expression would be interesting, as it was a part of the lipoprotein compositions and Magnifico et al. [309] showed that incubation of HUVEC with VLDL for 24 hours led to eNOS uncoupling [309]. PML-overexpressing EA-hy926 cells showed a strong decrease in eNOS protein levels.

Incubation with apoE4-homozygous HDL increased eNOS mRNA levels in a dose-dependent manner, while apoE4-homozygous LDL decreased eNOS mRNA levels. As apoE4 does not induce eNOS expression in many cell systems [328], the apoE4-homozygous HDL-dependent increase of eNOS protein expression after for 3 hours of incubation was unexpected. After 24 hours of incubation, low concentrations of apoE4-homozygous HDL and apoE4-homozygous LDL caused increased eNOS protein levels in EA.hy926 cells.

Incubation with sc-3088 led to higher eNOS protein levels, suggesting that PKC inhibits eNOS protein expression, a result that supports the established mechanism of PKCδ phosphorylating STAT3 on Ser-727 and thus activating it, causing inhibition of eNOS [198, 199]. Contradictory to these results, incubation of EA.hy926 cells with STATTIC, which suppresses STAT3 activation, did not change eNOS protein expression. To better understand these results, the effect of STAT3 on eNOS expression further needs to be investigated.

4.10. The effect of a physiologically concentrated lipoprotein composition on the flow-dependent vasodilation of coronary arteries

As the flow-dependent vasodilation of coronary arteries plays a role in the progression of atherosclerosis [270], the influence of the lipoprotein composition with physiological lipoprotein concentrations on the flow-dependent vasodilation was investigated. Only an

insignificant effect on the flow-dependent vasodilation of coronary arteries was found, regardless which flow rate was used.

Nevertheless, as this experiment was conducted on the coronary arteries of one patient only, further coronary arteries obtained from different patients would be needed to validate this speculation. Investigating the influence of lipoprotein compositions with different LDL/HDL ratios on the flow-dependent vasodilation would also be interesting, as LDL negatively affects the flow-dependent vasodilation [271], while it is positively affected by HDL [273]. In previous studies, apoE4-homozygous lipoproteins alone negatively affected the flow-dependent vasodilation of human coronary arteries [49, 329]. Therefore, it would also be interesting to obtain detailed insights on how apoE4-homozygous lipoproteins in compositions affect the flow-dependent vasodilation. Furthermore, it would be beneficial to determine the levels of cAMP and cGMP in the coronary arteries, as eNOS plays a role in the flow-dependent vasodilation [330] by inducing cGMP through NO release [240].

4.11. General limitations of this study

Some general drawbacks limit the scientific value of this study:

1. EA.hy926 cells are derived from an immortalized endothelial cell line, which causes difficulties of transferring the results of this study to the human organism.
2. Furthermore, the experiments were conducted *in vitro* only, also impeding the direct correlation to a living human organism.
3. The availability of apoE4-homozygous lipoproteins was limited. Therefore, not all experiments were conducted with apoE4-homozygous lipoproteins.
4. As most of the experiments were carried out during the COVID-19 pandemic, sufficient numbers of fully functional coronary arteries were not obtained, causing the flow-dependent vasodilation examination to be restricted to the coronary arteries of one patient only.

4.12. Clinical relevance and prospects

This study showed that lipoproteins are not only important for plaque formation in atherosclerosis and AD, but also in immunomodulatory pathways. As the results suggest that LDL triggers an immune response on top of its involvement in plaque formation, progression of atherosclerosis and AD might be faster than known before. Especially PML appears to act as a ‘node point’ in this interaction network and thus might be of interest as a possible drug

target, as for instance inhibition could lead to a decline of inflammatory processes and additional induction of eNOS expression. Even if using PML as a drug target would not pay out as reasonable, it could still be of relevance as it can be used as a specific marker for inflammatory processes in atherosclerosis and AD patients. To further investigate the role of PKC in this mechanism, it would be necessary to specify the isoforms that are involved in PML-mediated signalling transduction. Furthermore, investigating whether lowering of LDL by medication, for instance HMG-CoA reductase-inhibitors or PCSK9-inhibitors, efficiently affects PML expression could be relevant. As oxLDL plays an important role in the development of atherosclerosis and AD, conducting the experiments of this study using oxLDL could possibly provide further insights on the role of PML in the two diseases.

4.13. Conclusion

Lipoproteins of any kind have been under investigation for a long period of time, underlining their relevance in several physiological and pathophysiological processes in the human organism. Investigations focussing on PML in pathological processes likewise come up more frequently lately. Inflammatory processes are important in the development of atherosclerosis and AD, as is PML, and as a conclusion of the results of this study, LDL implements a pathway (Figure 58) that pushes the immunomodulatory effect of PML by activating PKC and possibly leading to chronic inflammation and enhanced plaque formation in atherosclerosis and AD patients with PML being the consolidating factor. This underlines the relevance of further studies regarding new roles of PML in atherosclerosis and AD.

5. Lists of tables, figures and references

5.1. List of tables

5.2. List of figures

5.3. List of references

1. Organization, W.H., *Global Health Estimates 2019: Deaths by Cause, Age, Sex, by Country and by Region, 2000-2019. Geneva; 2020*. 2021.
2. Kobiyama, K. and K. Ley, *Atherosclerosis.* Circ Res, 2018. **123**(10): p. 1118-1120.
3. Renz-Polster, H., S. Krautzig, and J. Braun, *Basislehrbuch Innere Medizin*. 2012: Elsevier Health Sciences Germany.
4. Debus, E., et al., *Ursachen und Risikofaktoren der Arteriosklerose.* Gefässchirurgie, 2013. **18**(6): p. 544-550.
5. Libby, P., P.M. Ridker, and A. Maseri, *Inflammation and atherosclerosis.* Circulation, 2002. **105**(9): p. 1135-1143.
6. Freissmuth, M., S. Offermanns, and S. Böhm, *Pharmakologie und Toxikologie.* 2016.
7. Stary, H.C., et al., *A definition of initial, fatty streak, and intermediate lesions of atherosclerosis. A report from the Committee on Vascular Lesions of the Council on Arteriosclerosis, American Heart Association.* Circulation, 1994. **89**(5): p. 2462-78.
8. Schaftenaar, F., et al., *Atherosclerosis: the interplay between lipids and immune cells.* Curr Opin Lipidol, 2016. **27**(3): p. 209-15.
9. Riccioni, G. and V. Sblendorio, *Atherosclerosis: from biology to pharmacological treatment.* J Geriatr Cardiol, 2012. **9**(3): p. 305-17.
10. Siegel, G., et al., *Lipoprotein binding to anionic biopolyelectrolytes and the effect of glucose on nanoplaque formation in arteriosclerosis and Alzheimer's disease.* Adv Colloid Interface Sci, 2016. **232**: p. 25-35.
11. Stary, H., *Macrophages, macrophage foam cells, and eccentric intimal thickening in the coronary arteries of young children.* Atherosclerosis, 1987. **64**(2-3): p. 91-108.
12. Stary, H., *Evolution and progression of atherosclerotic lesions in coronary arteries of children and young adults.* Arteriosclerosis (Dallas, Tex.), 1989. **9**(1 Suppl): p. I19-32.
13. Insull, W. and G. Bartsch, *Cholesterol, triglyceride, and phospholipid content of intima, media, and atherosclerotic fatty streak in human thoracic aorta.* J Clin Investig, 1966. **45**(4): p. 513-523.
14. Smith, E.B., *The influence of age and atherosclerosis on the chemistry of aortic intima: Part 1. The lipids.* Journal of atherosclerosis research, 1965. **5**(2): p. 224-240.
15. Geer, J.C. and G.T. Malcom, *Chlolesterol ester fatty acid composition of human aorta fatty streaks and normal intima.* Exp Mol Pathol, 1965. **4**(5): p. 500-507.
16. Stary, H., *The sequence of cell and matrix changes in atherosclerotic lesions of coronary arteries in the first forty years of life.* Eur Heart J, 1990. **11**(suppl_E): p. 3-19.
17. Stary, H.C., et al., *A definition of advanced types of atherosclerotic lesions and a histological classification of atherosclerosis. A report from the Committee on*

Vascular Lesions of the Council on Arteriosclerosis, American Heart Association. Arterioscler Thromb Vasc Biol, 1995. **15**(9): p. 1512-31.
18. Herder, M., et al., *Risk factors for progression of carotid intima-media thickness and total plaque area: a 13-year follow-up study: the Tromso Study.* Stroke, 2012. **43**(7): p. 1818-23.
19. Schulte, H. and G. Assmann, *Ergebnisse der «Prospective Cardiovascular Münster»(PROCAM)-Studie.* Sozial-und Präventivmedizin/Social and Preventive Medicine, 1988. **33**(1): p. 32-36.
20. van der Meer, I.M., et al., *Risk factors for progression of atherosclerosis measured at multiple sites in the arterial tree: the Rotterdam Study.* Stroke, 2003. **34**(10): p. 2374-9.
21. Moriya, J., *Critical roles of inflammation in atherosclerosis.* J Cardiol, 2019. **73**(1): p. 22-27.
22. Hansson, G.K., A.-K.L. Robertson, and C. Söderberg-Nauclér, *Inflammation and atherosclerosis.* Annu Rev Pathol Mech Dis, 2006. **1**: p. 297-329.
23. Kametani, F. and M. Hasegawa, *Reconsideration of amyloid hypothesis and tau hypothesis in Alzheimer's disease.* Front Neurosci, 2018. **12**: p. 25.
24. Atwood, C.S., et al., *Senile plaque composition and posttranslational modification of amyloid-β peptide and associated proteins.* Peptides, 2002. **23**(7): p. 1343-1350.
25. Siegel, G., et al., *Inhibition of arteriosclerotic plaque development by garlic.* Wien Med Wochenschr, 2004. **154**(21): p. 515-522.
26. Geisslinger, G., et al., *Mutschler Arzneimittelwirkungen.* 2019.
27. Masters, C.L., et al., *Amyloid plaque core protein in Alzheimer disease and Down syndrome.* Proc Natl Acad Sci USA, 1985. **82**(12): p. 4245-4249.
28. Spillantini, M.G. and M. Goedert, *Tau protein pathology in neurodegenerative diseases.* Trends Neurosci, 1998. **21**(10): p. 428-433.
29. Buée, L., et al., *Tau protein isoforms, phosphorylation and role in neurodegenerative disorders.* Brain Res Rev, 2000. **33**(1): p. 95-130.
30. Francis, P.T., et al., *The cholinergic hypothesis of Alzheimer's disease: a review of progress.* J Neurol Neurosurg Psychiatry, 1999. **66**(2): p. 137-147.
31. Danysz, W., et al., *Neuroprotective and symptomatological action of memantine relevant for Alzheimer's disease—a unified glutamatergic hypothesis on the mechanism of action.* Neurotox Res, 2000. **2**(2-3): p. 85-97.
32. Scheyer, O., et al., *Female sex and Alzheimer's risk: the menopause connection.* J Prev Alzheimer's Dis, 2018. **5**(4): p. 225-230.
33. Tilley, L., K. Morgan, and N. Kalsheker, *Genetic risk factors in Alzheimer's disease.* Mol Pathol, 1998. **51**(6): p. 293.
34. Butterfield, D.A. and M.P. Mattson, *Apolipoprotein E and oxidative stress in brain with relevance to Alzheimer's disease.* Neurobiol Dis, 2020. **138**: p. 104795.
35. Huang, Y. and R.W. Mahley, *Apolipoprotein E: structure and function in lipid metabolism, neurobiology, and Alzheimer's diseases.* Neurobiol Dis, 2014. **72**: p. 3-12.
36. Huang, Y., et al., *Apolipoprotein e.* J Mol Neurosci, 2004. **23**(3): p. 189-204.
37. Mahley, R.W. and S.C. Rall Jr, *Apolipoprotein E: far more than a lipid transport protein.* Annu Rev Genomics Hum Genet, 2000. **1**(1): p. 507-537.
38. Mahley, R.W., K.H. Weisgraber, and Y. Huang, *Apolipoprotein E: structure determines function, from atherosclerosis to Alzheimer's disease to AIDS.* J Lipid Res, 2009. **50**: p. S183-S188.
39. Zannis, V.I., P.W. Just, and J.L. Breslow, *Human apolipoprotein E isoprotein subclasses are genetically determined.* Am J Hum Genet, 1981. **33**(1): p. 11.

40. Mahley, R.W., *Apolipoprotein E: from cardiovascular disease to neurodegenerative disorders.* J Mol Med, 2016. **94**(7): p. 739-746.
41. van Duijn, C.M., et al., *Apolipoprotein E4 allele in a population–based study of early–onset Alzheimer's disease.* Nat Genet, 1994. **7**(1): p. 74-78.
42. Wächtershäuser, A. and J. Stein, *Lipid-und Lipoproteinstoffwechsel: Physiologie und Pathophysiologie.* Pharmazie in unserer Zeit, 2007. **36**(2): p. 98-107.
43. Aktories, K., et al., *Allgemeine und spezielle Pharmakologie und Toxikologie: Begründet von W. Forth, D. Henschler, W. Rummel*. 2017: Elsevier Health Sciences.
44. Rader, D.J. and H.H. Hobbs, *Disorders of lipoprotein metabolism.* Harrisons principles of internal medicine, 2005. **16**(2): p. 2286.
45. Biggerstaff, K.D. and J.S. Wooten, *Understanding lipoproteins as transporters of cholesterol and other lipids.* Adv Physiol Educ, 2004. **28**(3): p. 105-106.
46. Krohn, S., *Zur Wirkung vaskulärer Adrenorezeptoren in der High-Density-Lipoprotein-induzierten Relaxation menschlicher Koronararterien*. 2016.
47. Tulenko, T.N. and A.E. Sumner, *The physiology of lipoproteins.* J Nucl Cardiol, 2002. **9**(6): p. 638-649.
48. Rost, R., *Zusammensetzung der Lipoproteine*, in *Bewegungstips bei erhöhten Blutfettwerten*. 1992, Springer. p. 10-13.
49. Mockenhaupt, F., et al., *IDL-apolipoprotein E isoform navigates human coronary artery tone.* Arterioscler Thromb Vasc Biol, 2014. **34**(suppl_1): p. A416-A416.
50. Camejo, G., et al., *Association of apo B lipoproteins with arterial proteoglycans: pathological significance and molecular basis.* Atherosclerosis, 1998. **139**(2): p. 205-222.
51. Anber, V., et al., *Interaction of very-low-density, intermediate-density, and low-density lipoproteins with human arterial wall proteoglycans.* Arterioscler Thromb Vasc Biol, 1997. **17**(11): p. 2507-2514.
52. Bass, K.M., et al., *Plasma lipoprotein levels as predictors of cardiovascular death in women.* Arch Intern Med, 1993. **153**(19): p. 2209-2216.
53. Hermansen, K., et al., *Effects of soy and other natural products on LDL: HDL ratio and other lipid parameters: a literature review.* Adv Ther, 2003. **20**(1): p. 50-78.
54. Fernandez, M.L. and D. Webb, *The LDL to HDL cholesterol ratio as a valuable tool to evaluate coronary heart disease risk.* J Am Coll Nutr, 2008. **27**(1): p. 1-5.
55. Ramasamy, I., *Recent advances in physiological lipoprotein metabolism.* Clin Chem Lab Med (CCLM), 2014. **52**(12): p. 1695-1727.
56. Mahley, R.W., et al., *Plasma lipoproteins: apolipoprotein structure and function.* J Lipid Res, 1984. **25**(12): p. 1277-1294.
57. Steinmetz, A., et al., *Human apolipoprotein A-IV binds to apolipoprotein AI/A-II receptor sites and promotes cholesterol efflux from adipose cells.* J Biol Chem, 1990. **265**(14): p. 7859-7863.
58. Mahley, R.W., *Apolipoprotein E: cholesterol transport protein with expanding role in cell biology.* Science, 1988. **240**(4852): p. 622-630.
59. Kingwell, B.A., et al., *HDL-targeted therapies: progress, failures and future.* Nat Rev Drug Discov, 2014. **13**(6): p. 445-464.
60. Rye, K.-A., M.A. Clay, and P.J. Barter, *Remodelling of high density lipoproteins by plasma factors.* Atherosclerosis, 1999. **145**(2): p. 227-238.
61. Ridker, P.M., et al., *Non–HDL cholesterol, apolipoproteins AI and B100, standard lipid measures, lipid ratios, and CRP as risk factors for cardiovascular disease in women.* Jama, 2005. **294**(3): p. 326-333.
62. Getz, G.S. and C.A. Reardon, *Apoprotein E and reverse cholesterol transport.* Int J Mol Sci, 2018. **19**(11): p. 3479.

63. Bradley, W.A. and S.H. Gianturco, *ApoE is necessary and sufficient for the binding of large triglyceride-rich lipoproteins to the LDL receptor; apoB is unnecessary.* J Lipid Res, 1986. **27**(1): p. 40-48.
64. Blanco-Vaca, F., et al., *Role of apoA-II in lipid metabolism and atherosclerosis: advances in the study of an enigmatic protein.* J Lipid Res, 2001. **42**(11): p. 1727-1739.
65. Shapiro, M.D. and S. Fazio, *Apolipoprotein B-containing lipoproteins and atherosclerotic cardiovascular disease.* F1000Research, 2017. **6**.
66. Lee, N., H. Brewer, and J. Osborne, *beta 2-Glycoprotein I. Molecular properties of an unusual apolipoprotein, apolipoprotein H.* J Biol Chem, 1983. **258**(8): p. 4765-4770.
67. Rassart, E., et al., *Apolipoprotein d.* Biochim Biophys Acta Prot Struct Mol Enzym, 2000. **1482**(1-2): p. 185-198.
68. Olofsson, S.O., W.J. McConathy, and P. Alaupovic, *Isolation and partial characterization of a new acidic apolipoprotein (apolipoprotein F) from high density lipoproteins of human plasma.* Biochemistry, 1978. **17**(6): p. 1032-1036.
69. Dahlbäck, B. and L.B. Nielsen, *Apolipoprotein M–a novel player in high-density lipoprotein metabolism and atherosclerosis.* Curr Opin Lipidol, 2006. **17**(3): p. 291-295.
70. Duchateau, P.N., et al., *Apolipoprotein L, a new human high density lipoprotein apolipoprotein expressed by the pancreas: Identification, cloning, characterization, and plasma distribution of apolipoprotein L.* J Biol Chem, 1997. **272**(41): p. 25576-25582.
71. Koren, E., W.J. McConathy, and P. Alaupovic, *Isolation and characterization of simple and complex lipoproteins containing apolipoprotein F from human plasma.* Biochemistry, 1982. **21**(21): p. 5347-5351.
72. McConathy, W. and P. Alaupovic, *Isolation and partial characterization of apolipoprotein D: a new protein moiety of the human plasma lipoprotein system.* FEBS Lett, 1973. **37**(2): p. 178-182.
73. Havel, R.J., *Chylomicron remnants: hepatic receptors and metabolism.* Curr Opin Lipidol, 1995. **6**(5): p. 312-316.
74. Löffler, G. and P.E. Petrides, *Biochemie und pathobiochemie*. 2019: Springer-Verlag.
75. Gibbons, G., et al., *Synthesis and function of hepatic very-low-density lipoprotein.* Biochemical Society Transactions, 2004. **32**(1): p. 59-64.
76. Hevonoja, T., et al., *Structure of low density lipoprotein (LDL) particles: basis for understanding molecular changes in modified LDL.* Biochim Biophys Acta Mol Cell Biol Lipids, 2000. **1488**(3): p. 189-210.
77. Lewis, G.F. and D.J. Rader, *New insights into the regulation of HDL metabolism and reverse cholesterol transport.* Circ Res, 2005. **96**(12): p. 1221-1232.
78. Lammert, E. and M. Zeeb, *Metabolism of human diseases*. 2014: Springer.
79. Barter, P., *CETP and atherosclerosis*. 2000, Am Heart Assoc.
80. Mead, J.R., S.A. Irvine, and D.P. Ramji, *Lipoprotein lipase: structure, function, regulation, and role in disease.* J Mol Med, 2002. **80**(12): p. 753-769.
81. Sambandam, N., et al., *Localization of lipoprotein lipase in the diabetic heart: regulation by acute changes in insulin.* Arterioscler Thromb Vasc Biol, 1999. **19**(6): p. 1526-1534.
82. Itabe, H., *Oxidative modification of LDL: its pathological role in atherosclerosis.* Clin Rev Allergy Immunol, 2009. **37**(1): p. 4-11.
83. Yoshida, H. and R. Kisugi, *Mechanisms of LDL oxidation.* Clin Chim Acta, 2010. **411**(23-24): p. 1875-1882.

84. Dutrieux, J., et al., *PML/TRIM19-dependent inhibition of retroviral reverse-transcription by Daxx.* PLOS Pathog, 2015. **11**(11): p. e1005280.
85. Kastner, P., et al., *Structure, localization and transcriptional properties of two classes of retinoic acid receptor alpha fusion proteins in acute promyelocytic leukemia (APL): structural similarities with a new family of oncoproteins.* EMBO J, 1992. **11**(2): p. 629-642.
86. Bernardi, R., A. Papa, and P. Pandolfi, *Regulation of apoptosis by PML and the PML-NBs.* Oncogene, 2008. **27**(48): p. 6299-6312.
87. Lavau, C., et al., *The acute promyelocytic leukaemia-associated PML gene is induced by interferon.* Oncogene, 1995. **11**(5): p. 871-876.
88. Brand, P., T. Lenser, and P. Hemmerich, *Assembly dynamics of PML nuclear bodies in living cells.* PMC Biophys, 2010. **3**(1): p. 3.
89. Jensen, K., C. Shiels, and P.S. Freemont, *PML protein isoforms and the RBCC/TRIM motif.* Oncogene, 2001. **20**(49): p. 7223-7233.
90. Saurin, A.J., et al., *Does this have a familiar RING?* Trends Biochem Sci, 1996. **21**(6): p. 208-214.
91. Duprez, E., et al., *SUMO-1 modification of the acute promyelocytic leukaemia protein PML: implications for nuclear localisation.* J Cell Sci, 1999. **112**(3): p. 381-393.
92. Cheng, X. and H.-Y. Kao, *Post-translational modifications of PML: consequences and implications.* Front Oncol, 2013. **2**: p. 210.
93. Shen, T.H., et al., *The mechanisms of PML-nuclear body formation.* Mol Cell, 2006. **24**(3): p. 331-339.
94. Fogal, V., et al., *Regulation of p53 activity in nuclear bodies by a specific PML isoform.* EMBO J, 2000. **19**(22): p. 6185-6195.
95. Condemine, W., et al., *Characterization of endogenous human promyelocytic leukemia isoforms.* Cancer Res, 2006. **66**(12): p. 6192-6198.
96. Everett, R.D. and M.K. Chelbi-Alix, *PML and PML nuclear bodies: implications in antiviral defence.* Biochimie, 2007. **89**(6-7): p. 819-830.
97. De Stanchina, E., et al., *PML is a direct p53 target that modulates p53 effector functions.* Mol Cell, 2004. **13**(4): p. 523-535.
98. Chelbi-Alix, M., et al., *Induction of the PML protein by interferons in normal and APL cells.* Leukemia, 1995. **9**(12): p. 2027-2033.
99. Hsu, K.-S. and H.-Y. Kao, *PML: Regulation and multifaceted function beyond tumor suppression.* Cell Biosci, 2018. **8**(1): p. 1-21.
100. Regad, T. and M.K. Chelbi-Alix, *Role and fate of PML nuclear bodies in response to interferon and viral infections.* Oncogene, 2001. **20**(49): p. 7274-7286.
101. Tavalai, N. and T. Stamminger, *New insights into the role of the subnuclear structure ND10 for viral infection.* Biochim Biophys Acta Mol Cell Res, 2008. **1783**(11): p. 2207-2221.
102. Wu, W.-S., et al., *Promyelocytic leukemia protein sensitizes tumor necrosis factor α-induced apoptosis by inhibiting the NF-κB survival pathway.* J Biol Chem, 2003. **278**(14): p. 12294-12304.
103. Geoffroy, M.-C. and M.K. Chelbi-Alix, *Role of promyelocytic leukemia protein in host antiviral defense.* J Interferon Cytokine Res, 2011. **31**(1): p. 145-158.
104. Van Damme, E., et al., *A manually curated network of the PML nuclear body interactome reveals an important role for PML-NBs in SUMOylation dynamics.* Int J Biol Sci, 2010. **6**(1): p. 51.
105. Ishov, A.M., et al., *PML is critical for ND10 formation and recruits the PML-interacting protein daxx to this nuclear structure when modified by SUMO-1.* J Cell Biol, 1999. **147**(2): p. 221-234.

106. Sternsdorf, T., et al., *Nuclear dots: actors on many stages.* Immunobiology, 1997. **198**(1-3): p. 307-331.
107. Hodges, M., et al., *Structure, organization, and dynamics of promyelocytic leukemia protein nuclear bodies.* Am J Hum Genet, 1998. **63**(2): p. 297-304.
108. Li, C., et al., *C-terminal motifs in promyelocytic leukemia protein isoforms critically regulate PML nuclear body formation.* J Cell Sci, 2017. **130**(20): p. 3496-3506.
109. Zhong, S., et al., *Role of SUMO-1–modified PML in nuclear body formation.* Blood, 2000. **95**(9): p. 2748-2752.
110. Lallemand-Breitenbach, V., *PML nuclear bodies.* Cold Spring Harb Perspect Biol, 2010. **2**(5): p. a000661.
111. Lallemand-Breitenbach, V., et al., *Role of promyelocytic leukemia (PML) sumolation in nuclear body formation, 11S proteasome recruitment, and As2O3-induced PML or PML/retinoic acid receptor α degradation.* J Exp Med, 2001. **193**(12): p. 1361-1372.
112. Liu, Y., et al., *Manipulating PML SUMOylation via silencing UBC9 and RNF4 regulates cardiac fibrosis.* Mol Ther, 2017. **25**(3): p. 666-678.
113. Borden, K.L., *Pondering the promyelocytic leukemia protein (PML) puzzle: possible functions for PML nuclear bodies.* Mol Cell Biol, 2002. **22**(15): p. 5259-5269.
114. Wang, L., et al., *Disruption of PML nuclear bodies is mediated by ORF61 SUMO-interacting motifs and required for varicella-zoster virus pathogenesis in skin.* PLOS Pathog, 2011. **7**(8): p. e1002157.
115. Liang, Y.-C., et al., *SUMO5, a novel poly-SUMO isoform, regulates PML nuclear bodies.* Sci Rep, 2016. **6**(1): p. 1-15.
116. Seeler, J.-S. and A. Dejean, *The PML nuclear bodies: actors or extras?* Curr Opin Genet Dev, 1999. **9**(3): p. 362-367.
117. Maul, G.G., et al., *Nuclear domain 10 (ND10) associated proteins are also present in nuclear bodies and redistribute to hundreds of nuclear sites after stress.* J Cell Biochem, 1995. **59**(4): p. 498-513.
118. Takahashi, Y., et al., *PML nuclear bodies and apoptosis.* Oncogene, 2004. **23**(16): p. 2819-2824.
119. Sachdev, S., et al., *PIASy, a nuclear matrix–associated SUMO E3 ligase, represses LEF1 activity by sequestration into nuclear bodies.* Genes Dev, 2001. **15**(23): p. 3088-3103.
120. Lallemand-Breitenbach, V., et al., *Arsenic degrades PML or PML–RARα through a SUMO-triggered RNF4/ubiquitin-mediated pathway.* Nat Cell Biol, 2008. **10**(5): p. 547-555.
121. Chen, R.-H., Y.-R. Lee, and W.-C. Yuan, *The role of PML ubiquitination in human malignancies.* J Biomed Sci, 2012. **19**(1): p. 1-7.
122. Scaglioni, P.P., et al., *A CK2-dependent mechanism for degradation of the PML tumor suppressor.* Cell, 2006. **126**(2): p. 269-283.
123. Karle, W., et al., *Promyelocytic leukemia protein promotes the phenotypic switch of smooth muscle cells in atherosclerotic plaques of human coronary arteries.* Clin Sci, 2021. **135**(7): p. 887-905.
124. Corbett, C.B., A.K. St. Paul, and M.V. Autieri, *Promyelocytic leukemia protein: an atherosclerosis suppressor protein?* Clin Sci, 2021. **135**(13): p. 1557-1561.
125. Marks, D., et al., *Amyloid precursor protein elevates fusion of promyelocytic leukemia nuclear bodies in human hippocampal areas with high plaque load.* Acta Neuropathol Commun, 2021. **9**(1): p. 1-16.
126. Simpson, R.J., et al., *Interleukin-6: Structure-function relationships.* Protein Sci, 1997. **6**(5): p. 929-955.

127. Mihara, M., et al., *IL-6/IL-6 receptor system and its role in physiological and pathological conditions.* Clin Sci, 2012. **122**(4): p. 143-159.
128. Akira, S. and T. Kishimoto, *IL-6 and NF-IL6 in acute-phase response and viral infection.* Immunol Rev, 1992. **127**: p. 25-50.
129. Hirano, T., *Interleukin 6 and its receptor: ten years later.* Int Rev Immunol, 1998. **16**(3-4): p. 249-284.
130. Bickel, M., *The role of interleukin-8 in inflammation and mechanisms of regulation.* J Periodontol, 1993. **64**(5 Suppl): p. 456-460.
131. Ghasemi, H., et al., *Roles of IL-8 in ocular inflammations: a review.* Ocul Immunol Inflamm, 2011. **19**(6): p. 401-412.
132. Harvey, K. and R.A. Siddiqui, *Interleukin-8: An autocrine inflammatory mediator.* Curr Pharm Des, 1999. **5**(4): p. 241-253.
133. Ning, Y., et al., *Co-culture of ovarian cancer stem-like cells with macrophages induced SKOV3 cells stemness via IL-8/STAT3 signaling.* Biomed Pharmacother, 2018. **103**: p. 262-271.
134. Hubackova, S., et al., *Regulation of the PML tumor suppressor in drug-induced senescence of human normal and cancer cells by JAK/STAT-mediated signaling.* Cell cycle, 2010. **9**(15): p. 3157-3171.
135. Hubackova, S., et al., *Interleukin 6 signaling regulates promyelocytic leukemia protein gene expression in human normal and cancer cells.* J Biol Chem, 2012. **287**(32): p. 26702-26714.
136. Ohgiya, D., et al., *Association of promyelocytic leukemia protein with expression of IL-6 and resistance to treatment in multiple myeloma.* Acta Haematol, 2012. **128**(4): p. 213-222.
137. Guo, Y., et al., *IL-8 promotes proliferation and inhibition of apoptosis via STAT3/AKT/NF-κB pathway in prostate cancer Corrigendum in/10.3892/mmr. 2019.9942.* Mol med Rep, 2017. **16**(6): p. 9035-9042.
138. De La Iglesia, N., et al., *Deregulation of a STAT3–interleukin 8 signaling pathway promotes human glioblastoma cell proliferation and invasiveness.* J Neurosci, 2008. **28**(23): p. 5870-5878.
139. Hartman, J. and W.H. Frishman, *Inflammation and atherosclerosis: a review of the role of interleukin-6 in the development of atherosclerosis and the potential for targeted drug therapy.* Cardiol Rev, 2014. **22**(3): p. 147-151.
140. Seino, Y., et al., *Interleukin 6 gene transcripts are expressed in human atherosclerotic lesions.* Cytokine, 1994. **6**(1): p. 87-91.
141. Yeh, M., et al., *Increased transcription of IL-8 in endothelial cells is differentially regulated by TNF-α and oxidized phospholipids.* Arterioscler Thromb Vasc Biol, 2001. **21**(10): p. 1585-1591.
142. Gharavi, N.M., et al., *Role of the Jak/STAT pathway in the regulation of interleukin-8 transcription by oxidized phospholipids in vitro and in atherosclerosis in vivo.* J Biol Chem, 2007. **282**(43): p. 31460-31468.
143. Liu, Y., L.M. Hultén, and O. Wiklund, *Macrophages isolated from human atherosclerotic plaques produce IL-8, and oxysterols may have a regulatory function for IL-8 production.* Arterioscler Thromb Vasc Biol, 1997. **17**(2): p. 317-323.
144. Rus, H., R. Vlaicu, and F. Niculescu, *Interleukin-6 and interleukin-8 protein and gene expression in human arterial atherosclerotic wall.* Atherosclerosis, 1996. **127**(2): p. 263-271.
145. Quintanilla, R.A., et al., *Interleukin-6 induces Alzheimer-type phosphorylation of tau protein by deregulating the cdk5/p35 pathway.* Exp Cell Res, 2004. **295**(1): p. 245-257.

146. Kim, H. and K.J. Lee, *Serum tumor necrosis factor-alpha and interleukin-6 levels in Alzheimer's disease and mild cognitive impairment.* Eur Neuropsychopharmacol, 2016. **26**: p. S335.
147. Altstiel, L.D. and K. Sperber, *Cytokines in Alzheimer's disease.* Prog Neuropsychopharmacol Biol Psychiatry, 1991. **15**(4): p. 481-495.
148. Alsadany, M.A., et al., *Histone deacetylases enzyme, copper, and IL-8 levels in patients with Alzheimer's disease.* Am J Alzheimers Dis Other Demen, 2013. **28**(1): p. 54-61.
149. Walker, D.G., L.-F. Lue, and T.G. Beach, *Gene expression profiling of amyloid beta peptide-stimulated human post-mortem brain microglia.* Neurobiol Aging, 2001. **22**(6): p. 957-966.
150. McLarnon, J.G., *Chemokine interleukin-8 (IL-8) in Alzheimer's and other neurodegenerative diseases.* J Alzheimers Dis Parkinsonism, 2016. **6**(273): p. 2161-0460.1000273.
151. Patterson, R.L., et al., *Phospholipase C-γ: diverse roles in receptor-mediated calcium signaling.* Trends Biochem Sci, 2005. **30**(12): p. 688-697.
152. Idris, I., S. Gray, and R. Donnelly, *Protein kinase C activation: isozyme-specific effects on metabolism and cardiovascular complications in diabetes.* Diabetologia, 2001. **44**(6): p. 659-673.
153. PEARS, C.J., et al., *Mutagenesis of the pseudosubstrate site of protein kinase C leads to activation.* Eur J Chem, 1990. **194**(1): p. 89-94.
154. Way, K.J., E. Chou, and G.L. King, *Identification of PKC-isoform-specific biological actions using pharmacological approaches.* Trends Pharmacol Sci, 2000. **21**(5): p. 181-187.
155. MELLOR, H. and P.J. PARKER, *The extended protein kinase C superfamily.* Biochem J, 1998. **332**(2): p. 281-292.
156. Alkon, D.L., M.-K. Sun, and T.J. Nelson, *PKC signaling deficits: a mechanistic hypothesis for the origins of Alzheimer's disease.* Trends Pharmacol Sci, 2007. **28**(2): p. 51-60.
157. Li, D., B. Yang, and J.L. Mehta, *Ox-LDL induces apoptosis in human coronary artery endothelial cells: role of PKC, PTK, bcl-2, and Fas.* Am J Physiol Heart Circ Physiol, 1998. **275**(2): p. H568-H576.
158. Poole, A.W., et al., *PKC-interacting proteins: from function to pharmacology.* Trends Pharmacol Sci, 2004. **25**(10): p. 528-535.
159. Huang, K.-P., *The mechanism of protein kinase C activation.* Trends Neurosci, 1989. **12**(11): p. 425-432.
160. Nishizuka, Y., *The role of protein kinase C in cell surface signal transduction and tumour promotion.* Nature, 1984. **308**(5961): p. 693-698.
161. Nishizuka, Y., *Intracellular signaling by hydrolysis of phospholipids and activation of protein kinase C.* Science, 1992. **258**(5082): p. 607-614.
162. Nishizuka, Y., *Protein kinase C and lipid signaling for sustained cellular responses.* FASEB J, 1995. **9**(7): p. 484-496.
163. Zhang, J., et al., *Protein kinase C (PKC) βII induces cell invasion through a Ras/Mek-, PKCι/Rac 1-dependent signaling pathway.* J Biol Chem, 2004. **279**(21): p. 22118-22123.
164. Langzam, L., et al., *Patterns of protein kinase C isoenzyme expression in transitional cell carcinoma of bladder: relation to degree of malignancy.* Am J Clin Pathol, 2001. **116**(3): p. 377-385.

165. Ren, S., S. Shatadal, and G.X. Shen, *Protein kinase C-β mediates lipoprotein-induced generation of PAI-1 from vascular endothelial cells.* Am J Physiol - Endocrinol Metab, 2000. **278**(4): p. E656-E662.
166. Fyrnys, B., et al., *Oxidized Low Density Lipoprotein Stimulates Protein Kinase C (PKC) Activity and Expression of PKC-Isotypes via Prostaglandin-H-Synthase in P388D 1 Cells*, in *Eicosanoids and other Bioactive Lipids in Cancer, Inflammation, and Radiation Injury 3*. 1997, Springer. p. 93-98.
167. Giardina, J.B., D.J. Tanner, and R.A. Khalil, *Oxidized-LDL enhances coronary vasoconstriction by increasing the activity of protein kinase C isoforms α and ε.* Hypertension, 2001. **37**(2): p. 561-568.
168. Churchill, E., et al., *PKC isozymes in chronic cardiac disease: possible therapeutic targets?* Annu Rev Pharmacol Toxicol, 2008. **48**: p. 569-599.
169. Marino, M., et al., *Activation of IP3-protein kinase C-α signal transduction pathway precedes the changes of plasma cholesterol, hepatic lipid metabolism and induction of low-density lipoprotein receptor expression in 17-β-oestradiol-treated rats.* Exp Physiol, 2001. **86**(1): p. 39-45.
170. Kapoor, G.S., et al., *pp90RSK-and protein kinase C-dependent pathway regulates p42/44MAPK-induced LDL receptor transcription in HepG2 cells.* J Lipid Res, 2003. **44**(3): p. 584-593.
171. Mehta, K.D., et al., *Critical role of diacylglycerol-and phospholipid-regulated protein kinase Cε in induction of low-density lipoprotein receptor transcription in response to depletion of cholesterol.* Mol Cell Biol, 2002. **22**(11): p. 3783-3793.
172. Cathcart, M., et al., *Superoxide anion participation in human monocyte-mediated oxidation of low-density lipoprotein and conversion of low-density lipoprotein to a cytotoxin.* J Immunol, 1989. **142**(6): p. 1963-1969.
173. Cathcart, M.K., D.W. Morel, and G.M. Chisolm III, *Monocytes and neutrophils oxidize low density lipoprotein making it cytotoxic.* J Leukoc Biol, 1985. **38**(2): p. 341-350.
174. Li, Q., et al., *Protein Kinase Cα Regulates Human Monocyte O·¯2Production and Low Density Lipoprotein Lipid Oxidation.* J Biol Chem, 1999. **274**(6): p. 3764-3771.
175. Murohara, T., R. Scalia, and A.M. Lefer, *Lysophosphatidylcholine promotes P-selectin expression in platelets and endothelial cells: possible involvement of protein kinase C activation and its inhibition by nitric oxide donors.* Circ Res, 1996. **78**(5): p. 780-789.
176. Niu, X., X. Yan, and Z. Guo, *Oxidized low-density lipoproteins stimulate adhesion of monocytes to endothelial cells.* Zhongguo yao li xue bao= Acta Pharmacol Sin, 1997. **18**(1): p. 59-62.
177. Ma, H.-T., et al., *Protein kinase C β and δ isoenzymes mediate cholesterol accumulation in PMA-activated macrophages.* Biochem Biophys Res Commun, 2006. **349**(1): p. 214-220.
178. Van Huynh, T., et al., *Reduced protein kinase C immunoreactivity and altered protein phosphorylation in Alzheimer's disease fibroblasts.* Arch Neurol, 1989. **46**(11): p. 1195-1199.
179. Etcheberrigaray, R., et al., *Potassium channel dysfunction in fibroblasts identifies patients with Alzheimer disease.* Proc Natl Acad Sci USA, 1993. **90**(17): p. 8209-8213.
180. Favit, A., et al., *Alzheimer's-specific effects of soluble β-amyloid on protein kinase C-α and-γ degradation in human fibroblasts.* Proc Natl Acad Sci USA, 1998. **95**(10): p. 5562-5567.

181. Zammarchi, F., et al., *Antitumorigenic potential of STAT3 alternative splicing modulation.* Proc Natl Acad Sci USA, 2011. **108**(43): p. 17779-17784.
182. Qi, Q.-R. and Z.-M. Yang, *Regulation and function of signal transducer and activator of transcription 3.* World J Biol Chem, 2014. **5**(2): p. 231.
183. Akira, S., *Roles of STAT3 defined by tissue-specific gene targeting.* Oncogene, 2000. **19**(21): p. 2607-2611.
184. Darnell, J.E., *STATs and gene regulation.* Science, 1997. **277**(5332): p. 1630-1635.
185. Ihle, J.N., *STATs: signal transducers and activators of transcription.* Cell, 1996. **84**(3): p. 331-334.
186. Levy, D.E. and J. Darnell, *Stats: transcriptional control and biological impact.* Nat Rev Mol Cell Biol, 2002. **3**(9): p. 651-662.
187. Coleman IV, D.R., et al., *Investigation of the binding determinants of phosphopeptides targeted to the SRC homology 2 domain of the signal transducer and activator of transcription 3. Development of a high-affinity peptide inhibitor.* J Med Chem, 2005. **48**(21): p. 6661-6670.
188. Schust, J., et al., *Stattic: a small-molecule inhibitor of STAT3 activation and dimerization.* Chem Biol, 2006. **13**(11): p. 1235-1242.
189. Zou, S., et al., *Targeting STAT3 in cancer immunotherapy.* Mol Cancer, 2020. **19**(1): p. 1-19.
190. K Lau, Y.-T., et al., *Targeting STAT3 in cancer with nucleotide therapeutics.* Cancers, 2019. **11**(11): p. 1681.
191. Zhang, T., et al., *The coiled-coil domain of Stat3 is essential for its SH2 domain-mediated receptor binding and subsequent activation induced by epidermal growth factor and interleukin-6.* Mol Cell Biol, 2000. **20**(19): p. 7132-7139.
192. Bharadwaj, U., et al., *Monoclonal antibodies specific for STAT3β reveal its contribution to constitutive STAT3 phosphorylation in breast cancer.* Cancers, 2014. **6**(4): p. 2012-2034.
193. Jain, N., et al., *Protein kinase C δ associates with and phosphorylates Stat3 in an interleukin-6-dependent manner.* J Biol Chem, 1999. **274**(34): p. 24392-24400.
194. Sakaguchi, M., et al., *Role and regulation of STAT3 phosphorylation at Ser727 in melanocytes and melanoma cells.* J Invest Dermatol, 2012. **132**(7): p. 1877-1885.
195. Gartsbein, M., et al., *The role of protein kinase C δ activation and STAT3 Ser727 phosphorylation in insulin-induced keratinocyte proliferation.* J Cell Sci, 2006. **119**(3): p. 470-481.
196. Niu, G., et al., *Role of Stat3 in regulating p53 expression and function.* Mol Cell Biol, 2005. **25**(17): p. 7432-7440.
197. Zouein, F.A., et al., *Pivotal importance of STAT3 in protecting the heart from acute and chronic stress: new advancement and unresolved issues.* Front Cardiovasc Med, 2015. **2**: p. 36.
198. Saura, M., et al., *Stat3 mediates interelukin-6 inhibition of human endothelial nitric-oxide synthase expression.* J Biol Chem, 2006. **281**(40): p. 30057-30062.
199. Sud, N., et al., *Modulation of PKCδ signaling alters the shear stress-mediated increases in endothelial nitric oxide synthase transcription: role of STAT3.* Am J Physiol Lung Cell Mol Physiol, 2009. **296**(3): p. L519-L526.
200. Akira, S., *IL-6-regulated transcription factors.* Int J Biochem Cell Biol, 1997. **29**(12): p. 1401-1418.
201. Harhous, Z., et al., *An update on the multifaceted roles of STAT3 in the heart.* Front Cardiovasc Med, 2019. **6**: p. 150.

202. Chung, S.S. and J.V. Vadgama, *Curcumin and epigallocatechin gallate inhibit the cancer stem cell phenotype via down-regulation of STAT3–NFκB signaling.* AntiCancer Res, 2015. **35**(1): p. 39-46.
203. Kato, M., et al., *PML suppresses IL-6-induced STAT3 activation by interfering with STAT3 and HDAC3 interaction.* Biochem Biophys Res Commun, 2015. **461**(2): p. 366-371.
204. Inghirami, G., et al., *New and old functions of STAT3: a pivitol target for individualized treatment of cancer.* Cell cycle, 2005. **4**(9): p. 1131-1133.
205. Levy, D.E. and C.-k. Lee, *What does Stat3 do?* J Clin Investig, 2002. **109**(9): p. 1143-1148.
206. Wegenka, U.M., et al., *Acute-phase response factor, a nuclear factor binding to acute-phase response elements, is rapidly activated by interleukin-6 at the posttranslational level.* Mol Cell Biol, 1993. **13**(1): p. 276-288.
207. Chen, R.-H., et al., *Interleukin-6 inhibits transforming growth factor-β-induced apoptosis through the phosphatidylinositol 3-kinase/Akt and signal transducers and activators of transcription 3 pathways.* J Biol Chem, 1999. **274**(33): p. 23013-23019.
208. Chapman, R.S., et al., *Suppression of epithelial apoptosis and delayed mammary gland involution in mice with a conditional knockout of Stat3.* Genes Dev, 1999. **13**(19): p. 2604-2616.
209. Hsu, K.-S., et al., *Dual regulation of Stat1 and Stat3 by the tumor suppressor protein PML contributes to interferon α-mediated inhibition of angiogenesis.* J Biol Chem, 2017. **292**(24): p. 10048-10060.
210. Ohbayashi, N., et al., *The IL-6 family of cytokines modulates STAT3 activation by desumoylation of PML through SENP1 induction.* Biochem Biophys Res Commun, 2008. **371**(4): p. 823-828.
211. Chen, Q., et al., *Targeted inhibition of STAT3 as a potential treatment strategy for atherosclerosis.* Theranostics, 2019. **9**(22): p. 6424.
212. Kong, X., et al., *JAK2/STAT3 signaling mediates IL-6-inhibited neurogenesis of neural stem cells through DNA demethylation/methylation.* Brain Behav Immun, 2019. **79**: p. 159-173.
213. Chiba, T., M. Yamada, and S. Aiso, *Targeting the JAK2/STAT3 axis in Alzheimer's disease.* Expert Opin Ther Targets, 2009. **13**(10): p. 1155-1167.
214. Vogelstein, B. and K.W. Kinzler, *p53 function and dysfunction.* Cell, 1992. **70**(4): p. 523-526.
215. Ashcroft, M., M.H. Kubbutat, and K.H. Vousden, *Regulation of p53 function and stability by phosphorylation.* Mol Cell Biol, 1999. **19**(3): p. 1751-1758.
216. Levine, A.J., *p53, the cellular gatekeeper for growth and division.* cell, 1997. **88**(3): p. 323-331.
217. El-Deiry, W.S. *Regulation ofp53downstream genes*. in *Seminars in cancer biology*. 1998. Elsevier.
218. Vousden, K.H., *p53: death star.* Cell, 2000. **103**(5): p. 691-694.
219. Murphy, M., A. Hinman, and A.J. Levine, *Wild-type p53 negatively regulates the expression of a microtubule-associated protein.* Genes Dev, 1996. **10**(23): p. 2971-2980.
220. Woods, D.B. and K.H. Vousden, *Regulation of p53 function.* Exp Cell Res, 2001. **264**(1): p. 56-66.
221. Guevara, N.V., et al., *The absence of p53 accelerates atherosclerosis by increasing cell proliferation in vivo.* Nat Med, 1999. **5**(3): p. 335-339.
222. Mercer, J. and M. Bennett, *The role of p53 in atherosclerosis.* Cell cycle, 2006. **5**(17): p. 1907-1909.

223. Di Domenico, F., et al., *Glutathionylation of the pro-apoptotic protein p53 in Alzheimer's disease brain: implications for AD pathogenesis.* Neurochem Res, 2009. **34**(4): p. 727-733.
224. Cenini, G., et al., *Effects of oxidative and nitrosative stress in brain on p53 proapoptotic protein in amnestic mild cognitive impairment and Alzheimer disease.* Free Radic Biol Med, 2008. **45**(1): p. 81-85.
225. Reed, S.M. and D.E. Quelle, *p53 acetylation: regulation and consequences.* Cancers, 2015. **7**(1): p. 30-69.
226. Haupt, Y., et al., *Mdm2 promotes the rapid degradation of p53.* Nature, 1997. **387**(6630): p. 296-299.
227. Kubbutat, M.H., S.N. Jones, and K.H. Vousden, *Regulation of p53 stability by Mdm2.* Nature, 1997. **387**(6630): p. 299-303.
228. Böttger, A., et al., *Design of a synthetic Mdm2-binding mini protein that activates the p53 response in vivo.* Curr Biol, 1997. **7**(11): p. 860-869.
229. Guo, A., et al., *The function of PML in p53-dependent apoptosis.* Nat Cell Biol, 2000. **2**(10): p. 730-736.
230. Langley, E., et al., *Human SIR2 deacetylates p53 and antagonizes PML/p53-induced cellular senescence.* EMBO J, 2002. **21**(10): p. 2383-2396.
231. Sessa, W.C., *eNOS at a glance.* J Cell Sci, 2004. **117**(12): p. 2427-2429.
232. Kawashima, S., *The two faces of endothelial nitric oxide synthase in the pathophysiology of atherosclerosis.* Endothelium, 2004. **11**(2): p. 99-107.
233. Yang, Z.-W., et al., *Mg2+-induced endothelium-dependent relaxation of blood vessels and blood pressure lowering: role of NO.* Am J Physiol - Regul Integr Comp Physiol, 2000. **278**(3): p. R628-R639.
234. Fleming, I. and R. Busse, *Signal transduction of eNOS activation.* Cardiovasc Res, 1999. **43**(3): p. 532-541.
235. Sessa, W., et al., *Molecular cloning and expression of a cDNA encoding endothelial cell nitric oxide synthase.* J Biol Chem, 1992. **267**(22): p. 15274-15276.
236. Fulton, D., J.-P. Gratton, and W.C. Sessa, *Post-translational control of endothelial nitric oxide synthase: why isn't calcium/calmodulin enough?* J Pharmacol Exp Ther, 2001. **299**(3): p. 818-824.
237. Radulović, S., et al., *Endothelial lipase increases eNOS activating capacity of high-density lipoprotein.* Biochim Biophys Acta Mol Cell Biol Lipids, 2020. **1865**(4): p. 158612.
238. Parton, R.G., *Caveolae and caveolins.* Current opinion in cell biology, 1996. **8**(4): p. 542-548.
239. Anderson, R.G., *The caveolae membrane system*. 1998, Annual Reviews 4139 El Camino Way, PO Box 10139, Palo Alto, CA 94303-0139, USA.
240. Denninger, J.W. and M.A. Marletta, *Guanylate cyclase and the .NO/cGMP signaling pathway.* Biochim Biophys Acta, 1999. **1411**(2-3): p. 334-50.
241. Andrews, A.M., et al., *Cholesterol enrichment impairs capacitative calcium entry, eNOS phosphorylation & shear stress-induced NO production.* Cell Mol Bioeng, 2017. **10**(1): p. 30-40.
242. Förstermann, U., *Janus-faced role of endothelial NO synthase in vascular disease: uncoupling of oxygen reduction from NO synthesis and its pharmacological reversal.* Biol Chem, 2006. **387**(12): p. 1521-1533.
243. Ota, H., et al., *SIRT1/eNOS axis as a potential target against vascular senescence, dysfunction and atherosclerosis.* J Atheroscler Thromb, 2010: p. 1003080195-1003080195.

244. Blair, A., et al., *Oxidized low density lipoprotein displaces endothelial nitric-oxide synthase (eNOS) from plasmalemmal caveolae and impairs eNOS activation.* J Biol Chem, 1999. **274**(45): p. 32512-32519.
245. Wesnigk, J., et al., *Impact of lifestyle intervention on HDL-induced eNOS activation and cholesterol efflux capacity in obese adolescent.* Cardiol Res Pract, 2016. **2016**.
246. Austin, S.A., et al., *Endothelial nitric oxide deficiency promotes Alzheimer's disease pathology.* J Neurochem, 2013. **127**(5): p. 691-700.
247. Aird, W.C., *Endothelium,* in *Consultative Hemostasis and Thrombosis*. 2013, Elsevier. p. 33-41.
248. Pober, J.S. and W.C. Sessa, *Evolving functions of endothelial cells in inflammation.* Nat Rev Immunol, 2007. **7**(10): p. 803-815.
249. Goncharov, N.V., et al., *Markers and biomarkers of endothelium: when something is rotten in the state.* Oxid Med Cell Longev, 2017. **2017**.
250. Rajendran, P., et al., *The vascular endothelium and human diseases.* Int J Biol Sci, 2013. **9**(10): p. 1057.
251. Libby, P., *Inflammation in atherosclerosis.* Arterioscler Thromb Vasc Biol, 2012. **32**(9): p. 2045-2051.
252. Szmitko, P.E., et al., *New markers of inflammation and endothelial cell activation: Part I.* Circulation, 2003. **108**(16): p. 1917-1923.
253. Michiels, C., *Endothelial cell functions.* J Cell Physiol, 2003. **196**(3): p. 430-443.
254. Liao, J.K., *Linking endothelial dysfunction with endothelial cell activation.* J Clin Investig, 2013. **123**(2): p. 540-541.
255. Thornhill, M. and D. Haskard, *IL-4 regulates endothelial cell activation by IL-1, tumor necrosis factor, or IFN-gamma.* J Immunol, 1990. **145**(3): p. 865-872.
256. Gimbrone Jr, M.A. and G. García-Cardeña, *Endothelial cell dysfunction and the pathobiology of atherosclerosis.* Circ Res, 2016. **118**(4): p. 620-636.
257. Glagov, S., et al., *Compensatory enlargement of human atherosclerotic coronary arteries.* N Engl J Med, 1987. **316**(22): p. 1371-5.
258. Iaizzo, P.A., *Handbook of cardiac anatomy, physiology, and devices*. 2010: Springer Science & Business Media.
259. JAMES, T.N., *Anatomy of the coronary arteries in health and disease.* Circulation, 1965. **32**(6): p. 1020-1033.
260. Loukas, M., et al., *The normal and abnormal anatomy of the coronary arteries.* Clin Anat, 2009. **22**(1): p. 114-128.
261. Vaupel, P., et al., *Anatomie, Physiologie, Pathophysiologie des Menschen.* 2015.
262. Le, T.Q., et al., *A dynamic systems approach for detecting and localizing of infarct-related artery in acute myocardial infarction using compressed paper-based electrocardiogram (ecg).* Sensors, 2020. **20**(14): p. 3975.
263. Ambrose, J.A. and M. Singh, *Pathophysiology of coronary artery disease leading to acute coronary syndromes.* F1000Prime Rep, 2015. **7**.
264. Grech, E.D., *Pathophysiology and investigation of coronary artery disease.* Bmj, 2003. **326**(7397): p. 1027-1030.
265. Libby, P. and P. Theroux, *Pathophysiology of coronary artery disease.* Circulation, 2005. **111**(25): p. 3481-3488.
266. Drexler, H., et al., *Flow-dependent coronary artery dilatation in humans.* Circulation, 1989. **80**(3): p. 466-474.
267. Greger, R. and U. Windhorst, *Comprehensive human physiology.* From Cellular Mechanisms to Integration, 1996: p. 1996.
268. Fleckenstein, A., M. Frey, and G. Fleckenstein-Grün, *Antihypertensive and arterial anticalcinotic effects of calcium antagonists.* Am J Cardiol, 1986. **57**(7): p. D1-D10.

269. Bayliss, W.M., *On the local reactions of the arterial wall to changes of internal pressure.* J Physiol, 1902. **28**(3): p. 220.
270. Mandinov, L., et al. *Flow-dependent vasodilation in the coronary circulation: alterations in diseased states*. in *Seminars in Interventional Cardiology: SIIC*. 1998.
271. Grün, D., *Die Interaktion zwischen Low-Density Lipoprotein und sympathischen Adrenorezeptoren an Koronararterien des Menschen*. 2017.
272. Abletshauser, C., et al., *Biosensing of arteriosclerotic nanoplaque formation and interaction with an HMG-CoA reductase inhibitor.* Acta Physiol Scand, 2002. **176**(2): p. 131-145.
273. Moutongo Missala, I., *Der Einfluss von verschiedenen HDL-Isoformen auf die flussabhängige Gefäßmodulation menschlicher Koronarien*. 2016.
274. Siegel, G., et al., *Atherogenesis and plaque rupture, surface/interface-related phenomena.* Colloids Surf A Physicochem Eng Asp, 2018. **557**: p. 28-35.
275. Dong, B., et al., *Electrospinning of collagen nanofiber scaffolds from benign solvents.* Macromolecular rapid communications, 2009. **30**(7): p. 539-542.
276. Ruzin, S.E., *Plant microtechnique and microscopy*. Vol. 198. 1999: Oxford University Press New York.
277. Chisari, F., L. Curtiss, and F. Jensen, *Physiologic concentrations of normal human plasma lipoproteins inhibit the immortalization of peripheral B lymphocytes by the Epstein-Barr virus.* J Clin Investig, 1981. **68**(2): p. 329-336.
278. Leonhardt, W., et al., *Recovery of cholesterol and triacylglycerol in very-fast ultracentrifugation of human lipoproteins in a large range of concentrations.* 1994.
279. Baumstark, D., *NMR-Spektroskopie an Lipoproteinen und Lipoproteinsubklassen*. 2012.
280. Giovannoni, F., et al., *Dengue non-structural protein 5 polymerase complexes with promyelocytic leukemia protein (PML) isoforms III and IV to disrupt PML-nuclear bodies in infected cells.* Front Cell Infect Microbiol, 2019: p. 284.
281. Liu, W. and C. Heckman, *The sevenfold way of PKC regulation.* Cell Signal, 1998. **10**(8): p. 529-542.
282. Shamloul, A., et al., *The Methyltransferase Smyd1 Mediates LPS-Triggered Up-Regulation of IL-6 in Endothelial Cells.* Cells, 2021. **10**(12): p. 3515.
283. Becker, S., et al., *Stability of Smyd1 in endothelial cells is controlled by PML-dependent SUMOylation upon cytokine stimulation.* Biochem J, 2021. **478**(1): p. 217-234.
284. Schneider, C.A., W.S. Rasband, and K.W. Eliceiri, *NIH Image to ImageJ: 25 years of image analysis.* Nat Methods, 2012. **9**(7): p. 671-675.
285. Schlangen, J., *Die Wirkung von VLDL-Isoformen auf die flussabhängige Dilatation an Koronararterien des Menschen*. 2010.
286. Jumar, A., *Die Wirkung von Katecholaminen auf die Koronararterien des Menschen*. 2012.
287. Siegel, G., et al., *Blood-flow sensing by anionic biopolymers.* J Autonom Nerv Syst, 1996. **57**(3): p. 207-213.
288. Frostegard, J., et al., *Biologically modified LDL increases the adhesive properties of endothelial cells.* Atherosclerosis, 1991. **90**(2): p. 119-126.
289. Rajavashisth, T., et al., *Induction of endothelial cell expression of granulocyte and macrophage colony-stimulating factors by modified low-density lipoproteins.* Nature, 1990. **344**(6263): p. 254-257.
290. Sata, M. and K. Walsh, *Oxidized LDL activates fas-mediated endothelial cell apoptosis.* J Clin Investig, 1998. **102**(9): p. 1682-1689.

291. Gisterå, A. and G.K. Hansson, *The immunology of atherosclerosis.* Nat Rev Nephrol, 2017. **13**(6): p. 368-380.
292. Chelbi-Alix, M.K., et al., *Resistance to virus infection conferred by the interferon-induced promyelocytic leukemia protein.* J Virol, 1998. **72**(2): p. 1043-1051.
293. Maarifi, G., M.K. Chelbi-Alix, and S. Nisole, *PML control of cytokine signaling.* Cytokine Grwoth Factor Rev, 2014. **25**(5): p. 551-561.
294. Cheng, X. and H.-Y. Kao, *Microarray analysis revealing common and distinct functions of promyelocytic leukemia protein (PML) and tumor necrosis factor alpha (TNF α) signaling in endothelial cells.* BMC Genom, 2012. **13**(1): p. 1-17.
295. Stiko-Rahm, A., et al., *Secretion of plasminogen activator inhibitor-1 from cultured human umbilical vein endothelial cells is induced by very low density lipoprotein.* Arteriosclerosis, 1990. **10**(6): p. 1067-1073.
296. Hsu, K., et al., *Translational control of PML contributes to TNFα-induced apoptosis of MCF7 breast cancer cells and decreased angiogenesis in HUVECs.* Cell Death Differ, 2016. **23**(3): p. 469-483.
297. Dichtl, W., et al., *Very low-density lipoprotein activates nuclear factor-κB in endothelial cells.* Circ Res, 1999. **84**(9): p. 1085-1094.
298. Yang, W., et al., *TRIM52 plays an oncogenic role in ovarian cancer associated with NF-kB pathway.* Cell Death Dis, 2018. **9**(9): p. 1-14.
299. Zhang, W.-Y., et al., *HDL inhibits saturated fatty acid mediated augmentation of innate immune responses in endothelial cells by a novel pathway.* Atherosclerosis, 2017. **259**: p. 83-96.
300. Kontush, A., et al., *Structure of HDL: particle subclasses and molecular components.* High Density Lipoproteins, 2015: p. 3-51.
301. Suc, I., et al., *HDL and ApoA prevent cell death of endothelial cells induced by oxidized LDL.* Arterioscler Thromb Vasc Biol, 1997. **17**(10): p. 2158-2166.
302. Sugano, M., K. Tsuchida, and N. Makino, *High-density lipoproteins protect endothelial cells from tumor necrosis factor-α-induced apoptosis.* Biochem Biophys Res Commun, 2000. **272**(3): p. 872-876.
303. Yin, K., D.-f. Liao, and C.-k. Tang, *ATP-binding membrane cassette transporter A1 (ABCA1): a possible link between inflammation and reverse cholesterol transport.* Mol Med, 2010. **16**(9): p. 438-449.
304. Wang, N., et al., *A PEST sequence in ABCA1 regulates degradation by calpain protease and stabilization of ABCA1 by apoA-I.* J Clin Investig, 2003. **111**(1): p. 99-107.
305. Hoshino, T., K. Kamino, and M. Matsumoto, *Gene dose effect of the APOE-ϵ4 allele on plasma HDL cholesterol level in patients with Alzheimer's disease.* Neurobiol Aging, 2002. **23**(1): p. 41-45.
306. Lunardi, A., et al., *A role for PML in innate immunity.* Genes Cancer, 2011. **2**(1): p. 10-19.
307. Ryoo, S.-W., et al., *Native LDL induces interleukin-8 expression via H2O2, p38 Kinase, and activator protein-1 in human aortic smooth muscle cells.* Cardiovasc Res, 2004. **62**(1): p. 185-193.
308. Gomaraschi, M., et al., *High-density lipoproteins attenuate interleukin-6 production in endothelial cells exposed to pro-inflammatory stimuli.* Biochim Biophys Acta Mol Cell Biol Lipids, 2005. **1736**(2): p. 136-143.
309. Magnifico, M.C., et al., *VLDL induced modulation of nitric oxide signalling and cell redox homeostasis in HUVEC.* Oxid Med Cell Longev, 2017. **2017**.

310. Tsoi, L.-M., et al., *Apoprotein E isoform-dependent expression and secretion of pro-inflammatory cytokines TNF-α and IL-6 in macrophages.* Arch Biochem Biophys, 2007. **460**(1): p. 33-40.
311. Hendrayani, S.-F., et al., *The inflammatory/cancer-related IL-6/STAT3/NF-κB positive feedback loop includes AUF1 and maintains the active state of breast myofibroblasts.* Oncotarget, 2016. **7**(27): p. 41974.
312. Singh, J.K., et al., *Recent advances reveal IL-8 signaling as a potential key to targeting breast cancer stem cells.* Breast Cancer Res, 2013. **15**(4): p. 1-9.
313. Lee, H.S., et al., *LDL stimulates collagen mRNA synthesis in mesangial cells through induction of PKC and TGF-β expression.* American Journal of Physiology-Renal Physiology, 1999. **277**(3): p. F369-F376.
314. Stranzl, A., et al., *Low-density lipoprotein receptor mRNA in human breast cancer cells: influence by PKC modulators.* Breast Cancer Res Treat, 1997. **42**(3): p. 195-205.
315. Sun, H., et al., *Kainate receptor activation induces glycine receptor endocytosis through PKC deSUMOylation.* Nat Commun, 2014. **5**(1): p. 1-17.
316. Ripperger, J.A., et al., *Transcription Factors Stat3 and Stat5b Are Present in Rat Liver Nuclei Late in an Acute Phase Response and Bind Interleukin-6 Response Elements (∗).* J Biol Chem, 1995. **270**(50): p. 29998-30006.
317. Jung, Y.Y., et al., *LDL cholesterol promotes the proliferation of prostate and pancreatic cancer cells by activating the STAT3 pathway.* J Cell Physiol, 2021. **236**(7): p. 5253-5264.
318. Kwon, M.-J., et al., *Protein kinase C-θ promotes Th17 differentiation via upregulation of Stat3.* J Immunol, 2012. **188**(12): p. 5887-5897.
319. Xiang, M., et al., *STAT3 induction of miR-146b forms a feedback loop to inhibit the NF-κB to IL-6 signaling axis and STAT3-driven cancer phenotypes.* Sci Signal, 2014. **7**(310): p. ra11-ra11.
320. Obi, S., et al., *Heat induces interleukin-6 in skeletal muscle cells via TRPV1/PKC/CREB pathways.* J Appl Physiol, 2017. **122**(3): p. 683-694.
321. Romberger, D., et al., *Hog barn dust extract stimulates IL-8 and IL-6 release in human bronchial epithelial cells via PKC activation.* J Appl Physiol, 2002. **93**(1): p. 289-296.
322. Gottifredi, V. and C. Prives, *P53 and PML: new partners in tumor suppression.* Trends Cell Biol, 2001. **11**(5): p. 184-187.
323. Suo, J., et al., *Influenza virus aggravates the ox-LDL-induced apoptosis of human endothelial cells via promoting p53 signaling.* J Med Virol, 2015. **87**(7): p. 1113-1123.
324. Abbas, T., et al., *Inhibition of human p53 basal transcription by down-regulation of protein kinase Cδ.* J Biol Chem, 2004. **279**(11): p. 9970-9977.
325. Ashcroft, M. and K.H. Vousden, *Regulation of p53 stability.* Oncogene, 1999. **18**(53): p. 7637-7643.
326. Pearson, M., et al., *PML regulates p53 acetylation and premature senescence induced by oncogenic Ras.* Nature, 2000. **406**(6792): p. 207-210.
327. Gonnissen, S., et al., *High Concentration of Low-Density Lipoprotein Results in Disturbances in Mitochondrial Transcription and Functionality in Endothelial Cells.* Oxid Med Cell Longev, 2019. **2019**.
328. Ulrich, V., et al., *Genetic variants of ApoE and ApoER2 differentially modulate endothelial function.* Proc Natl Acad Sci USA, 2014. **111**(37): p. 13493-13498.
329. Fabich, N., et al., *LDL-Apolipoprotein E Isoform Codetermines Human Coronary Artery Tone*. 2012, Am Heart Assoc.

330. Boo, Y.C. and H. Jo, *Flow-dependent regulation of endothelial nitric oxide synthase: role of protein kinases.* Am J Physiol Cell Physiol, 2003. **285**(3): p. C499-C508.